

Aspects of stochastic control and switching: from Parrondo's games to electrical circuits

by

Andrew Gordon Allison

B.Sc.(Mathematical Sciences), The University of Adelaide, 1978.

B.E. (Computer Systems Engineering, Honours), The University of Adelaide, 1995.

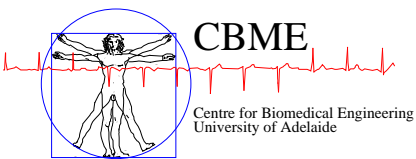
Thesis submitted for the degree of

Doctor of Philosophy

in

The School of Electrical and Electronic Engineering, Faculty of
Engineering, Computer and Mathematical Sciences,
The University of Adelaide

2009



© 2009
Andrew Gordon Allison
All Rights Reserved



Contents

Contents	iii
Abstract	ix
Statement of Originality	xi
Acknowledgements	xiii
Conventions	xv
Publications	xvii
List of Figures	xxi
List of Tables	xxv
Chapter 1. Introduction and motivation	1
1.1 Introduction	2
1.1.1 Brownian motors	2
1.2 Motivation	3
1.3 Thesis overview	3
1.4 Original contributions	7
1.5 Chapter summary	9
Chapter 2. Background for Parrondo's games	11
2.1 Brownian motion	12
2.2 Maxwell's demon	14
2.3 The ratchet and pawl machine	16
2.4 Flashing ratchets	18
2.5 Constructed Brownian ratchets	22
2.6 A brief history of finite discrete games of chance	23
2.7 Chapter summary	26

Chapter 3. The physical basis of Parrondo's games	27
3.1 Discrete transformations of continuous functions	29
3.2 Finite difference equations and Parrondo's games	38
3.3 Finite partial difference equations	40
3.4 Sampling the Fokker-Planck Equation	44
3.5 Parrondo's games, as a set of PDEs	47
3.5.1 Game A, as a partial difference equation	48
3.5.2 Game B, as a partial difference equation	50
3.5.3 Conditions for convergence of the solution	50
3.5.4 An appropriate choice of scale	51
3.5.5 Mean position and mean velocity of drift	53
3.5.6 An example of a simulation, including null-transitions	54
3.5.7 A more realistic simulation	55
3.6 Summary of results, regarding the sampling process	58
3.7 Estimating the moments of Parrondo's games	58
3.7.1 Evaluation of the discrete transforms of the solution function	59
3.7.2 Evaluation of first and second moments, of the solution	62
3.7.3 The Bernoulli process, a simple worked example	64
3.7.4 Stochastic processes with stationary probabilities of transition	66
3.7.5 The w-transforms of some well known distributions	68
3.7.6 Parrondo's Game A	69
3.7.7 Taleb's game, a game with highly asymmetrical rewards	70
3.7.8 Difference equations with periodic coefficients	72
3.7.9 Parrondo's game B	74
3.7.10 The small-matrix representation of Parrondo's games	77
3.8 Chapter summary	80
Chapter 4. Rates of return from discrete games of chance	81
4.1 Some definitions of terms	82
4.1.1 Phase space	84
4.1.2 Limiting fixed-points in phase-space	85

4.1.3	Parrondo's games	86
4.1.4	A definition for Parrondo's games	87
4.2	The unconstrained or <i>large-matrix</i> formulation	88
4.3	The spatially-periodic case, reduced modulo L	92
4.4	Asymptotic value of the first moment of the games	94
4.4.1	Markov Chains with Rewards	94
4.4.2	A matrix notation for the first moment	95
4.5	The matrix technique for the first moment	96
4.5.1	Parrondo's original games	96
4.5.2	The apparent paradox of Parrondo's games	100
4.5.3	Parrondo's games, with natural diffusion	115
4.5.4	A pair of discrete games with only two states	118
4.5.5	Astumian's games	121
4.5.6	Astumian's games, with absorbing boundary conditions	125
4.5.7	Summary of common features of the discrete games	130
4.6	Visualisation of the process	132
4.6.1	Time-homogeneous Markov chains and notation	132
4.6.2	Time-inhomogeneous Markov chains	134
4.6.3	Reduction of the periodic case	136
4.7	Long sequences of operators	136
4.8	Phase-space visualisation and fractal properties	138
4.8.1	Two Markov games that generate simple fractals	138
4.8.2	The Cantor middle-third fractal	139
4.8.3	Iterated Function Systems (IFS)	148
4.8.4	Parrondo's fractal	148
4.9	Equivalent representation	149
4.9.1	The average probability vector, over time	151
4.9.2	The average probability vector, over phase-space	153
4.9.3	Consistency of the two averages	155
4.10	An optimised form of Parrondo's games	156
4.10.1	An interesting fractal object	157
4.11	Chapter summary	158

Chapter 5. switched-mode circuits and switched Markov systems	161
5.1 Switched-mode circuits and switched Markov systems	162
5.1.1 Switched-mode circuits	162
5.1.2 Switched state-space and switched Markov systems	172
5.1.3 Fractals in the phase-space of switched-mode circuits	175
5.1.4 The limiting case of fast switching as $\tau \rightarrow 0$	177
5.2 A Parrondo effect for a switched-mode circuit	184
5.2.1 Construction of a simple switched-mode system	186
5.2.2 A switched state-space formulation	190
5.2.3 Internal stored energy	192
5.2.4 Proof of instability of plants A_1 and A_2	197
5.2.5 Proof of stability of the stochastically mixed processes	200
5.3 Sources of noise	202
5.4 Chapter summary	203
Chapter 6. Langevin equations as models for noise in circuits	205
6.1 Introduction, to noise techniques in electronics	206
6.2 Stochastic analysis of circuits	209
6.2.1 Outline of stochastic calculus of Itô	209
6.2.2 The Fokker Planck equation and the Langevin SDE	216
6.3 Modelling of electronic circuits, using SDEs	217
6.3.1 Infinitesimal forms of Kirchhoff's laws	217
6.3.2 Kirchhoff's current law	217
6.3.3 Kirchhoff's voltage law	220
6.3.4 Models for resistors	223
6.3.5 Modelling of capacitors	227
6.3.6 Modelling of inductors	227
6.4 A one-dimensional Langevin equation (SDE)	228
6.4.1 An approach, based on power spectral density	228
6.4.2 The Langevin SDE	234
6.5 A two-dimensional Langevin equation (SDE)	236

6.5.1	Nyquist’s approach, based on power spectral density	236
6.5.2	An approach, using the the Langevin stochastic differential equation	243
6.6	Noise models for the JFET	244
6.7	A simple JFET circuit	245
6.8	Analysis of the JFET circuit	246
6.9	Summary and open questions	247
 Chapter 7. Conclusions and future challenges		 251
7.1	Original contribution	252
7.2	Future prospects	253
7.2.1	The physical basis of Parrondo’s games	253
7.2.2	Rates of return from discrete games of chance	260
7.2.3	Switched-mode circuits and switched Markov systems	261
7.2.4	Langevin equations to model noise in electronic circuits	263
 Résumé		 267
 Methods of work		 269
 Epilogue		 273
 Bibliography		 275
 Glossary		 289
 Index		 291

Abstract

The first half of this thesis deals with the line of thought that leads to the development of discrete games of chance as models in statistical physics, with an emphasis on analysis of Parrondo's games.

The second half of the thesis is concerned with applying discrete games of chance to the modelling of other phenomena in the discipline of electrical engineering. The important features being the element of *switching* that is implicit in discrete games of chance and the element of *uncertainty*, introduced by the random aspect of discrete games of chance.

Statement of Originality

This work contains no material that has been accepted for the award of any other degree or diploma in any university or other tertiary institution and, to the best of my knowledge and belief, contains no material previously published written by another person, except where due reference has been made in the text.

I give consent to this copy of the thesis, when deposited in the University Library, being available for loan, photocopying and dissemination through the library digital thesis collection, subject to the provisions of the Copyright act of 1968. Copying or publication or use of this thesis or part thereof for financial gain is not allowed without the author's written permission. Due recognition shall be given to the author, and the University of Adelaide, in any scholarly use that may be made of any material in this thesis.

10th Sep. 2009

Acknowledgements

Whenever one writes about a scientific subject, one stands on the shoulders of giants. Some of these people are famous, and appear in the literature and are cited. Some are less famous, for their contributions to the work, and deserve special recognition here.

The period of time in which this thesis was completed was very stressful for me because both of my parents died. They deserve personal as well as professional acknowledgement. My mother, Gwen Anderson, encouraged my interest in chemistry and the natural world. My father, Robert Allison, encouraged my interest in electronics and statistics. He taught me to play cards and to take only reasonable risks, in cards or in life. If in doubt, he always encouraged me to “play it straight.”

I thank my supervisors, Professors Derek Abbott and Charles E. M. Pearce. I owe an enormous debt to Professor Derek Abbott. He has always encouraged me to think outside the square. He made every effort to bring me into contact with experts in the many fields in which he works. He has encouraged me to persevere in the face of difficulties. He had faith in my ideas when I had doubts. He brought me back to reality when my feet left the ground. He helped me to improve the precision of my prose.

I owe an equal debt to Professor Charles Pearce, who also had had faith in me and encouraged me to follow up my intuitive ideas until they were properly formulated. Charles also prevented me from committing a number of grievous mathematical errors. If any errors remain, they are certainly mine.

Thanks to Derek’s efforts, I have been able to have informal discussions with many scientists, whom I admire greatly. These include, Prof. Juan Parrondo (Universidad Computense), Prof. Dean Astumian (University of Maine), Prof. Eugene Stanley (Director, Center for Polymer Studies), Prof. Peter Hänggi (Universität Augsburg), Prof. Raúl Toral (Instituto de Física Interdisciplinaria Sistemas Complejos), Assoc. Prof. Martin Bier (East Carolina University), Prof. Charles Doering (University of Michigan), Prof. Erhard Behrends (Freie Universität Berlin) and Prof. Michael Barnsley (Australian

Acknowledgements

National University). I am honoured to have met these people and I feel very humble when I claim to have extended their ideas by even a small amount.

I particularly appreciate the efforts of the long suffering editors of my open publications, who also helped me to make my ideas more logical and coherent, and fit within the page limits. I particularly appreciate the efforts of Prof. Laszlo Kish (Texas A&M University) Dr. Sergey Bezrukov (National Institutes of Health, NIH) and Prof. Lutz Schimansky-Geier (Institut für Physik Humboldt, Universität zu Berlin).

I also appreciate the contributions of many of the staff and students at the School of Electrical and Electronic Engineering at the University of Adelaide, especially my very patient Heads of School, Dr Tony Parker, Dr Ken Sarkies and Assoc. Prof. Mike Liebelt. I thank Greg Harmer for the use of his fabulous Smoluchowski-ratchet figure, Matthew Berryman, Frederic Bonnet, Tze Wei Tang, Chris Illert and Pau Amengual for being very astute and reliable co-authors. I particularly thank Matthew for the use of his PERL code. I thank Mark McDonnell for the use of his laptop, for sharing a hotel room (at a conference) and for many interesting and discursive conversations about noise, correlation, and information. I thank Withawat Withayachumanankul for his tree diagram of our scientific genealogy.

I am especially grateful to Associate Professor John van der Hoek (University of South Australia) for his advice regarding stochastic differential equations. I am grateful to Chris Illert for many fruitful discussions regarding the calculus of variations and the application of variational techniques to problems in electronics. Finally, I thank my partner Mei Sheong Wong, and family, for putting up with my absence (at a computer) for very long periods of time and for help with proofs of some of the less technical material.

“Writing a book is a horrible, exhausting struggle, like a long bout of some painful illness. One would never undertake such a thing if one were not driven on by some demon whom one can neither resist nor understand.” George Orwell

Conventions

This thesis is typeset using L^AT_EX2e software, including the core packages tetex-base, tetex-bin and tetex-extra. All L^AT_EX software was obtained from the Debian Archive at: <http://www.debian.org>.

Numerical calculations were carried out in Matlab, and in the equivalent open-source packages GNU Octave and Gnuplot, which were also obtained from the Debian archive.

Many of the Figures were generated in Matlab and in GNU Octave. The other figures were drawn, or post-processed, in a number of other drawing packages, including Corel-Draw 9 under Windows 2000, Adobe Creative Suite 3 under Mac OS-X, or in xfig and Inkscape, under LINUX. The last two packages were downloaded from the Debian archive. All drawings have been converted or exported to encapsulated post-script (eps) format.

The complete editing environment, Emacs21 (Editing with MACroS, version 21.4.1) was used as an effective interface to L^AT_EX. The idiomatic conventions, for L^AT_EX, conform to standard described in (Lamport 1994).

Harvard style is used for referencing and citation in this thesis. British spelling is adopted, consistent with the Ispell package, using the British dictionary, in Emacs21. Additional words have been traced back to their original sources. Where we have needed to quote works in other languages, including works in US English, we have used the original spelling.

Publications

Book Chapters

ALLISON-A., ABBOTT-D. & AND PEARCE-C. E. M. (2005) State-space visualisation and fractal properties of Parrondo's games, in A. S. Nowak., and K. Szajowski. (eds.), *Proceedings of the Ninth International Symposium on Dynamic Games and Applications 2000, Advances in Dynamic Games: Applications to Economics, Finance, Optimization, and Stochastic Control.*, Vol. 7, The International Society of Dynamic Games (ISDG), Birkhauser, pp. 613–633.

Journal Articles

BERRYMAN-M. J., ALLISON-A., WILKINSON-C. R. & ABBOTT-D. (2005) Review of signal processing in genetics, *Fluctuation and Noise Letters*, **5**(4), pp. R13–R35.

AMENGUAL-P., ALLISON-A., TORAL-R. & ABBOTT-D. (2004) Discrete-time ratchets, the Fokker-Planck equation and Parrondo's paradox, *Proceedings of the Royal Society of London*, **460**(2048), pp. 2269–2284.

BERRYMAN-M. J., ALLISON-A., & ABBOTT-D. (2004) Mutual information for examining correlations in DNA, *Fluctuation and Noise Letters*, **4**, pp. L237–L246.

ILLERT-C. & ALLISON-A. (2004) Phono-genesis and the origin of accusative syntax in proto-Australian language, *Journal of Applied Statistics*, **31**(1), pp. 73–104.

TANG-T. W., ALLISON-A. & AND ABBOTT-D. (2004) Investigation of chaotic switching strategies in Parrondo's games, *Fluctuation and Noise Letters*, **4**, pp. L585–L596.

BERRYMAN-M. J., ALLISON-A. & ABBOTT-D. (2003) Statistical techniques for text classification based on word recurrence intervals, *Fluctuation and Noise Letters*, **3**(1), pp. L1–L10.

LEE-Y., ALLISON-A. & ABBOTT-D. (2003) Minimal Brownian ratchet: An exactly solvable model, *Phys. Rev. Lett.*, **91**(22), Art. No. 220601.

ALLISON-A. & ABBOTT-D. (2002) A MEMS Brownian ratchet, *Microelectronics Journal*, **33**(3), pp. 235–243.

Publications

ALLISON-A. & ABBOTT-D. (2002) The physical basis for Parrondo's games, *Fluctuation and Noise Letters*, **2**(4), pp. L327–L341.

ALLISON-A. & ABBOTT-D. (2001) Control systems with stochastic feedback, *Chaos Journal*, **11**(3), pp. 715–724.

ALLISON-A. & ABBOTT-D. (2001) Stochastic resonance in a Brownian ratchet, *Fluctuation and Noise Letters*, **1**(4), pp. L239–L244.

ALLISON-A. & ABBOTT-D. (2000) Some benefits of random variables in switched control systems, *Microelectronics Journal*, **31**, pp. 515–522.

Conference Articles

PEARCE-C. E. M., ALLISON-A. & ABBOTT-D. (2007) Perturbing singular systems and the correlating of uncorrelated random sequences, in T. E. Simos, G. Psihoyios and C. Tsitouras(eds.), *Proc. AIP, International Conference of Numerical Analysis and Applied Mathematics*, **936** (1), pp. 699–699.

ALLISON-A., ABBOTT-D. & PEARCE-C. E. M. (2007) , Finding keywords amongst noise: Automatic text classification without parsing, in J. Kertész., S. Bornholdt., and R. Mantegna. (eds.), *Proc. SPIE, Noise and Stochastics in Complex Systems and Finance*, Vol. 6601, Art. No. 660113.

BONNET-F. D. R., ALLISON-A. & ABBOTT-D. (2006) Bubbles in a minority game setting with real financial data, in A. Bender. (ed.), *Proc. SPIE, Complex Systems*, Vol. 6039, pp. 99–103.

ALLISON-A. & ABBOTT-D. (2005) Applications of Stochastic Differential Equations in electronics, in L. Reggiani and C. Penneta and V. Akimov and E. Alfinito and M. Rosini. (eds.), *Proc. AIP, Unsolved Problems of Noise and Fluctuations in Physics, Biology and High Technology*, Vol. 800, pp. 15–23.

BERRYMAN-M. J., ALLISON-A. & ABBOTT-D. (2005) Gene network analysis and design, in D. V. Nicolau. (ed.), *Proc. SPIE, Biomedical Applications of Micro- and Nanoengineering II*, Vol. 5651, pp. 126–133.

BERRYMAN-M. J., COUSSENS-S. W., PAMULA-Y., KENNEDY-D., LUSHINGTON-K., SHALIZI-C., ALLISON-A., MARTIN-J., SAINT-D. & ABBOTT-D. (2005) Nonlinear aspects of the EEG during sleep in children, *Proc. SPIE, Fluctuations and Noise in Biological, Biophysical, and Biomedical Systems*, Vol. 5841, Austin, Texas, pp. 40–48.

- BERRYMAN-M. J., **ALLISON-A.** & ABBOTT-D. (2004) Optimizing genetic algorithm strategies for evolving networks, *Proc. SPIE, Fluctuations and Noise in Biological, Biophysical and Biomedical Systems*, Vol. 5473, pp. 122–130.
- BERRYMAN-M. J., **ALLISON-A.** & ABBOTT-D. (2004) Stochastic evolution and multifractal classification of prokaryotes, in S. M. Bezrukov., H. Frauenfelder., and F. Moss. (eds.), *Proc. SPIE, Fluctuations and Noise in Biological, Biophysical and Biomedical Systems*, Vol. 5110, pp. 192–200.
- BERRYMAN-M. J., SPENCER-S. L., **ALLISON-A.** & ABBOTT-D. (2004) Fluctuations and noise in cancer development, in Z. Gingl. (ed.), *Proc. SPIE, Noise in Interdisciplinary Applications II, Fluctuations and Noise 2004*, Vol. 5471, pp. 322–332.
- BERRYMAN-M. J., **ALLISON-A.** & ABBOTT-D. (2004) Cellular automata for exploring gene regulation in drosophila segmentation, *Proc. SPIE, BioMEMS and Nanotechnology 2003*, pp. 266–277.
- BERRYMAN-M. J., KHOO-W. L., NGUYEN-H., O'NEILL-E., **ALLISON-A.** & ABBOTT-D. (2004) Exploring tradeoffs in pleiotrophy and redundancy using evolutionary computing, in D. V. Nicolau. (ed.), *Proc. SPIE, BioMEMS and Nanotechnology 2003*, Vol. 5275, pp. 49–58.
- BONNET-F. D. R., **ALLISON-A.** & ABBOTT-D., (2004) Path integrals in fluctuating markets, in Z. Gingl. (ed.), *Proc. SPIE, Noise in Complex Systems and Stochastic Dynamics II*, Vol. 5471, pp. 595–611.
- BONNET-F. D. R., **ALLISON-A.** & ABBOTT-D (2004) Review of quantum path integrals in fluctuating markets, in D. Abbott., and K. Eshraghian. (eds.), *Proc. SPIE, Microelectronics: Design, Technology, and Packaging*, Vol. 5274, pp. 569–580.
- TANG-T. W., **ALLISON-A.** & ABBOTT-D. (2004) Parrondo's games with chaotic switching, *Proc. SPIE, Fluctuations and Noise in Biological, Biophysical and Biomedical Systems*, Vol. 5471, pp. 520–530.
- ALLISON-A.** & ABBOTT-D. (2003) Brownian ratchets with distributed charge, in S. M. Bezrukov., H. Frauenfelder., and F. Moss. (eds.), *Proc. SPIE, Fluctuations and Noise in Biological, Biophysical, and Biomedical Systems*, Vol. 5110, pp. 302–311.
- ALLISON-A.** & ABBOTT-D. (2003) Discrete games of chance as models for continuous stochastic transport processes, in L. Schimansky-Geier., D. Abbott., A. Neiman., and C. V. den Broeck. (eds.), *Proc. SPIE, Noise in Complex Systems and Stochastic Dynamics*, Vol. 5114, pp. 363–371.
- BERRYMAN-M.J, **ALLISON-A.**, CARPEÑA-P & ABBOTT-D. (2002) Signal processing and statistical methods in analysis of text and DNA, D. V. Nicolau (ed.), *Proc. SPIE, Biomedical Applications of Micro-*

and *Nanoengineering*, Vol. 4937, pp. 231–240.

ALLISON-A. & **ABBOTT-D.** (2002) Stochastic resonance, Brownian ratchets and the Fokker-Planck equation, in S. M. Bezrukov. (ed.), *Proc. SPIE, Unsolved Problems of Noise and Fluctuations: UPoN 2002*, Vol. 665, pp. 74–83.

ALLISON-A. & **ABBOTT-D.** (2001) MEMS implementation of a Brownian ratchet, in D. Abbott., V. K. Varadan., and K. F. Boehringer. (eds.), *Proc. SPIE, Smart Electronics and MEMS II*, Vol. 4236, pp. 319–329.

HOO-T. L., **TING-A. S. C.**, **O'NEILL-E.**, **ALLISON-A.** & **ABBOTT-D.** (2001) Real life: A cellular automation for investigating competition between pleiotrophy and redundancy, *Proc. SPIE, Electronics and Structures for MEMS II*, Vol. 4591, pp. 380–390.

ALLISON-A. & **ABBOTT-D.** (2000) Stable processes in econometric time series: Are prices made out of noise?, in D. Abbott., and L. B. Kish. (eds.), *Proc. AIP, Second. Int. Conf. Unsolved Problems of Noise and Fluctuations (UPoN 99)*, Vol. 511, pp. 221–232.

ALLISON-A. & **ABBOTT-D.** (2000) Stochastically switched control systems, in D. Abbott. (ed.), *Proc. SPIE, Second. Int. Conf. Unsolved Problems of Noise and Fluctuations (UPoN 99)*, Vol. 511, pp. 249–254.

ALLISON-A. & **ABBOTT-D.** (1999) Simulation and properties of randomly switched control systems, in B. Courtois., and S. N. Demidenko. (eds.), *Proc. SPIE, Design, Characterization, and Packaging for MEMS and Microelectronics*, Vol. 3893, pp. 204–213.

List of Figures

1.1	Probability density in a flashing ratchet	4
<hr/>		
2.1	Maxwell's demon	15
2.2	The ratchet and pawl machine	18
2.3	The flashing ratchet	20
2.4	Top view of an inter-digital flashing ratchet	21
2.5	Side view of an inter-digital flashing ratchet	22
2.6	Charge separation in a Brownian ratchet	23
<hr/>		
3.1	A single sample path of Parrondo's original process	49
3.2	Time-evolution of the mean of the distribution $p(t, x)$	55
3.3	The time-evolution of $p(t, x)$	56
3.4	The mean position of a Brownian particle in a ratchet	57
3.5	Point probabilities and probabilities of transition for the Bernoulli process	60
<hr/>		
4.1	The decision tree for Game A	87
4.2	The decision tree for Game B	88
4.3	State transitions of Parrondo's games, with no limits on position	90
4.4	Results from a simulation based on the large matrix approach	91
4.5	State transitions of Parrondo's games, (reduced modulo L)	93
4.6	Expected rates of return ϱ for various choices of the mixing fraction γ	98
4.7	The zero-gain surface for Parrondo's games	99
4.8	The quasi-stable forms in Onsager's model	100
4.9	The winning and losing regions in the 2D version of Parrondo's games	105
4.10	An example of a linear reward function, ϱ_1	110
4.11	An example of a non-linear reward function, ϱ_2	111

List of Figures

4.12	A stereo-pair plot of the winning and losing regions of Parrondo's games	116
4.13	The state transitions of Parrondo's games, with natural diffusion	117
4.14	The expected rates of return ϱ for various choices of the mixing fraction γ	118
4.15	Definitions for a simple two-state game	119
4.16	Simulation of a two-state version of Parrondo's games	120
4.17	The expected rates of return ϱ for various choices of the mixing fraction γ	121
4.18	State transitions for Astumian's rule-set number 1	124
4.19	State transitions for Astumian's rule-set number 2	125
4.20	The expected rates of return ϱ for various choices of the mixing fraction γ	126
4.21	A rule-set for Astumian's games	127
4.22	The phase-space of a simple Markov chain	134
4.23	A fractal attractor generated by games S and T	139
4.24	A histogram of a distribution in phase-space	142
4.25	The fractal object generated by Parrondo's original games	150
4.26	The scaling properties of the attractor generated by Parrondo's games .	151
4.27	Fractal attractor generated by a limiting case of Parrondo's games	158
<hr/>		
5.1	A simple switched capacitor energy converting circuit	163
5.2	Switched-capacitor, equivalent circuit, during the <i>ON</i> mode	165
5.3	Switched-capacitor, equivalent circuit, during the <i>OFF</i> mode	165
5.4	A sketch of V_c as a function of time	167
5.5	A detailed numerical simulation of the switched-capacitor circuit	170
5.6	A histogram of the scaled voltage, $x = V_c/V_s - 1/2$	176
5.7	The output from a switched-capacitor circuit	178
5.8	The result from an SDE model for a switched capacitor circuit	180
5.9	The scaling of variance with switching frequency	182
5.10	General plan of a second-order system with one feedback loop	187
5.11	Root locus plot for a second order system	189
5.12	A model for the open-loop transfer function, $G(s)$	193
5.13	A model for the feedback transfer function, $G(s)$	194

5.14	Discrete state-space simulation of the neutral system	197
5.15	Discrete state-space simulation of system A_1	198
5.16	Discrete state-space simulation of system A_2	199
5.17	Discrete state-space simulation of the randomly switched system	200

6.1	Some sample paths from Geometric Brownian Motion (GBM)	215
6.2	The infinitesimal form of Kirchhoff's Current Law (KCL)	218
6.3	The infinitesimal form of Kirchhoff's Voltage Law (KVL)	221
6.4	Linear noise models for a resistor	224
6.5	Modelling of capacitors	227
6.6	Modelling of inductors	228
6.7	Parallel, or Norton, representation of an RC circuit	229
6.8	A Thévenin Equivalent Circuit for the RC circuit	230
6.9	The Poles of the PSD function for an RC circuit	233
6.10	SDE models for an RC parallel circuit	235
6.11	A parallel RCL circuit	237
6.12	Positions of poles of a second-order under-damped circuit	238
6.13	The normalised poles of a second-order under-damped circuit	238
6.14	Poles of the power spectral density function	240
6.15	An RCL parallel circuit	243
6.16	Noise model for a JFET	245
6.17	Large-signal, schematic circuit diagram for a Colpitts oscillator	245
6.18	Small signal equivalent circuit of a Colpitts oscillator	246

7.1	The Gaussian function, as a <i>basis</i> function	256
7.2	Fundamental limitations of computation	273

List of Tables

3.1	Notation for discrete transformation and associated calculations	31
3.2	Notation for transformed version of $p_{m,n}$	37
3.3	Semantic interpretations of variously transformed versions of $p_{m,n}$. . .	37
3.4	Transforms of solutions to the Bernoulli process	62
3.5	Transforms of some one-dimensional probability mass functions	69
3.6	The generators for some stationary stochastic processes	71
4.1	Rule-set number one, for Astumian's games	122
4.2	Rule-set number two, for Astumian's games	122
4.3	Parameters for the rule-sets, for Astumian's games	128
4.4	Steady state probabilities, for Astumian's games	130
5.1	Some values for the poles, s_1 and s_2 , as functions of the loop gain K . . .	188

Chapter 1

Introduction and motivation

BROWNIAN motors are very small devices by which are able to transduce energy from one form into another. Electrical, or chemical, energy can be used to produce directed motion in space. This chapter provides a very brief introduction to Brownian motors, and how they relate to the motivation for this thesis.

1.1 Introduction

1.1.1 Brownian motors

In ordinary motors, on the human scale, the dominant forms of energy storage are due to inertia, gravity and elasticity. To this, we could also add the energy stored in the electric and magnetic fields, for electrical machines. Mathematically, these fields are all conservative. The associated forces are spatial gradients of a conservative work function, or field.

Energy loss, or dissipation is related to non-conservative forces. These forces cannot be expressed as gradients of a work function (Lanczos 1949). Non-conservative forces are examples of the second law of thermodynamics. Energy that is associated with macroscopic observable degrees of freedom is transferred irreversibly to numerous microscopic un-observable degrees of freedom. There is mixing involved at a microscopic scale. Once some energy has been partitioned amongst many small particles, it cannot be un-mixed, without the expenditure of more energy. The mixing is irreversible.

If a motor, on the human scale, is well designed then the energy loss due to friction is small and does not affect the qualitative behaviour of the machine. Fluctuations, due to the discrete nature of the underlying phenomena, are small and may be neglected, or added to the standard theory as a small perturbation. The situation is reversed if we consider microscopic machines that are constructed on a similar scale to underlying phenomena, to the molecules, carriers, fluxoids¹, or whatever they may be. When we consider microscopic machines the viscous and frictional forces dominate all the other forces and the fluctuations are more evident than any long-term time-average changes. At first, we might expect that *no* machine could possibly operate under these conditions. On closer consideration, it can be seen that the natural machinery inside living cells, not only operates very well, but actually benefits from the presence of fluctuations. A machine that makes use of microscopic fluctuations to transduce energy from one form to another is called a *Brownian motor*.

Brownian motors are strongly dependent on random impacts of molecules (thermal noise), which means that they are only feasible at the nanometer scale. At this small

¹A fluxoid is a quantum of magnetic flux, $\Phi_0 = h / (2q_e) \approx 2.067 \times 10^{-15}$ Wb.

scale, the forces due to viscosity are much greater than the forces due to inertia. The apparently random movements due to fluctuations will be very substantial, in comparison with the scale of the machine. Even in a well designed device, the motion in the required direction will be very small, compared with all the other motion due to random forces exerted by the environment.

Some authors have speculated that protein-based molecular motors in living cells are Brownian motors. The more detailed modelling of Brownian motors seems to have promise in helping us to understand processes in biology. There is the possibility that engineers could mimic the systems that are found in nature. There is the further possibility that we may discover things that we were not even expecting. The dynamics of Brownian motors is an interesting field, which is amenable to mathematical analysis.

1.2 Motivation

Parrondo (1996b) devised a set of discrete games of chance that mimic some aspects of Brownian motors. The main motivation for this thesis is to understand Parrondo's game-theoretical model and to place that model on a rigorous basis. In this thesis the dynamics are modelled using the Fokker-Planck equation, and using the Langevin equation.

1.3 Thesis overview

This thesis investigates transport phenomena associated with inhomogeneous systems. To investigate *all* possible systems or *all* possible phenomena is a task that will probably never be finished. It is prudent to restrict attention to certain special cases where progress appears to be possible. In this thesis, we have mostly used a constructive approach to demonstrate mathematical concepts, rather than an existential approach. Progress is made through worked examples of a general theme.

This thesis first investigates some discrete games of chance, introduced by Parrondo (1996b) and investigated by Harmer and Abbott (1999a) and others. Parrondo's Games

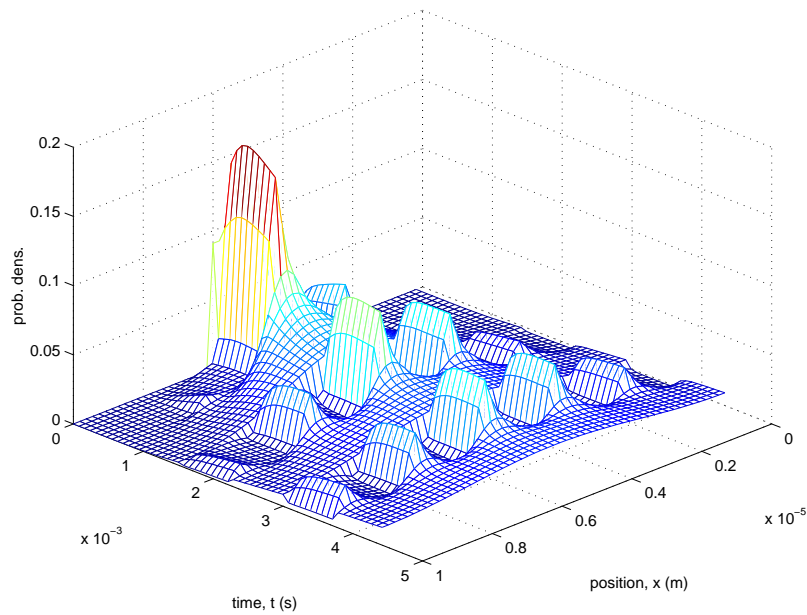


Figure 1.1. Probability density in a flashing ratchet. This figure shows the probability density of finding a Brownian particle within a particular type of Brownian motor, called a *flashing ratchet*. This device is also known as an *on-off ratchet*. The x -axis, on the right, shows spatial position, x , in metres. The y -axis, on the left, shows time, t , in seconds. The spacing of the teeth of this ratchet is about 200 nm. the z -axis on the far left shows probability density, p in units of m^{-1} . If the probability density is integrated over all positions, x , at any given time, t , then the total probability is always one. This simulation was carried out using methods that follow in logical progression from the Fokker-Planck equation and from Parrondo's games. One purpose of this thesis is to make the connection, between the Fokker-Planck equation and Parrondo's games more explicit.

appear to be paradoxical because playing each of the games individually is a losing proposition, with negative expected return. Conversely, playing a mixture of the two different games is a winning proposition, with positive expected return. The useful thing about Parrondo's games is that they are "simple" but not "too simple."² If the games were simplified any further then they would not adequately model actual phenomena in the real physical world. If the model was more detailed then we might not be able to solve the resulting equations analytically. Numerical solutions might not give the insight that can be obtained from an exact solution to a slightly simplified

²Albert Einstein is purported to have said that "We should make things as simple as possible, but not simpler."

model.

In this thesis, Parrondo's games are placed on a sound physical basis. We obtain the equations for Parrondo's games by sampling the Fokker-Planck equation description of a flashing ratchet. Techniques are derived for estimating the moments of Parrondo's games. These are equivalent to the rates of return (or loss) of the games and the degree of uncertainty associated with those estimates. The small-matrix representation of Parrondo's games is also placed on a more rigorous basis.

The small-matrix technique, for the first moment of Parrondo's games, is applied to a variety of different but related discrete games, from the literature, including: (i) Parrondo's original games, (ii) Parrondo's games with natural diffusion, (iii) a pair of discrete games with only two states, (iv) Astumian's games (with boundaries at infinity), and (v) Astumian's original games (with absorbing boundary conditions). All of these, apparently different, games can be analysed by applying the same mathematical methods. We analyse all of them, within the one framework that is developed in this thesis.

It is shown, by construction, that the presence (or absence) of self-transitions in discrete Markov games is independent of the presence, of absence, of the paradoxical behaviour.

Visualisation techniques are applied to the representation of the games in phase-space and it is shown that the resulting attracting set has fractal properties. The methods of Barnsley (1988) are extended to derive expressions of the moments of fractals, in phase-space. The average value of the time varying probability vector (over time) is shown to give the same result as averaging the time varying probability vector (over phase-space). This is an important result for establishing the consistency of the two approaches.

The equations for the time-evolution of Parrondo's games have the same form as the equations for the time-evolution of switched-mode electrical circuits. It is shown that the attracting set in the phase-space for a switched-mode circuit can also be a fractal. This is quite analogous to the case for Parrondo's games. It is possible to construct a version of Parrondo's paradox for a physical switched-mode circuit, if the measure of *winning* or *losing* is based on changes in the internal stored energy of the system. This

proof is achieved by construction. It is possible to construct a physical switched-mode circuit that is unstable in either mode but is stable when switched between modes. This stable situation persists, even if the modes are selected at random. These results are analogous to the paradoxical behaviours that are exhibited by Parrondo's games.

The *winning* and *losing* regions of Parrondo's games are considered. In Parrondo's games, the act of choosing games, at random, forms an equivalent game that is a linear convex combination of the other, more basic games. This is a strictly linear process but the reward function that is applied to determine whether the games are *winning* and *losing* is non-linear, and the winning and losing regions of the parameter space are non-convex³. Viewed in this way it can be seen that paradoxes of the Parrondo type are possibly very common, and will be found in a number of different problem domains.

Parrondo's games are shown to have models of the form

$$p_{m+1,n} = \sum_{\forall v} p_{m,v} \cdot q_{v,n}. \quad (1.1)$$

which can be written using the standard notation of linear algebra:

$$\underline{p}_{m+1} = \underline{p}_m \cdot [\mathbf{q}]. \quad (1.2)$$

This is very concise, and has the same mathematical form as discrete-time state-space models for dynamical systems, including switched-mode electrical circuits. The consideration of random switching policies, in Parrondo's games, naturally leads to the consideration of random switching policies in other dynamical systems governed by equations with the same form, as Equation 1.2.

Parrondo's games exemplify interesting behaviour brought about by a switching process. This simple model inspires us to generalise this behaviour in the areas of stochastic control, and stochastic switching. This naturally leads to questions of random switching policies, in Markov systems and in electrical circuits.

³Any subset, \mathcal{M} , of real linear space, \mathcal{L} , is either convex or non-convex. A set, \mathcal{M} , is *convex* if, whenever it contains two points $x \in \mathcal{M}$ and $y \in \mathcal{M}$, it also contains all points in the finite line segment joining x and y . The convex set, \mathcal{M} must contain all points of the form $z = \gamma \cdot x + (1 - \gamma)y$ are in \mathcal{M} , where $\gamma \in \mathcal{R}$ and $0 \leq \gamma \leq 1$ (Kolmogorov and Fomin 1970). Sets that are not convex are called *non-convex*, rather than *concave*.

The limiting case, for a switched-mode electrical circuit, as the switching time becomes very small $\tau \rightarrow 0$ is examined. The state variable of the circuit seems to undergo a random walk that is reminiscent of Brownian motion. It is postulated that a more elegant way to analyse problems of this type would be to take the limiting case of a continuous-time stochastic process, which should include idealised Brownian motion, as a standard part of the model. Viewed from this point of view, fast switching is only one of many methods of introducing Gaussian white-noise into a circuit. The new method of analysis should be able to incorporate all possible sources of Gaussian white noise in the circuit and to formulate Stochastic Differential Equations that describe the time evolution of the circuit. This goal is achieved by applying the Stochastic Calculus of Itô to devise one consistent method for analysing all linear electrical circuits that include sources of Gaussian white noise.

The stochastic analysis of circuits is introduced. This includes models for resistors, capacitors and inductors. The method is tested by applying it to a couple of well known circuits, and comparing the results with the more orthodox result, obtained using Power Spectral Density. A functional mapping between electrical and mechanical systems is demonstrated and it is shown that the equations obtained by the new method are equivalent to the Langevin equations, from statistical mechanics. Finally some of the issues that arise from the noise model for a Junction Field Effect Transistor are discussed.

1.4 Original contributions

This thesis makes a number of important contributions to the application of models of the type used in Parrondo's games. Firstly in the development of the games themselves, and secondly in the application of these models to electrical circuits.

In Chapter 3 we establish the physical basis for Parrondo's games. This is based on our earlier work (Allison and Abbott 2002) where the results were published for the first time. These results were later followed up and verified in Toral *et al.* (2003b). This work places the work of earlier authors, including Harmer *et al.* (2000b) on a more rigorous basis. We establish conditions for realistic simulations of Brownian ratchets,

which we refer to as Parrondo's games with *natural diffusion*. This extends our earlier work in Amengual *et al.* (2004), where the results were established for the first time. We also show, for the first time, how to evaluate the moments of Parrondo's games using a discrete transform method. This can be carried out without explicitly solving the difference equations represented by Parrondo's games.

In Chapter 4 we establish a unified small-matrix technique for evaluating expected return from all sets of games in the same class as Parrondo's games. This extends our earlier work in Allison *et al.* (2005), where the method was developed for the first time. By construction, we establish that Parrondo's games still manifest their apparently paradoxical behaviour, even if self-transitions are included. We also examine the conditions for the minimum number of states and develop a set of games with only two states, which demonstrates the same paradoxical behaviour as Parrondo's games.

We reveal that fractals are generated in the phase-space for Parrondo's games, this extends our earlier work in Allison *et al.* (2005), where the result was published for the first time. These results were later independently confirmed by Behrends (2006). We devise methods for evaluating all the moments of fractals, including second and higher moments. These results appear to be new to the literature. They extend the work of Barnsley (1988).

In Chapter 5, the concepts embodied in Parrondo's games are applied to electrical circuits. We extend our earlier work in Allison and Abbott (2001), where we showed, for the first time, that a form of Parrondo's paradox exists for electronic circuits.

In this chapter we also extended the methods of Middlebrook and Čuk (1976) and use stochastic differential equations (SDEs) to model switching noise in switched-mode circuits, in the case where there is a random aspect in the switching rule. This result appears to be new to the literature. We show fractals exist in the phase spaces of switched mode circuits, where there is a random, or stochastic, aspect in the switching rule. It then becomes possible to use the methods developed in Chapter 4, to evaluate the mean values and variances of state variables.

In Chapter 6, we develop methods to model electrical circuits using stochastic differential equations (SDEs). In order to make these rigorous, we also develop new differential forms for Kirchhoff's laws and for the device laws. This chapter extends our earlier work in Allison and Abbott (2005), where the results were established for the first time.

1.5 Chapter summary

In this introductory chapter we have introduced the concept of a Brownian motor, as a motivation for the consideration of discrete models of transport processes, such as Parrondo's games. We provide an overview of the thesis and a statement of original contributions.

Chapter 2

Background for Parrondo's games

THE historical background and important features of Brownian motion, Maxwell's demon, the ratchet and pawl machine and flashing ratchets, are presented and discussed. We describe the physical construction of a flashing Brownian ratchet and cite some successful artificially-constructed Brownian ratchets. We provide an overall historical time-line for the subject and give an outline of the motivations for using discrete games of chance as models for stochastic transport processes.

2.1 Brownian motion

Feynman *et al.* (1963) begin their famous series of books with a statement that the most important fact that we need to know about the physical world is that it is made out of atoms. This is now the standard paradigm for chemistry, but this truth was not always universally acknowledged. The history of the atomic theory of matter is interesting.

There are ancient sources that refer to atoms. Democritus, Lucretius and Epicurus all expounded theories regarding atoms. The first modern European reference to atoms appears to be by Gassendi (1649), who cites Epicurus. Gassendi lived from 1592 to 1655, and after his death, number of other scientists write about atoms, including Boyle (1627–1691), Newton (1642–1727) and Lémery (1645–1715). Boyle (1661) refers to the ancient sources and explicitly discusses the *particles* and *corpuscles* of matter that have shapes and properties and are immutable. Newton (1704) was an active chemist and personally carried out a great number of chemical and alchemical experiments. He writes at length about particles of matter in his book on optics (Newton 1704), Book Three, Part I, Quest. 31:

Have not the small Particles of Bodies certain Powers, Virtues, or Forces, by which they act at a distance, not only upon the Rays of Light for reflecting, refracting, and inflecting them, but also upon one another for producing a great part of the Phænomena of Nature?"

Certainly the particle view of matter was common, as early as, Newton (1704), but was not necessarily the majority view until Dalton (1808) was able to present the case for atoms, based on evidence from quantitative experiments in chemistry and physics. Specifically, Dalton refers to the gas laws (Boyle's law, Gay-Lussac's law, Charles' law and Dalton's law of partial pressures). He also refers to the fact that in quantitative chemical experiments, the reagents of binary chemical reactions always combine in fixed proportions. After Dalton, there is a period of about a hundred years where the issue is vigorously debated, but the atomic view seems to be the majority opinion, amongst scholars. The atomic view of matter was not universal though. We should not forget that Boltzmann had to endure criticism of his theories in his own lifetime (Bryan 1906). The debate is completed with the theoretical contributions of

Einstein (1905), the practical observations of Perrin (1909)⁴, and the complete victory of the atomic view of matter.

One difficulty with the acceptance of the atomic view of matter is that atoms are so small. It is difficult to observe them directly. One measure of scale is given by Avogadro's number \mathcal{N}_A , being the number of atoms, in 12 grams of Carbon 12. Maxwell (1888) obtained a value of $\mathcal{N}_A = 4.1 \times 10^{23}$. Perrin (1909) obtained a value of $\mathcal{N}_A = 7.15 \times 10^{23}$. The currently accepted value of Avogadro's number is $\mathcal{N}_A = 6.0221367(36) \times 10^{23}$. The correct value of the exponent has been known since the time of Maxwell and Boltzmann. Avogadro's number is a *very* large number, in human terms. Most people cannot visualise a number as large as 10^{23} , and cannot form a distinct mental picture of the difference between 10^{23} and 10^{22} or 10^{24} . Any physical object that is large enough to be seen by a human being, without the aid of instruments, will contain an enormous number of atoms.

The numbers are so large that it that it is quite infeasible to track the course of each and every particle, in most physical systems. Statistical methods have to be used. This was understood and stated by Laplace (1814), Maxwell (1888) and Gibbs (1902), and is clear in the thinking of Boltzmann and his students, who pointed out the statistical nature of the laws of thermodynamics (Bryan 1906). An important aspect of *statistical* laws, as opposed to *deterministic* laws, is that measurements will not always yield the same result. If we consider the equation of state for an ideal gas, $pV = NkT$, as an example. This law will not always hold exactly. There will always be fluctuations about the mean values. Any attempt to measure the pressure, p , or the temperature T , will be subject to fluctuations. These are not due to experimental error they are fundamental aspects of the quantities being measured. These fluctuations lead to some difficult problems. Maxwell is clearly aware that a world composed of atoms would appear to be very different to a sentient being who could perceive individual atoms. Without the aid of instruments, human beings, can only perceive the bulk average properties of matter, but it would be possible, in principle, for a sentient being to track the paths of some individual molecules, given the right instruments. This leads to an interesting philosophical problem.

⁴This work appears in English, translated by F. Soddy, as Perrin (1910).

2.2 Maxwell's demon

In his book about the theory of heat, Maxwell (1888) proposes a thought experiment that still concerns scientists today: *“if we conceive of a being whose faculties are so sharpened that he can follow every molecule in its course, such a being, whose attributes are as essentially finite as our own, would be able to do what is impossible to us. For we have seen that molecules in a vessel full of air at uniform temperature are moving with velocities by no means uniform, though the mean velocity of any great number of them, arbitrarily selected, is almost exactly uniform. Now let us suppose that such a vessel is divided into two portions, A and B, by a division in which there is a small hole, and that a being, who can see the individual molecules, opens and closes this hole, so as to allow only the swifter molecules to pass from A to B, and only the slower molecules to pass from B to A. He will thus, without expenditure of work, raise the temperature of B and lower that of A, in contradiction to the second law of thermodynamics.”* This thought-experiment is shown in Figure 2.1.

Maxwell's *being* was christened as *Maxwell's demon* by Lord Kelvin. Smoluchowski (1912) points out that the door-mechanism and the demon are also subject to bombardment from the surrounding molecules. This means that they will also be subject to Brownian motion and will not be able to operate reliably. This means that the demon will not be able to reliably carry out the operations required to violate the second law of thermodynamics.

Szilard (1929) adds a new point of view to the discussion. He points out that the demon is acting on detailed information that he has collected about the motion of the particles of the gas. He establishes that there is a fundamental relationship between the information collected by the demon and the reduction of entropy⁵ caused by the demon's activities. The second law of thermodynamics requires that the total entropy

⁵Entropy, S , is a term proposed by Clausius in 1868. It is an extensive state variable of a thermodynamic system. It is an exact differential. Clausius' original expression was $dS = dQ_{\text{rev}}/T$, where dQ_{rev} is the heat that is exchanged reversibly into a system and T is the temperature. The more modern definition, following Gibbs and Boltzmann is that entropy is the logarithm of the number of micro-states in a macro-state. This leads to Boltzmann's famous equation $S = k \times \log \Omega$, where k is Boltzmann's constant and Ω is the probability of a micro-state, given a certain macro-state. This approach ultimately leads to the work of Nyquist and Shannon regarding information. The quantity $-S$ is called *negative entropy* or *negentropy*. Szilard's result is that the negentropy generated by the demon is equal or less than the information collected by the demon.

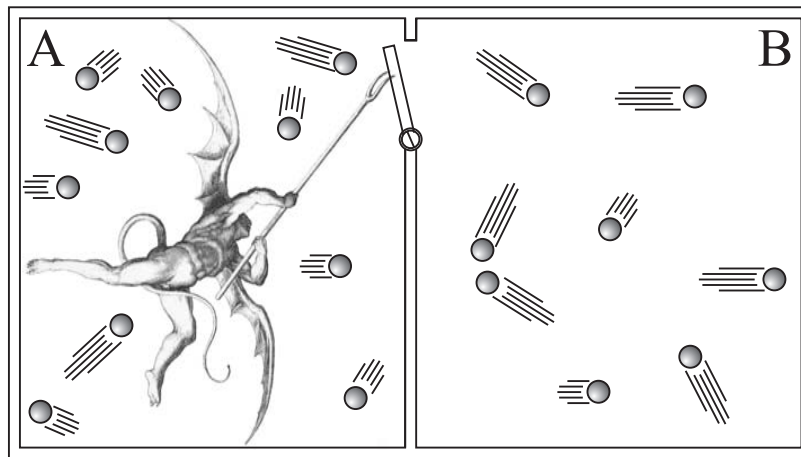


Figure 2.1. Maxwell's demon. This figure is an artist's impression of Maxwell's being with sharpened faculties. He can follow every molecule in its course and allows the fast molecules to pass from region "A" on the left to region "B" in the right. In principle the door can be opened and closed without net expenditure of work. After a period of time the being will, without expenditure of work, raise the temperature of region B and lower that of region A. This is in apparent contradiction to the second law of thermodynamics. Maxwell considered this to be a limitation of the range of applicability of the second law of thermodynamics, which is only statistical in nature and may not apply to each and every molecule in a large mass of matter. Maxwell correctly perceived that the difference between the imaginary being and us is due to a state of information. The being is presumed to be able to collect information about the trajectories of the individual molecules, whereas we cannot. This approach to the problem, based on information, was carried further by Szilard (1929) and Brillouin (1956). It is also important to note that the demon is enclosed within the system and will be subject to collisions with the molecules, which will interfere with his attempt to undermine the laws of thermodynamics. The demon cannot remain at a different temperature than his surroundings, without the expenditure of energy. This is Smoluchowski's argument.

of a closed system cannot diminish, $\frac{dS}{dT} \geq 0$. The apparent reduction of entropy in regions A and B, dS , is balanced by the need, of the demon, to obtain a certain amount of information, dI , which must be paid for by an increase in entropy within the demon and his surroundings, dS_d . This means that the total change in entropy, $d(S + S_d) \geq 0$, even if $dS < 0$.

Brillouin (1956) argues that the demon will not actually be able to *see* the individual atoms, because at thermal equilibrium he will be immersed inside a black-body and

2.3 The ratchet and pawl machine

will only see black-body thermal-radiation in all directions. The demon cannot *see* the molecules in order to operate the door at the right times. If the demon is equipped with some other apparatus, such as a torch, then this will consume energy, which is shared amongst the molecules of region A, which will, in turn, generate more entropy than the reduction that is generated by the demon's other activities.

A final and important stage in the study of Maxwell's demon results from the work of Landauer (1961), who argued that *“Computing machines inevitably involve devices which perform logical functions that do not have a single-valued inverse. This logical irreversibility is associated with physical irreversibility and requires a minimal heat generation, per machine cycle, typically of the order of kT for each irreversible function.”* This means that if the demon collects information, about the trajectories of particles, then he must collect and carry out computations in order to make a decision, as to whether the door should be opened or not. This computation is associated with a minimum energy cost. The work of Bennett (1982) established that the irreducible cost for the demon is not in opening and closing the door, nor in deciding whether to open and close the door. The irreducible cost lies in restoring the demon's computational machinery to a default state, before performing the next computation.

2.3 The ratchet and pawl machine

Gabriel Lippmann discussed a ratchet and pawl device, shown in Figure 2.2, as early as 1900 (Smoluchowski 1912). The basic idea is that the vanes (labelled “V”) in the heat-bath on the right, at temperature T_1 , are agitated by numerous collisions with molecules in the bath. If the vanes are not constrained then they undergo a rotational form of Brownian motion. The ratchet mechanism consists of a ratchet wheel (marked “R”), a pawl (marked “P”), and a spring and damper mechanism (marked “S”). The ratchet provides a constraint that allows rotation in one direction and not the other. In principle, this motion may be used to raise the weight (marked “W”) and hence to perform mechanical work. Naïvely, it seems possible to use the ratchet to cool down the heat bath, T_1 and to perform mechanical work on the weight, W , but Smoluchowski (1912) correctly argued that at thermal equilibrium, with ($T_1 = T_2$), it is impossible for the machine to perform work.

The general aim of this thought experiment is to investigate whether, or not, a micro-mechanical version of Maxwell's demon could be constructed in order to harness the thermal Brownian fluctuations of gas molecules, by a process of rectification. If such a device could be constructed, for $T_1 = T_2$, then it would violate the second law of thermodynamics and it would be a perpetual motion machine of the second kind.

Marian von Smoluchowski, who had worked with Gabriel Lippmann in 1896, discussed the ratchet and pawl device (Smoluchowski 1912). This machine was also discussed by Feynman *et al.* (1963), who added the refinement that the ratchet and pawl mechanism and the vanes can be visualised as being immersed in different heat baths, at different temperatures. The vanes are at temperature T_1 and the ratchet mechanism is kept at temperature T_2 . The essential scenario painted by Smoluchowski and Feynman is that when the pawl, P, responds to the impulse from the ratchet wheel, R, it acquires some energy. If this energy is not dissipated then the pawl will vibrate and bounce and will not be able to perform the necessary locking function. This means that it cannot prevent rotations in the wrong direction unless pawl is damped and cooled in the second heat bath at temperature T_2 . Feynman *et al.* (1963) state that the mechanism does not produce the required motion unless $T_2 < T_1$, in which case the ratchet and pawl machine is just a heat engine, and Maxwell's demon is exorcised, when $T_1 = T_2$. Of course, if we wanted to build a microscopic heat engine then it might be sensible to build a machine like the ratchet in Figure 2.2, but we would have to provide energy to maintain $T_2 < T_1$. This is essentially the same issue as erasing the mental state of Maxwell's demon, as discussed by Bennett (1982). A heat engine that uses energy to reset a selection mechanism, like the pawl, is a Brownian motor.

Parrondo (1996a) states that there are errors in the analysis in Feynman *et al.* (1963). Parrondo argues that Feynman incorrectly invokes the quasi-static assumption, resulting in an incorrect expression for the engine efficiency. The efficiency issue does not affect the question of detailed balance, that is whether the motor can have net rotation in the required direction when $T_2 = T_1$. Abbott *et al.* (2000) have mathematically shown that will work as a motor when $T_1 > T_2$, and that the ratchet will work as a motor in reverse when $T_1 < T_2$, and that no net motion will occur when $T_1 = T_2$. This establishes that the ratchet and pawl machine is only a heat engine, and conforms to

2.4 Flashing ratchets

NOTE:

This figure is included on page 18 of the print copy of the thesis held in the University of Adelaide Library.

Figure 2.2. The ratchet and pawl machine. The machine consists of vanes, V , a ratchet wheel, R , and a weight, W , all connected to a common axle. The pawl mechanism, P , is connected to a spring and damper, S , which should only allow movement in one direction. Any movement in this direction should lift the weight, W , and perform mechanical work. The energy-cost of this work has to be paid for by a reduction in the mean energy of the molecules in the heat bath, T_1 . This should cause T_1 to reduce. At first sight this appears to be a perpetual motion of the second kind, which violates the second law of thermodynamics. Closer analysis reveals that the ratchet and pawl machine is a heat engine and that it can only operate as required if $T_2 < T_1$ (Feynman *et al.* 1963). This figure is reproduced, with permission, from Harmer (2001).

the laws of thermodynamics.

2.4 Flashing ratchets

Another important line of development, that intersects with the ideas of Brownian ratchets and Maxwell's demon, is the idea of the *molecular motor*. The earliest major development, is the identification of the roles of actin, myosin and adenosine-triphosphate in movement in muscles (Guba and Györgyi 1946)⁶. It becomes clear that stored energy in the form of chemicals can be transduced into mechanical work and that this is a normal part of animal physiology. The molecules of myosin and adenosine-triphosphate are rather like molecular machines and the molecule adenosine-triphosphate is like fuel. This metaphor is developed further and the term *molecular*

⁶A. Szent Györgyi won the Nobel Prize in Medicine and Physiology in 1937.

motor appears literature, in the late 1980s (Warrick and Spudich 1987). Simon *et al.* (1992) propose a mechanism for driving the trans-location of proteins and the term *Brownian ratchet* is used. Quite detailed analyses of the structures and mechanics of molecular motors are later carried out by Bier (1997) and by Astumian and Derényi (1998). Molecular motors and pumps can be driven by molecular fluctuations, as long as energy is provided, from an external source⁷. The details of very large molecules, like proteins, are complicated and this is still an area of active research.

Ajdari and Prost (1992) and Magnasco (1993) are generally considered to have proposed the idea of a Brownian ratchet, as a method of performing chemical separation, similar to electrophoresis (Seader and Henley 2006). Further early analysis of Brownian ratchets was carried out by Doering (1995). The Brownian Ratchet idea was influential, and motivated Parrondo (1996b) to formulate discrete games of chance, to model the essential features of Brownian ratchets.

The interaction between fluctuating potentials and Brownian motion are important factors in Brownian ratchets and in molecular motors and the term *Brownian motor* is coined. The mechanism described here is for a flashing Brownian ratchet, although some of these principles are applicable to molecular motors and to Brownian motors.

The basic operation of a flashing ratchet is shown in Figure 2.3. When the field is turned on, the particles accumulate at positions of lowest electric potential. The distribution will approach a time-invariant equilibrium. This is shown at position “d” in part (ii) of the figure. When the field is turned off, the distribution will approach a different time-invariant equilibrium. This is shown at position “e” in part (iii) of the figure. If the field were left off for long enough the distribution of particles would reach a state of maximum entropy, a flat uniform distribution. This is the relevant time-invariant equilibrium when the field is off.

We consider the probability density of a charged Brownian particle near the reference plane (b) in the ratchet. While the field is turned off the distribution, shown at position “d” relaxes and spreads out to form a broader distribution at position “e”. The resulting flux across reference plane (a) is J_1 and the resulting flux across reference plane (c) is J_2 . The bulk of the distribution is near reference plane (b), which is closer to reference

⁷Typically this energy is provided in chemical form, such as Adenosine-Tri-Phosphate (ATP).

2.4 Flashing ratchets

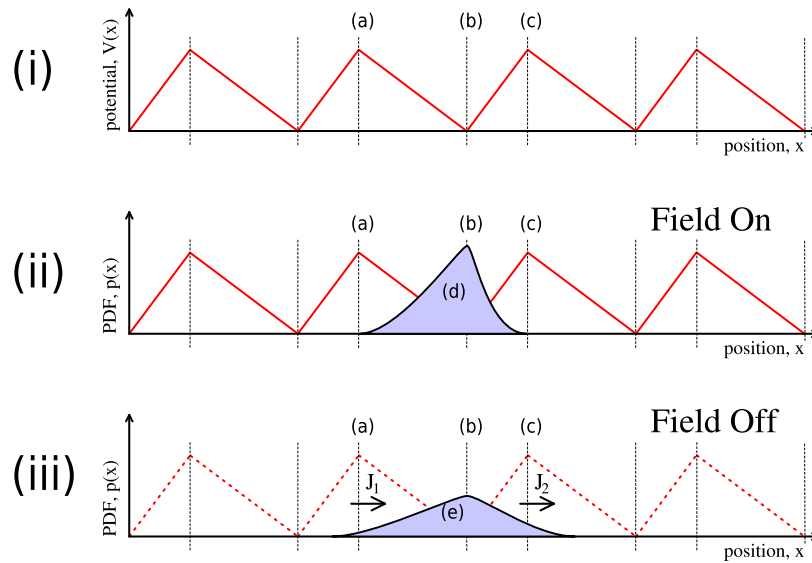


Figure 2.3. The flashing ratchet. This figure shows the flashing ratchet, as proposed by Ajdari and Prost (1992). Part (i) shows the electric field, as a function of position. This field can be turned on and off, or *flashed* as required. Part (ii) shows the distribution of mobile charged particles if the field is turned on. The distribution will approach a time-invariant equilibrium, if the field is kept on for long enough. Part (iii) shows what happens to the distribution of the particles when the field is turned off, for a short time. Please note that there is a net drift of particles to the right. When the sloped edges are turned on, they impart energy to the particles. There is a net movement to the right, simply because the longer slope on the right has a greater capture cross-section, and thus ‘wins’ over the shorter slope.

plane (c) than it is to reference plane (a). It is intuitively plausible that the resulting flux across reference plane (c) will be larger than the flux across reference plane (a). We expect $J_2 - J_1 > 0$. The net flow should be positive. More accurate analysis, based on the Fokker-Planck equation shows that this is correct. The result of flashing the ratchet is that the Brownian particles will move more frequently to the right than to the left. This gives rise to a net flow or transport effect. This effect depends on the charge and mobility of the particles and can be used for chemical separation.

Possible physical construction

The structure described here is loosely based on an actual device built and tested by Bader *et al.* (1999). Many other structures are possible but this particular one maps

neatly onto the mathematical structure required for a flashing ratchet of the type described by Doering (1995).

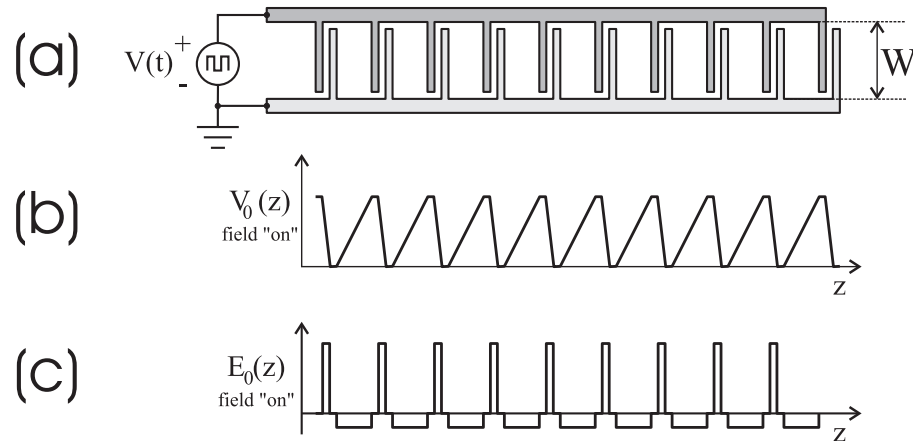


Figure 2.4. Top view of an inter-digital flashing ratchet. Part (a) shows comb-shaped electrodes connected to a voltage source that can be turned on or off according to any desired pattern, in time. Part (b) shows the electric potential, or voltage, $V_0(z)$, generated by the ratchet when it is turned on, as a function of position, z . Part (c) shows the electric field, $E_0(z)$ generated by the ratchet when it is turned on, as a function of position, z . For the quasi-static case E_0 and V_0 are related by $E_0 = -\nabla V_0$. Please note that the electric field, $E_0(z)$, is sometimes positive (when the voltage is rapidly sloping downwards) and sometimes negative (when the voltage is more gradually sloping upwards). Sometimes the electric field is more or less zero (in the spaces where the voltage is constant). For a real ratchet with finite depth, there will be fringing effects and the profiles of the fields may not be quite as described, with straight lines and sharp corners. There would be some rounding of the curves. This figure does give a reasonable view of the effect of the field though, which will be asymmetrical. The lack of spatial symmetry is important.

In most analyses of Brownian ratchets, only a single charged particle is considered, an otherwise neutral medium. This is not always very realistic. The effectiveness of the transport process depends strongly on how we model the effect of ion to ion interactions. At high local ion concentrations the effect of the crowding of charge is significant. It is necessary to include this effect in the models. If we are interested in average ion currents then we can replace the complicated many-body problem with a time-average mean-field for the distribution of charge. It is necessary to make use of Poisson's equation. To date, most analyses of artificial, human-made, ratchets require us to neglect the effect of distributed charge. This means that the standard analysis is only strictly

2.5 Constructed Brownian ratchets

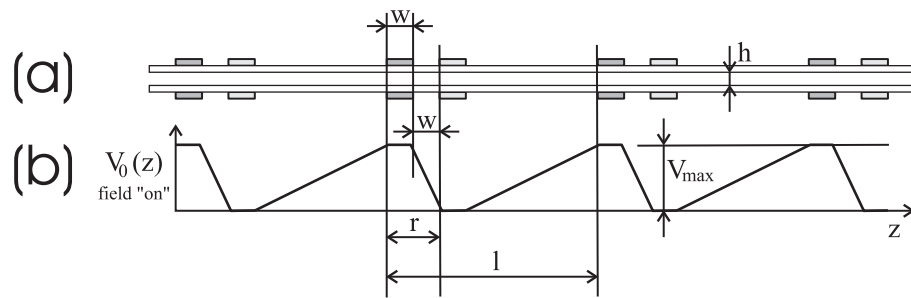


Figure 2.5. Side view of an inter-digital flashing ratchet. Part (a) shows a side view of the ratchet. For more symmetrical fields it would be desirable to place electrodes above and below the channel containing the Brownian particles. Ideally the channel should be very shallow. The depth h should be as small as the manufacturing process would allow. Ideally the electrodes should be isolated from the fluids in the channel. Otherwise it would be possible for electrolysis to occur. At the very least, the electrodes could be subjected to corrosion and the resulting chemical changes could affect the contents of the channel. For any given MEMS fabrication process there will be a minimum feature size, w . For maximum ratchet effect the electrodes, shown, should be minimal width with minimum separation. The length between pairs of teeth, l , is the spatial period of the ratchet. In general this will be larger than the minimum feature size, w . This asymmetry is important. Part (b) shows the resulting electric field, $V_0(z)$, generated by the ratchet when it is turned on, as a function of position, z . For the one dimensional ratchet we can write down the approximate value for the electric field as $E_0 \approx -\Delta V/\Delta z$.

valid for dilute solutions.

There is some evidence, from simulations (Allison and Abbott 2003a), that the presence of oppositely charged mobile ions in the channel, reduces the ability of the ratchet to transport ions, of either charge. This should not be too surprising since the ratchet will have to carry out work in order to separate the oppositely charged ions from each other, even if that work is recovered later when the ions recombine with other oppositely charged ions. To date, this area is still relatively undeveloped.

2.5 Constructed Brownian ratchets

Faucheux *et al.* (1995) constructed a physical device, using optical tweezers to modulate the potential around a single Brownian particle. Since then a number of other

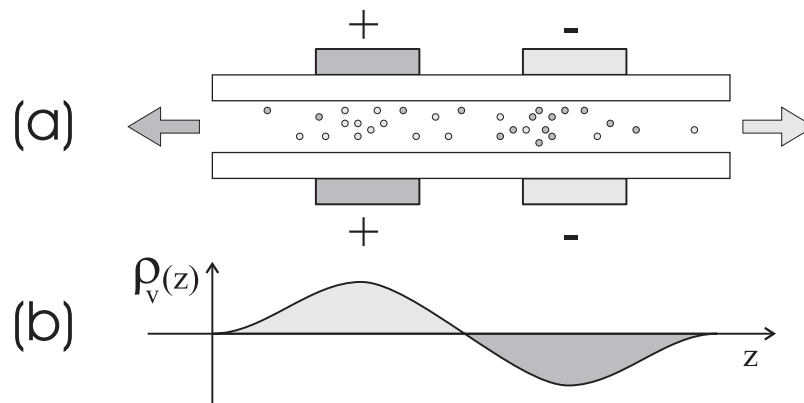


Figure 2.6. Charge separation in a Brownian ratchet. The positive and negative ions are shown with vastly exaggerated scale. They will congregate near the electrodes of opposite charge. This gives rise to the crowding of charge in a distributed fashion through space. The presence of the crowded charge gives rise to an electric field that will counteract the effect of the field from the electrodes. If the device were turned on long enough for the charges to reach equilibrium positions then no further flow would occur. The Brownian particles would experience no electric field and would undergo normal Brownian motion. The ratchet can still operate, however, away from equilibrium.

physical devices have been constructed, including (Slater *et al.* 1997, Ertas 1998, Duke and Austin 1998, Bader *et al.* 1999). The work of Bader *et al.* (1999) is particularly interesting, in that it realised the ideas of Ajdari and Prost (1992) and Magnasco (1993) by achieving chemical separations of large molecules. The geometry of their device had the general form, shown in Figure 2.4.

The brief history and overview presented, up to this point, concentrates on systems that can be modelled using continuous functions, on scales that are large, compared with molecules or carriers. The bulk of this thesis deals with discrete models of continuous systems. The use of discrete models has its own history, which we now summarise.

2.6 A brief history of finite discrete games of chance

The subject, stochastic transport, has a history that can be traced back for over ninety years. It is clear that many people made important contributions, and there are many

2.6 A brief history of finite discrete games of chance

different lines of thought. There is not enough space to cover them all here. We concentrate mainly on the ideas that lead to discrete games of chance as models for stochastic processes. We present a brief summary as follows:

- 1905** Einstein (1905) proposes the use of Brownian motion to estimate Avogadro's number and verify some predictions of the atomic theory of matter.
- 1905** Pearson (1905) invents the term *random walk* and applies it to the problem of mosquito population. Lord Rayleigh solves the problem within a week (Pearson 1905).
- 1909** Perrin (1909) verifies Einstein's results and establishes a more accurate estimate for Avogadro's number.
- 1916** Smoluchowski (1916) uses discrete time and discrete space to model Brownian motion of a single particle. The concept of the *random walk* is used to solve problems in physics.
- 1946** Guba and Györgyi (1946) establish the roles of actin, myosin and adenosine-triphosphate in movement in muscles. This is an important step along the path to the development of molecular motors.
- 1956** King and Altman (1956) use structures that are equivalent to Markov chains, with discrete states and continuous time, to devise a schematic method for deriving the rate laws for enzyme-catalysed reactions.
- 1977** Hill (1977) extends (King and Altman 1956), and uses the techniques to investigate free energy transduction and biochemical cycle kinetics.
- 1986** Westerhoff *et al.* (1986) show that enzymes can capture and transmit free energy from an oscillating electric field. Their model follows King and Altman (1956) and uses discrete states, and continuous time. Reaction rates, rather than probabilities of transition, are used and a game setting is *not* explicitly used.
- 1992** Simon *et al.* (1992) propose a mechanism for driving the trans-location of proteins. The phrase *Brownian ratchet* is used.
- 1992** Ajdari and Prost (1992) propose the flashing ratchet mechanism.
- 1996** Reimann *et al.* (1996) analyse molecular motors, driven by temperature oscillations. The phrase *Brownian motor* is used.

- 1996** Parrondo (1996b) proposes games that are intended to provide a simple model for a Brownian ratchet. A *game* setting is explicitly used. The model uses discrete time and discrete space. Harmer *et al.* (2000a) refer to these games as *Parrondo's games*.
- 2001** Astumian (2001) publishes a set of games, which translate the essential features of the model used in Westerhoff *et al.* (1986) and in Astumian *et al.* (1987) into a discrete time and discrete space model. A game setting is explicitly used. The system has five states. These games have become known as *Astumian's games* (Piotrowski and Sladkowski 2004).
- 2002** Allison and Abbott (2002) show an explicit mapping between Brownian ratchets and Parrondo's games. This mapping is independently confirmed by Toral *et al.* (2003b). These two approaches are brought together and systematised by Amengual *et al.* (2004).
- 2004** Astumian (2004) points out that Parrondo's original games do not include self-transitions. He also makes the mapping between the model of Westerhoff *et al.* (1986) and the model of Astumian (2001) explicit.
- 2005** Amengual *et al.* (2004) publish a generalised version of Parrondo's games, which includes self-transitions. This game only has three states.
- 2009** Ethier and Lee (2009) establish formulae for the mean rate of return, and variance, of nearly all scenarios of the Parrondo type, using an approach based on the Central Limit Theorem (CLT).

It could be argued that Smoluchowski (1916) carried out the first use of discrete games of chance to the model stochastic processes in physical chemistry. In one sense the technique is very old. What makes this technique very useful today, is that we have the advantage of many other developments that have occurred since the technique was invented. We have much more powerful computers and we have access to efficient numerical methods that make the best use of the available computing power. Discrete games of chance are naturally suited to solution on digital computers. It is our belief that is an old tool that will find new life in the years ahead.

2.7 Chapter summary

In this chapter we have described the background and context for Parrondo's games. We begin with a consideration of Brownian motion, Maxwell's demon and the ratchet and pawl machine. This then leads on to a consideration of flashing ratchets and the possible physical construction, of a flashing ratchet. We discuss some physical Brownian ratchets that have been constructed, and tested. Finally, we give a brief history of finite discrete games of chance, and how this relates to the thesis. In the next chapter we establish the relationship between Brownian ratchets and Parrondo's games with more rigour.

Chapter 3

The physical basis of Parrondo's games

THIS chapter contains detailed material regarding two groups of transformation that have proved to be useful in the study of Brownian ratchets and Parrondo's games. One group of transformations is the use of finite differences, which has a long tradition that can be traced back to Newton and Gregory. The other group transformations is made up from integral transformations, including those of Fourier and Laplace. We accept the result from Kolmogorov (1931), that the dynamics of a Brownian particle can be represented using a Partial Differential Equation (PDE) called the Fokker-Planck Equation. The use of finite differences allows us to transform the PDE into a system of finite-difference equations, which have the same form as the equations for Parrondo's games. This places Parrondo's games on a sound physical basis.

We do not have to solve the resulting equations directly, though. If our main interest is to calculate moments, such as rates of flow, then we can use transform techniques to solve directly for the z -transform of the solutions. We show that it is possible to estimate the moments of Parrondo's games by working directly with gradients of the z -transforms of the solutions. Parrondo's games are multiplexed in space and we investigate the effect of multiplexing on the z -transforms, and devise formulae to evaluate the moments of multiplexed functions. Finally we examine the effect of randomised or periodic sequences of Parrondo's games.

3.1 Discrete transformations of continuous functions

We seek a method to model the behaviour of a one-dimensional Brownian ratchet. Several physical devices have been constructed, and have worked and are described in the literature, including work by Faucheux *et al.* (1995), Slater *et al.* (1997), Ertas (1998), Duke and Austin (1998) and Bader *et al.* (1999). The performance has been compared against fairly simplified theories. In the analysis by Bader *et al.* (1999), for example, it is assumed that the *off* time of the ratchet is small, in the sense that a Brownian particle will typically only diffuse at most from one tooth of the ratchet to the next in that time. Some of the other approximations assume that the *off* time is large in that sense. We seek a method of simulation, which could be useful in the design, and optimisation, of flashing Brownian ratchets for a wide range of different possible parameter values, under a uniform set of assumptions. The two obvious practical effects that need to be modelled are the transport effect, where particles are transported through the device, and a spreading or deviation⁸ effect, where identical particles travel through the device at different speeds. Any useful method of simulation should be able to model transport and deviation over a wide range of different possible parameter values.

Sampling of smooth functions of space and time

The behaviour of Brownian motors and Brownian ratchets can be accurately described in terms of a partial differential equation called the Fokker-Planck equation (Gardiner 1983, Risken 1996). This takes the form:

$$\frac{\partial}{\partial x} \left(D^{(2)}(t, x) \cdot \frac{\partial}{\partial x} p(t, x) \right) - \frac{\partial}{\partial x} \left(D^{(1)}(t, x) \cdot p(t, x) \right) - \frac{\partial}{\partial t} p(t, x) = 0. \quad (3.1)$$

The formulation of this equation is given in Risken (1996). One important approach to the derivation, is to assume that the process is Markov and to begin with the Chapman-Kolmogorov equations. The conditional density function can be approximated using a Taylor expansion (in space) and the result can be integrated (in time) to yield the Kramers-Moyal expansion. This is the approach devised by Einstein (1905). It has been summarised in Wang and Uhlenbeck (1945) and also in Reif (1965), Pauli (1973)

⁸Reif (1965) refers to mean square displacement, due to diffusion, as *dispersion*. We prefer the term *deviation* to refer to the amount of spread that can occur due to a physical process, such as *diffusion*.

3.1 Discrete transformations of continuous functions

and Risken (1996). In the case of a linear diffusion law (Fick's law) and Gaussian conditional density function, the Kramers-Moyal expansion only requires spatial differentiation to the second degree. The Kramers-Moyal reduces to the Fokker-Planck Equation 3.1. The solution to this equation will be a real function of two real variables, $p(t, x)$. If we were to attempt to solve these equations numerically on a computer, without some form of approximation, then the amount of information to be stored and processed would be infinite, which is clearly not feasible. We must accept some degree of approximation in order to make progress. The aim is to make an initial approximation, which leads to some error, and then to take precautions to guarantee that the error is within acceptable limits. The approach used here is to sample the partial differential equation and to re-formulate the time-evolution of a system in terms of discrete partial difference equations. This approach has been widely used to solve diffusive transport problems since the early work of von Neumann. It is still a standard approach for solving parabolic partial differential equations (Press *et al.* 1995, Iserles 1996, Scheisser and Silebi 1997, Korn and Korn 2000, Chapra 2006). The main alternative approaches are solution by spectral methods (Trefethen 2000) and solution by the finite element methods (Buchanan 1995, Iserles 1996, Chapra 2006). Trefethen (2000) points out that the finite difference approach is not the most computationally efficient method. On the other hand, it is simple to visualise and to formulate. It has a long history. It is well understood and, as we shall see, leads directly to Parrondo's games.

A description of the important variables and operators

The names and purposes of the most important variables for this section are summarised in Table 3.1. There are two types of transformation to be discussed: transformation from continuous time and space, t and x , to discrete time and space, m and n , and the further transformation to generating functions, in terms of z and w .

In order to calculate finite differences, the function, $p(t, x)$, must be sampled and the simplest method for sampling a continuous function is to collocate the sampled points with the underlying physical function, at certain specified points:

$$p_{m,n} = p(m\tau, n\lambda). \quad (3.2)$$

The main issue arising from this approach is how to account for variations in $p(t, x)$ in between the sampling points. This is related to the problems of approximation and

Physical Concept	Time variable	Position variable
Natural variable	t	x
Frequency	$f = 1/t$	$\nu = 1/x$
Angular frequency	$\omega = 2\pi f$	$k = 2\pi\nu$
Laplace variable	$s = j\omega$	$r = jk$
Sampling interval	τ	λ
Sampled integer variable	$m = \text{floor}(t/\tau)$	$n = \text{floor}(x/\lambda)$
Translation operator	$z = e^{s\tau}$	$w = e^{r\lambda}$

Table 3.1. Notation for discrete transformation and associated calculations. The names and purposes of the most important variables needed for transformation. There are two important classes of independent variables, time-like and space-like.

interpolation. There is a very large literature regarding these topics (Atkinson 1985, Maron and Lopez 1990, Press *et al.* 1995, Chapra 2006). The usual approach is to assume that $p(t, x)$ is sufficiently smooth and that Taylor's theorem, with remainder, applies up to some finite order of differentiation. It is then possible to manipulate the finite Taylor series algebraically to obtain expressions for the degree of error involved in the sampling process. It is assumed that the sampling intervals, τ and λ , are small enough to allow the errors of sampling to be neglected. If this is not sufficiently accurate then it will be necessary to decrease the sampling intervals, τ and λ . In principle, it is always possible to improve accuracy by reducing the sampling intervals.

Choice of sampling method, operators and basis functions

Sampling at an exact point is equivalent to convolution with Dirac delta functions, as follows:

$$p_{m,n} = p(m\tau, n\lambda) = \int_{-\infty}^{+\infty} \int_{-\infty}^{+\infty} \delta(t - m\tau) \cdot \delta(x - n\lambda) \cdot p(t, x) dt dx. \quad (3.3)$$

In this case the inner kernel function for sampling is $\kappa(t, n, x, m) = \delta(t - n \cdot \tau) \cdot \delta(x - m \cdot \lambda)$. This particular choice of sampling kernel yields information about the value the function at the sampling points, but does not give us complete information about what happens in-between the sampling points. Our point estimates of $p(t, x)$ may be in error at points in-between the sampling points.

3.1 Discrete transformations of continuous functions

The situation becomes more complicated if there is the possibility of error, noise or round-off in the evaluation of $p(t, x)$. Various trade-offs between the different types of error are made possible by choosing a different kernel function. An early reference to this appears in Lanczos (1954), where he points out that numerical differentiation takes the form of integration with respect to a specially chosen kernel function. He notes that expressing the derivative in integral form could establish a derivative even at points where a derivative does not exist, in the ordinary sense. He points out that this would be true, even in the presence of noise. Lanczos' kernel functions were constructed by inverting Taylor's formula and making certain assumptions about the analytic nature of the function and the ability to neglect the effect of higher derivatives. No specific rules were offered for constructing an optimal kernel for any specific family of functions or any given level and distribution of noise. It should be noted that differentiation is equivalent to sampling a function at specified points, together with taking limits as finite differences approach zero. We could write, for example:

$$f'(x) = \lim_{\Delta X \rightarrow 0} \frac{f(x + \Delta X) - f(x - \Delta X)}{2\Delta X} \quad (3.4)$$

$$= \int_{-\infty}^{+\infty} \lim_{\Delta X \rightarrow 0} \left(\frac{1}{2\Delta X} \delta(x + \Delta X) + \frac{1}{2\Delta X} \delta(x - \Delta X) \right) \cdot f(x) dx. \quad (3.5)$$

In this case, the kernel function is a generalised function, or *distribution* in the sense defined by Soboleff and Schwartz (Zemanian 1965). Ideal sampling and ideal differentiation are singular functionals. More complicated operators, such as differentiation depend on the simpler operation of sampling.

Differentiation, multiple differentiation, and sampling can all be expressed in terms of integration with respect to a suitably chosen kernel function. They can all be expressed as integral functionals. Given this, it is possible to formulate the problems of sampling, differentiation, integration, and integral transformation within the framework of functional analysis (Simmons 1963, Zemanian 1965). Classes of possible solution functions, $p(t, x)$, are equivalent to multi-dimensional vectors in a topological space. The space can be defined to have inner-products and a metric. We can also consider possible solution functions, $p(t, x)$, as limits of sequences of sums of basis functions, Cauchy sequences. We could, if the situation required, choose those basis functions to be orthogonal or to be eigenfunctions or Green's functions of the underlying equations that we seek to solve or we could choose some other complete set of basis functions. If

we take the standpoint of functional analysis then variables of interest, such as the expected value of the flow (the first moment) or the variance (the central second moment) can also be expressed as integral functionals, which map functions in function space to real numbers. The overall aim of this approach is to reduce the problem of solving Ordinary Differential Equations (ODEs) and Partial Differential Equations (PDEs) to a generalised problem in linear algebra.

The purpose of integral transforms is to make the problem of the linear algebra simpler, because differential operators have a simpler representation in the transformed domain. One reason for using transforms of a discrete (sampled) functions is to reduce the amount of information to be processed and hopefully to make the problem tractable. The aim is to make the formulation of the problem reasonably accurate and yet simple enough to allow the idealised problem to be solved analytically. This is consistent with Richard Hamming's maxim that the aim of simulation is not just numbers but insight. The aim is to arrive at algebraic expressions, which show (at least approximately) how the solutions vary with the choice of parameters.

One important application of functional analysis is to approximate a function, such as the postulated solution to a differential equation, with a finite sum of basis functions. Under certain circumstances it is possible to reduce the difference between the unknown function and the approximation to arbitrarily small levels. This difference is based on the metric for the topological space. Accurate representation is generally possible if the space is constructed in such a way that it is *complete*, in the sense that all Cauchy sequences of functions in the space converge (Simmons 1963). It is generally possible to construct the space so that it includes all linear sums of a set of a set of basis functions. The Cauchy sequences are sequences of sums of basis functions. These sequences can be indefinitely long. There is a very large literature regarding the choice of basis functions and very common choices include the use of complex exponential functions (Bracewell 2000, Press *et al.* 1995), or orthogonal polynomials (Press *et al.* 1995, Maron and Lopez 1990), or even wavelets (Hubbard 1998). The choice of basis functions does affect whether the operators have simple representations or whether they appear to be complicated. Ideally, the operators and basis functions should be matched in order to make the resulting equations easy to manipulate. If we use finite differences then the sampling kernel functions are effectively delta functions

3.1 Discrete transformations of continuous functions

and the basis functions are polynomials, which are considered to be locally equivalent to the truncated Taylor series for the underlying function. This is a common and well accepted choice but it is only one of a great multitude of possible choices.

The idea that each sample may include contributions from more than a single idealised point suggests that we should use a kernel function of non-zero width, σ . A Gaussian function is a good example. We could choose a kernel function of $\kappa(x, \mu) = \exp(-(x - \mu)^2 / (2\sigma^2)) / (\sigma\sqrt{2\pi})$. This function has a mean square width of σ and is centred in space at a position $x = \mu$. We can write a formula for sampling the function $p(t, x)$ in the region near $x = \mu$:

$$p(t, \mu) \approx \int_{-\infty}^{+\infty} \frac{1}{\sigma\sqrt{2\pi}} e^{-\frac{(x-\mu)^2}{2\sigma^2}} \cdot p(t, x) dx. \quad (3.6)$$

The definition of the word “near” depends in the choice of σ . This type of sampling sacrifices some accuracy, regarding the value of the function at the point to be sampled, $x = \mu$, in order to make the result less sensitive to noise and to obtain information about the behaviour of the function $p(t, x)$ at points near the sampling point. This attitude to sampling has some aspects in common with wavelet theory (Hubbard 1998), where wavelet functions can be localised in space. The approach also has aspects in common with the idea of a *fuzzy set* here all points near the point to be sampled, $x = \mu$, share some degree of membership if the fuzzy set labelled μ . We could choose $\mu = n\lambda$ and regard the kernel $\kappa(x, n\lambda)$ as a membership function, which expresses the degree to which the number x belongs to the fuzzy set centred at the discrete spatial position labelled n . There are signal processing applications where Gaussian functions or other fuzzy-kernels have been used to good effect (Bezdek and Pal 1992).

In summary, we can represent the sampling of a function using a convolution:

$$p_{m,n} = \int_{-\infty}^{+\infty} \int_{-\infty}^{+\infty} \kappa(t, n, x, m) \cdot p(t, x) dt dx. \quad (3.7)$$

In general, the optimal choice of kernel function $\kappa(t, n, x, m)$ should allow a trade-off between errors due to noise and errors due to variation of the function between the sampling points. For the present discussion, it is assumed that $\kappa(t, n, x, m) = \delta(t - n\tau) \cdot \delta(x - m\lambda)$, which is optimal in the absence of errors due to noise of measurement, or round-off error. The underlying basis functions will be polynomials, which can be expanded locally around the sampling points, and can be related back to the

underlying function, $p(t, x)$, using Taylor's theorem.

Discrete transforms in time and in space

Equation 3.3 shows that the act of sampling a function, $p(t, x)$, to obtain discrete samples, $p_{m,n}$ is equivalent to an integral transform. More conventional integral transforms, such as the Laplace integral transformation, have the same general form:

$$\mathbb{F}(s) = \int_0^{+\infty} e^{-st} \cdot f(t) dt \quad (3.8)$$

where the kernel function is $\kappa(t, s) = e^{-st}$. The Laplace transform has been developed into a widely used and very practical tool for engineering and applied mathematics (Fodor 1965, Doetsch 1974, LePage 1980, Zemanian 1965, Kreyszig 2006). If we then take a Laplace transform of a sampled function, then we obtain a discrete version of the Laplace transform called the *z-transform*. This is the approach used by many authors (Jury 1964, Fodor 1965, Blackman 1975, LePage 1980), including Jury who is widely credited with development of the *z-transform*. We can write a one-sided *z-transform*, in time, in terms of a one-sided Laplace transform, in time, as follows:

$$\mathbb{F}(s) = \int_0^{+\infty} e^{-st} \left(\sum_{m=0}^{+\infty} \delta(t - m\tau) \cdot f(t) \right) dt, \quad (3.9)$$

which reduces to the sum of a series

$$\mathbb{F}(s) = \sum_{m=0}^{+\infty} (e^{+st})^{-m} \cdot f(m\tau) \quad (3.10)$$

$$= \sum_{m=0}^{+\infty} z^{-m} \cdot f_m, \quad (3.11)$$

which is a standard one-sided *z-transform* in time, where $z = e^{s\tau}$ and $f_m = f(m\tau)$. The equations for the shifting, and derivative, theorems for two-sided transforms do not include an explicit reference to the initial value of a function, in time (Bracewell 2000). In contrast, the same theorems for one-sided transforms do include explicit references to initial values (Ogata 1987, Kuo 1992, Proakis and Manolakis 1992, Ersoy 1997). This makes initial-value problems easier to formulate initial-value problems, using a *one-sided* transform.

The use of two-sided Laplace transforms leads to a two-sided *z-transform*, provided that the relevant integrals and sums converge absolutely. The *z-transform* is a widely

3.1 Discrete transformations of continuous functions

used and contemporary version of the older concept of the generating function (Knuth 1978, Papoulis 1991, Wackerley *et al.* 1996, Yates and Goodman 1999). Theorems, properties and tables of transform pairs appear in many engineering textbooks (Ogata 1987, Kuo 1992, Proakis and Manolakis 1992, Ersoy 1997). It is a well understood technique and the standard results are used when needed, without proof. Two forms of the z-transform are required. To process distributions in space, which are potentially unbounded, above and below, one needs to use a two sided transform. The two-sided spatial Laplace transform can be defined as:

$$\mathbb{F}(r) = \int_{-\infty}^{+\infty} e^{-rx} \cdot f(x) dx. \quad (3.12)$$

This leads to a two-sided discrete transform based on a spatial shift operator, $w = e^{r\lambda}$. The w -transform can be written as:

$$\mathbb{P}_m(w) = \mathbb{W}[p_{m,n}] = \sum_{n=-\infty}^{+\infty} w^{-n} p_{m,n}. \quad (3.13)$$

All the usual theorems of the two-sided z-transform also applies to the w-transform, if we perform a suitable change of variables.

In order to manipulate functions of time, with initial values at $t = 0$, it is more appropriate to use one sided z-transform in time, which is defined in terms of the temporal shift operator, $z = e^{s\tau}$, as follows:

$$\mathbb{P}(z)_n = \mathbb{Z}[p_{m,n}] = \sum_{m=0}^{+\infty} z^{-n} p_{m,n}. \quad (3.14)$$

Of course a dual transform, in space and time, is possible:

$$\mathbb{P}(z, w) = \mathbb{Z}[\mathbb{W}[p_{m,n}]] = \mathbb{W}[\mathbb{Z}[p_{m,n}]]. \quad (3.15)$$

The transforms commute as long as the sums converge absolutely, for some non-empty region of convergence. The effects of applying one or other, or both transforms are described in Table 3.2.

It is possible to distinguish the various types of function, in Table 3.2 by making a note of the types of arguments and subscripts. Some aspects of this notation should be stated explicitly. Certain symmetries have been used in constructing the notation in Table 3.2. Lower-case function names, such as p , refer to natural functions of time

time vs space	n	w
m	$p_{m,n}$	$\mathbb{P}_m(w)$
z	$\mathbb{P}(z)_n$	$\mathbb{P}(z, w)$

Table 3.2. Notation for transformed version of $p_{m,n}$. The same dependent variable, $p(t, x)$, appears differently in different domains. When it is sampled it appears as a discrete function of discrete time and space, $p_{m,n}$. With two different transforms, there are four different types of discrete transformed function, which are listed in the table. It is possible to distinguish which transforms have been applied by referring to the typeface, arguments and subscripts.

function identifier	semantic interpretation
$p(t, x)$	$p(t, x)$ is the probability density function, as a function of time, t , and space, x . It is a real function of real variables
$p_{m,n}$	$p_{m,n}$ is the discrete sampled probability mass function, of integer variables: discrete time, m , and discrete space, n . It is a real function of integer indices.
$\mathbb{P}_m(w)$	$p(t, x)$ has been transformed in space. Discrete space, n has been replaced with the spatial shift operator $w = e^{r\lambda}$. $\mathbb{P}_m(w)$ is a complex function of an integer index and a complex argument.
$\mathbb{P}(z)_n$	$p(t, x)$ has been transformed in time. Discrete time, m has been replaced with the temporal shift operator $z = e^{s\tau}$. $\mathbb{P}(z)_n$ is a complex function of a complex argument and an integer index.
$\mathbb{P}(z, w)$	$p(t, x)$ has been transformed in space and time. $\mathbb{P}(z, w)$ is a complex function of two complex arguments.

Table 3.3. Semantic interpretations of variously transformed versions of $p_{m,n}$. The symbol p can be overloaded in a number of ways. The semantic interpretation depends on the use of typeface, subscripts, and arguments.

3.2 Finite difference equations and Parrondo's games

and space or to sampled functions of discrete-time and discrete-space. Upper-case function names, such as \mathbb{P} , refer to sampled functions that have been transformed in either discrete-space or in discrete-time. The use of arguments and subscripts indicates which transforms have been performed. The first function argument, or subscript, is always temporal and the second function argument, or subscript, is always spatial. The subscripts, m and n , are always integers and represent discrete time and discrete space respectively. The function arguments, x and t , are always real and represent time and space respectively. The function arguments, z and w , are always complex and represent transformed discrete-time and transformed discrete-space respectively. All of these mathematical objects in Table 3.2 represent the same physical situation. They just represent the same processes with different parametrisation.

3.2 Finite difference equations and Parrondo's games

Parrondo's games were devised by J. M. R Parrondo in 1996 as a simplified didactic model for flashing Brownian ratchets. Harmer and Abbott published early papers confirming that Parrondo's insight was correct (Harmer and Abbott 1999a, Harmer and Abbott 1999b, Harmer *et al.* 2000a). Pearce also undertook early work on the analysis of the games (Pearce 2000a, Pearce 2000b). Parrondo's games have been studied and simulated by a number of other authors and Harmer *et al.* have published extensive reviews of the early work on Parrondo's games (Harmer *et al.* 2000b, Harmer and Abbott 2001, Harmer and Abbott 2002). The first work to show that Parrondo's games can be obtained by sampling the Fokker-Planck Equation can be found in Allison and Abbott (2002) and Allison and Abbott (2003b). The approach here is to re-formulate the equations that govern flashing ratchet in the form of a set of partial difference equations, which are shown to be equivalent to the rules for Parrondo's games, in certain limiting cases. Toral and Amengual *et al.* verified and extended these results (Toral *et al.* 2003b, Toral *et al.* 2003a). Most existing work, on Parrondo's games, concentrates on the expected value of the possible return from playing the games. The expected value is the first moment of the sample paths. Very few authors have considered or calculated the second, or higher, moments of the sample paths of Parrondo's games.

It is practically important to know at least the first *two* moments. As an illustration, we may consider the similar and well understood process of chromatography, which is governed by a partial differential equation formulated by Carta (1988) and is described in Seader and Henley (2006). This PDE is analogous to the Fokker-Planck Equation, which governs the dynamics of Brownian ratchets. In chromatography, the components of a mixture are separated by the transport effect caused by a flow of eluting solvent. The overall rate of movement of molecules from the sample is a function of the relative affinities of the molecules to the stationary phase and to the moving phase. This is beneficial because it allows analytic separation and chemical analyses to be performed, based on different rates of adsorption. This transport effect can be expressed in terms of the first moment. On the other hand, identical molecules from the sample will diffuse, as they are transported. They will disperse, relative to the position of the bulk of the sample. This effect is related to the second moment. The separation effect, represented by the first moment, could be completely ruined if the components were to disperse into each other. Examples of this are described in Seader and Henley (2006). In short, physical devices with very large second moment are not very useful for separation, even if the first moment appears to be very favourable. The same problem arises for chromatography, electrophoresis, Brownian ratchets, Brownian motors, or any form of separation that includes diffusion.

At the present time, there does not seem to be any complete analysis of the second moment of transport in Brownian ratchets, which is analogous to Carta's analysis of chromatography. The second moment does not seem to have been considered very extensively. To his credit, Toral (2001) considered second moments when he calculated the numerical variances for his *cooperative Parrondo's games*. There is, presently, no reference in the existing literature to any algebraic expression for the second, or higher, moments of Parrondo's games. To derive algebraic expressions for these moments, it is necessary to directly evaluate some rather complicated infinite series or to find some indirect method for performing the summation. The traditional approach to this type of problem, in mathematical statistics, is to use a generating function (Muth 1977, Papoulis 1991, Wackerley *et al.* 1996, Yates and Goodman 1999, Bracewell 2000). This fits in very well with the fact that Parrondo's games can be represented as difference equations and the fact that these difference equations can be solved using generating functions. This suggests the following approach to evaluating all of the moments of Parrondo's games:

3.3 Finite partial difference equations

1. Sample the relevant Fokker-Planck Equation to obtain a set of partial-difference equations, which are equivalent to Parrondo's games.
2. Use a generating-function approach to derive expressions for transforms of the solution to the partial difference equations.
3. Differentiate the transforms to obtain expressions for the moments of Parrondo's games. These will be exact expressions for the moments of Parrondo's games and should provide approximate numerical estimates for the corresponding moments of the true solution to the original Fokker-Planck equations.

One of the most powerful aspects of this approach is that it is not necessary to evaluate to inverse transform and write the solution in closed-form. It is possible to work directly with the transforms to obtain the moments. The expressions for the moments are generally more simple than the expressions for the complete solutions in time and space. The first step in the procedure, outlined above, is to sample the Fokker-Planck equation. This is described in the next section.

3.3 Finite partial difference equations

We consider a problem, discussed by Einstein (1956), of a Brownian particle. We consider a small microscopically-visible particle suspended in a liquid. The huge numbers of molecules in the liquid are in constant thermal motion. They frequently strike the Brownian particle at random intervals giving rise to small random variations in the motion of the Brownian Particle. The course of the Brownian particle appears to be very irregular. The number of parameters in such a system are enormous. The value of the Avogadro number tells us that there are about 6×10^{23} atoms in a single mole of substance. Even if we knew the correct equations of motion, there is no way that we could collect enough data to specify the initial conditions of an Avogadro number of particles. We are forced to follow the approach of Boltzmann, Maxwell and Gibbs. We must use probability models and statistics to describe the essential features of the process. Information is lost in the process. As Maxwell put it: *"And here I wish to point out that, in adopting this statistical method of considering the average number of groups of molecules selected according to their velocities, we have abandoned the strict*

kinetic method of tracing the exact circumstances of each individual molecule in all of its encounters" (Maxwell 1888). This actually echoes the earlier statement by Laplace: "The curve described by a single molecule [of] air or vapour is regulated in a manner just as certain as the planetary orbits; the only difference between them is that which comes from our ignorance" (Laplace 1814)⁹. In summary, we use probability in order to partially compensate for our ignorance. We are fully aware that something is lost in the process.

According to Pauli (1973), Langevin, Lorenz, and Einstein each used statistical methods to arrive at expressions for the mean square displacement of a Brownian particle. Einstein (1905) showed that the probability density function for the Brownian particle at any given instant in time, $p(t, x)$ was governed by the diffusion equation (Gardiner 1983):

$$D^{(2)} \cdot \frac{\partial^2 p(t, x)}{\partial x^2} - \frac{\partial p(t, x)}{\partial t} = 0, \quad (3.16)$$

where we denote the probability of finding a Brownian particle at a certain point in space, x , and time, t , by $p = p(t, x)$. The diffusion equation becomes modified if the Brownian particle is charged and an external field is applied. It can be shown that the time-evolution of $p(t, x)$ is then governed by a partial differential equation called the Fokker-Planck Equation (Gardiner 1983, Risken 1996):

$$\frac{\partial}{\partial x} \left(D^{(2)}(t, x) \cdot \frac{\partial p(t, x)}{\partial x} \right) - \frac{\partial}{\partial x} \left(D^{(1)}(t, x) \cdot p(t, x) \right) - \frac{\partial p(t, x)}{\partial t} = 0. \quad (3.17)$$

There are many ways to obtain the Fokker-Planck Equation, see Risken (1996) or Gardiner (1983) for example, but one simple approach is to begin with the law for diffusion, derived by Graham and Fick (Cussler 1997):

$$J(t, x) = - \left(D^{(2)}(t, x) \cdot \frac{\partial p(t, x)}{\partial x} \right) + \left(D^{(1)}(t, x) \cdot p(t, x) \right), \quad (3.18)$$

where $J(t, x)$ is the probability flow and $p(t, x)$ is the probability density. Fick's law can be combined with the law of continuity,

$$\frac{\partial p(t, x)}{\partial t} + \frac{\partial J(t, x)}{\partial x} = 0, \quad (3.19)$$

to yield the Fokker-Planck Equation 3.17. The functions $D^{(1)}(z, t)$ and $D^{(2)}(z, t)$ are referred to as the infinitesimal first and second moments of diffusion. In practice, the infinitesimal second moment does sometimes depend on concentration of the solute, $p(z, t)$, but is usually regarded as constant and is called the *Fick's law constant*.

⁹The essay (Laplace 1814) is also reproduced in Hawking (2005).

3.3 Finite partial difference equations

A typical value (e.g. for a hydrated sodium ion in water) is of the order $D^{(2)} \approx 1.3 \times 10^{-9} \text{ m}^2\text{s}^{-1}$ (Bird *et al.* 1960, Atkins 1994). The probability flow, $J(t, x)$, is sometimes called the *convective flux*, because the flux is equivalent to an externally applied convective flux (Atkins 1994). Some other authors refer to this flow as the *Kolmogorov flow*.

Further simplification of Equation 3.17 is possible if $D^{(2)}(t, x)$ and $D^{(1)}(t, x)$ are piecewise-constant. In fact, Equation 3.17 becomes separable under those conditions. The procedure is very similar to that for the standard diffusion equation (Farlow 1982), and there are analytic solutions in any closed sub-domain where $D^{(2)}(t, x)$ and $D^{(1)}(t, x)$ are piecewise-constant. If the fundamental solutions have the form $p(t, x) = F(x) \cdot G(t)$ then the Fokker-Planck Equation separates out as:

$$D^{(2)} \cdot \frac{\partial^2 F}{\partial x^2} - D^{(1)} \frac{\partial F}{\partial x} - C_1 F = 0 \quad (3.20)$$

$$\frac{\partial G}{\partial t} - C_1 G = 0, \quad (3.21)$$

$$(3.22)$$

where C_1 is a constant, to be determined by the boundary conditions. The complete and general solution for the sub-domain must be written as an infinite sum of fundamental solutions:

$$p(t, x) = \sum_{v=0}^{\infty} A_v \cdot F_v(x) \cdot G_v(t) \quad (3.23)$$

where A_v are a series of constants to be determined by the constraints imposed by the initial condition and the continuity requirements at the sub-domain boundaries. There are nontrivial technical issues associated with solving for the undetermined coefficients A_v and C_1 within each sub-domain. There are an infinite number of equations to be solved. Another problem with this method is that $D^{(1)}(t, x)$ can, in general, change rapidly and the piecewise-constant approximation may not be physically reasonable.

It seems easier to make the sub-domains very small and to make the computation for each sub-domain very simple. We assume that $D^{(2)}(t, x)$ is constant, which is physically reasonable, and to allow $D^{(1)}(t, x)$ to take arbitrary form. This is required in order to realistically analyse the behaviour of Brownian ratchets and leads to the following

form of the Fokker-Planck Equation:

$$D^{(2)}(t, x) \cdot \frac{\partial^2}{\partial x^2} p(t, x) - \frac{\partial}{\partial x} \left(D^{(1)}(t, x) \cdot p(t, x) \right) - \frac{\partial}{\partial t} p(t, x) = 0. \quad (3.24)$$

The infinitesimal first moment, or *drift*, $D^{(1)}(t, x)$, depends on the magnitude of externally imposed forces and on the mobility, u , of the Brownian particle that is given by

$$u = \frac{Z_e}{6\pi\eta a} \quad (3.25)$$

where Z_e is the electrical charge on the particle, η is the kinematic viscosity of the solvent and a is the effective radius of the particle.¹⁰

It is easy to become lost in mathematical abstraction, and to forget the physical processes that are involved here. A physical example to give an idea of scale is helpful in this regard. A typical value for the mobility (of a hydrated sodium ion in water) is

$$u \approx 51.9 \times 10^{-9} \text{m}^2 \text{s}^{-1} \text{volt}^{-1}. \quad (3.26)$$

Sodium is a good choice because it is such a common ion, on the planet Earth, and in living tissue. The mobilities of ions depend on their state of charge, Z_e , and their physical size, a , as described in Equation 3.25. A range of different molecules will have a range of different mobilities. Further descriptions and numerical data may be found in books on physical chemistry and statistical physics (Bird *et al.* 1960, Reif 1965, Atkins 1994, Cussler 1997).

If we apply an electrical potential, or voltage, of $V(z, t)$ then the infinitesimal first moment is given by

$$D^{(1)}(t, x) = -u \frac{\partial}{\partial x} V(t, x). \quad (3.27)$$

The speed of drift is proportional to the applied force. The theory behind Equations 3.25 and 3.27 is due to Stokes and was used by Einstein (Atkins 1994).

When we take into account the functional forms of $D^{(2)}$ and $D^{(1)}$ then we can rewrite the Fokker-Planck equation as:

$$D^{(2)}(t, x) \cdot \frac{\partial^2 p(t, x)}{\partial x^2} - \frac{\partial D^{(1)}(t, x)}{\partial x} \cdot p(t, x) - D^{(1)}(t, x) \cdot \frac{\partial p(t, x)}{\partial x} - \frac{\partial p(t, x)}{\partial t} = 0. \quad (3.28)$$

¹⁰The symbol, u , is used here in accordance with the notation used by Atkins (1994). Some authors use the symbol, μ , to refer to mobility, but we prefer not to overload the use of this symbol. We use the symbol, μ_k , to refer to non-central moments.

3.4 Sampling the Fokker-Planck Equation

This can be written more concisely as

$$D^{(2)} \cdot \frac{\partial^2 p}{\partial x^2} - \frac{\partial D^{(1)}}{\partial x} \cdot p - D^{(1)} \cdot \frac{\partial p}{\partial x} - \frac{\partial p}{\partial t} = 0 \quad (3.29)$$

provided that we remember that all the functions depend on t and x . This is the form of the Fokker-Planck equation that we sample at regular intervals in time and space, to yield finite difference equations.

3.4 Sampling the Fokker-Planck Equation

Many Partial Differential Equations, or PDEs, including Equation 3.28, can be very difficult to solve analytically. One well established approach to this problem is to sample possible solutions to a PDE at regular intervals, called mesh points (Lapidus 1962, Press *et al.* 1995, Iserles 1996, Scheisser and Silebi 1997, Korn and Korn 2000, Chapra 2006). The true solution is approximated locally by a collocating polynomial. The values of the derivatives of the true solution are approximated by the corresponding derivatives of the collocating polynomial. This is the approach outlined in the previous section.

We can define local coordinates, expanded locally about a point (t_0, x_0) we can map points between a real space (t, x) and an integer or discrete space (m, n) . Time, t , and position, x , are modelled by real numbers, $t, x \in \mathcal{R}$ and the corresponding sampled position, m , and sampled time, n , are modelled by integers $m, n \in \mathcal{Z}$. We sample the space using a simple linear relationship

$$(t, x) = (t_0, x_0) + (\Delta m \cdot \tau, \Delta n \cdot \lambda) \quad (3.30)$$

$$= (t_0 + (\Delta m \cdot \tau), x_0 + (\Delta n \cdot \lambda)) \quad (3.31)$$

where λ is the sampling length and τ is the sampling time.

In order to map Equation 3.28 into discrete space, we need to make suitable finite difference approximations to the partial derivatives. The notation is greatly simplified if we define a family of difference operators:

$$\Delta_{\Delta m, \Delta n} \cdot p = p(t_0 + (\Delta m \cdot \tau), x_0 + (\Delta n \cdot \lambda)) - p(t_0, x_0). \quad (3.32)$$

This allows us to calculate finite differences of P in terms of small integer offsets in time and space, Δm and Δn . In principle, this is a doubly infinite family of operators but in practice we only use a small finite subset of these operators. This is determined by our choice of sampling points. This choice is not unique and is not trivial. The set of sampling points is called a *computational molecule* (Lapidus 1962). Some choices lead to over-determined sets of equations with no solution. Some other choices lead to under-determined sets of equations with infinitely many solutions. We chose a computational molecule that leads to what is called *explicit* computation with the following sample points: $(\Delta m, \Delta n) \in \{(0, 0), (-1, -1), (-1, 0), (-1, +1)\}$. We also need to make a choice regarding the form of the local collocating polynomial. This is not unique and inappropriate choices do not lead to unique solutions. A polynomial that is quadratic in x and linear in t is the simplest feasible choice:

$$p(t, x) = p(t_0, x_0) + A_1 \cdot (x - x_0) + A_2 \cdot (x - x_0)^2 + B_1 \cdot (t - t_0) \quad (3.33)$$

where A_1 , A_2 and B_1 are the real coefficients of the polynomial. Equations 3.31, 3.32 and 3.33 imply a simple system of linear equations that can be expressed in matrix form:

$$\begin{bmatrix} -\lambda & +\lambda^2 & -\tau \\ 0 & 0 & -\tau \\ +\lambda & +\lambda^2 & -\tau \end{bmatrix} \begin{bmatrix} A_1 \\ A_2 \\ B_1 \end{bmatrix} = \begin{bmatrix} \Delta_{-1,-1} \cdot p \\ \Delta_{-1,0} \cdot p \\ \Delta_{-1,+1} \cdot p \end{bmatrix}. \quad (3.34)$$

These can be solved algebraically, using Cramer's method to obtain expressions for A_1 , A_2 and B_1 :

$$A_1 = \frac{p(t_0 - \tau, x_0 + \lambda) - p(t_0 - \tau, x_0 - \lambda)}{2\lambda} \quad (3.35)$$

and

$$A_2 = \frac{p(t_0 - \tau, x_0 - \lambda) - 2p(t_0 - \tau, x_0) + p(t_0 - \tau, x_0 + \lambda)}{2\lambda^2} \quad (3.36)$$

and

$$B_1 = \frac{p(t_0, x_0) - p(t_0 - \tau, x_0)}{\tau}. \quad (3.37)$$

These are all intuitively reasonable approximations but their choice is not arbitrary. Equations 3.35, 3.36, 3.37 form a complete and consistent set. We could not change one without adjusting the others. We can evaluate the derivatives of Equation 3.33 to obtain a complete and consistent set of finite difference approximations for the partial derivatives:

$$\left. \frac{\partial p}{\partial x} \right|_{t=t_0, x=x_0} \approx A_1 = \frac{p(t_0 - \tau, x_0 + \lambda) - p(t_0 - \tau, x_0 - \lambda)}{2\lambda} \quad (3.38)$$

3.4 Sampling the Fokker-Planck Equation

and

$$\frac{\partial^2 p}{\partial x^2} \Big|_{\substack{t=t_0 \\ x=x_0}} \approx 2A_2 = \frac{p(t_0 - \tau, x_0 - \lambda) - 2p(t_0 - \tau, x_0) + p(t_0 - \tau, x_0 + \lambda)}{\lambda^2} \quad (3.39)$$

and

$$\frac{\partial p}{\partial t} \Big|_{\substack{t=t_0 \\ x=x_0}} \approx B_1 = \frac{p(t_0, x_0) - p(t_0 - \tau, x_0)}{\tau}. \quad (3.40)$$

We can apply the same procedure to $D^{(1)}(z, t)$ to obtain

$$\frac{\partial D^{(1)}}{\partial z} \Big|_{\substack{t=t_0 \\ x=x_0}} \approx A_1 = \frac{D^{(1)}(t_0 - \tau, x_0 + \lambda) - D^{(1)}(t_0 - \tau, x_0 - \lambda)}{2\lambda}. \quad (3.41)$$

Equations 3.38, 3.39, 3.40 and 3.41 can be substituted into Equation 3.28 to yield the required finite partial difference equation:

$$p(t_0, x_0) = q_{n-1, n} \cdot p(t_0 - \tau, x_0 - \lambda) + q_{n, n} \cdot p(t_0 - \tau, x_0) + q_{n+1, n} \cdot p(t_0 - \tau, x_0 + \lambda) \quad (3.42)$$

where

$$q_{n-1, n} = \frac{D^{(2)}\tau/\lambda^2 + D^{(1)}(t_0, x_0)\tau/2\lambda}{(D^{(1)}(t_0 - \tau, x_0 + \lambda) - D^{(1)}(t_0 - \tau, x_0 - \lambda))\tau/(2\lambda) + 1} \quad (3.43)$$

and

$$q_{n, n} = \frac{-2D^{(2)}\tau/\lambda^2 + 1}{(D^{(1)}(t_0 - \tau, x_0 + \lambda) - D^{(1)}(t_0 - \tau, x_0 - \lambda))\tau/2\lambda + 1} \quad (3.44)$$

and

$$q_{n+1, n} = \frac{D^{(2)}\tau/\lambda^2 - D^{(1)}(t_0, x_0)\tau/2\lambda}{(D^{(1)}(t_0 - \tau, x_0 + \lambda) - D^{(1)}(t_0 - \tau, x_0 - \lambda))\tau/(2\lambda) + 1}. \quad (3.45)$$

The coefficients $q_{v, n}$ are conditional single-step probabilities of transition, which are locally expanded about the position, $[t_0, x_0]$. The meaning of the subscripts is more clear if we note that $t_0 = m\tau$ and $x_0 = n\lambda$. The precise semantic interpretation of the probabilities of transition is $q_{v, j} = \mathbf{P}[n = j \text{ at time } m + 1 \mid n = v \text{ at time } m]$. Equation 3.42 can be written more concisely in terms of sampled quantities with discrete subscripts:

$$p_{m, n} = p_{m-1, n-1} \cdot q_{n-1, n} + p_{m-1, n} \cdot q_{n, n} + p_{m-1, n+1} \cdot q_{n+1, n} \quad (3.46)$$

$$= \sum_{v=n-1}^{n+1} p_{m-1, v} \cdot q_{v, n}, \quad (3.47)$$

which is a system of difference equations in the real variable p , indexed by strictly integer time and space coordinates, $m \in \mathcal{Z}$ and $n \in \mathcal{Z}$, respectively. We can write

$$p_{m, n} = \sum_{v=-\infty}^{+\infty} p_{m-1, v} \cdot q_{v, n}, \quad (3.48)$$

provided that all the non-essential probabilities of transition are defined to be zero. Equation 3.48 is consistent with the laws of conditional probability. The process is clearly Markovian, since $p_{m,n}$ depends only on values of $p_{m-1,v}$ and not on probabilities at earlier times. This is consistent with the fact that the Fokker-Planck Equation describes a Markov process (Risken 1996). Equation 3.48 is linear and can be written using the standard notation of linear algebra, in matrix form. Finally, Equation 3.48 is a set of Partial Difference Equations (PDEs), and has precisely the form required for Parrondo's games.

3.5 Parrondo's games, as a set of PDEs

In the original formulation, the conditional probabilities of winning or losing depended on the state, n , but not on any other information about the past history of the games. The definitions of Parrondo's games are essentially statements about the conditional discrete probabilities of transition:

$$q_{v,j} = \mathbf{P} [n = j \text{ at time } m + 1 \mid n = v \text{ at time } m]. \quad (3.49)$$

We can define the games as follows:

- Game A is a toss of a biased coin:

$$q_{n,n+1} = \mathbf{P} [\text{win}] = \frac{1}{2} - \epsilon \quad (3.50)$$

$$q_{n,n-1} = \mathbf{P} [\text{loss}] = \frac{1}{2} + \epsilon, \quad (3.51)$$

where ϵ is an adverse external bias that the game has to overcome. This bias, ϵ , is typically a small number such as $\epsilon = 1/200 = 0.005$, for example. These values were used in many of the early papers (Harmer and Abbott 1999a, Harmer and Abbott 1999b, Harmer *et al.* 2000a).

- Game B does depend on the discrete position of the particle, n :

If $(n \bmod 3) = 0$, then the probability of increase is high.

$$q_{n,n+1} = \mathbf{P} [\text{win}] = \frac{1}{10} - \epsilon \quad (3.52)$$

$$q_{n,n-1} = \mathbf{P} [\text{loss}] = \frac{9}{10} + \epsilon \quad (3.53)$$

If $(n \bmod 3) \neq 0$, then the probability of increase is low.

$$q_{n,n+1} = \mathbf{P}[\text{win}] = \frac{3}{4} - \epsilon \quad (3.54)$$

$$q_{n,n-1} = \mathbf{P}[\text{loss}] = \frac{1}{4} + \epsilon. \quad (3.55)$$

For all of these games, all transition probabilities, $q_{n,v}$, not listed explicitly above, are zero. The language being used here is taken from games of chance, where the aim is to win. An increase in the value of the discrete position, n , is regarded as a “win” and a decrease is regarded as a “loss.” The typical game of this type is called *Gambler's ruin* (Ross 1970, Taylor and Karlin 1998).

The conditional probabilities defined in Parrondo's games are forward probabilities, $q_{n,n+1}$ and $q_{n,n-1}$ at discrete time m . The difference equations are easier to formulate and solve as reverse equations in terms of $q_{n-1,n}$ and $q_{n+1,n}$ at discrete time $m - 1$. The transformation between the two points of view is essentially a shift of origin. It is a detail, of notation, to be carefully handled but it does not lead to any new physics, or mathematics. It is straightforward to simulate a randomised sequence of Parrondo's games on a computer using a very simple algorithm (Harmer and Abbott 2001). The simulations are easiest to code in terms of forward conditional probabilities. An example is shown in Figure 3.1.

3.5.1 Game A, as a partial difference equation

The immediate aim is to determine the relationship between the physical process, defined by the Fokker-Planck Equation and the definitions of Parrondo's games. We can write the requirements for game A in the form of Equation 3.48, as

$$p_{m,n} = \left(\frac{1}{2} - \epsilon\right) \cdot p_{m-1,n-1} + 0 \cdot p_{m-1,n} + \left(\frac{1}{2} + \epsilon\right) \cdot p_{m-1,n+1}. \quad (3.56)$$

This implies a constraint that $q_{n,n} = 0$, which implies that $D^{(2)} \cdot \tau / \lambda^2 = 1/2$, which defines the relative scales of λ and τ so we can give it a special symbol, β , where

$$\beta = \frac{D^{(2)} \cdot \tau}{\lambda^2}. \quad (3.57)$$

The constraints on $q_{n-1,n}$ and $q_{n+1,n}$ imply a value for Parrondo's bias parameter:

$$\epsilon = \frac{-\lambda \cdot D^{(1)}(t_0, x_0)}{4D^{(2)}}, \quad (3.58)$$

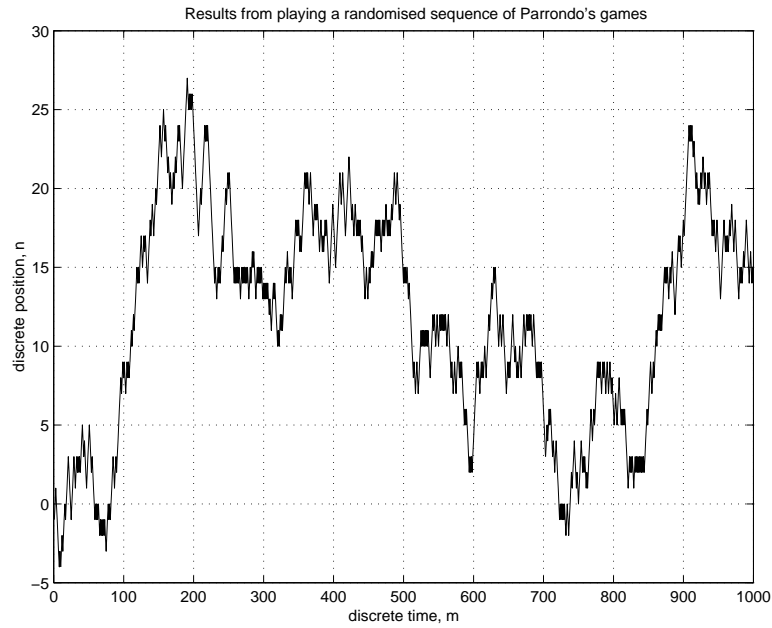


Figure 3.1. A single sample path of Parrondo's original process. The original process, described by Harmer and Abbott, was encoded in Matlab and simulated, one discrete time-step at a time. The results were recorded and are displayed in the graph. It can be seen that the general drift is upwards, towards larger values of discrete position, n , but this is not established, beyond reasonable doubt. The mean path, or trend, is hidden within a large amount of deviation. If an ensemble average is formed from a large number of sample paths, then the amount of deviation is greatly reduced and the upward trend is more apparent. It is possible to use probability models to re-formulate the notions of *drift* and *deviation*. We can make these ideas more precise by reformulating them in terms of the *moments* of the games. For Parrondo's original games, we note that the first moment is positive but this is partially concealed because the second moment is large.

which can be related back to an externally imposed electric field, $\mathbf{E} = -\partial V/\partial z$ using Equations 3.25 and 3.27:

$$\epsilon = \left(\frac{\lambda}{4D^{(2)}} \right) \left(\frac{Z_e}{6\pi\eta a} \right) \left(-\frac{\partial V}{\partial z} \right) = - \left(\frac{\lambda}{4D^{(2)}} \right) \left(\frac{Z_e}{6\pi\eta a} \right) \cdot \mathbf{E}. \quad (3.59)$$

The small bias, ϵ , is proportional to the applied external field which, justifies Parrondo's original intuition.

3.5.2 Game B, as a partial difference equation

The further aim is to determine the relationship between the physical process, defined by the Fokker-Planck equation and the definition of Parrondo's game B. Game B, as defined here, is quite general and actually includes game A as a special case. There is still zero probability of remaining in the same state, which implies a constraint that $q_{n,n} = 0$, which implies that we still have the same scale, $\beta = 1/2$. If we are in state n then we can denote the probability of winning by $q_{n,n+1} = P(\text{win} \mid \text{initial position is } n)$. We can write the difference equations for Game B in the form:

$$p_{m,n} = q_{n-1,n} \cdot p_{m-1,n-1} + 0 \cdot p_{m-1,n} + q_{n+1,n} \cdot p_{m-1,n+1}, \quad (3.60)$$

which, together with Equations 3.43, 3.44 and 3.45, gives

$$\frac{q_{n+1,n}}{q_{n-1,n}} = \frac{1 - \frac{D^{(1)} \cdot \lambda}{2D^{(2)}}}{1 + \frac{D^{(1)} \cdot \lambda}{2D^{(2)}}}, \quad (3.61)$$

which implies that

$$D^{(1)}_{m,n} = \frac{2D^{(2)}}{\lambda} \cdot \frac{q_{n-1,n} - q_{n+1,n}}{q_{n-1,n} + q_{n+1,n}}. \quad (3.62)$$

This can be combined with Equation 3.27 and then directly integrated to calculate the required voltage profile. We can approximate the integral with a Riemann sum:

$$V_{m,n} = \frac{-2D^{(2)}}{u} \sum_{v=0}^n \frac{q_{v-1,v} - q_{v+1,v}}{q_{v-1,v} + q_{v+1,v}}, \quad (3.63)$$

so we can construct the required voltage profile for the ratchet. Given the values of $q_{v,n}$, at time m , it is always possible to calculate the required voltage profile, $V_{m,n}$. Conversely, given the voltage profile, we can use Equation 3.27 to calculate the infinitesimal first moment, $D^{(1)}$ and then use Equations 3.43, 3.44 and 3.45 to calculate the probabilities of transition, $q_{v,n}$. There is a one to one and onto mapping between voltage profile of a hypothetical physical device, $V_{m,n}$, and probabilities of transition, $q_{v,n}$. We can conclude that Parrondo's games are literally a finite difference model of a flashing Brownian ratchet.

3.5.3 Conditions for convergence of the solution

We need to know the conditions under which the solution to the finite partial difference Equation 3.48 converges to the true solution of the partial differential Equation 3.28, as

the mesh size, λ goes to zero. There is a theorem due to O'Brien *et al.* (1951) that establishes the numerical integration of a parabolic PDE, in explicit form, converges to the correct solution as $\lambda \rightarrow 0$ and $\tau \rightarrow 0$ provided $\beta = D^{(2)} \cdot \tau/\lambda^2 \leq \frac{1}{2}$. We see that Parrondo's choice of diffusion operator, with $\beta = \frac{1}{2}$ is at the very edge of the stable region.

3.5.4 An appropriate choice of scale

There is a possible range of values for β . As $\beta \rightarrow 0$ we require the time step $\tau \rightarrow 0$. The only way to achieve this is to make the number of time steps required to simulate a given time interval, to increase without bound $N_{\text{steps}} = T/\tau \rightarrow \infty$. It is computationally infeasible to perform simulations with extremely small values of $\beta \rightarrow 0$. On the other hand, the value of $\beta = \frac{1}{2}$ implied in original Parrondo's games is at the very limit of stability. In fact, the presence of small round-off errors in the arithmetic could cause the discrete simulation to diverge significantly from the continuous solution.

In defence of Parrondo's original choice of diffusion operator, it is fortuitous that Parrondo's diffusion operator lies just inside the convergent region. Parrondo was not the first scientist to make that choice. Lapidus (1962) points out that the case with $\beta = \frac{1}{2}$ leads to a standard numerical method called the *Schmidt formula*. Taylor and Karlin (1998) point out that Ehrenfest's model of diffusion involves a change of state by ± 1 , for each time tick, and does not allow a null or self-transition. On the other hand, a model of diffusion that excludes self-transitions is not very realistic. At one moment, we have a group of particles confined in a small region. Then we have a vacuum and then particles move back in that region again, and so on. Boltzmann argued that fluctuations do occur but *extreme* fluctuations, which leave a vacuum behind are extremely improbable. There is something very non-physical about Parrondo's original choice of diffusion operator.

We propose that choosing $\beta = \frac{1}{4}$, in the middle of the feasible range, is much more appropriate. If we consider the case of pure diffusion, with $D^{(1)} = 0$, then Equation 3.48 reduces to

$$p_{m,n} = \beta \cdot p_{m-1,n-1} + (1 - 2\beta) \cdot p_{m-1,n} + \beta \cdot p_{m-1,n} \quad (3.64)$$

3.5 Parrondo's games, as a set of PDEs

and if we choose $\beta = 1/4$ then this reduces to

$$p_{m,n} = \frac{1 \cdot p_{m-1,n-1} + 2 \cdot p_{m-1,n} + 1 \cdot p_{m-1,n+1}}{4}, \quad (3.65)$$

which is the same as Pascal's triangle with every second row removed. This is essentially a half-period, or double frequency, Bernoulli process. The solution to the case where the initial condition is a Kronecker delta function, $p_{i,0} = \delta_{i,0}$ is easy to write down, using Binomial coefficients:

$$p_{m,n} = \frac{C_{2m,m+n}}{2^{2n}} = \binom{2m}{m+n} \cdot \frac{1}{2^{2n}} = \frac{(2m)!}{(n+m)! \cdot (n-m)!} \cdot \frac{1}{2^{2n}}, \quad (3.66)$$

which is a half period, or double frequency binomial, with position in the range $-m \leq n \leq +m$. Outside this range, we have $p_{m,n} = 0$. We can apply Stirling's approximation to the factorial¹¹ and arrive at the Laplace and De Moivre form of the Central Limit Theorem which, establishes a correspondence between Binomial (or Bernoulli) distribution and the Gaussian distribution to obtain

$$p_{m,n} = \frac{1}{\sqrt{\pi m}} \exp\left(\frac{-n^2}{m}\right). \quad (3.67)$$

This expression is only approximate but is true in the limiting case as $m \rightarrow \infty$. This approximation is sometimes known as the Normal approximation to the Binomial distribution (Wackerley *et al.* 1996).

In the case where $D^{(1)} = 0$; the Fokker-Planck Equation 3.28 reduces to a diffusion equation:

$$D \frac{\partial^2 p}{\partial x^2} - \frac{\partial p}{\partial t} = 0. \quad (3.68)$$

Einstein's solution¹² to the diffusion equation is a Gaussian probability density function:

$$p(t, x) = \frac{1}{\sigma \sqrt{2\pi}} \exp\left(\frac{-x^2}{2\sigma^2}\right) \quad (3.69)$$

where the variance, σ^2 , is a linear function of time:

$$\sigma^2 = 2D^{(2)}t. \quad (3.70)$$

This last result is referred to as the Einstein-Smoluchowski equation (Atkins 1994) and appears in Einstein's original papers (Einstein 1905, Einstein 1956, Pauli 1973). Maxwell (1888) attributes the solution in Equation 3.69 to Fourier. Wannier (1966) points

¹¹Reif (1965) uses a Taylor expansion of Equation 3.66, and Stirling's formula, to arrive at Equation 3.67.

¹²Einstein applied Fourier's solution (Maxwell 1888) to the heat equation in a new context.

out that Equation 3.70 is also implicit in the Nernst equation, and that this result was probably known before it was used by Einstein (1905) and Smoluchowski (1916). It is possible to verify that Equation 3.69 is a solution to Equation 3.68 by direct substitution:

$$D^{(2)} \cdot \frac{\partial^2 p}{\partial x^2} = \frac{\partial p}{\partial t} \quad (3.71)$$

$$= \left(\frac{-1}{2t} \right) \cdot \left(1 - \left(\frac{x}{\sigma} \right)^2 \right) \cdot p(t, x) . \quad (3.72)$$

If we sample this solution in Equation 3.69 using the mapping in Equation 3.31 then we obtain Equation 3.67 again. This is an exact result. We also obtain a result regarding the variance, $2D^{(2)} \cdot t = \frac{\lambda^2}{2\tau} \cdot t$ and hence, $\beta = \frac{D^{(2)}\tau}{\lambda^2} = \frac{1}{4}$, which was the original scaling assumption. We conclude that the choice of $\beta = \frac{1}{4}$ is very appropriate for the solution to the diffusion equation. We suggest that this would also be true for the Fokker-Planck Equation, in the case where $D^{(1)}$ is small. The appropriate choice of β , given arbitrarily large, or rapidly varying, $D^{(1)}$ is still an unsolved problem. In general, we would expect that much smaller values, $\beta \rightarrow 0$, would be needed to accommodate more extreme choices of $D^{(1)}$.

3.5.5 Mean position and mean velocity of drift

We can define the mean position of a Brownian particle in terms of expected value, with respect to position x :

$$\mu(t) = E_x [p(t, x)] = \int_{-\infty}^{+\infty} xp(t, x) dx. \quad (3.73)$$

The mean velocity of drift can be calculated as follows:

$$\frac{\partial \mu}{\partial t} = \frac{\partial}{\partial t} \int_{-\infty}^{+\infty} xp dx \quad (3.74)$$

$$= \int_{-\infty}^{+\infty} x \frac{\partial p}{\partial t} dx \quad (3.75)$$

$$(3.76)$$

and, making use of the law of continuity, in Equation 3.19, we obtain

$$\frac{\partial \mu}{\partial t} = - \int_{-\infty}^{+\infty} x \frac{\partial J}{\partial x} dx. \quad (3.77)$$

3.5 Parrondo's games, as a set of PDEs

We can apply integration by parts to obtain

$$\frac{\partial \mu}{\partial t} = - [J(t, x) \cdot x]_{-\infty}^{+\infty} + \int_{-\infty}^{+\infty} J(t, x) dx \quad (3.78)$$

and since the boundary conditions at infinity are assumed to be zero, we obtain:

$$\frac{\partial \mu}{\partial t} = \int_{-\infty}^{+\infty} J(t, x) dx, \quad (3.79)$$

so the mean velocity of drift is related to the flow of probability, $J(t, x)$, integrated over space. If we have sampled the solution to the Fokker-Planck Equation then we can approximate the integral in Equation 3.73 using a Riemann sum:

$$\mu_m = E_n [p_{m,n}] = \lambda \cdot \sum_{n=-\infty}^{+\infty} n p_{m,n}. \quad (3.80)$$

This can be used to evaluate the mean position of a Brownian particle in computer simulations.

3.5.6 An example of a simulation, including null-transitions

We simulated a physically reasonable ratchet with a moderately large modulo value, $L = 8$. (The value for the original Parrondo's games was $L = 3$.) We used the value of $\beta = 1/4$. The simulation was based on a direct implementation of Equation 3.48 in Matlab. We chose an example sampling time of $\tau = 12 \mu s$ and a sampling distance of $\lambda \approx 0.25 \mu m$. The result is shown in Figure 3.2, where we indicate how the expected position of a particle can move within a Brownian flashing ratchet during four cycles of the modulating field. We can see a steady drift of the mean position of the particle in response to the ratchet action.

This simulation includes a total of 500 time samples. Note that the average rate of transport quickly settles down to a steady value, even after only four cycles of the ratchet. It is worth noting that this is a discrete simulation. It is an example of a generalised version of Parrondo's games. It is a version of Parrondo's games with null transitions, with $\beta = \frac{1}{4}$. This result was first published by Allison and Abbott (2002) and shows that Parrondo's games can produce a non-zero transport effect even when null transitions are included. This establishes that *Parrondo's paradox* does not depend on the absence of null-transitions.

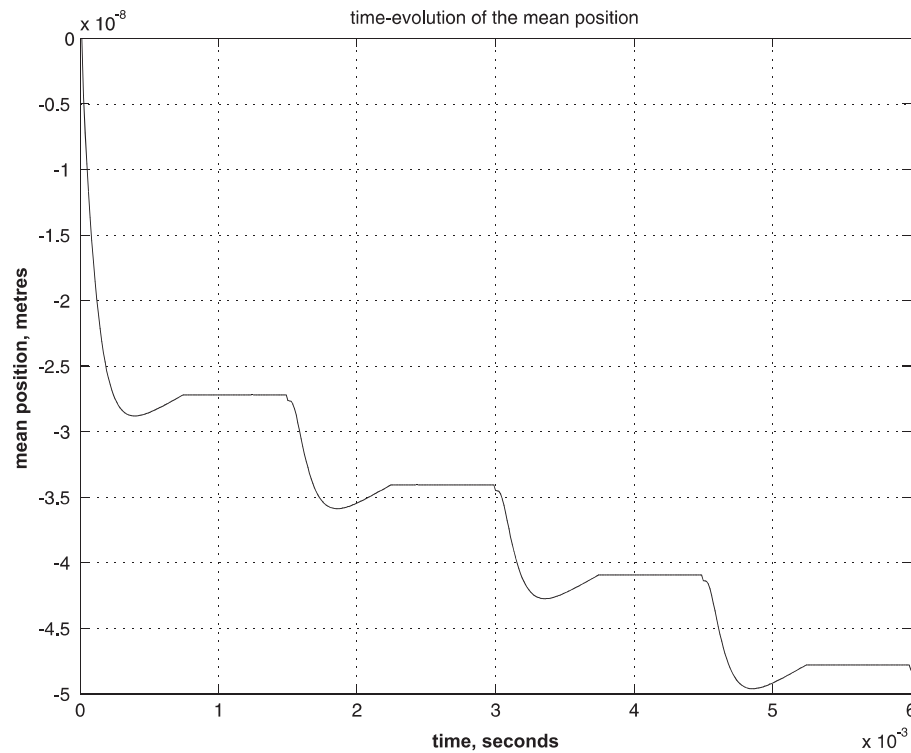


Figure 3.2. Time-evolution of the mean of the distribution $p(t, x)$. When the field is asserted, the mean position of the particles moves in a generally downward direction. There is some relaxation towards the end of that part of the cycle. When the field is turned off, the mean remains constant although diffusion causes the distribution to disperse. The total shift in mean position of this ratchet is very modest, about $0.005 \mu\text{m}$, compared with the spacing between the teeth of the ratchet, of $2.0 \mu\text{m}$. Part of the motivation of this work is to optimise the transport effect of the Brownian ratchet, subject to constraints.

3.5.7 A more realistic simulation

Parrondo's games can be used to simulate the operation of a Brownian ratchet, by simply including more samples in the simulation. For example, a one dimensional Brownian ratchet device is tested with the following parameters: There are 11 teeth either side of the initial condition with 11 samples per tooth, in the spatial dimension. The spatial period is $L = 2.0 \times 10^{-6}$ m. The temporal period is $T_0 = 1.5 \times 10^{-3}$ s. The maximum, on, voltage is $V_{\text{max}} = 60.0 \times 10^{-3}$ V. This is deliberately kept low enough to avoid significant heating or electrolysis effects. The physical constants for diffusion are chosen to be diffusion coefficient: $D^{(2)} = 1.3 \times 10^{-9} \text{ m}^2\text{s}^{-1}$ and particle mobility $u = 51.9 \times 10^{-9} \text{ ms}^{-1}\text{V}^{-1}$, which are the typical values for a hydrated sodium ion in water (Atkins 1994). The duty cycle is chosen to be $\mathcal{D} = 1 - \gamma = 1/2$. The ratchet

3.5 Parrondo's games, as a set of PDEs

is *on* and *off* for equal periods of time. The value of the scaling variable, β , defined in Equation 3.57, is chosen as $\beta = 1/4$ in order to be consistent with the recommendation for Parrondo's games with natural diffusion. The results of this simulation are shown in Figures 3.3 and 3.4.

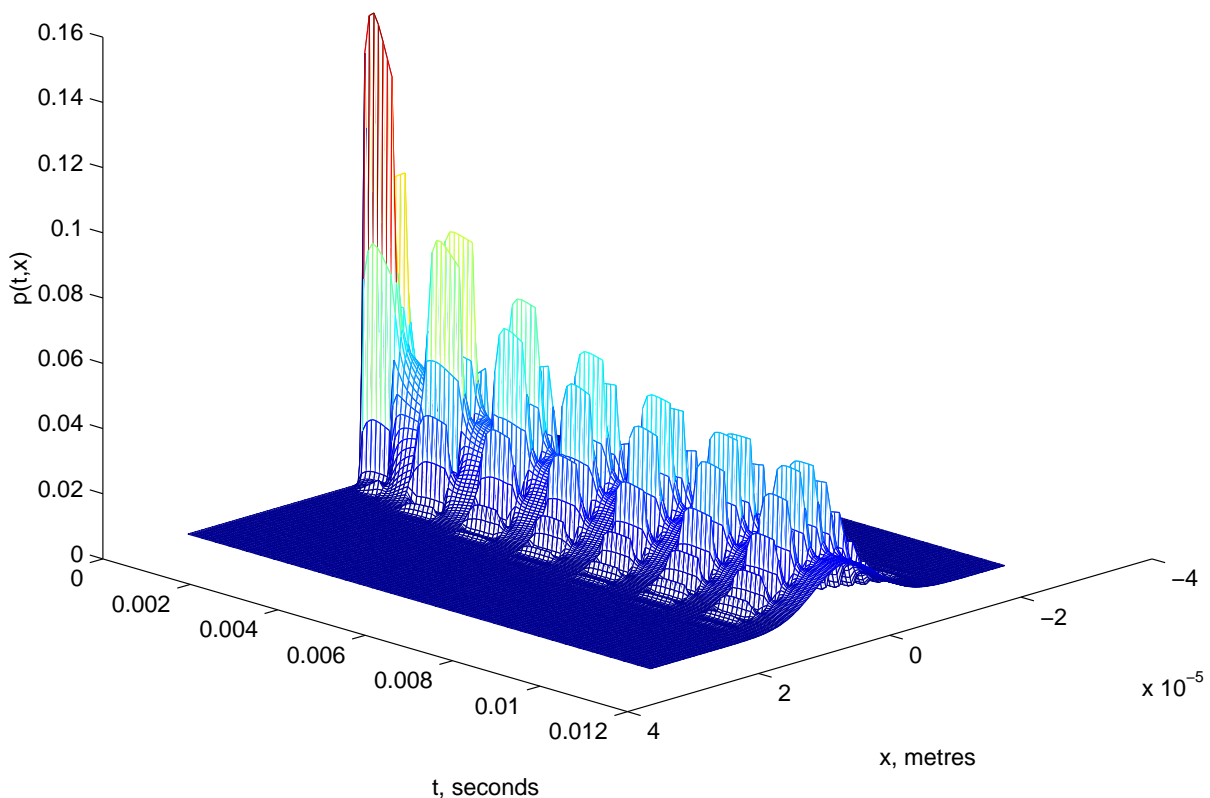


Figure 3.3. The time-evolution of $p(t,x)$. The coordinate system is a right-handed Cartesian system, x, y, z . The x -axis shows position x in metres. The y -axis shows time t in seconds and the z -axis shows probability density $p(t,x)$. The units of probability density are m^{-1} . The probability density is normalised to a total probability of one, at each point in time, t . The grouping of particles in the teeth of the ratchet can clearly be seen during the *on* times and the relaxation of the particles during the *off* can also be clearly seen. The overall drift is present but may be hard to see in this figure. This entire simulation of a ratchet is quite realistic and yet is really only a special case of Parrondo's games. It differs from Parrondo's original games in that there are null-transitions, more samples in time and in space, and the scale has been adjusted to be realistic for hydrated sodium ions in water.

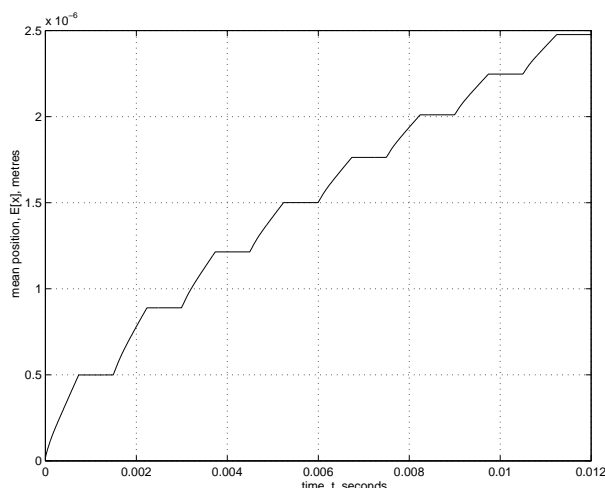


Figure 3.4. The mean position of a Brownian particle in a ratchet. The distributions, calculated in Figure 3.3 are averaged to give an estimate of the mean position of a Brownian particle in the ratchet. The shift in mean position can clearly be seen. Once again, this simulation is really only a special case of Parrondo's games. It differs from Parrondo's original games in that there are self-transitions, more samples in time and in space, and the scale has been adjusted to be realistic for hydrated sodium ions in water. The change in mean position is positive, indicating that the games would be *winning* if the simulation had been formulated as a game of chance, rather than a physical simulation of a Brownian process.

These are simulations of a Brownian ratchet but they are also instances of Parrondo's games with natural diffusion. It is clear that we could include more and more samples into the simulation and make the simulation more and more realistic, as required. The limit theorem of Kaplan guarantees convergence. Parrondo's games with natural diffusion would be useful for simulating a proposed ratchet device. Alternatively, we could simplify the games down to a minimal case, where the games could be solved exactly using mathematical techniques. The purpose of analysis is to gain some insight, which might not be clear amongst the large amounts of data generated by brute-force simulations. The analytical approach is the one pursued by Parrondo.

3.6 Summary of results, regarding the sampling process

We acknowledge the similar, but independent, work of Heath *et al.* (2002). The focus here different; we seek to establish the physical, and mathematical, basis of Parrondo's games and to derive a practical numerical technique for simulation.

We conclude that Parrondo's games *are* a valid finite-element simulation of a flashing Brownian ratchet, which justifies Parrondo's original intuition. We have established that Parrondo's ϵ parameter is a reasonable way to simulate a gradual externally imposed electric field, or voltage gradient. We have established that Parrondo's implied choice of the β parameter does lead to a stable simulation, but we suggest that the choice of $\beta = 1/4$ is more appropriate from a mathematical point of view. The transport effect does not depend on the absence of null-transitions.

Finally, we have generalised Parrondo's games, in the form of a set of finite difference equations and we have shown that these can be implemented on a computer. This justifies the claim that Parrondo's games are a discrete-time, discrete-space version of a flashing Brownian ratchet. Parrondo's games are, in effect, a particular way of sampling a Fokker-Planck Equation.

3.7 Estimating the moments of Parrondo's games

The aim is to design a Brownian ratchet device to produce a transport effect. Devices of this type could be used to amplify signals, in a manner similar to the way that the diffusion of minority carriers amplifies a signal in a bipolar transistor. The transport effect could also be used for sorting (Bader *et al.* 1999) or to perform analytic separations, in a manner similar to chromatography (Seader and Henley 2006). In order to produce a workable design, we must have a model that allows us to estimate the magnitude of the transport or drift effect. It can be seen, in Figure 3.1, that calculating the effective drift is not sufficient for practical purposes. We must also measure the amount of deviation involved.

Calculation of the higher moments should not be necessary. This follows from the central limit theorem. The disordered or random part of the motion of a Brownian particle

tends to have infinitesimal increments that are Gaussian and the Gaussian distribution is completely determined by the first two moments, so the immediate aim is to determine the first two moments of a Brownian ratchet process.

We assume that the process has been sampled in discrete time and space, as suggested in the last section and that we have arrived at a set of Parrondian games that approximate the device under enquiry. These games can be written as a set of partial difference equations in point probabilities, $p_{m,n}$. There is a large literature on the use of z-transforms to solve ordinary difference equations (McEliece *et al.* 1989, Kuo 1992, Proakis and Manolakis 1992, Jerri 1996, Ersoy 1997). In fact this motivation was present in the earliest works on the z-transform, such as those of Jury (1964), who considered the problem of electrical ladder circuits. More recently, Proakis and Manolakis (1992) considered the well-known problem of the Fibonacci sequence, using the z-transform and Kuo (1992) considered the problem of regular repayments on a loan, under compound interest, using the z-transform.

Many of the results, obtained using the z-transform, were anticipated using an earlier technique called the *generating function*. Knuth (1978) attributes the invention of generating functions to de Moivre (1730) who used the technique to solve the difference equations for the Fibonacci sequence. Goldberg (1986) used the generating function technique and extended it to apply to partial difference equations in two independent variables. He used the technique to solve the problem of Bernoulli trials, to derive the standard expression for the Binomial distribution, $p_{m,n} = C_{m,n} q^n (1 - q)^{(m-n)}$. This example problem contains the essential features required to solve the partial difference equations that arise in the analysis of Parrondo's games. The analysis is presented here, using the z-transform and the notation from Tables 3.1, 3.2 and 3.3.

3.7.1 Evaluation of the discrete transforms of the solution function

It is possible to derive an expression for the z-transform of the solution to a system of difference equations directly from the difference equations. This is clearly seen if we examine the recurrence relationship for Bernoulli trials, which is shown graphically in

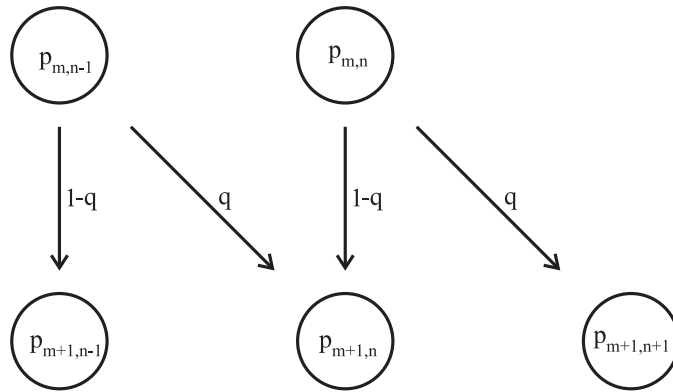


Figure 3.5. Point probabilities and probabilities of transition for the Bernoulli process. The probability that the system is at discrete state n at discrete time m is $p_{m,n}$. If we are given the fact that system is in state n at time m then there are two possible transitions from that state. The probability of transition to state n at time $m + 1$ is $1 - q$ and the probability of transition to state $n + 1$ at time $m + 1$ is q . All other transitions have a conditional probability of zero. If we know that the system has arrived at state n at time $m + 1$ then there are two possible pathways by which the system can have reached that state. There could have been a transition from state $n - 1$, with probability of q , or a self-transition from state n , with probability of $1 - q$. All other transitions have a conditional probability of zero.

Figure 3.5 and algebraically as follows:

$$p_{m+1,n} = q \cdot p_{m,n-1} + (1 - q) \cdot p_{m,n}. \tag{3.81}$$

This recurrence relationship is a partial difference equation. It can be derived by summing over all the possible histories, using the laws of conditional probabilities. The probability that the system is at discrete state n at discrete time m is $p_{m,n}$. We can recall that the single-time-step conditional probability of transition is

$$q_{v,j} = \mathbf{P} [n = j \text{ at time } m + 1 \mid n = v \text{ at time } m]. \tag{3.82}$$

It then follows from the laws of conditional probability that

$$p_{m+1,n} = \sum_{v=-\infty}^{+\infty} p_{m,v} \cdot q_{v,n}. \tag{3.83}$$

For the case of Bernoulli trials, we can define $q_{v,n} = (1 - q) \cdot \delta_{v,n} + q \cdot \delta_{v+1,n}$, where δ refers to the Kronecker delta operator. Note that q (without subscripts) refers to the probability of success in the original Bernoulli trials scheme and that $q_{v,n}$ (with subscripts) refers to a more general conditional probability of transition. In the case of

Parrondo's games the transition probabilities $q_{v,n}$ can depend on the values of the initial position, v , the final position n , and the time, m . In the case of Bernoulli trials, these transition probabilities are stationary and $q_{v,n} = q = \text{constant}$.

If we take the two-sided spatial w -transform of Equation 3.81 then we obtain

$$\mathbb{P}_{m+1}(w) = q \cdot w^{-1} \cdot \mathbb{P}_m(w) + (1 - q) \cdot \mathbb{P}_m(w). \quad (3.84)$$

We can then take the one-sided temporal z -transform of Equation 3.84 to obtain

$$z^{+1} \cdot \mathbb{P}(z, w) - z^{+1} \cdot \mathbb{P}_0(w) = q \cdot w^{-1} \cdot \mathbb{P}(z, w) + (1 - q) \cdot \mathbb{P}(z, w) \quad (3.85)$$

and hence

$$\mathbb{P}(z, w) = \frac{1}{1 - z^{-1} \cdot ((1 - q) + q \cdot w^{-1})} \cdot \mathbb{P}_0(w). \quad (3.86)$$

If we use the initial condition, that the system is in state zero at time zero then $p_{0,n} = \delta_{0,n}$ and hence $\mathbb{P}_0(w) = 1$. This gives:

$$\mathbb{P}(z, w) = \frac{1}{1 - z^{-1} \cdot ((1 - q) + q \cdot w^{-1})}. \quad (3.87)$$

This is the dual transform of the solution to the difference Equation 3.81. This transform is simple enough to invert. We can take the inverse w -transform, \mathbb{W}^{-1} , to obtain

$$\mathbb{P}_m(w) = \left(q \cdot w^{-1} + (1 - q) \right)^m. \quad (3.88)$$

If we then apply the inverse z -transform, we obtain

$$p_{m,n} = C_{m,n} \cdot q^n \cdot (1 - q)^{m-n} \quad (3.89)$$

where $C_{m,n} = m! / (n!(m - n)!)$ is a binomial coefficient. Equation 3.89 is the standard result for Bernoulli trials and is called the Binomial distribution (Papoulis 1991). In this simple case, the inverse transformations from Equation 3.87 to Equation 3.89 are simple enough to be performed in closed form. The problem with solutions of the form of Equation 3.89 is that there is too much detail. It is not possible to make general statements about the expected value of a transport effect or about the amount of deviation without calculating moments. This would require us to evaluate further sums over the probabilities in Equation 3.89. This can be quite tedious and time consuming. A far more elegant and direct approach is to work with transforms of the solutions, such as Equations 3.87 or 3.88, and to regard these transforms as modified moment generating functions.

3.7 Estimating the moments of Parrondo's games

time vs space	n	w
m	$p_{m,n} = C_{m,n} q^n (1-q)^{(m-n)}$	$\mathbb{P}_m(w) = (qw^{-1} + (1-q))^m$
z	$\mathbb{P}(z)_n = \frac{q^n z^{-n}}{(1-(1-q)z^{-1})^{n+1}}$	$\mathbb{P}(z, w) = \frac{1}{1-z^{-1}(qw^{-1}+(1-q))}$

Table 3.4. Transforms of solutions to the Bernoulli process. It is fairly easy to write down the solutions to the equations for the Bernoulli process, in all the different domains. After careful consideration, it turns out that the solution in the time domain, $p_{m,n}$, is not the easiest starting point for calculating the spatial moments of the process, $\mu_1'(m)$ and $\sigma^2(m)$. The easiest starting point for calculating the moments is $\mathbb{P}_m(w)$.

3.7.2 Evaluation of first and second moments, of the solution

We make use of the differentiation properties of the w -transform. It is possible to show by direct substitution, and by swapping of the order of differentiation and summation that:

$$\frac{\partial \mathbb{P}_m(w)}{\partial w} \Big|_{w=1} = -E[n]_m = -\mu_1'_m, \quad (3.90)$$

which gives an expression for the first moment, in space, as a function of time

$$\mu_1'_m = E[n]_m = -\frac{\partial \mathbb{P}_m(w)}{\partial w} \Big|_{w=1}. \quad (3.91)$$

The corresponding expression for the non-central second moment can be obtained in the same way

$$\mu_2'_m = E[n^2]_m = +\frac{\partial^2 \mathbb{P}_m(w)}{\partial w^2} \Big|_{w=1} + \frac{\partial \mathbb{P}_m(w)}{\partial w} \Big|_{w=1}. \quad (3.92)$$

These are the relevant formulae for the z -transform. The corresponding results for the Fourier transform are given in Leon-Garcia (1994). Equations 3.91 and 3.92 are valid as long as the relevant sums converge absolutely for some non-empty region of convergence, which justifies the swapping of the order of summation and differentiation. It is possible that some distributions for actual real-world random variables have an unbounded second moment. Clearly, Equation 3.92 does not apply in those cases, where the infinite sums do not converge. For example, we cannot sample a Cauchy distribution and then evaluate the moments using this technique, since the sums do not converge. On the other hand, we could sample a Gaussian function and evaluate the moments using Equations 3.91 and 3.97. Equations 3.91 and 3.92 can also be evaluated in the doubly transformed, $\{z, w\}$, domain. We can write

$$\mu_1'(z) = E[n](z) = -\frac{\partial \mathbb{P}(z, w)}{\partial w} \Big|_{w=1} \quad (3.93)$$

and the second moment follows in a similar way

$$\mu_2'(z) = E \left[n^2 \right] (z) = + \frac{\partial^2 \mathbb{P}(z, w)}{\partial w^2} \Big|_{w=1} + \frac{\partial \mathbb{P}(z, w)}{\partial w} \Big|_{w=1}. \quad (3.94)$$

This follows from the linearity of the operators. The central second moment, or variance, can be calculated from the non-central second moments using the *parallel axis theorem*¹³, for moments,

$$\sigma^2 [n] = E \left[(n - E [n])^2 \right] = E \left[n^2 \right] - E [n]^2 \quad (3.95)$$

$$= \mu_2' - (\mu_1')^2. \quad (3.96)$$

Equation 3.95 is sometimes referred to, by engineers, as *Steiner's theorem* (Apostol and Mnatsakanian 2003). We can use this result to calculate the variance of the sample paths, as a function of discrete time:

$$\sigma_m^2 = E \left[n^2 \right]_m - (E [n]_m)^2 \quad (3.97)$$

$$= \frac{\partial^2 \mathbb{P}_m(w)}{\partial w^2} \Big|_{w=1} + \frac{\partial \mathbb{P}_m(w)}{\partial w} \Big|_{w=1} - \left(\frac{\partial \mathbb{P}_m(w)}{\partial w} \Big|_{w=1} \right)^2. \quad (3.98)$$

The last term in Equation 3.95 involves a square, which is a non-linear operation. This means that there is no simple expression, corresponding to Equation 3.97, in the doubly transformed, $\{z, w\}$, domain. The squared term can be transformed, using a convolution integral in the z -plane, but the result can be complicated. It would usually be easier to take the inverse z -transform of Equations 3.93 and 3.94 to use Equation 3.97 to evaluate the variance as a function of time. We should note that the inverse z -transform can also be expressed as a convolution integral, so taking the inverse z -transform is usually less complicated than taking the z -transform of the square of a function.

In summary; if we can evaluate the transform of the solutions, $\mathbb{P}(z, w)$, then we can easily evaluate the non-central first and second moments, as functions of z , using Equations 3.93 and 3.92. If we take inverse z -transforms of those non-central moments then we can evaluate the non-central moments as functions of m and use Equation 3.95 to evaluate the central second moment, or variance. Alternatively we can take the inverse z -transform of $\mathbb{P}(z, w)$ to obtain $\mathbb{P}_m(w)$ then we can use Equation 3.97 to evaluate the variance.

¹³This is described in Weisstein (1999), page 1190, Equation (6).

3.7.3 The Bernoulli process, a simple worked example

Derivatives of $\mathbb{P}_m(w)$ and the moments of $p_{m,n}$

The transforms of the solutions to the Bernoulli process are already evaluated in Equations 3.87 and 3.88. These can be differentiated and transformed, or inverse transformed. These results are summarised below. The derivatives of $\mathbb{P}_m(w)$ are as follows:

$$\mathbb{P}_m(w) = (qw^{-1} + 1 - q)^m \quad (3.99)$$

and

$$\frac{\partial \mathbb{P}_m(w)}{\partial w} = -mqw^{-2} (qw^{-1} + 1 - q)^{m-1} \quad (3.100)$$

and

$$\frac{\partial^2 \mathbb{P}_m(w)}{\partial w^2} = (m(m+1)q^2w^{-4} + 2mq(1-q)w^{-3}) (qw^{-1} + 1 - q)^{m-2}. \quad (3.101)$$

This leads to some special cases. The zeroth derivative, at $w = 1$, is

$$\mathbb{P}_m(w) |_{w=1} = 1, \quad (3.102)$$

which implies a total probability of one for all values of m , which is a requirement for any feasible probability mass function. We must have

$$\left(\sum_{n=-\infty}^{+\infty} p_{m,n} \right) = 1 \quad (3.103)$$

for all feasible values of discrete time, $m \in \mathcal{Z}$ and $m \geq 0$. The higher derivatives are:

$$\frac{\partial \mathbb{P}_m(w)}{\partial w} |_{w=1} = -mq \quad (3.104)$$

and

$$\frac{\partial^2 \mathbb{P}_m(w)}{\partial w^2} |_{w=1} = m(m+1)q^2 + 2mq(1-q). \quad (3.105)$$

If we then apply Equations 3.91 and 3.97 to Equations 3.104 and 3.105 we can derive expressions for the first two moments of the Bernoulli process:

$$\mu_1'_m = mq, \quad (3.106)$$

and

$$\mu_2'_m = mq(1-q + mq) \quad (3.107)$$

and hence

$$\sigma^2_m = mq(1-q), \quad (3.108)$$

which are consistent with the standard results for the Bernoulli process (Reif 1965, Abramowitz and Stegun 1970, Wackerley *et al.* 1996, Taylor and Karlin 1998, Korn and Korn 2000). It is also possible in the doubly-transformed domain, $\{z, w\}$.

Derivatives of $\mathbb{P}(z, w)$ and the moments of $p_{m,n}$

The calculation of the moments is easier with the single transform, $\mathbb{P}_m(w)$, than the dual transform, $\mathbb{P}(z, w)$ but it is possible to work in the other domain, without the need to immediately perform the inverse z-transform. The derivatives of the dual transform are listed below. The zeroth derivative is simply the dual transform

$$\mathbb{P}(z, w) = \frac{1}{1 - z^{-1} \cdot ((1 - q) + q \cdot w^{-1})}. \quad (3.109)$$

This is the same as Equation 3.87. The higher derivatives are

$$\frac{\partial \mathbb{P}(z, w)}{\partial w} = \frac{-qz^{-1}w^{-2}}{(1 - z^{-1} \cdot ((1 - q) + q \cdot w^{-1}))^2} \quad (3.110)$$

and

$$\frac{\partial^2 \mathbb{P}(z, w)}{\partial w^2} = \frac{2qz^{-1}w^{-3} (1 - (1 - q)z^{-1})}{(1 - z^{-1} \cdot ((1 - q) + q \cdot w^{-1}))^3}. \quad (3.111)$$

These equations lead to some results for the special case when $w = 1$,

$$\mathbb{P}(z, w) |_{w=1} = \mathbb{P}(z, 1) = \frac{1}{1 - z^{-1}}, \quad (3.112)$$

which is the z-transform of Equation 3.102. The first derivative becomes

$$\frac{\partial \mathbb{P}(z, w)}{\partial w} |_{w=1} = -q \frac{z^{-1}}{(1 - z^{-1})^2}, \quad (3.113)$$

which is the z-transform of Equation 3.104.

The second derivative is

$$\frac{\partial^2 \mathbb{P}(z, w)}{\partial w^2} |_{w=1} = \frac{2qz^{-1} (1 - (1 - q)z^{-1})}{(1 - z^{-1})^3}, \quad (3.114)$$

which is the z-transform of Equation 3.105. The equation for the first moment is linear so the corresponding equation in the dual transformed domain is not surprising,

$$\mu_1'(z) = +q \frac{z^{-1}}{(1 - z^{-1})^2}, \quad (3.115)$$

3.7 Estimating the moments of Parrondo's games

which follows from Equation 3.110 and is consistent with Equation 3.106. The second non-central moment is calculable in the same way,

$$\mu_2'(z) = \frac{qz^{-1} + q(2q-1)z^{-2}}{(1-z^{-1})^3}, \quad (3.116)$$

which is the z-transform of Equation 3.107. The equation for the variance cannot be obtained directly from Equations 3.110 and 3.111 because of the non-linear squared term in Equation 3.95. In order to obtain an expression for the second moment, it is necessary perform the inverse z-transforms on Equations 3.115 and 3.116 and then apply Equation 3.95. Of course, that result is consistent with Equation 3.108.

3.7.4 Stochastic processes with stationary probabilities of transition

It can be seen that the equations for the Bernoulli process begin with a very simple expression for the difference equation, in Equation 3.81. The expression for the dual transform, in Equation 3.87, is also quite simple. The expressions for the derivatives, such as Equation 3.111, are more complicated and yet the final results for the moments, Equations 3.106 and 3.108 are very simple. One might suspect that there is a simple symmetry in the problem, which can be exploited, to reduce the amount of effort required to calculate the moments. One important key to this is to note that the probabilities of transition, $q_{v,n}$, are stationary with respect to time and that they do not depend on position either. This means that there are constant repeated terms, which appear in the recurrence relations. This can be readily seen in Equation 3.87 where all the dependency on space appears in a single instance of the spatial shift operator, w , and all the dependency on time appears in a single instance of the temporal shift operator, z . This suggests that further simplification is possible. It should be possible to find a simpler method for obtaining expressions for the moments of the Bernoulli process and a large class of processes that are related to the Bernoulli process, including Parrondo's game A.

Suppose that we are analysing a process that has stationary probabilities of transition and that the dual transform has the form

$$\mathbb{P}(z, w) = \frac{1}{1 - z^{-1} \cdot \alpha(w)}. \quad (3.117)$$

The function $\alpha(w)$ plays the role of a generator. If we take the inverse z-transform of Equation 3.117 then we obtain

$$\mathbb{P}_m(w) = \alpha(w)^m, \quad (3.118)$$

which confirms what we had already suggested, that the spatial generating function, at time m , can be obtained by raising a generator, $\alpha(w)$, to a power, m . If the probabilities of transition are stationary then the process essentially convolves the same set of transition probabilities with each other, over and over gain. This gives rise to powers of the generator in the transformed, w , space. If we take the w -transform of Equation 3.83 then we can write down an expression for the generator, $\alpha(w)$, in terms of the transition probabilities, $q_{v,n}$:

$$\alpha(w) = \sum_{v=-\infty}^{+\infty} q_{v,n} \cdot w^{v-n}. \quad (3.119)$$

In the case of the Bernoulli process, we have

$$q_{v,n} = (1 - q) \delta_{v,n} + q \delta_{v+1,n}, \quad (3.120)$$

which gives the generator

$$\alpha(w) = (1 - q) w^0 + q w^{-1} \quad (3.121)$$

and if we substitute this into Equation 3.117 then we obtain Equation 3.88. This is a very systematic way to derive the generator and the dual $\{z, w\}$, transform of the solution to the partial difference equation. It is possible to directly evaluate the derivatives of Equation 3.117 and to show that the non-central moments can be evaluated in terms of the derivatives of the generator $\alpha(w)$. The first moment is given by

$$\mu'_{1m} = \left(-\frac{\partial \alpha(w)}{\partial w} \Big|_{w=1} \right) \cdot m, \quad (3.122)$$

and the second central moment, or variance, is given by

$$\sigma^2_m = \left(\frac{\partial^2 \alpha(w)}{\partial w^2} \Big|_{w=1} + \frac{\partial \alpha(w)}{\partial w} \Big|_{w=1} - \left(\frac{\partial \alpha(w)}{\partial w} \Big|_{w=1} \right)^2 \right) \cdot m, \quad (3.123)$$

which is an elegant result. This also proves that the variance always expands linearly with time, as long as the sum for the generator in Equation 3.119 converges. There might be certain *fat-tailed* distributions, such as the ones found in financial time series, where the variance does not scale linearly with time, but the infinite-sums for the

3.7 Estimating the moments of Parrondo's games

generators for these functions will not converge. This is clear if one examines Equations 3.12 and 3.13 and considers how the w -transform is derived from the two-sided spatial Laplace transform. The integral for the two-sided Laplace transform generally diverges for large negative values of x , unless the density function diminishes to zero very quickly. For example, the two-sided transform converges for a Gaussian function but diverges for a Cauchy distribution. For most practical situations, the sum for the generator, in Equation 3.119 does converge and the variance does increase linearly with time, according to Equation 3.123.

Equation 3.123 has the same form as the Einstein-Smoluchowski equation 3.70. We can estimate an effective diffusion coefficient, $D_{\text{eff}}^{(2)}$, for the whole macroscopic distribution given the detailed, microscopic, probabilities of transition, embodied in the generator $\alpha(w)$,

$$D_{\text{eff}}^{(2)} = D^{(2)} \cdot \frac{1}{2\beta} \left(\frac{\partial^2 \alpha(w)}{\partial w^2} \Big|_{w=1} + \frac{\partial \alpha(w)}{\partial w} \Big|_{w=1} - \left(\frac{\partial \alpha(w)}{\partial w} \Big|_{w=1} \right)^2 \right). \quad (3.124)$$

This is an interesting equation because it relates the macroscopic effective diffusion coefficient, $D_{\text{eff}}^{(2)}$, to the actual diffusion coefficient, in the physical medium of the ratchet, $D^{(2)}$, through the scaling factor, β , and the minute detailed probabilities of transition, embodied in the generator, $\alpha(w)$. It should be noted that the probabilities of transition depend on the first infinitesimal moment, $D^{(1)}$, which depends on the applied voltage, $V(t, x)$. It follows that the effective diffusion coefficient depends on the applied voltages and well as the actual diffusion coefficient of the medium. We can alter the rate of diffusion by applying fields and the magnitude of this effect is described by Equation 3.124. Being able to alter the rate of diffusion, by applying external fields suggests a number of useful applications. The Parrondo transport effect, would only be one of these.

3.7.5 The w -transforms of some well known distributions

Any theory that is developed as a result of a long sequence of supposedly logical deductions is always subject to challenge because these deductions are carried out by fallible human beings. Mistakes are always possible. We are fortunate to have opportunities to test the theory from the last section against practical examples, where the results are known in advance. A summary of our results is shown in Table 3.5. All

Distribution and Properties	Mass Function, p_n	\mathbb{W} transform	mean, μ_1'	variance σ^2
Geometric	$(1 - q)q^n$	$\frac{1-q}{1-qw^{-1}}$	$\frac{q}{1-q}$	$\frac{q}{(1-q)^2}$
Poisson	$e^{-\mu} \frac{\mu^n}{n!}$	$e^{\mu(w^{-1}-1)}$	μ	μ
Binomial	$C_{m,n} q^n (1 - q)^{(m-n)}$	$((1 - q) + qw^{-1})^m$	mq	$mq(1 - q)$
Sampled Gaussian	$\frac{1}{\xi\sqrt{2\pi}} e^{\left(\frac{-(n\lambda-\mu)^2}{2\xi^2}\right)}$	$w^{-\frac{\mu}{\lambda}} \cdot e^{\left(\frac{1}{2}\left(\frac{\xi}{\lambda}\right)^2 \ln(w)^2\right)}$	$\frac{\mu}{\lambda}$	$\left(\frac{\xi}{\lambda}\right)^2$
Delta function	$\delta_{n,\mu/\lambda}$	$w^{-\frac{\mu}{\lambda}}$	$\frac{\mu}{\lambda}$	0

Table 3.5. Transforms of some one-dimensional probability mass functions. The discrete \mathbb{W} transform can be used to solve partial difference equations and then to calculate the moments of the resulting distributions, without having to explicitly determine the inverse transform, \mathbb{W}^{-1} . The common distributions have been extensively studied, are well understood and provide a means of testing the theory from the last section.

the moments were calculated using the methods in the previous section. They agree with the standard results in the literature (Abramowitz and Stegun 1970). An interesting feature of the sampled-Gaussian distribution is that the sampling process does not affect the value of the mean or the variance. All the small errors introduced by the sampling process cancel out, in the case of the Gaussian function, at least as far as the *moments* are concerned. This is not generally true of all functions. In general, the Riemann sum of a sampled function differs from the true indefinite integral. This is evident if one studies the error formulae for the rectangle rule for integration, for example (Chapra 2006). There is no *a priori* reason to expect that the moments of the discrete sampled-Gaussian would be identical with the moments of the original real Gaussian function, especially if the sampling length, λ , were very large. This invariant property suggests that Gaussian functions might be useful as basis functions, especially where the intention is to calculate moments.

3.7.6 Parrondo's Game A

If we play a uniform sequence of Parrondo's Game A then the generator method can be applied. The definition of the generator for Parrondo's Game A is determined by the rules of the game:

$$\alpha(w) = \left(\frac{1}{2} - \epsilon\right) \cdot w^{-1} + \left(\frac{1}{2} + \epsilon\right) \cdot w^{+1}. \quad (3.125)$$

3.7 Estimating the moments of Parrondo's games

The moments of a uniform sequence of Parrondo's game A can be calculated by applying Equations 3.123 and 3.122 to obtain

$$\mu_1'(m) = -2\epsilon m \quad (3.126)$$

and

$$\sigma^2(m) = 4 \cdot \left(\frac{1}{2} + \epsilon\right) \cdot \left(\frac{1}{2} - \epsilon\right) \cdot m, \quad (3.127)$$

which are consistent with numerical simulations of Parrondo's Game A.

3.7.7 Taleb's game, a game with highly asymmetrical rewards

The Bernoulli process and Parrondo's Game A are examples of a more general process where there is chance involved and there are rewards. More generally, these rewards are *outcomes*, which can be positive or negative. An interesting case is a game described by Taleb (2004), where the probabilities and rewards are highly asymmetrical.

Using the same language that was used to define Parrondo's games, we can define Taleb's game as:

$$q_{n,n+R_1} = \mathbf{P}[\text{Reward } R_1] = q \quad (3.128)$$

$$q_{n,n+R_2} = \mathbf{P}[\text{Reward } R_2] = 1 - q, \quad (3.129)$$

where R_1 and R_2 are the *rewards*. Taleb's original game required that $q = q_{n,n+R_1} = 999/1000$, $R_1 = +\$1$, $(1 - q) = q_{n,n+R_2} = 1/1000$ and $R_2 = -\$10,000$. The issue is that the investor may become accustomed to the small rewards presented by R_1 and forget about the large, but infrequent, penalty, or negative reward¹⁴, represented by R_2 . This game was surprisingly prescient. It was devised long before the *sub-prime mortgage crisis*¹⁵. Of course, Taleb's game is an extremely simplified model but it does describe certain key aspects of asymmetrical investment situations. Taleb's game can

¹⁴Taleb refers to this infrequent but catastrophic event, which cannot be logically deduced from past experience, as a *black swan* event. This is a reference to the writings of John Stuart Mill.

¹⁵Kiviat (2007) described the essence of the sub-prime crisis as follows: "At its core, the entire process is based on using borrowed money (home mortgages) as collateral to borrow more money (mortgage-backed securities) to borrow yet more money (CDOs [Collateralized-Debt-Obligations]), and hoping that the payment chain doesn't break. Once home mortgage defaults rise, the whole system can unravel." A scholarly, although less concise description is found in (Krinsman 2007). Soros (2008) provides a very philosophical view of the credit crisis of 2008, and what it probably means for the future of financial markets.

Process	Generator
Bernoulli	$\alpha(w) = q \cdot w^{-1} + (1 - q) \cdot w^0$
Parrondo's Game A	$\alpha(w) = (\frac{1}{2} - \epsilon) \cdot w^{-1} + (\frac{1}{2} + \epsilon) \cdot w^{+1}$
Taleb's game	$\alpha(w) = q \cdot w^{-R_1} + (1 - q) \cdot w^{-R_2}$

Table 3.6. The generators for some stationary stochastic processes. The Bernoulli process, Parrondo's Game A, and Taleb's game are really just re-scaled versions of the same process. The same method of analysis can be used to calculate the moments for all of these processes.

be analysed using the techniques given in the previous section, even though is an extremely asymmetrical game. The generators for various stationary stochastic processes are given in Table 3.6. Equations 3.123 and 3.122 can be applied to obtain

$$\mu_1'(m) = (q \cdot R_1 + (1 - q) \cdot R_2) \cdot m, \quad (3.130)$$

which is as expected. The variance is given by

$$\sigma^2(m) = q \cdot (1 - q) \cdot (R_1 - R_2)^2 \cdot m. \quad (3.131)$$

These results are consistent with numerical simulations of Taleb's game. The relationship to the Bernoulli process is clear. In fact, The Bernoulli process *is* Taleb's game with $R_1 = +1$ and $R_2 = 0$. Parrondo's Game A is Taleb's game with $R_1 = +1$, $q = 1/2 - \epsilon$, $R_2 = -1$ and $(1 - q) = 1/2 + \epsilon$, so Taleb's game generalises the Bernoulli process and Parrondo's game A. The moments of all of these stationary stochastic processes can be calculated using Equations 3.130 and 3.131.

If we use Taleb's original values, and units¹⁶, then we obtain $\mu_1' = -9.001 \cdot m$ \$ and $\sigma^2 = 99,919.980999 \cdot m$ \$². In terms of powers of ten we have approximately $\mu_1' \approx -10^1 \cdot m$ \$ and $\sigma^2 \approx 10^5 \cdot m$ \$². Taleb pointed out that the process is losing and that a typical player might have to play for a long time before discovering this fact. This is true. Another way of looking at the same situation is that the process is also extremely volatile. The sample paths may stray a very large distance from the mean line

¹⁶The units of discrete position, n , for a sampled Brownian ratchet device are dimensionless. The SI units for the sampling length, λ , are in metres. If the games are used to represent games of chance, played for money, then the units of discrete position, n , are still dimensionless, but the units of the sampling length are now those of currency. For Taleb's game, this is US dollars, \$, or equivalently, \$¹. The units of variance in Taleb's game will be the units of the square of the sampling length, \$².

3.7 Estimating the moments of Parrondo's games

of expectation, described by Equation 3.130. This divergence may be very positive, and lure investors into a sense of false optimism or it may be very negative, which would be disastrous for the individual investor. It would be very easy to lose a lot of money by playing Taleb's game, even if the coefficients were adjusted to make the mean rate of return slightly positive. It is possible to overcome this volatility, by creating an ensemble of many thousands of independent sample paths of Taleb's game. This is effectively what large insurance companies and investment trusts attempt to do. The key problems are adjusting the coefficients to make the expected return positive and ensuring that the individual sample paths are *truly* independent. A correlated downturn in all of the sample paths at the same time would be a disaster, like the great crash of 1929 (Galbraith 1954). Taleb's point is that, every now and then, disasters do happen.

3.7.8 Difference equations with periodic coefficients

Parrondo's Game B differs significantly from Game A because it is not uniform in space. This makes the generator, $\alpha(w)$, harder to calculate, even if we apply a strictly uniform sequence of Game B in time, which makes the process stationary, in time. Some new fundamental theory has to be developed, to deal with spatially-periodic stochastic processes, such as Parrondo's Game B. Fortunately, discrete transforms have symmetries, which can be exploited in the case of periodic functions. This capability was known from the earliest application of discrete transform (Jury 1964).

Multiplexed spatial functions

The function of multiplexing is widely used in electrical engineering for compiling a single sequence of sampled values from some other set of less-frequently sampled signals (Proakis and Manolakis 1992). Mathematical analysis of the process of multiplexing led Shannon to arrive at his celebrated sampling theorem (Lüke 1999).

For our immediate purpose, we shall use other symbols to indicate the functions, to be multiplexed. We can imagine a function of discrete-position, p_n , which is composed from multiplexed copies of another function of discrete-position, f_n . The simplest form of multiplexing is to space the function out, f_n , modulo L and to pack the intervening spaces with zeros. We can write:

$$p_n = f_n \text{ if } (n \bmod L) = 0$$

$$p_n = 0 \text{ if } (n \bmod L) \neq 0.$$

We could say that p_n is a re-packing of f_n with a spatial period of L , and with zero packing, in between. This can be more formally written in terms of the Kronecker delta tensor, $\delta_{n,v}$:

$$p_n = \sum_{v=-\infty}^{+\infty} \delta_{\text{floor}(v/L),0} \cdot f_{\text{floor}(v/L)}. \quad (3.132)$$

The delta function selects the appropriate elements of f_n and inserts it in the correct position in the sequence for p_n . If we take the \mathbb{W} transform of Equation 3.132 then we obtain:

$$\mathbb{P}(w) = \sum_{v=-\infty}^{+\infty} w^{-L \cdot v} f_v = \mathbb{F}(w^L) \quad (3.133)$$

so the \mathbb{W} transform of the interleaved function p_v is the \mathbb{W} transform of the original function, evaluated at w^L . Suppose now that we have a finite set of base functions, $f_{u,v}$, where $0 \leq u \leq L-1$, and u is an index to select the required base function and v is a dummy variable to stand in for the spatial variable. We can multiplex these base functions by spacing, zero-padding, shifting and then adding. The multiplexing function is best described in terms of the mod and floor functions. Of course, we can express any integer, n , in terms of a quotient and a remainder, $n = L \cdot \text{floor}(n/L) + \text{mod}(n, L)$. The formula for the multiplexed function then takes on the form:

$$p_n = f_{u,v} = f_{\text{mod}(n,L), \text{floor}(n/L)} \quad (3.134)$$

and if we take the \mathbb{W} transform of this form, we obtain

$$\mathbb{P}(w) = \sum_{u=0}^{L-1} w^{-u} \cdot \mathbb{F}_u(w^L), \quad (3.135)$$

which is just a sum of functions of the type used in Equation 3.133.

The moments of multiplexed spatial functions

To evaluate the moments of the multiplexed function, we need to evaluate the derivatives of the \mathbb{W} transform of the multiplexed function. We can explicitly write:

$$\frac{\partial \mathbb{P}(w)}{\partial w} = \sum_{u=0}^{L-1} \frac{\partial}{\partial w} \left(w^{-u} \cdot \mathbb{F}_u(w^L) \right) \quad (3.136)$$

3.7 Estimating the moments of Parrondo's games

and conclude that

$$E [n] = -\frac{\partial \mathbb{P}(w)}{\partial w} \Big|_{w=1} = -L \cdot \sum_{u=0}^{L-1} \frac{\partial \mathbb{F}_u(w)}{\partial w} \Big|_{w=1} + \sum_{u=0}^{L-1} u \cdot \mathbb{F}_u(1). \quad (3.137)$$

The expected values, evaluated with respect to the base functions, $\mathbb{F}_u(w)$, are expanded by a factor of L and there is a correction term, which allows for the effects of the off-sets, u .

The formula for the non-central second moment is similar but more complicated

$$\begin{aligned} E [n^2] &= \frac{\partial^2 \mathbb{P}(w)}{\partial w^2} \Big|_{w=1} + \frac{\partial \mathbb{P}(w)}{\partial w} \Big|_{w=1} \\ &= \sum_{u=0}^{L-1} L \cdot \frac{\partial^2 \mathbb{F}_u(w)}{\partial w^2} \Big|_{w=1} \\ &\quad + \sum_{u=0}^{L-1} (L^2 - 2Lu) \cdot \frac{\partial \mathbb{F}_u(w)}{\partial w} \Big|_{w=1} \\ &\quad + \sum_{u=0}^{L-1} u^2 \cdot \mathbb{F}_u(1) \end{aligned} \quad (3.138)$$

$$(3.139)$$

and if we are given the \mathbb{W} transforms of the base functions, $\mathbb{F}_u(w) = \mathbb{W} [f_{u,n}]$ then we can calculate the moments of the composite function, p_n .

3.7.9 Parrondo's game B

The question that remains is whether we can use the equations for Parrondo's games to arrive directly at transforms for the multiplexed function components, $f_{u,v}$ in Equation 3.134. We could then apply Equations 3.137 and 3.138 to obtain the moments. Once we allow that Parrondo's Game B has different probabilities of transition, which vary with a spatial modulo of $L = 3$, then we obtain three coupled sets of difference equations,

$$p_{m+1,3l} = \left(\frac{3}{4} - \epsilon\right) \cdot p_{m,3l-1} + \left(\frac{1}{4} + \epsilon\right) \cdot p_{m,3l+1} \quad (3.140)$$

$$p_{m+1,3l+1} = \left(\frac{1}{10} - \epsilon\right) \cdot p_{m,3l} + \left(\frac{1}{4} + \epsilon\right) \cdot p_{m,3l+2} \quad (3.141)$$

$$p_{m+1,3l+2} = \left(\frac{3}{4} - \epsilon\right) \cdot p_{m,3l+1} + \left(\frac{9}{10} + \epsilon\right) \cdot p_{m,3l+3}. \quad (3.142)$$

If we take the \mathbb{W} transform of these equations and choose the notations, $n = 3l + u$ and $\mathbb{W} [p_{m,3l+u}] = \mathbb{F}_{m,u} (w)$, to avoid overloading the symbol $\mathbb{P}_m (w)$, which has already been used in earlier sections. We arrive at a matrix equation

$$[\mathbb{F}_{m+1,0}(w), \mathbb{F}_{m+1,1}(w), \mathbb{F}_{m+1,2}(w)] = [\mathbb{F}_{m,0}(w), \mathbb{F}_{m,1}(w), \mathbb{F}_{m,2}(w)] \times \mathbf{G}(w), \quad (3.143)$$

where $\mathbf{G}(w)$ is given by

$$\mathbf{G}(w) = \begin{bmatrix} 0 & \left(\frac{1}{10} - \epsilon\right) & \left(\frac{9}{10} + \epsilon\right) \cdot w^{+1} \\ \left(\frac{1}{4} + \epsilon\right) & 0 & \left(\frac{3}{4} - \epsilon\right) \\ \left(\frac{3}{4} - \epsilon\right) \cdot w^{-1} & \left(\frac{1}{4} + \epsilon\right) & 0 \end{bmatrix}. \quad (3.144)$$

This can be written in a more concise form¹⁷

$$\underline{\mathbb{F}}_{m+1} (w) = \underline{\mathbb{F}}_m (w) \cdot \mathbf{G}(w). \quad (3.145)$$

If we allow an initial condition $\underline{\mathbb{F}}_0 (w) = [1, 0, 0]$, which is appropriate for an initial condition of a delta function then we can write down the solution explicitly

$$\underline{\mathbb{F}}_m (w) = \underline{\mathbb{F}}_0 (w) \cdot \mathbf{G}(w)^m. \quad (3.146)$$

It should be clear that the transition matrix $\mathbf{G} (w)$ in Equation 3.146 plays an analogous role to the generator $\alpha (w)$ in Equation 3.118. The effect of multiplexing is to replace the original 1×1 generator with an $L \times L$ array. We can refer to $\mathbf{G} (w)$ as a generating matrix. It is also worth noting that the generating matrix, $\mathbf{G} (w)$, has a very similar format to the one-step transition matrix, defined by Pearce (2000b),

$$\mathbf{P} = \begin{pmatrix} 0 & r_1 & 1 - r_1 \\ 1 - r_2 & 0 & r_2 \\ r_3 & 1 - r_3 & 0 \end{pmatrix}. \quad (3.147)$$

¹⁷Here we use bold characters, \mathbf{G} , to represent matrices, bold double-stroke characters, \mathbb{F} , to represent discrete transforms of functions of position and/or time. We could represent vectors as degenerate cases of matrices, where one dimension is collapsed to a single row, but this would tend to be ambiguous. We use an underscore, $\underline{\mathbb{F}}_m (w)$, to indicate a row vector. The double-stroke bold font indicates that the objects in the vector are transforms. The subscript, m , indicates that these spatial transforms were evaluated at discrete-time m . The complex argument, w , indicates that discrete space, n , has been transformed out and has been replaced with the complex variable, w . We can use an underscore and a transpose superscript \underline{u}^T to indicate a column vector.

3.7 Estimating the moments of Parrondo's games

This is a stochastic matrix, with unit row sums (Meyer 2000). All the matrix elements are one-step probabilities of transition. The matrices, $\mathbf{G}(w)$ and \mathbf{P} , are very similar if we allow $r_1 = \frac{1}{10} - \epsilon$, $r_2 = \frac{3}{4} - \epsilon$ and $r_3 = \frac{3}{4} - \epsilon$. The generating matrix, $\mathbf{G}(w)$, differs from \mathbf{P} because it contains the operator, w , which ranges over the entire complex plane. Pearce's transition matrix, \mathbf{P} , is only relevant to Parrondo's games under certain asymptotic conditions but the generating matrix, $\mathbf{G}(w)$, describes the evolution of the system at all positions, although position appears indirectly, as operator w . The presence of the operator, w , in the generating matrix, $\mathbf{G}(w)$, accounts for the indefinite periodic extension of the matrix in discrete space, n .

If we keep to the convention of using the symbol, q , to represent probabilities of transition, and we use the format suggested by Pearce in Equation 3.147, then this suggests the following general form for the generating matrix for Parrondo's games:

$$\mathbf{G}(w) = \begin{pmatrix} 0 & q_1 & (1 - q_1) \cdot w^{+1} \\ 1 - q_2 & 0 & q_2 \\ q_3 \cdot w^{-1} & 1 - q_3 & 0 \end{pmatrix}. \quad (3.148)$$

Of course, we reproduce Parrondo's game B by choosing, $q_1 = \frac{1}{10} - \epsilon$, $q_2 = q_3 = \frac{3}{4} - \epsilon$ and $\epsilon = \frac{1}{200}$. Parrondo's game A can also be represented within this framework, using $q_1 = q_2 = q_3 = \frac{1}{2} - \epsilon$ and $\epsilon = \frac{1}{200}$.

Equation 3.146 can be solved by taking the temporal \mathbb{Z} -transform and performing some algebraic simplification,

$$\underline{\mathbb{F}}(z, w) = \underline{\mathbb{F}}_0(w) \cdot \left(\mathbf{I} - z^{-1} \cdot \mathbf{G}(w) \right)^{-1}. \quad (3.149)$$

This is the matrix extension of the one-dimensional Equation 3.117, for functions that have not been multiplexed. The more complicated matrix form, in Equation 3.149, is needed when the transition probabilities are periodic in space and we are using multiplexed functions to represent the solution. We can solve explicitly for the transforms of the base functions

$$\underline{\mathbb{F}}(z, w) = [1, 0, 0] \times \mathbf{H}(z, w), \quad (3.150)$$

where $\mathbf{H} = \mathbf{H}(z, w)$ is defined by

$$\mathbf{H} = \begin{bmatrix} +1 & -z^{-1} \cdot \left(\frac{1}{10} - \epsilon\right) & -z^{-1}w^{+1} \cdot \left(\frac{9}{10} + \epsilon\right) \\ -z^{-1} \cdot \left(\frac{1}{4} + \epsilon\right) & +1 & -z^{-1} \cdot \left(\frac{3}{4} - \epsilon\right) \\ -z^{-1}w^{-1} \cdot \left(\frac{3}{4} - \epsilon\right) & -z^{-1} \cdot \left(\frac{1}{4} + \epsilon\right) & +1 \end{bmatrix}^{-1} \quad (3.151)$$

This can also be written in the concise form

$$\underline{\mathbb{F}}(z, w) = \underline{\mathbb{F}}_0(w) \cdot \mathbf{H}. \quad (3.152)$$

This relates the transforms of the solutions, $\underline{\mathbb{F}}(z, w)$, to the initial conditions, $\underline{\mathbb{F}}_0(w)$, through the operator matrix, $\mathbf{H}(z, w) = (\mathbf{I} - z^{-1} \cdot \mathbf{G}(w))^{-1}$. Equation 3.152 describes the evolution of the system at all times and at all positions, although time and position appear indirectly, as operators, z and w . Equation 3.152 is a more generalised matrix version of the special case described in Equation 3.117.

The next step is to explicitly solve Equation 3.150 for the \mathbb{W} transforms of the base functions, $\underline{\mathbb{F}}_u(z, w)$ and then to apply Equations 3.137 and 3.138 to evaluate the moments of the process, for Parrondo's Game B, explicitly.

3.7.10 The small-matrix representation of Parrondo's games

At time m , the time varying probabilities are a function of spatial position, n , and are denoted by $p_{m,n}$. At one time-step earlier, the time varying probabilities are $p_{m-1,k}$, where the discrete time is $m - 1$ and the discrete position is k . The laws of conditional probability imply that

$$p_{m,n} = \sum_{k=-\infty}^{+\infty} p_{m-1,k} \cdot q_{m-1,k,n} \quad (3.153)$$

where $q_{m-1,k,n}$ is the conditional probability from discrete position k to discrete position n at discrete time $m - 1$.

Our immediate purpose is to study the effect of aggregation of states, modulo- L . In Parrondo's original games, this parameter is $L = 3$. In order to avoid the excessive use of subscripts, we will use the convention that time subscript on the left-hand side of the equations is m and the subscript on the right hand side is $m - 1$. In order to preserve this convention, we refrain from swapping terms across the equals sign, during

3.7 Estimating the moments of Parrondo's games

algebraic manipulations. This means that we can re-write Equation 3.153 as

$$p_n = \sum_{k=-\infty}^{+\infty} p_k \cdot q_{k,n}. \quad (3.154)$$

Reduction modulo- L requires us to consider the structure of the transition probabilities, $q_{k,n}$. For Parrondo's original games, with $L = 3$, this structure has a tri-diagonal form. The first three rows, with $0 \leq k \leq 2$ appear as follows:

$$\begin{array}{ccccc} q_{0,-1} & q_{0,0} & q_{0,1} & 0 & 0 \\ 0 & q_{1,0} & q_{1,1} & q_{1,2} & 0 \\ 0 & 0 & q_{2,1} & q_{2,2} & q_{2,3}. \end{array} \quad (3.155)$$

After reduction modulo-3, the matrices should take the form, indicated by the one-step transition matrix, defined by Pearce (2000b), shown in Equation 3.147. We reproduce the structure here:

$$\begin{array}{ccc} r_{1,1} & r_{1,2} & r_{1,3} \\ r_{2,1} & r_{2,2} & r_{2,3} \\ r_{3,1} & r_{3,2} & r_{3,3}. \end{array} \quad (3.156)$$

We expect relationships to exist between $r_{1,1}$ and $q_{0,0}$, and $r_{1,2}$ and $q_{0,1}$, and $r_{2,1}$ and $q_{1,0}$, and $r_{2,2}$ and $q_{1,1}$, and $r_{2,3}$ and $q_{1,2}$, and $r_{3,2}$ and $q_{2,1}$, and $r_{3,3}$ and $q_{2,2}$. These follow the fairly simple rule that relationships exist between $r_{k+1,n+1}$ and $q_{k,n}$. The offset of +1 in the subscripts is for historical reasons, because of the way that they were chosen in (Pearce 2000b). After reduction, modulo-3 we also expect a relationship between $r_{1,3}$ and $q_{0,-1}$, which is of the form $r_{k+1,n+1}$ and $q_{k,n+3}$. The additional increment, of 3, is due to reduction modulo-3. This reduction also assumes that $q_{0,2} = 0$, which is true for Parrondo's original games. After reduction, modulo-3 we also expect a relationship between $r_{3,1}$ and $q_{2,3}$, which is of the form $r_{k+1,n+1}$ and $q_{k,n-3}$. The additional decrement, of 3, is due to reduction modulo-3. This reduction also assumes that $q_{2,0} = 0$, which is true for Parrondo's original games.

In consideration of these requirements, there are three important factors to be considered in the reduction of a general structure $q_{k,n}$ to a reduced matrix $r_{i,j}$:

- reduction modulo-3
- the historical offsets in subscripts , $k + 1$ and $n + 1$

- The tri-diagonal aspect of the games $|k - n| > 1 \Rightarrow q_{k,n} = 0$, so some terms do not enter into the summation.

To achieve a reduction modulo- L , we can re-write the subscript n to take the form, $n = L \cdot u + j - 1$, where L is the modulo base, and u and $j, 0 \leq j \leq L - 1$ are integers. This leads to a summation formula of

$$r_{i,j} = \sum_{u=-\infty}^{+\infty} q_{i-1, L \cdot u + j - 1}, \quad (3.157)$$

together with the rule that most terms in the summation make no contribution, because $|k - n| > 1 \Rightarrow q_{k,n} = 0$. We can also sum the probability vectors, p_n , modulo- L to obtain a reduced row vector,

$$s_i = \sum_{u=-\infty}^{+\infty} p_{L \cdot u + i - 1}. \quad (3.158)$$

This reduces the probability vector, modulo- L , subject to the subscript convention, $1 \leq i \leq L$.

The next important question to resolve, is whether (or not) the reductions defined in Equations 3.157 and 3.158 are consistent with the requirements for matrix multiplication. Given We need to show that Equations 3.157 and 3.158 and Equation 3.154 are consistent with the requirement that

$$s_j = \sum_{i=1}^L s_i \cdot r_{i,j}. \quad (3.159)$$

If we begin with Equation 3.159 and directly substitute Equation 3.157, and swap the order of summation then we obtain

$$s_j = \sum_{v=0}^{L-1} \sum_{u=-\infty}^{+\infty} p_{L \cdot u + v} \cdot r_{L \cdot u + v + 1, j}. \quad (3.160)$$

Normally, these summations cannot be separated, but for $L \geq 3$, the tri-diagonal nature of $r_{L \cdot u + v + 1, j}$ implies that only one element is present in the entire sum, so the summations can be split, to yield

$$s_j = \left(\sum_{v=0}^{L-1} p_{L \cdot u + v} \right) \cdot \left(\sum_{u=-\infty}^{+\infty} r_{L \cdot u + v + 1, j} \right), \quad (3.161)$$

which then takes the form

$$s_j = \sum_{v=0}^{L-1} s_{v+1} \cdot r_{v+1, j} \quad (3.162)$$

3.8 Chapter summary

and since v is only a dummy summation variable we can re-write this as

$$s_j = \sum_{i=1}^L s_i \cdot r_{i,j}. \quad (3.163)$$

which is of the required form for reduced matrix multiplication, In Equation 3.159 as used in (Pearce 2000b), provided that $L \geq 3x$.

We have shown that it is possible to represent the large tri-diagonal games of the form in Equation 3.153 in the reduced form of Equation 3.162. The important factors that make this reduction possible are, the periodic (modulo- L) spatial structure of the games, careful choice of subscript conventions and the tri-diagonal structure of the transition probabilities $|k - n| > 1 \Rightarrow q_{k,n} = 0$.

3.8 Chapter summary

In this chapter, Parrondo's games (which are a set of Partial Difference Equations) are placed on a sound physical basis, by relating the difference equations to the diffusion of Brownian particles. We obtained the equations for Parrondo's games by sampling the Fokker-Planck equation description of a flashing ratchet. Techniques were derived for estimating the moments of Parrondo's games. These techniques can be applied to difference equations with periodic coefficients, which reduce to functions that are multiplexed in space, or in time. Finally, the small-matrix representation of Parrondo's games has been placed on a more rigorous basis. In the next chapter, these ideas are applied to a number of discrete games of chance that appear in the literature.

Chapter 4

Rates of return from discrete games of chance

IT can be shown that if we allow the diffusive system, represented by Parrondo's original games, to evolve for a very long time, as $m \rightarrow \infty$, then the solution has a periodic factor, both in space and in time. If the only interest is to calculate asymptotic behaviour of the system, as $m \rightarrow \infty$, then it is possible to make use of the periodicity to simplify the way in which the problem is formulated. It is possible to reduce the difference equations, modulo L , in the spatial dimension. This means that it is no longer necessary to manipulate arbitrarily large matrices, or to transform the problem, leading to matrices that contain operators. It is only necessary to manipulate L by L matrices, containing real numbers. These reduced, L by L , matrices have the form of finite discrete games of chance. Parrondo's original formulation of the games was written in this modulo L form. The finite discrete games of Parrondo and Astumian are discussed, analysed and compared. The history of these games, and their analysis, is also documented.

4.1 Some definitions of terms

We review the relevant properties of Markov transition operators and then introduce some terminology and visualisation techniques from the theory of dynamical systems. We will then use these tools, later in the chapter, to define and investigate some interesting properties of Parrondo's games. We must first discuss and introduce the terms and notation that we will use. The key concepts are :

state A *state* contains all of the information that we need to specify what is happening in the system at any given time. It has a strict and well defined meaning in the study of Markov chains. This is described in the text book Karlin and Taylor (1975) and we preserve their meaning here. In the case of a sampled Brownian ratchet, such as Parrondo's games, the state is indexed as the discrete position in space, n .

state-space Karlin and Taylor (1975) refer to *state-space* as the set of all possible values of the state. In the case of a sampled Brownian ratchet, this is the set of all possible values of n , which is contained in the set of all integers, \mathcal{Z} , unless boundary conditions are imposed, or the Markov chain is reduced by aggregating states.

transition probabilities are the probabilities of transition from one state to another in a Markov chain. We follow the notation used in Meyer (2000),

$$q_{v,j} = \mathbf{P} [n = j \text{ at time } m + 1 \mid n = v \text{ at time } m] .$$

transition matrix contains the probabilities of transition expressed in matrix form and $[\mathbf{q}]$ refers to the complete set of transition probabilities, $q_{v,j}$, written in matrix form. The usual subscript conventions for matrix indices, $v \in \mathcal{Z}$, and $j \in \mathcal{Z}$ apply (Meyer 2000). The matrices are operators and can be referred to as *Markov transition operators*. If the matrices represent a Markov transition operator then they will be *stochastic matrices*, with row sums of unity and they will have all the standard properties of stochastic matrices (Meyer 2000).

probability distribution vector is the vector of probabilities,

$\underline{p}_m = p_{m,n} = [\cdots p_{-1}, p_0, p_{+1}, p_{+2}, \cdots]$, which specifies the probabilities that the system will be in various states, $n \in \mathcal{Z}$, at a given discrete-time, m (Meyer 2000). In general, this is time varying and can be called the time-varying probability vector. Strictly speaking, this vector only describes our degree of knowledge about the state of a particle, not the actual *state* of the particle. Probability is only

needed because we have limited information about the state. This limitation can arise in a number of ways. We may be considering a large ensemble of Brownian particles. This is the case for a colloidal suspension. There are many individual states, one for each particle. There are too many individual states for us to be able to track each one individually. It is sensible to think in terms of a probability distribution for these states. Alternatively, we may be considering the possible motions of a single particle and it may have been a long time since the last direct observation of the state of that particle. In this case it is sensible to consider the actual sample path of the single particle as belonging to an ensemble of possible sample paths. This attitude is expressed eloquently by Gibbs (1902) who wrote: *“It is in fact customary in the discussion of probabilities to describe anything which is imperfectly known as something taken at random from a great number of things which are completely described.”*

initial probability distribution vector describes our initial degree of knowledge about the state of the system, \underline{p}_0 . If we initially have complete information about the system then this will be a Kronecker delta function. For example, if the particle was at position $n = 0$ at time $m = 0$ then the initial probability distribution vector would be $\underline{p}_0 = \delta_{n,0}$.

phase-space is the abstract space that contains all possible probability vectors, \underline{p}_m . Since all probabilities lie in the closed interval, $[0, 1]$, the phase space will always be embedded within the larger space $[0, 1]^L$ which is the Cartesian product of L independent intervals, where there are a total of L states. It should be noted that L can be very large and still be finite. It is sometimes convenient to ignore the constraints and embed the phase-space within the Euclidean vector space, \mathcal{R}^L .

time evolution The laws of conditional probability result in a very simple form for the time-evolution of the Markov chain $\underline{p}_{m+1} = \underline{p}_m \cdot [\mathbf{q}]$. The case where the Markov transition operator is constant has been extensively studied and is described in text books, such as Karlin and Taylor (1975). The case where the Markov transition operator is a function of discrete time, $[\mathbf{q}] = [\mathbf{q}]_m$ is less well understood. There is some recent work by Douc *et al.* (2004), where bounds are placed on rates of convergence. The main application here is the simulated annealing algorithm. Unfortunately, the results are very complex and it is difficult to see

4.1 Some definitions of terms

how these results could be applied to the rates of return or moments from time-inhomogeneous Markov chains.

4.1.1 Phase space

The phase-space, contains the time-varying probability-vectors, and the stable limiting probability vector, if it exists. It is a vector space in the sense that it satisfies all the axioms for a linear Euclidean vector, as stated in the standard texts, such as space Kolmogorov and Fomin (1970) and Apostol (1974). In this sense, this space resembles *state-space* that is widely used in control theory (Levine 1996). Yates and Goodman (1999) use the term *state probability vector* to refer to the probability vector. This is presumably a passing reference to the analogies between state-space and the space of probabilities in a Markov chain. The use of the word *state* has a special meaning in the theory of Markov chains. Karlin and Taylor (1975) reserve the term *state-space* to refer to the set of all possible values of a random variable. We prefer to avoid confusion and not to overload the use of the word *state*. In classical dynamics there is a space, called *configuration space*, which is used to define the configuration of a mechanical system at any given instant of time. This is summarised in texts such as Lanczos (1949) and Greenwood (1977). This space has some similarities to state-space but it may not be topologically identical with a Euclidean space (Penrose 2004) and may not obey all of the laws required for it to be a vector space, in the strict mathematical sense. There is another abstract vector space, which is widely used in mechanics and statistical mechanics, due to Gibbs (1902) (Perrot 1998) and to Poincaré (Diacu and Holmes 1996). It is called *phase space* and is widely used in text books, such as Reif (1965) and Diacu and Holmes (1996). We propose the use of the term *phase-space* to refer to the space that contains all possible probability vectors for a Markov chain.

Strong analogies exist between the phase-space of physics and the phase-space of Markov chains, but we must be careful not to press these analogies too far since the transition operators are different and they obey different conservation laws.

The set of reachable points, for any system, can be embedded within a larger space such as \mathcal{R}^L . For Markov chains, the law of total probability, $\sum_{n=-\infty}^{+\infty} p_{m,n} = 1$, represents a constraint. This reduces the dimension of the of the set of reachable points, by

one. For example, an L dimensional Markov chain with one constraint can be represented within an $L - 1$ dimensional phase-space, which is naturally embedded within the first, L dimensional space, \mathcal{R}^L . In general, the set of reachable points must lie within the phase-space and we can embed the phase-space within a larger space, if this makes the analysis, or visualisation, easier. We will refer to any larger space, which contains the phase-space as a subspace, as an embedding space. For example we can embed the $L - 1$ dimensional phase-space for an L -dimensional Markov chain within the real Euclidean space \mathcal{R}^L . This is a very convenient representation, both for numerical calculations and for visualisation. For example, Parrondo's original games had three states and the set of reachable points lies on a two dimensional plane, $p_1 + p_2 + p_3 = 1$. Sometimes it is convenient to use the embedding space \mathcal{R}^3 and sometimes it is convenient to represent the phase-space as a subset of a two dimensional space \mathcal{R}^2 .

4.1.2 Limiting fixed-points in phase-space

Time-homogeneous sequences of regular Markov transition operators have unique stable limiting state-probabilities. This was first shown by Erdős *et al.* (1949) and this result appears in many of the standard texts, including Karlin and Taylor (1975), Taylor and Karlin (1998), Norris (1997) and Yates and Goodman (1999). In phase-space this means that the sequence of probability vectors \underline{p}_m converges to a unique value, $\lim_{m \rightarrow \infty} \underline{p}_m = \underline{\pi}$. This steady-state or *stationary* value is referred to as the *stationary probability vector*. The phase-space representations of the probability-vectors converge to unique points.

In contrast, if the sequence of Markov transition operators is not homogeneous in time then the sequence probability-vectors generated by the products of different operators need not converge to a single point, in the phase-space. The conditions for the fixed-point are violated. It is possible to show, by construction, that this is the case for Parrondo's games.

4.1 Some definitions of terms

This is a different issue from periodicity. An operator of the form

$$A = \begin{bmatrix} 0 & 1 & 0 \\ 0 & 0 & 1 \\ 1 & 0 & 0 \end{bmatrix} \quad (4.1)$$

is periodic. If we apply a homogeneous sequence of periodic operators then the probability vector may not converge to a single unique value. There is a fixed point, with $\underline{p} = [1/3, 1/3, 1/3]^T$, but that fixed point cannot be reached just by iterating, with $\underline{p}_{m+1} = \underline{p}_m \cdot A$.

The time varying probability vectors for Parrondo's games do not converge either, but this lack of convergence has a different cause. Parrondo's games are inhomogeneous, not necessarily periodic.

4.1.3 Parrondo's games

In Parrondo's games, the apparently paradoxical situation occurs where individually losing games combine to win. The basic formulation and definitions of Parrondo's games are described in Harmer and Abbott (1999a), Harmer and Abbott (1999b), Harmer *et al.* (2000a), Harmer *et al.* (2000b), Pearce (2000a), Pearce (2000b), Harmer and Abbott (2001) and Toral (2001). A wide range of applications have been suggested. Some of these are described in McClintock (1999), Moraal (2000a) Davies (2001) Reed (2007). A good summary is included in Harmer and Abbott (2002).

Parrondo's games were originally described as games of chance, played for money. This approach to probability has a long history that can easily be traced back as far as *De Ludo Aleae* in 1565, by Cardano (Todhunter 1865, Jaynes 2003). The early work by Pascal and Fermat was motivated by consideration of a problem posed by the Chevalier De Mere, in 1654, regarding gambling on the outcomes of throwing dice (Todhunter 1865). In Parrondo's original formulation, the state variable, n , was the amount of capital a gambler had accumulated, which fluctuates in analogy to the physical position of a particle. Parrondo's games were later shown to be rigorously related to Brownian ratchets (Allison and Abbott 2002, Allison and Abbott 2003b, Toral *et al.* 2003b, Toral *et al.* 2003a), but the language of games and gambling still predominates, in much

of the literature, due to game-theoretic applications.

4.1.4 A definition for Parrondo's games

The games have been formally defined in the previous chapter. A different way of presenting the same ideas is to represent the games as rule-sets or decision trees. This is the logical way to think about the games if one needs to code them for simulation in the time domain. Parrondo's original parameters for the games were $a_1 = a_2 = a_3 =$

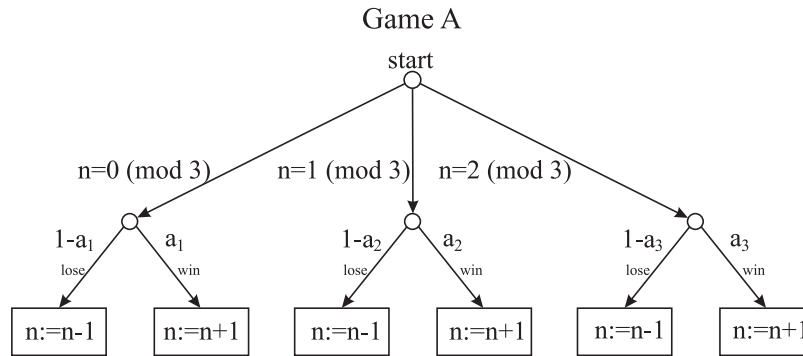


Figure 4.1. The decision tree for Game A. One of the main branches is chosen, depending on the value of $v = n \bmod 3$. A further branch is then taken at random with $P[\text{win}] = a_v$ and $P[\text{lose}] = 1 - a_v$. The corresponding action is then taken. In the case of a win, n is replaced by $n + 1$ and in the case of a loss, n is replaced with $n - 1$. The parameters for this game are essentially the conditional probabilities of a win, $[a_1, a_2, a_3]$. More formally, we can write $a_{v,j} = \mathbf{P}[n = j \bmod 3 \text{ at time } m + 1 \mid n = v \bmod 3 \text{ at time } m]$.

$\frac{1}{2} - \epsilon$, and $\epsilon = \frac{1}{200}$, for Game A, as shown in Figure 4.1. The values for for Game B were $b_1 = \frac{1}{10} - \epsilon$, $b_2 = b_3 = \frac{3}{4} - \epsilon$ and $\epsilon = \frac{1}{200}$, as shown in Figure 4.2. The rules for choosing Game A or Game B, for each trial, are left open to choice. Most studies have selected games at random with $P[\text{Game A}] = \gamma$ and $P[\text{Game B}] = 1 - \gamma$, where γ is a probability, or *mixing parameter*, in the range $0 \leq \gamma \leq 1$. Another popular scheme for choosing the games it to repeat them according to a periodic pattern, rather like a *refrain* in music. We could, for example, repeat the pattern $[A, B, B, A, B]$, to get an indefinite sequence $[A, B, B, A, B, A, B, A, B, B, A, B \dots]$.

4.2 The unconstrained or *large-matrix* formulation

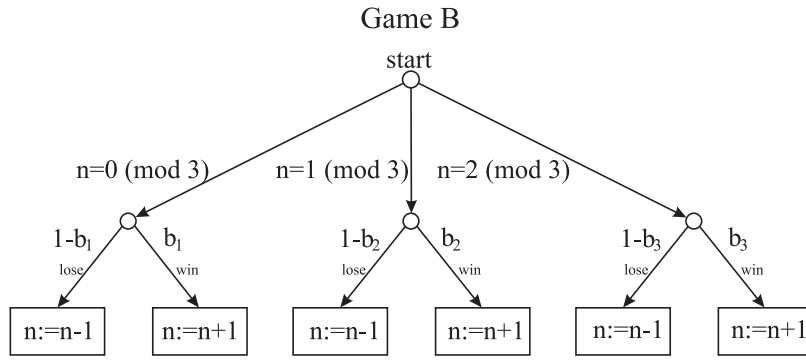


Figure 4.2. The decision tree for Game B. The semantics for Game B are the same as for Game A, in Figure 4.1 excepting that the parameters, $[a_1, a_2, a_3]$ are replaced with different parameters $[b_1, b_2, b_3]$.

4.2 The unconstrained or *large-matrix* formulation

We assume that the physical process has been sampled. The point probabilities at time, m , and position, n , are represented by $p_{m,n}$. The one-step probabilities of transition, from position v to position n at the same time, are represented by, $q_{v,n}$, for a general game¹⁸. It then follows from the laws of conditional probability that

$$p_{m+1,n} = \sum_{\forall v} p_{m,v} \cdot q_{v,n}. \quad (4.2)$$

In principle, the spatial indices can span over the entire set of integers. They can be positive or negative and they can be arbitrarily large in magnitude. We can avoid problems with the infinite limit by regarding the number of dimensions as being potentially very large but still finite, so the symbol $\forall v$ can be interpreted as $v_{\min} \leq v \leq v_{\max}$, for some large, but finite limits, $v_{\min} \in \mathcal{Z}$ and $v_{\max} \in \mathcal{Z}$.

The probabilities of transition would be in a matrix of two potentially indefinitely large dimensions. For example, the Bernoulli process would have a one-step transition matrix of the form:

$$[\mathbf{q}] = \begin{bmatrix} \ddots & & & & & & \\ & \ddots & & & & & \\ & & 1-q & q & & & \\ & & & 1-q & q & & \\ & & & & 1-q & q & \\ & & & & & \ddots & \ddots \end{bmatrix}, \quad (4.3)$$

¹⁸We could have $q_{v,n} = a_{v,n}$, for Game A or $q_{v,n} = b_{v,n}$, for Game B. The choice of letters, a , b , or the more general q , should be clear from the context.

4.2 The unconstrained or *large-matrix* formulation

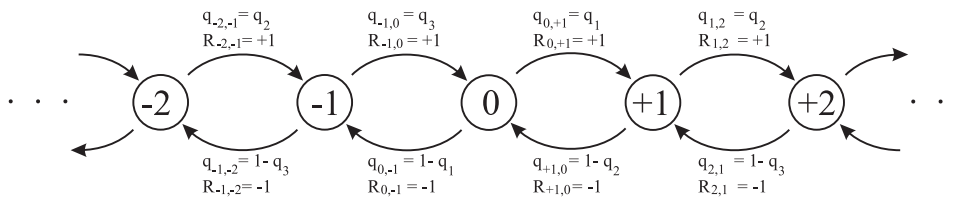


Figure 4.3. State transitions of Parrondo's games, with no limits on position. The values of n are enclosed within the circles that represent states of a discrete Markov process. The arrows represent the transitions between states. The rewards are indicated by $R_{v,n}$. The probabilities of transition are represented by $q_{v,n}$. In general, a transition from state v to state n would have a probability of $q_{v,n}$, and the transition would be associated with a reward of $R_{v,n}$. Indefinitely long state-transition graphs are associated with indefinitely large state-transition matrices, of the type in Equation 4.3.

numerical computing programs, such as Matlab and Octave, have special features for sparse matrices, which require only non-zero matrix elements to be stored. There is also the issue that if the matrices are not *actually* large enough then errors could occur at the boundaries. This is not really a practical problem either, since it is possible to test the boundary elements after each time-step to check whether or not they are still zero. If a problem is about to occur then the matrix can be re-packed, inside a matrix with greater dimensions, to avoid the problem. The results from a simulation with *large matrices* is shown in Figure 4.4.

Throughout this discussion, it should be understood that the matrices may be very large, but not infinite. It might be thought that we could approach infinite matrices, by using sequences of finite matrices and taking a limit. Unfortunately there is no guarantee that the limits will exist. A further problem is that the laws that apply for finite matrices, such as the associative law, do not necessarily apply to infinite operators.

A practical issue with the manipulation of *large* matrices is that it is very difficult to perform *algebraic* manipulations when the matrices become very large. The individual elements inside the vectors and the matrices quickly become very long and complicated. Even if we used a computer-algebra package, such as Maple or Axiom, then the expressions could rapidly expand to the point where they are beyond human comprehension. The longer term aim of analysis must be to seek a symmetry, which allows the problem to be simplified to the point where some human insight can be gained. Exact numerical simulation gives answers but no insight regarding functional forms. Exact

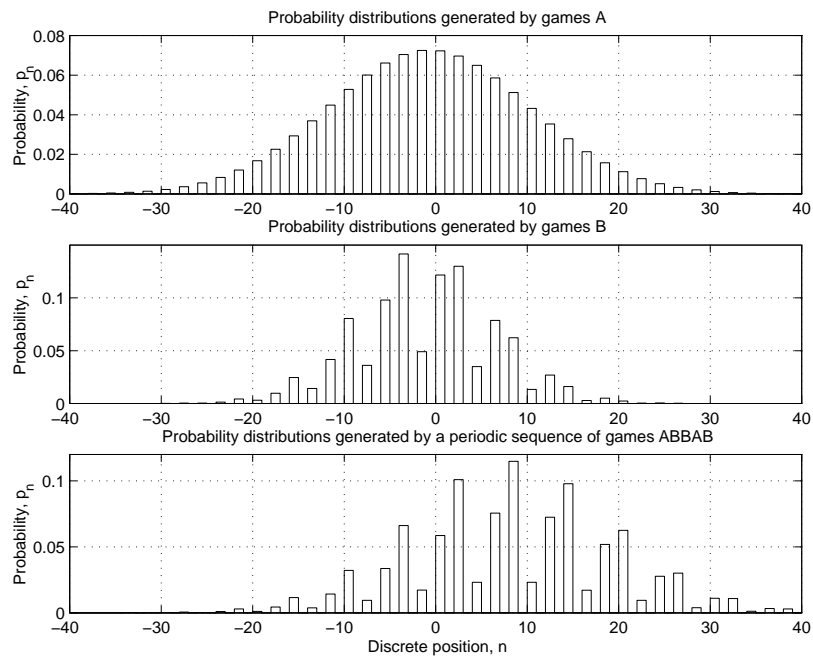


Figure 4.4. Results from a simulation based on the large matrix approach. The horizontal axes represent discrete position, n . The vertical axes represent the point probabilities, p_n of finding a particle at each given position, n . The result for Game A was produced using 40 successive trials of identical copies of Game A. The result for Game B was produced using 40 successive trials of identical copies of Game B. The result for Game C was produced using a periodic mixing of Game A and Game B. This was achieved by repeating the sequence of games $[A, B, B, A, B]$ eight times, giving a total of 40 games in the simulation, which matches the numbers of games in the other simulations. It can be seen that the mean position of the distribution produced by the mixed sequence of games is further to the right than the mean position of the distributions produced by Games A and Game B, individually. This is verified by numerical calculations and by more exact analysis of the asymptotic behaviour of the games.

algebraic expansion of a model can give an answer that is too unwieldy and gives no insight. Our aim is to find a useful approximation that can be solved exactly, and therefore gives insight regarding functional forms. On the other hand, we do not want this approximation to be so coarse that the results are physically unrealistic.

One useful approach is to consider the asymptotic case where the system has been evolving for a long time, $m \rightarrow \infty$. In this case, the modulo 3, spatial symmetry of Parrondo's games is crucial. It is possible to aggregate probabilities of transitions and point probabilities, modulo 3. This results in a smaller set of games, where the number

states of reduced to just three.

4.3 The spatially-periodic case, reduced modulo L

In their original form, Parrondo's games spanned unbounded domains of all integers or all non-negative integers (Harmer and Abbott 1999a). If our interest is to examine the asymptotic behaviour of the games as $m \rightarrow \infty$ and to study asymptotic rates of return or moments then it is possible to reduce these games by aggregating states of the Markov chain modulo three. Surprisingly, we can do this without losing any information about the asymptotic rate of return from the games, as $m \rightarrow \infty$. After reduction, the transition operators for Parrondo's games take the form :

$$[\mathbf{A}] = \begin{bmatrix} 0 & q_1 & 1 - q_1 \\ 1 - q_2 & 0 & q_2 \\ q_3 & 1 - q_3 & 0 \end{bmatrix}, \quad (4.6)$$

where q_0, q_1 and q_2 are the conditional probabilities of winning, given the current state, n , which has been reduced to $n \bmod L$, where $L = 3$. This is the reduced form of the games used by Pearce (2000b). The probability vector also has to be reduced by aggregating all probabilities, p_n , into a finite vector of probabilities, $p_{n \bmod L}$. This is the *small-matrix* formulation of Parrondo's games. The equations for the time-evolution of this system have the same mathematical form as Equation 4.5, for the time-evolution of the large-matrix version of Parrondo's games:

$$\underline{p}_{m+1} = \underline{p}_m \cdot [\mathbf{q}]. \quad (4.7)$$

The main difference is that, with the aggregated approach, the matrices and vectors are smaller. This means that they are easier to manipulate but some information is lost in the process. Information about the short term transient behaviour is lost. It is not possible to recover information about the higher moments of Parrondo's games, unless the small matrices include operators, such as the w and z operators, from the last chapter. A rather surprising result is that the *small-matrix version* of the games does capture enough information for us to make statements about the first moment of Parrondo's games. This is useful because it allows us to calculate the rate at which we are winning (or losing) money in a game of chance, or to calculate the rate of drift of a particle in a Brownian ratchet. If we could calculate the first moment, without having to use the

cumbersome mathematical machinery of discrete w and z transforms, or the need to manipulate extremely large matrices, then we would be making progress. It is useful to be able to estimate the first moment of a set of games, without having to engage in very long or very large calculation.

The state transitions associated with this reduced form of the games are shown in Figure 4.5

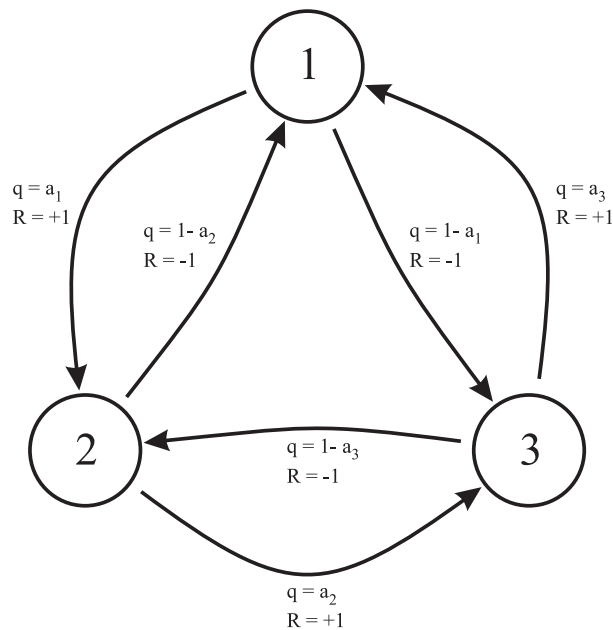


Figure 4.5. State transitions of Parrondo's games, (reduced modulo L). The reduced discrete spatial values, $n \bmod L$, are enclosed within the circles that represent states of a discrete Markov process. The arrows represent the transitions between states. The rewards are indicated by R , without subscripts. The probabilities of transition are represented by q , without subscripts. The absence of subscripts is intended to simplify the figure. In general, a transition from state v to state n has a probability of $q_{v,n}$, and the transition is associated with a reward of $R_{v,n}$. The procedure of reducing the Parrondo's games from the indefinitely large process in Figure 4.3 requires states to be aggregated into equivalence classes, modulo L , and probabilities of transition and rewards have to be averaged. In the case of Parrondo's games there is no particular difficulty in evaluating the averages, since all the rewards and probabilities of transition are identical, modulo L .

4.4 Asymptotic value of the first moment of the games

4.4.1 Markov Chains with Rewards

Parrondo's games can be represented as games of chance, played for rewards. Parrondo's games are Markov chains with rewards. These rewards can be represented in matrix form:

$$R_{v,j} = \text{reward if } [n = j \text{ at time } m + 1 \mid n = v \text{ at time } m]. \quad (4.8)$$

There is a specific reward associated with each specific state transition. We can think of $R_{v,j}$ as the reward that we earn when a transition occurs from state v to state j . For Parrondo's original games we have $R_{v,j} = (j - v) \pmod 3$.

If we play a mixed game, composed from Game A and Game B, then we can represent this mixture as an equivalent game, which we call Game C. In the case of a randomised choice, the matrix for Game C is a linear convex combination of the matrices for Game A and Game B:

$$\mathbf{C} = \gamma \mathbf{A} + (1 - \gamma) \mathbf{B}, \quad (4.9)$$

where $0 \leq \gamma \leq 1$, and γ represents the proportion of the mixing¹⁹. In the case of a deterministic periodic sequence, such as $[A, B, B, A, B]$, then the matrix for the equivalent Game C would have to satisfy:

$$\mathbf{C} = \mathbf{A} \cdot \mathbf{B} \cdot \mathbf{B} \cdot \mathbf{A} \cdot \mathbf{B} \quad (4.10)$$

or more generally

$$\mathbf{C} = \prod_{m=1}^L \mathbf{Q}_m, \quad (4.11)$$

where $\mathbf{Q}_m \in \{\mathbf{A}, \mathbf{B}\}$. The more general \mathbf{Q} matrices are chosen from the matrices for the available games, \mathbf{A} or \mathbf{B} , and the matrix for the equivalent game. Game \mathbf{C} , is an aggregate games that replaces L of the previous Game \mathbf{A} or Game \mathbf{B} .

Each application of the matrix \mathbf{C} now replaces the application of L of the previous operators, \mathbf{A} or \mathbf{B} . This means that the time axis becomes re-scaled. For this reason it is

¹⁹A formal definition of convex combination can be found in Trustrum (1971). A vector \underline{x} is a convex combination of \underline{u}_k , for $1 \leq k \leq N$, if $\underline{x} = \sum_{k=1}^N \lambda_k \underline{u}_k$, where $\lambda_k \geq 0$, and $\sum_{k=1}^N \lambda_k = 1$.

easier to simulate in time steps of $L \cdot \tau$ at each step of the simulation. It is then possible to step forwards by single steps, using Equation 4.7, one game at a time.

The state transition diagrams for Game A and Game B and the time averaged Game C would have identical topology and have identical reward structure, although the probabilities of transition between states would be different. Systems of this type have been analysed by Howard (1960) although we use different notation to perform the necessary multiplications and summations. The essence of his approach is that rewards have to be averaged over transitions between all recurrent states, in proportion to their rate of occurrence. In our notation, the expected reward from each transition of the time-averaged homogeneous process is :

$$\varrho_{v,j} = E [R_{v,j} \cdot C_{v,j}] . \quad (4.12)$$

This is a scalar equation in the real numbers, $R_{v,j}$ and $C_{v,j}$.

4.4.2 A matrix notation for the first moment

If we wish to calculate the mean expected reward, for the whole process, then we must sum over transitions from all recurrent states in proportion to their probability of occurrence. This will be a function of the transition matrix, C , and the relevant stationary probability-vector, Π_C :

$$\varrho [C] = \sum_{v,j} \varrho_{v,j} = \Pi_C \cdot ([R] \circ [C]) \cdot \mathbf{U}^T \quad (4.13)$$

where “ \circ ” represents the Hadamard, or element by element, product and \mathbf{U}^T is a unit column vector of dimension N . Post-multiplication by \mathbf{U}^T has the effect of performing the necessary summation. We recall that Π_C represents the steady-state probability-vector for matrix C . The function $\varrho(C)$ represents the expected asymptotic return, in units of reward, per unit time when the games are played. If we include the definition of C in Equation 4.130 in Equation 4.12 then we can write :

$$\varrho [\gamma[A] + (1 - \gamma)[B]] = E [R_{i,j} \cdot (\gamma A_{i,j} + (1 - \gamma) B_{i,j})] \quad (4.14)$$

$$= \gamma E [R_{i,j} \cdot A_{i,j}] + (1 - \gamma) E [R_{i,j} \cdot B_{i,j}] . \quad (4.15)$$

We can also define :

$$\varrho[A] = \Pi_A ([R] \circ [A]) \mathbf{U}^T \quad (4.16)$$

4.5 The matrix technique for the first moment

and

$$\varrho[\mathbf{B}] = \mathbf{\Pi}_B ([R] \circ [B]) \mathbf{U}^T. \quad (4.17)$$

We make use of Equations 4.16, 4.17, and 4.13 to calculate the asymptotic rates of return from a number of standard games, described in the literature. These equations lead directly to a matrix technique, for calculating the asymptotic value of the first moment.

4.5 The matrix technique for the first moment

4.5.1 Parrondo's original games

We can adopt the notation of Pearce (2000b), and generalise the *small-matrix* forms for Game A and Game B as follows:

$$[\mathbf{A}] = \begin{bmatrix} 0 & a_1 & 1 - a_1 \\ 1 - a_2 & 0 & a_2 \\ a_3 & 1 - a_3 & 0 \end{bmatrix} \quad (4.18)$$

and

$$[\mathbf{B}] = \begin{bmatrix} 0 & b_1 & 1 - b_1 \\ 1 - b_2 & 0 & b_2 \\ b_3 & 1 - b_3 & 0 \end{bmatrix}. \quad (4.19)$$

We recall that Parrondo's original parameters were $a_1 = a_2 = a_3 = 1/2 - \epsilon$, $b_1 = 1/10 - \epsilon$, $b_2 = b_3 = 3/4 - \epsilon$ and $\epsilon = 1/200$. These parameters define a special case of the more general problem, which we consider here.

One form of Parrondo's games is to mix the two games by selecting them at random, with fixed probabilities:

Choose Game A with probability $P[\mathbf{C}' = \mathbf{A}] = \gamma$

Choose Game B with probability $P[\mathbf{C}' = \mathbf{B}] = 1 - \gamma$,

where \mathbf{C}' is the step by step choice, made for the transition matrix for the stochastic process. Since γ is a probability it must be a real number in the range, $0 \leq \gamma \leq 1$. We can define a mixed time-average game

$$\mathbf{C} = E[\mathbf{C}'] = \begin{bmatrix} 0 & c_1 & 1 - c_1 \\ 1 - c_2 & 0 & c_2 \\ c_3 & 1 - c_3 & 0 \end{bmatrix}, \quad (4.20)$$

where $c_1 = \gamma \cdot a_1 + (1 - \gamma) b_1$, $c_2 = \gamma \cdot a_2 + (1 - \gamma) b_2$ and $c_3 = \gamma \cdot a_3 + (1 - \gamma) b_3$. We can express this linear convex combination more concisely as:

$$\mathbf{C} = \gamma \cdot \mathbf{A} + (1 - \gamma) \mathbf{B}. \quad (4.21)$$

The matrix, \mathbf{C} , is a stochastic matrix, with row-sums of one. This matrix will always have at least one eigenvalue of unity and there will always be a stationary distribution vector, $\underline{\pi}_{\mathbf{C}}$, satisfying $\underline{\pi}_{\mathbf{C}} = \underline{\pi}_{\mathbf{C}} \cdot \mathbf{C}$.

We can use standard techniques (Meyer 2000) to evaluate the stationary distribution vector for the mixed game:

$$\underline{\pi}_{\mathbf{C}} = \frac{[1 - c_2 + c_2c_3, 1 - c_3 + c_1c_3, 1 - c_1 + c_1c_2]}{3 - (c_1 + c_2 + c_3) + (c_1c_2 + c_1c_3 + c_2c_3)}, \quad (4.22)$$

which is consistent with the formulae derived by Pearce (2000b). The reward matrix is:

$$R = \begin{bmatrix} 0 & +1 & -1 \\ -1 & 0 & +1 \\ +1 & -1 & 0 \end{bmatrix}, \quad (4.23)$$

so the weighting vector for the rewards is

$$[\mathbf{R} \circ \mathbf{C}] \underline{u}^T = \begin{bmatrix} 2c_1 - 1 \\ 2c_2 - 1 \\ 2c_3 - 1 \end{bmatrix}. \quad (4.24)$$

We can then apply Equation 4.13 to calculate the expected rate of reward:

$$q = \frac{3 \cdot (c_1c_2c_3 - (1 - c_1)(1 - c_2)(1 - c_3))}{c_1c_2c_3 + (1 - c_1)(1 - c_2)(1 - c_3) + 2}, \quad (4.25)$$

which is consistent with the formula in Harmer *et al.* (2000a).

The coefficients, c_n , in Equation 4.25 are dependent on the mixing fraction, γ . If we choose $\gamma = 1$ then the mixed game reduces to a pure sequence of Game A, and if we choose $\gamma = 0$ then the mixed game reduces to a pure sequence of Game B. Games A and B are chosen to be slightly losing, due to the ϵ parameter. In contrast, the mixed game with an intermediate value of γ can be winning, with $q > 0$. The results, for various choices of γ are shown graphically in Figure 4.6. It is clear that q is a non-

4.5 The matrix technique for the first moment

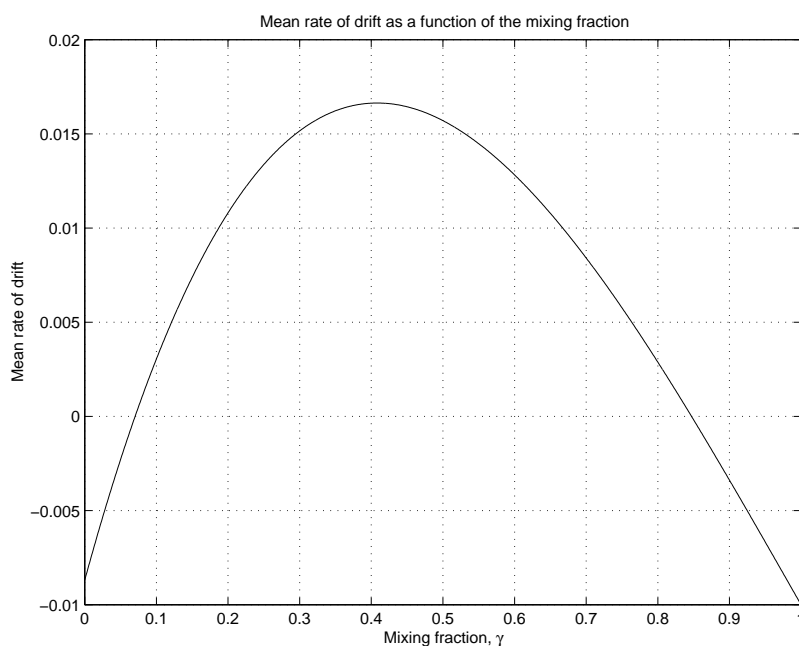


Figure 4.6. Expected rates of return q for various choices of the mixing fraction γ . The parameters for Game A and Game B are fixed, using Parrondo's original values. The parameters for the mixed game, C, are derived as a linear convex combination of the parameters for Game A and Game B according to Equation 4.21. The rate of return for Game C is calculated according to Equation 4.25 and plotted in Matlab.

linear function of the mixing parameter, $q(\gamma)$. Changes of sign are possible because the reward function, q is nonlinear. For example, $q(0) < 0$, $q(1) < 0$ and $q(0.5) > 0$. This change of sign in the rate of return, $q(\gamma)$, with changes in the mixing fraction, γ , has been referred to as *Parrondo's paradox* in the literature (Harmer and Abbott 1999a).

The zero-gain surface

The numerator of Equation 4.25 can be written as

$$\text{numerator} = 3 \cdot (c_1 \cdot c_2 \cdot c_3 - (1 - c_1) \cdot (1 - c_2) \cdot (1 - c_3)), \quad (4.26)$$

which gives rise to a condition for zero-gain, or zero-return, from the games,

$$c_1 c_2 c_3 = (1 - c_1) (1 - c_2) (1 - c_3). \quad (4.27)$$

This is shown graphically in Figure 4.7. The denominator of Equation 4.25 is always positive. Equation 4.27 is not entirely new to physical chemistry. Onsager (1931) derived an equivalent condition for detailed balance in a cyclic chemical reaction. It is an interesting coincidence that the reaction, which was considered had three quasi-stable

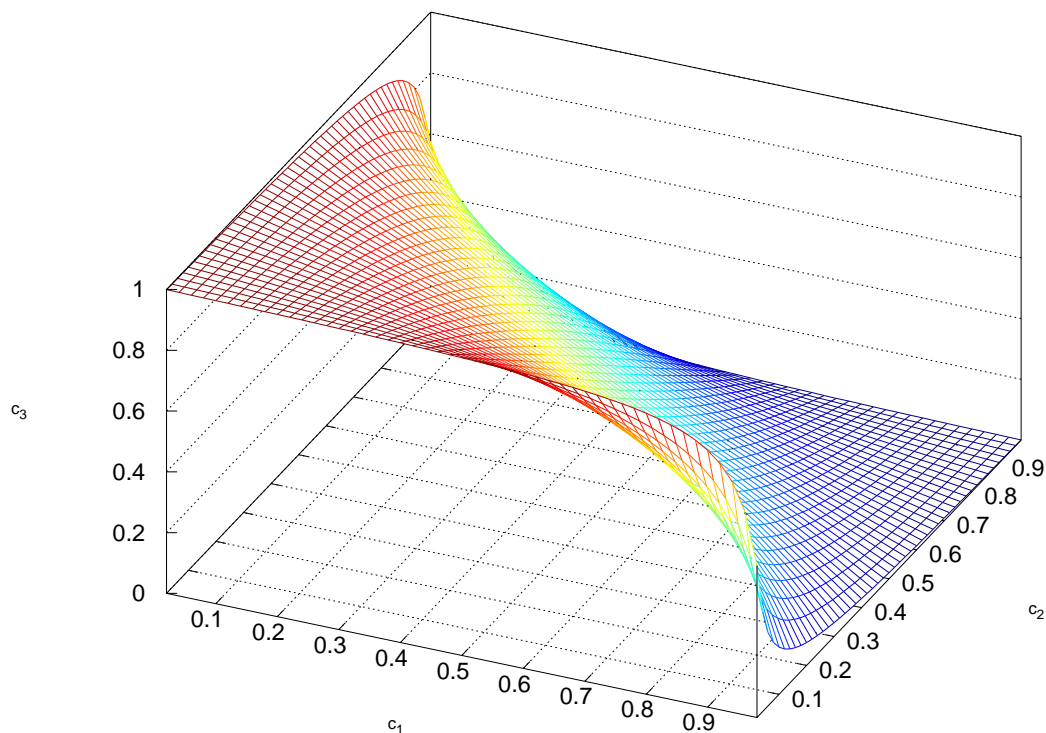


Figure 4.7. The zero-gain surface for Parrondo's games. The condition for zero-return, or zero-gain, from Parrondo's original games is given by $c_1c_2c_3 = (1 - c_1)(1 - c_2)(1 - c_3)$. This condition defines a surface in the parameter-space, $[c_1, c_2, c_3]$. This surface is contained entirely within the cube, defined by $0 \leq c_1 \leq 1$, $0 \leq c_2 \leq 1$ and $0 \leq c_3 \leq 1$. Even a cursory visual inspection reveals that the surface is not a plane. It would be possible to choose points on one side of the surface and the line connecting these points would pass through to the other side of the surface. This is a geometric representation of Parrondo's paradox.

states, A , B and C , as reproduced in in Figure 4.8.

Onsager (1931) assumes that a substance can exist in a homogeneous phase in three different forms, labelled A , B and C . He further assumes that any one of these forms can spontaneously transform itself into either of the others, according to the scheme shown in Figure 4.8. It is assumed that simple laws of mass action apply. This gives rise to a system of linear ordinary differential equations in the total numbers of molecules in

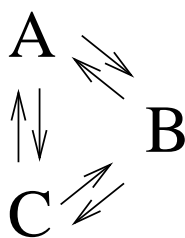


Figure 4.8. The quasi-stable forms in Onsager's model. Onsager (1931) assumes that a substance can exist in a homogeneous phase in three different forms, labelled A , B and C . He further assumes that any one of these forms can spontaneously transform itself into either of the others, according to the scheme shown in this figure.

each phase, n_A , n_B and n_C . These continuous-time differential equations are analogous to the discrete-time difference equations that appear in Parrondo's games. Onsager uses the system of ODEs to derive a condition for equilibrium, which he writes in terms of reaction-rate coefficients:

$$k_{AC} \cdot k_{CB} \cdot k_{BA} = k_{AB} \cdot k_{BC} \cdot k_{CA}. \quad (4.28)$$

If equilibrium is to be possible, then the products of the forward and reverse rates must be equal. This is the condition for detailed balance. The similarity of Equation 4.28 to Equation 4.27 is clear. This is also reflected in the similarity between Figures 4.5 and 4.8. The connection between Onsager's work and Parrondo's games was first pointed out by Van den Broeck *et al.* (1999).

In summary, the condition for zero-return from Parrondo's games is analogous to the condition for detailed balance in a cyclic chemical reaction. If we could vary the rates of reaction by varying some physical parameter then we could possibly disrupt the condition for detailed balance, in the same way that switching between games, in Parrondo's games, can produce a change in the expected return from the games.

4.5.2 The apparent paradox of Parrondo's games

Some commentators have claimed that there is nothing paradoxical about Parrondo's games (Philips and Feldman 2004). Harmer and Abbott (2002) point out that some claims of the absence of paradox are based on a straw-man argument. They also point out that Parrondo's games were never meant to be more than an *apparent paradox*, and

state that Parrondo's paradox is in the same category as *Simpson's paradox*, *the Braess paradox*, and *the renewal paradox*.

Parrondo *et al.* (2000) state that the counterintuitive aspect of Parrondo's games is that "Two losing games can yield, when combined, a paradoxical tendency to win." In this case, *combination* is mathematically represented by forming a linear convex combination of the parameters, which are the conditional probabilities of winning (Harmer and Abbott 2002). Moraal (2000b) points out that the counterintuitive aspect of Parrondo's games is essentially a statement about the convexity, or concavity, of the losing region in the parameter space.

We argue that Parrondo's games are *apparently paradoxical* because the expected rewards from the games differ from what we would expect for games that are composed from completely independent memory-less random events. The apparent paradox is possible, in Parrondo's games, because the conditional probabilities, of winning or losing, depend on the current state of the player. This introduces memory into the process. We represent the long-term expected return from the games using a reward function, ϱ . There are two aspects of the reward function that have been used to describe the apparent paradox:

Non-linear reward function The parameters embedded within the games specify a manifold that can be referred to as *parameter space*. For completely independent random games, the reward function is a linear function of the parameters. Our human intuition has taught us to rely on this as a heuristic rule, because independent random events are common in daily life. Situations that violate the heuristic rule are apparently paradoxical. We will show that a non-linear reward function is a necessary but not sufficient condition for Parrondo's paradox to exist.

Non-Convex winning and losing regions The reward function, ϱ , partitions the parameter space into three disjoint subsets: the winning region with $\varrho > 0$, the losing region with $\varrho < 0$ and the the zero gain region, with $\varrho = 0$. For independent memory-less games, *and* for Parrondo's games, the zero gain region is a surface, with the winning region on one side and the losing region on the other. The *difference* between independent memory-less games and Parrondo's games is that in Parrondo's games: the zero gain surface is not a flat plane, the losing

4.5 The matrix technique for the first moment

region is non-convex, and the winning region is non-convex. This lack of convexity is the essential feature that gives rise to the apparent paradox.

A possible source of confusion

In his famous Tractatus, Wittgenstein (1918) writes:

4.003 Most of the propositions and questions to be found in philosophical works are not false but nonsensical. Consequently we cannot give any answer to questions of this kind, but can only point out that they are nonsensical. Most of the propositions and questions of philosophers arise from our failure to understand the logic of our language. (They belong to the same class as the question whether the good is more or less identical than the beautiful.) And it is not surprising that the deepest problems are in fact not problems at all.

The misuse, misunderstanding, or overloading, of words can lead to great confusion. In Wittgenstein's view²⁰, it is the main task of philosophers to clear up these misunderstandings. This is not science, but it is necessary preparation *before* science can proceed.

In the humble case of Parrondo's games the use of the word "convex" seems to raise pseudo-philosophical issues of the type that Wittgenstein was keen to dispel. This is our attempt at clarification of a few key technical terms:

Convex set: Given a real linear space L , Kolmogorov and Fomin (1970) define a convex set as follows "A set $M \subset L$ is said to be convex if and whenever it contains the points x and y , it also contains the straight line segment joining x and y ." For our present purpose the losing region, with $q > 0$ would be convex if, given any points in the parameter space, \underline{c}_A and \underline{c}_B , with $q(\underline{c}_A) < 0$ and $q(\underline{c}_B) < 0$ then $q(\gamma \cdot \underline{c}_A + (1 - \gamma) \cdot \underline{c}_B) < 0$, for $0 \leq \gamma \leq 1$. An equivalent definition appears in Trustrum (1971).

Convex functional: Kolmogorov and Fomin (1970) define a convex functional as follows "A functional p defined on a real linear space L is said to be convex if (1) $p(x) \geq 0$

²⁰It should be noted that Wittgenstein often changed his views, but his opposition to the inconsistent use of language was constant throughout his career (Monk 1991).

for all $x \in L$ (nonnegativity), and (2) $p(\alpha \cdot x) = \alpha \cdot p(x)$ for all $x \in L$ and for all $\alpha \geq 0$ and (3) $p(x + y) \leq p(x) + p(y)$ for all $x, y \in L$. " Kolmogorov and Fomin (1970) go on to prove a theorem that "if p is a convex functional on a linear space L , and k is any positive real number then the set $\{x : p(x) \leq k\}$ is convex."

Linear convex combination: Trustrum (1971) defines a linear convex combination as follows "A vector \underline{x} is a convex combination of $\{\underline{u}_k\}$, for $1 \leq k \leq N$, if $\underline{x} = \sum_{k=1}^N \lambda_k \underline{u}_k$, where $\lambda_k \geq 0$, and $\sum_{k=1}^N \lambda_k = 1$." He goes on to state that "The convex hull of a set $\mathbf{X} \subset \mathcal{R}^n$, written $\langle \mathbf{X} \rangle$, is the set of all convex combinations of points in \mathbf{X} . If \mathbf{X} is a finite set then the convex hull is called a convex polytope." Using this definition, the convex hull of a finite set of vectors, $\{\underline{u}_k\}$, is a convex set.

Concave functional: A functional p defined on a real linear space L is said to be concave if $-p$ is convex. Using this definition, there are functionals that are neither convex, nor concave. The use of the word "concave" when we really mean "non-convex" is a source of confusion and we have avoided this usage. If a set is non-convex then it can be said to lack the property of "convexity."

These definitions are relevant to Parrondo's games, as follows:

- The winning region in Parrondo's games is a non-convex set.
- The losing region in Parrondo's games is a non-convex set.
- Game C is a linear convex combination of Game A and Game B, within the space of parameters.
- The reward functional, ϱ , is neither convex nor concave, within the parameters space.

We illustrate these concepts, further, with the aid of worked examples.

4.5 The matrix technique for the first moment

Parameter space

Parameter space is an abstract manifold, constructed by using the parameters of a system as generalised coordinates. For Parrondo's games, the parameter space is a subset of \mathcal{R}^3 , with generalised coordinates, c_1 , c_2 and c_3 that represent the three conditional probabilities of winning under various circumstances (Pearce 2000a). Since the generalised coordinates are probabilities, there are additional constraints, $0 \leq c_1 \leq 1$, $0 \leq c_2 \leq 1$ and $0 \leq c_3 \leq 1$. The entire parameter space is a unit cube, embedded within \mathcal{R}^3 . The three parameters for any given instance of Parrondo's games can be written as a vector $\underline{c} = [c_1, c_2, c_3]$, which is called the parameter vector.

A special two-dimensional case

In Parrondo's original games the parameters have certain symmetries. Game A has the symmetry, $c_1 = c_2 = c_3$, and Game B has the symmetry $c_2 = c_3$. These symmetries have led some investigators to consider only the special two-dimensional case with $c_2 = c_3$. This restricted two-dimensional version of Parrondo's games has a two-dimensional parameter space, spanned by vectors of the type $[c_1, c_2]$, with $0 \leq c_1 \leq 1$ and $0 \leq c_2 \leq 1$. The restricted two-dimensional parameter space is shown in Figure 4.9. A very similar figure, based on spin models, appears in Moraal (2000b). The set of points $[c_1, c_2]$ in the parameter space that corresponds to losing games is called the *losing region*. The set of points $[c_1, c_2]$ in the parameter space that corresponds to winning games is called the *winning region*. The statement, that two losing games can combine to win, is equivalent to saying that the losing region is non-convex. This has been stated in various ways in several papers, (Moraal 2000a, Harmer and Abbott 2001, Allison and Abbott 2001, Harmer and Abbott 2002, Costa *et al.* 2005).

To prove that the losing region is non-convex in the parameter space, we only need to show that it is not convex. We only need one counter-example, to the rules for convexity. Parrondo's original example is sufficient. The rate of return from the games is given by the reward function in Equation 4.25. We can simply evaluate ρ , for the various parameter sets. For Game A the parameter vector is $[c_1, c_2, c_3] = [a_1, a_1, a_1] = [99/200, 99/200, 99/200]$ and the corresponding return from the games is $\rho = -1/100 = -0.01$, which is losing. For Game B the parameter vector is $[c_1, c_2, c_3] = [b_1, b_2, b_2] = [19/200, 149/200, 149/200]$ and the corresponding return from the games is given by,

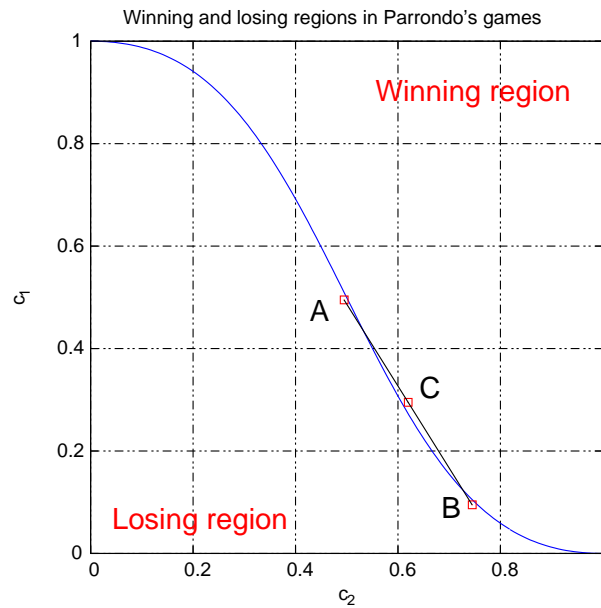


Figure 4.9. The winning and losing regions in the 2D version of Parrondo's games. If we restrict the choice of parameters, by enforcing the constraint, $c_2 = c_3$, then the parameter space only has two dimensions and can be represented using a unit square, shown in this figure. The zero-gain surface collapses to a zero-gain curve with condition $c_1 \cdot (c_2)^2 = (1 - c_1) \cdot (1 - c_2)^2$. The zero-gain curve connects the top left corner, $[c_1, c_2] = [0, 1]$, and bottom right hand corner, $[c_1, c_2] = [1, 0]$, of the figure. The region above the curve, near $[c_1, c_2] = [1, 1]$ is the winning region, with $\rho > 0$. The region below the curve, near $[c_1, c_2] = [0, 0]$ is the losing region, with $\rho < 0$. The parameters for Parrondo's original Game A are represented as the point marked "A" on the figure. The parameters for Parrondo's original Game B are represented as the point marked "B" on the figure. The mixed game C is constructed using equal proportions of Games A and B, with a mixing fraction of $\gamma = 1/2$. Game C is marked as point "C" in the figure. The entire figure, including points A, B and C, is drawn to scale. Points A and B are in the losing region, with $\rho < 0$. This corresponds to the fact that Games A and B are losing, on average. Point C is in the winning region with $\rho > 0$. This corresponds to the fact that Game C is winning, on average. It can be seen that the losing region of the parameter space is non-convex, since some points on the finite line segment joining A and B, such as point C, are not in the losing region. The apparently paradoxical behaviour of Parrondo's games is only possible because the losing region is non-convex. This is one of the issues first discussed by Moraal (2000b).

$\rho = -73,443/8,446,300 \approx -0.0086953$, which is also losing. Both of these points lie below the zero-gain surface in Figure 4.12. The returns associated with these parameters are negative, $\rho[\underline{a}] < 0$ and $\rho[\underline{b}] < 0$. We can create a version of Game C,

4.5 The matrix technique for the first moment

which is an average of Game A and Game B, in the parameter space, $\underline{c} = \frac{1}{2}(\underline{a} + \underline{b})$, which evaluates to $[c_1, c_2, c_3] = [118/400, 248/400, 248/400]$ and the corresponding return from the games is $\varrho = +223/14,200 \approx +0.015704$, which is winning. This lies above the zero-gain surface. The return associated with these, mixed, parameters is positive $\varrho \left[\frac{1}{2}(\underline{a} + \underline{b}) \right] > 0$. This single counter-example is sufficient to prove that the losing region, with $\varrho < 0$, is non-convex. To prove the same result for the winning region, $\varrho > 0$, we only need to exchange all probabilities with their complements $\underline{a}' = [a'_1, a'_2, a'_3] = [101/200, 101/200, 101/200]$, $\underline{b}' = [b'_1, b'_2, b'_3] = [181/200, 51/200, 51/200]$ and $\underline{c}' = [c'_1, c'_2, c'_3] = [282/400, 152/400, 152/400]$. Equation 4.49 is anti-symmetric with respect to complementary exchange. The corresponding returns are the negative of the former gains $\varrho[\underline{a}'] = -\varrho[\underline{a}]$, $\varrho[\underline{b}'] = -\varrho[\underline{b}]$ and $\varrho[\underline{c}'] = -\varrho[\underline{c}]$. This establishes an *anti-Parrondo* effect, which proves that the winning region is non-convex. For Parrondo's games, both the winning and losing regions are non-convex. This can also be seen, intuitively by inspecting Figure 4.9.

In summary, Parrondo's games *do* combine two losing games to create a winning game. In more formal mathematical language, the losing region of Parrondo's games, in the parameter space, is non-convex. There is also an anti-Parrondo effect.

Linear and non-linear reward functions

We investigate the rôle of linearity. A reward function is linear if we can write

$$\varrho(\gamma_1 \cdot \underline{c}_1 + \gamma_2 \cdot \underline{c}_2) = \gamma_1 \cdot \varrho(\underline{c}_1) + \gamma_2 \cdot \varrho(\underline{c}_2), \quad (4.29)$$

for any vectors \underline{c}_1 and \underline{c}_2 in the parameter space and for any real numbers $\gamma_1 \in \mathcal{R}$ and $\gamma_2 \in \mathcal{R}$. This places a very strong constraint on the form of the function. It must be possible to re-write all linear reward functions in the form

$$\varrho(\underline{c}) = \underline{N} \cdot \underline{c}, \quad (4.30)$$

where \underline{N} is a normal vector. The components of \underline{N} are the values reward function for each of the unit vectors of the coordinate system. For a three dimensional coordinate system, this is $\underline{N} = [\varrho(\underline{u}_1), \varrho(\underline{u}_2), \varrho(\underline{u}_3)]$.

The proof that all function of the form of Equation 4.30 are linear is fairly straightforward,

$$q(\gamma_1 \cdot \underline{c}_1 + \gamma_2 \cdot \underline{c}_2) = \underline{N} \cdot (\gamma_1 \cdot \underline{c}_1 + \gamma_2 \cdot \underline{c}_2) \quad (4.31)$$

$$= \gamma_1 \cdot \underline{N} \cdot \underline{c}_1 + \gamma_2 \underline{N} \cdot \underline{c}_2 \quad (4.32)$$

$$= \gamma_1 \cdot q(c_1) + \gamma_2 \cdot q(c_2), \quad (4.33)$$

which establishes linearity.

If $q(\underline{c}) = q_C$ is constant then this places a constraint on the possible values of \underline{c} ,

$$\underline{N} \cdot \underline{c} = q_C, \quad (4.34)$$

which is the equation for a flat plane in three dimensional space²¹. The planes described in Equation 4.34, are surfaces of equal reward.

In conclusion, any function of the form of Equation 4.30 is linear and all linear functions can be written in this form. The surfaces of equal reward, for linear reward functions, always have the form of Equation 4.34.

Linear reward functions and convex winning and losing regions

Once the linearity property, in Equation 4.33, is established it is possible to show that the winning region is convex. Suppose that the vectors, \underline{a} and \underline{b} are in the winning region, then

$$q(\underline{a}) > 0 \quad (4.35)$$

$$q(\underline{b}) > 0. \quad (4.36)$$

If we choose a mixing fraction in the range $0 \leq \gamma \leq 1$ then we can place limits on γ and $(1 - \gamma)$,

$$\gamma \geq 0 \quad (4.37)$$

$$1 - \gamma \geq 0. \quad (4.38)$$

²¹This would be a straight line in two dimensional space, or a flat hyperplane in higher dimensional spaces.

4.5 The matrix technique for the first moment

The linearity property, in Equation 4.33, now gives

$$q(\underline{c}) = q(\gamma \cdot \underline{a} + (1 - \gamma) \cdot \underline{b}) \quad (4.39)$$

$$= \gamma \cdot q(\underline{a}) + (1 - \gamma) \cdot q(\underline{b}). \quad (4.40)$$

All the quantities in Equation 4.40 are non-negative. In the case where, $0 < \gamma < 1$ then all the constants are strictly positive

$$\gamma > 0 \quad (4.41)$$

$$1 - \gamma > 0, \quad (4.42)$$

and all the constants in Equation 4.40 are positive, which leads to a strictly positive outcome, $q(\underline{c}) > 0$.

The cases where $\gamma = 0$ and $1 - \gamma = 0$ can be treated separately. When $\gamma = 0$, we have $q(\underline{c}) = q(\underline{b}) > 0$. When $1 - \gamma = 0$, we have $q(\underline{c}) = q(\underline{a}) > 0$. This means that in all cases, for all possible values of γ , we have $q(\underline{c}) > 0$. This can be written, using the formalism of predicate logic, as:

$$(q(\underline{a}) > 0) \wedge (q(\underline{b}) > 0) \Rightarrow (q(\underline{c}) > 0). \quad (4.43)$$

If \underline{a} and \underline{b} are in the winning region then the mixed game, \underline{c} , must also be in the winning region.

If the reward function, q , is linear then the winning region is a convex set. Similar arguments applies to the losing and zero-gain regions, as well. The linearity property, in Equation 4.33, places such a strong constraint on the functions that all the regions are convex:

$q > 0$: The winning region is convex. $(q(\underline{a}) > 0) \wedge (q(\underline{b}) > 0) \Rightarrow (q(\underline{c}) > 0)$.

$q = 0$: The zero-gain region is convex. $(q(\underline{a}) = 0) \wedge (q(\underline{b}) = 0) \Rightarrow (q(\underline{c}) = 0)$.

$q < 0$: The losing region is convex. $(q(\underline{a}) < 0) \wedge (q(\underline{b}) < 0) \Rightarrow (q(\underline{c}) < 0)$.

In summary, if the reward function, q , is linear then all the regions are convex and there is no paradoxical behaviour. If we wish to construct systems that exhibit apparent paradoxes of the Parrondo type then we must use a non-linear reward function, q , to do this. Non-linearity is a necessary condition before an apparent paradox can be constructed.

Some linear and non-linear reward functions

Some two dimensional worked examples can make the rôle of linearity more clear. A good example of a linear function in two dimensional space is

$$q_1(\underline{c}) = c_2 - c_1, \quad (4.44)$$

over the unit square, $0 \leq c_1 \leq 1$ and $0 \leq c_2 \leq 1$. This function can be written as

$$q_1([c_1, c_2]) = \begin{bmatrix} -1 & +1 \end{bmatrix} \cdot \begin{bmatrix} c_1 \\ c_2 \end{bmatrix}, \quad (4.45)$$

which is of the form of Equation 4.30. This proves that the function is linear, and that the contours of this function are straight lines. This is shown in Figure 4.10.

A different but closely-related and non-linear function is

$$q_2(\underline{c}) = \frac{c_2 - c_1}{\left(c_1^2 + c_2^2 + \frac{1}{2}\right)^2}, \quad (4.46)$$

over the same range. This is shown in Figure 4.11.

The plots in Figure 4.11 indicate but do not prove that q_2 is nonlinear. The easiest proof is by counterexample. We can evaluate q_2 at three points along a straight line, in the parameter space. $q_2([1/2, 1/2]) = 0$ and $q_2([0, 1]) = 2/3$ and $q_2([1/4, 3/4]) = 4/9$, so

$$\frac{1}{2}q_2\left(\left[\frac{1}{2}, \frac{1}{2}\right]\right) + \frac{1}{2}q_2([0, 1]) = \frac{1}{3} \neq \frac{4}{9} = q_2\left(\left[\frac{1}{4}, \frac{3}{4}\right]\right), \quad (4.47)$$

which contradicts Equation 4.29 and demonstrates that the function q_2 in Equation 4.46 is nonlinear. An interesting feature of the functions q_1 and q_2 is that they have the same winning, losing and zero-reward regions. All of these regions are convex. This is easy to understand if we consider that the denominator in Equation 4.46 is always positive. Dividing by this nonlinear denominator causes q_2 to be nonlinear, but the signs of q_1 and q_2 will always be identical. This means that the winning and losing regions for the two functions will be identical. The linear function must have a convex winning region, as indicated in Equation 4.43. This means that we have constructed a non-linear function with a convex winning region.

4.5 The matrix technique for the first moment

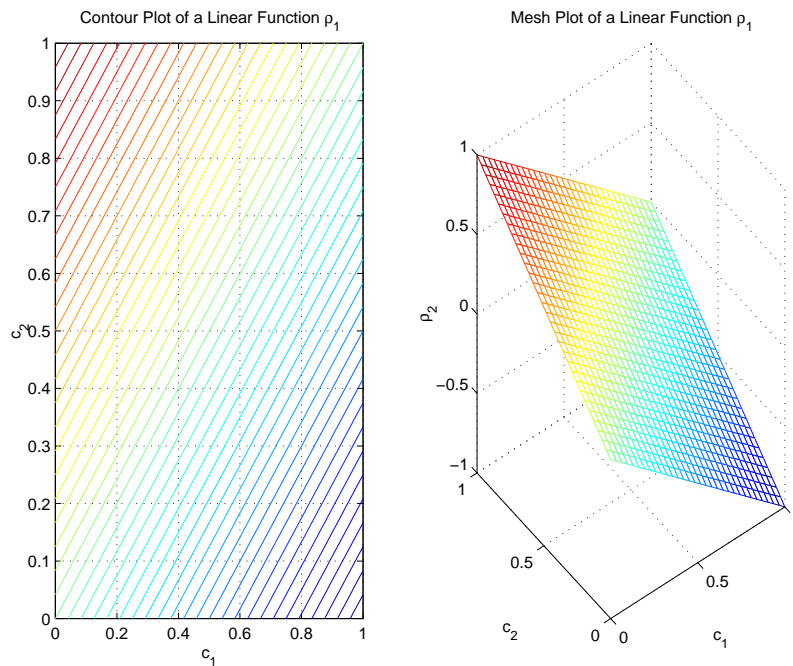


Figure 4.10. An example of a linear reward function, q_1 . The left half of the figure shows a contour plot of $q_1(\underline{c})$. The x -axis represents c_1 . The y -axis represents c_2 . The contours are straight and equally spaced. These are indications of linearity. The right half of the figure shows a mesh plot of $q_1(\underline{c})$. The x and y axes represent c_1 and c_2 respectively. The z -axis represents the value of the function, $q_1(\underline{c})$. The surface is a flat plane. This is an indication of linearity. The line of zero return is $c_2 - c_1 = 0$. The region of zero return is the line segment that satisfies $0 \leq c_1 = c_2 \leq 1$. The triangular region with $0 \leq c_1 < c_2 \leq 1$ is the winning region. The triangular region with $0 \leq c_2 < c_1 \leq 1$ is the losing region.

In summary, non-linear functions can give rise to convex winning and losing regions in parameter space. Non-linear reward functions, q , do not guarantee that the winning or losing regions are non-convex.

Alternatively, we can state that non-linearity is a necessary but not sufficient condition to generate a paradox of the Parrondo type. A necessary *and* sufficient condition is that the winning region should be non-convex in the parameter space.

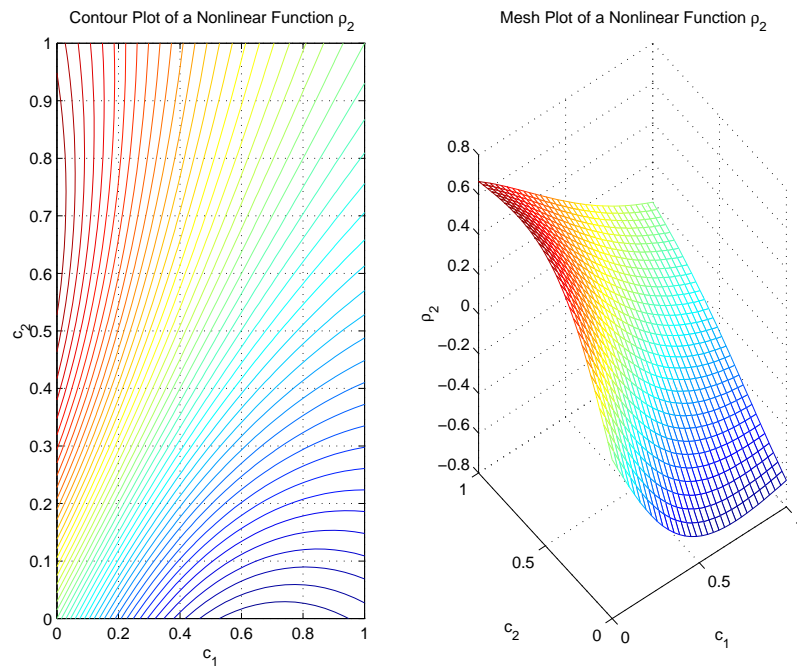


Figure 4.11. An example of a non-linear reward function, q_2 . The left half of the figure shows a contour plot of $q_2(\underline{c})$. The x -axis represents c_1 . The y -axis represents c_2 . Most of the contours are not straight. The contours are not equally spaced. These are indications of nonlinearity. The right half of the figure shows a mesh plot of $q_2(\underline{c})$. The x and y axes represent c_1 and c_2 respectively. The z -axis represents the value of the function, $q_2(\underline{c})$. The surface is not a flat plane. This is an indication of nonlinearity. The line of zero return is $c_2 - c_1 = 0$. The region of zero return is the line segment that satisfies $0 \leq c_1 = c_2 \leq 1$. The triangular region with $0 \leq c_1 < c_2 \leq 1$ is the winning region. The triangular region with $0 \leq c_2 < c_1 \leq 1$ is the losing region.

Summary of linearity results

- Linear reward functions always give rise to convex winning and losing regions in the parameter space. There is nothing, even *apparently*, paradoxical about linear reward functions.
- Nonlinear reward functions can give rise to either convex or non-convex, winning or losing regions in the parameter space. A nonlinear reward function is a *necessary* but not sufficient condition to guarantee a non-convex losing region.
- The apparent paradox of Parrondo's games where "two losing games combine to win" is equivalent to the statement that the losing region for Parrondo's games,

4.5 The matrix technique for the first moment

in the parameter space, is non-convex. The apparent paradox is made possible by a nonlinear reward function, but not all nonlinear reward functions give rise to apparent paradoxes.

Independent games without memory

Suppose that we play a simple dichotomous game of chance. We call it Game A. For example, we could draw a card from a shuffled but suitably weighted deck. There is a probability of a *win* of q_A and a reward of $w_A > 0$. The probability of a *loss* is $1 - q_A$ and the reward, in this case, is $l_A < 0$. The parameter for this Game A is a single real number $0 < q_A < 1$. Simple application of the laws of expectation reveals that the expected return from a round of Game A is $e_A = q_A \cdot w_A + (1 - q_A) \cdot l_A$.

Suppose that we also set up another similar game called Game B. We could draw a card from a different shuffled, and differently weighted, deck. There is a probability of a *win* of q_B and a reward of $w_B > 0$. The probability of a *loss* is $1 - q_B$ and the reward, in this case, is $l_B < 0$. The parameter for this Game B is a single real number $0 < q_B < 1$. Application of the laws of expectation reveals that the expected return from a round of Game B is $e_B = q_B \cdot w_B + (1 - q_B) \cdot l_B$.

These games, Game A and Game B are simple chance events of the type encountered in casino games such as cards or dice. Suppose now that some enterprising casino operator offers a new game, which plays Game A at random with probability of γ , or plays Game B at random with probability of $1 - \gamma$. This is precisely the type of mixture that has been used for Parrondo's games. We can refer to this new combined game as Game C. The probabilities for Games A and B are independent, so the laws of probability allow us to write $e_C = \gamma \cdot q_A \cdot w_A + \gamma \cdot (1 - q_A) \cdot l_A + (1 - \gamma) \cdot q_B \cdot w_B + (1 - \gamma) \cdot (1 - q_B) \cdot l_B$. This can be reduced to the simpler form

$$e_C = \gamma \cdot e_A + (1 - \gamma) \cdot e_B, \quad (4.48)$$

which is the condition for linearity.

The losing region for this Game C has to be convex in the parameter space because the reward function is linear. This is the usual situation for games of chance, which are independent and have no memory. If we were playing games at a casino and we were

losing money on the dice and we were losing money at cards then we could not reverse our fortune by playing a mixture of dice and cards. This is because the outcome from our mixed game is a linear combination of the outcomes of the component games, as described in Equation 4.48.

Summary: Independent memoryless games of chance always lead to linear reward functions and to convex winning and losing regions in the parameter space. The fact that independent memoryless events are so common in our everyday experience has conditioned us, at least subconsciously, to expect linear reward functions. Parrondo's games appear to be paradoxical, or counterintuitive, because they violate one of the consequences of linearity. The winning and losing regions are non-convex and, linear combinations of games can lead to reversals of fortune. This would never happen with independent memoryless games.

Properties of the reward function for Parrondo's games

The reward function for Parrondo's original games can be written in terms of the parameters. For Parrondo's original games the expected return from a mixed set of games is given by

$$q(\underline{c}) = \frac{3 \cdot (c_1 c_2 c_3 - (1 - c_1)(1 - c_2)(1 - c_3))}{c_1 c_2 c_3 + (1 - c_1)(1 - c_2)(1 - c_3) + 2}, \quad (4.49)$$

which is a re-statement of Equation 4.25. If we plot the zero gain surface, with $q = 0$, then the result is a smooth surface, as shown in Figure 4.12. Analysis of Equation 4.49 reveals a few interesting properties:

- The function $q(\underline{c})$ is invariant to permutations of c_1, c_2 and c_3 .
- The function $q(\underline{c})$ is anti-symmetric with respect to complimenting, if $c_1' = 1 - c_1, c_2' = 1 - c_2$ and $c_3' = 1 - c_3$ and we construct a complementary parameter vector, $\underline{c}' = [c_1', c_2', c_3']$ then $q(\underline{c}) = -q(\underline{c}')$.
- The function $q(\underline{c})$ can be written in simplified form as

$$q = \frac{3 \cdot (G - H)}{G + H + 2}, \quad (4.50)$$

4.5 The matrix technique for the first moment

where

$$G = c_1 \cdot c_2 \cdot c_3 \quad (4.51)$$

$$H = (1 - c_1) \cdot (1 - c_2) \cdot (1 - c_3), \quad (4.52)$$

which are the products of the forward and reverse probabilities that appear in Equation 4.27. The numerator of Equation 4.50 is identical with Equation 4.27.

- The function $\varrho(\underline{c})$ is smooth and differentiable everywhere in the parameter space.
- The partial derivatives of ϱ can be written in closed form

$$\frac{\partial \varrho}{\partial c_1} = 6 \cdot \left(\frac{(1+H) \cdot G}{c_1} + \frac{(1+G) \cdot H}{1-c_1} \right) / (G+H+2)^2 \quad (4.53)$$

$$\frac{\partial \varrho}{\partial c_2} = 6 \cdot \left(\frac{(1+H) \cdot G}{c_2} + \frac{(1+G) \cdot H}{1-c_2} \right) / (G+H+2)^2 \quad (4.54)$$

$$\frac{\partial \varrho}{\partial c_3} = 6 \cdot \left(\frac{(1+H) \cdot G}{c_3} + \frac{(1+G) \cdot H}{1-c_3} \right) / (G+H+2)^2 \quad (4.55)$$

All the quantities in these equations are positive.

- The function $\varrho(\underline{c})$ is monotonic with respect to all of the coordinates:

$$\frac{\partial \varrho}{\partial c_1} > 0 \quad (4.56)$$

$$\frac{\partial \varrho}{\partial c_2} > 0 \quad (4.57)$$

$$\frac{\partial \varrho}{\partial c_3} > 0, \quad (4.58)$$

which means that the reward function, ϱ , does not have any internal local maxima or minima.

- The maximum and minimum values occur at the boundaries

$$\varrho_{\min} = \varrho([0, 0, 0]) = -1 \quad (4.59)$$

$$\varrho_{\max} = \varrho([1, 1, 1]) = +1. \quad (4.60)$$

The extreme cases represent a certain win or a certain loss.

- The zero gain surface, $q = 0$, divides the parameter space into two regions, the losing region, near $[0, 0, 0]$, with $q < 0$ and the winning region, near $[1, 1, 1]$, with $q > 0$.
- The zero gain surface satisfies Equation 4.27 and is not a flat plane.

The function $q(\underline{c})$ is displayed in Figure 4.12. It is possible to appreciate the non-convex winning and losing regions, and also the symmetries of the function by considering the geometry of Figure 4.12.

4.5.3 Parrondo's games, with natural diffusion

Allison and Abbott (2002) pointed out that the diffusion operator used in Parrondo's original games was not optimal. A simulation of a flashing ratchet, using a discrete set of games, with a more realistic model for diffusion, was first published by Allison and Abbott (2002). These ideas were further developed in Amengual *et al.* (2004) and the term "*natural diffusion*" was used to describe discrete games that employed more realistic models for diffusion. We present a simple set of games here. They entail minimal change to Parrondo's original games, and use a more realistic model for diffusion.

In Parrondo's games, with natural diffusion, Game A is represented as:

$$\mathbf{A} = \begin{bmatrix} \frac{1}{2} & \frac{1}{4} & \frac{1}{4} \\ \frac{1}{4} & \frac{1}{2} & \frac{1}{4} \\ \frac{1}{4} & \frac{1}{4} & \frac{1}{2} \end{bmatrix}. \quad (4.61)$$

This corresponds to a half-period or double-frequency Bernoulli process and converges to the same result as the diffusion equation in the asymptotic limit over long times, as $m \rightarrow \infty$. The leading diagonal elements are nonzero and these correspond to self-transitions. This results in a more physical choice of diffusion operator than in the original version of Parrondo's games. Game B includes some biases, $[\eta_1, \eta_2, \eta_3]$, which

4.5 The matrix technique for the first moment

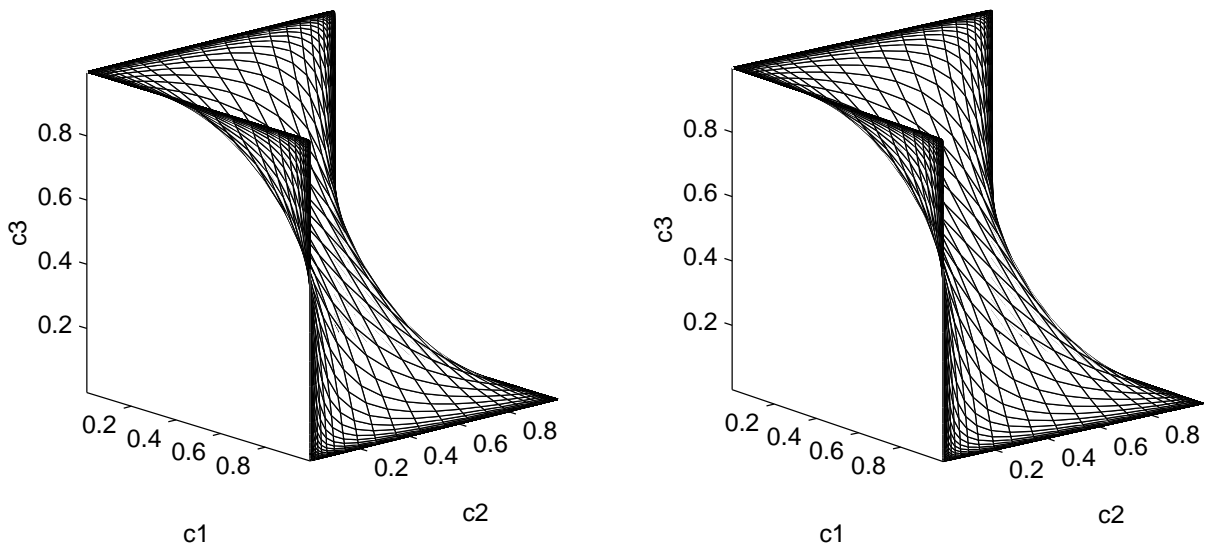


Figure 4.12. A stereo-pair plot of the winning and losing regions of Parrondo's games.

This figure shows the zero gain surface for Parrondo's games, within the parameter space $[c_1, c_2, c_3]$, where the c_k values are the probabilities in the reduced matrices for Parrondo's games. The losing region is below the surface and the winning region is above the surface. The complete parameter space is three dimensional. The zero-gain surface that divides the two regions has a topological dimension of two. It is possible to mentally reconstruct a three-dimensional image of the surface by viewing the stereo pair in the appropriate way. The left image should be viewed with the left eye and the right image should be viewed with the right eye. Some people can reconstruct these images by just looking at them. This works quite well if the eyes are kept about 300 mm from the page and the orientation of the page is adjusted until the images merge. Some people may need optical assistance, such as a stereoscope. Some readers may find the task of stereo reconstruction to be too difficult, even with a stereoscope. It is still possible to gain some idea of the three dimensional structure of the surface, by viewing one half of this figure, or by studying Figure 4.7, which is larger.

are small offsets in probability that are induced by the fields in the ratchet device,

$$\mathbf{B} = \begin{bmatrix} \frac{1}{2} & \frac{1}{4} + \eta_1 & \frac{1}{4} - \eta_1 \\ \frac{1}{4} - \eta_2 & \frac{1}{2} & \frac{1}{4} + \eta_2 \\ \frac{1}{4} + \eta_3 & \frac{1}{4} - \eta_3 & \frac{1}{2} \end{bmatrix}. \quad (4.62)$$

Of course all the probability offsets must lie in the range $-1/2 < \eta_i < +1/2$, for $i = 1, 2, 3$. Game B reduces to Game A in the special case when all the offsets are zero, $\eta_1 = \eta_2 = \eta_3 = 0$. Game B corresponds to the case when the field is turned on and Game A corresponds to the case when the field is turned off. Any time average game

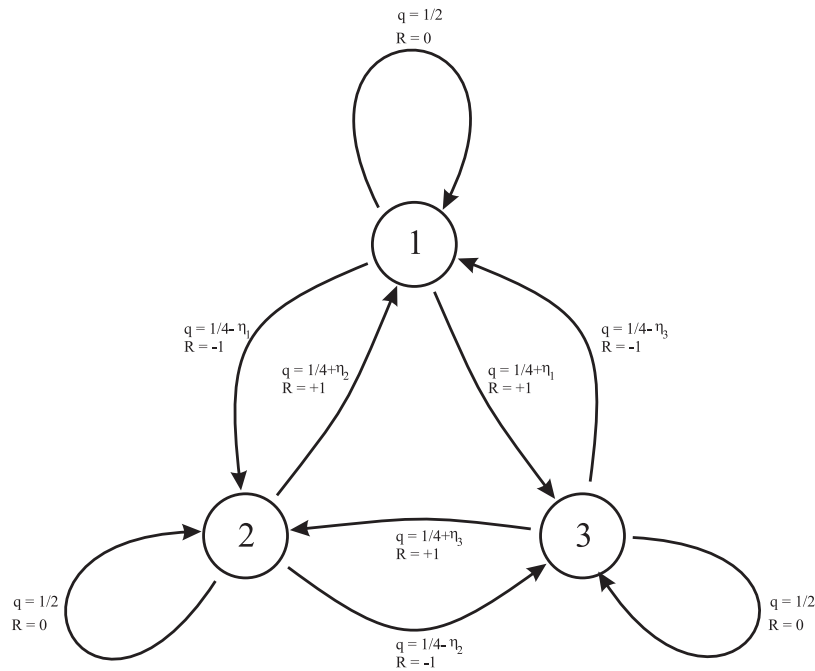


Figure 4.13. The state transitions of Parrondo’s games, with natural diffusion. The reduced discrete spatial values, $n \bmod L$, are enclosed within the circles that represent states of a discrete Markov process. The arrows represent the transitions between states. The rewards are indicated by R , without subscripts. The probabilities of transition are represented by q , without subscripts. The absence of subscripts is intended to simplify the figure.

$C = \gamma \cdot A + (1 - \gamma) \cdot B$, will still have the form of Game B, in Equation 4.62, with different offsets, $[\eta_1, \eta_2, \eta_3]$.

The steady state probabilities are

$$\underline{\pi}_B = \frac{\left(\frac{3}{16} - \frac{1}{4}\eta_2 + \frac{1}{4}\eta_3 + \eta_2\eta_3, \frac{3}{16} - \frac{1}{4}\eta_3 + \frac{1}{4}\eta_1 + \eta_1\eta_3, \frac{3}{16} - \frac{1}{4}\eta_1 + \frac{1}{4}\eta_2 + \eta_1\eta_2 \right)}{\eta_1\eta_2 + \eta_1\eta_3 + \eta_2\eta_3 + \frac{9}{16}}. \quad (4.63)$$

If we apply the theory to Game C, which is really a modified form of Game B, then we obtain

$$\rho = \frac{6 \left(16(1 - \gamma)^3 \eta_1\eta_2\eta_3 + (1 - \gamma)(\eta_1 + \eta_2 + \eta_3) \right)}{16(1 - \gamma)^2 (\eta_1\eta_2 + \eta_1\eta_3 + \eta_2\eta_3) + 9}. \quad (4.64)$$

This gives the expected rate of return from a randomised sequence of Parrondo’s games with natural diffusion, as a function of the mixing parameter, γ . The result of this calculation is shown in Figure 4.14. The change of sign in the rate of return, ρ with change in γ , can be clearly seen. The significance of this result is that it shows how Parrondo’s

4.5 The matrix technique for the first moment

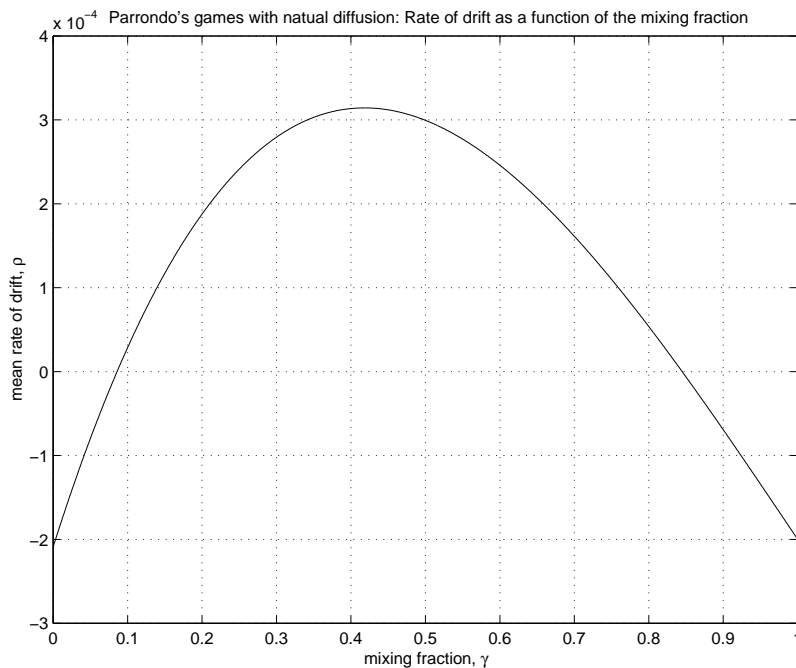


Figure 4.14. The expected rates of return ρ for various choices of the mixing fraction γ . The parameters for Game A and Game B have been fixed at values that more realistically represent the natural process of diffusion, with scaling parameter of $\beta = 1/4$. The parameters for the mixed game, C, are derived as a linear convex combination of the parameters for Game A and Game B. The expected rate of return for Game C is calculated and plotted. The y -axis represents the expected asymptotic rate of return, ρ . The x -axis represents the mixing fraction, γ .

games can be modified in a way that includes a more natural model for diffusion. The use of a natural model for diffusion does not prevent us from demonstrating the Parrondo effect. It is possible to demonstrate a Parrondo effect, using games that include self-transitions, as shown in Figure 4.13.

4.5.4 A pair of discrete games with only two states

The previous two examples involved games with three states. The question arises, whether we can construct games with less than three states that can still generate a Parrondo effect. It turns out that it is possible to construct games of this type, only if one is prepared to adopt a rather unusual reward structure that is not skip-free. The state transitions, rewards and probabilities of transition, for Game A are shown in Figure 4.15.

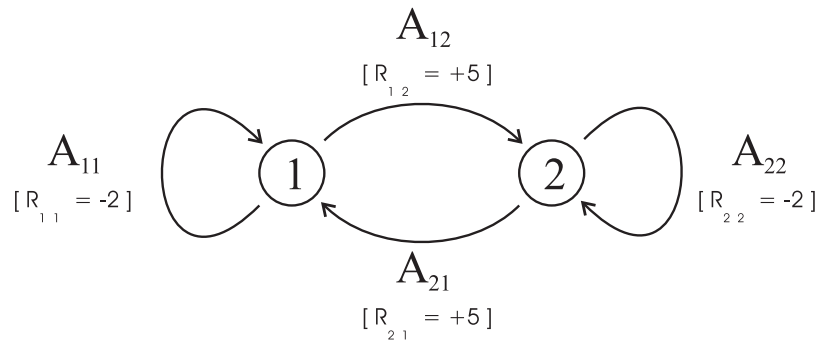


Figure 4.15. Definitions for a simple two-state game. The probability of transitions are given by $A_{v,j} = \mathbf{P}[n = j \text{ at } m + 1 \mid n = v \text{ at } m]$. There are only two states $n = 1$ and $n = 2$. The rewards associated with these transitions are given by $R_{v,j} =$ reward if $[n = j \text{ at } m + 1 \mid n = v \text{ at } m]$ The probabilities and rewards are indicated next to the line arcs, which represent the transitions. In this sense, the Markov chain resembles a type of Finite State Automaton (FSA) called a *Mealy machine* (Hopcroft and Ullman 1979), where the output from the system is associated with the state-transitions, rather than the states themselves. The reward matrix is indicated in Equation 4.67. The probabilities of transition may vary depending on the game that is being played at the time. The game in the figure is labelled as Game A and the probabilities of transition for Game A are indicated in Equation 4.65. If Game B is being played then the relevant probabilities of transition are given in Equation 4.66.

We can show that Parrondo’s paradox does exist for this simple example by working through the same method as for Parrondo’s original games. We can define Game A as

$$[\mathbf{A}] = \begin{bmatrix} \frac{5}{6} & \frac{1}{6} \\ \frac{1}{2} & \frac{1}{2} \end{bmatrix} \tag{4.65}$$

and Game B as

$$[\mathbf{B}] = \begin{bmatrix} \frac{1}{2} & \frac{1}{2} \\ \frac{1}{6} & \frac{5}{6} \end{bmatrix}. \tag{4.66}$$

The stationary probability-vectors are: $\Pi_{\mathbf{A}} = [\frac{3}{4}, \frac{1}{4}]$ and $\Pi_{\mathbf{B}} = [\frac{1}{4}, \frac{3}{4}]$. We can define the reward matrix as:

$$[\mathbf{R}] = \begin{bmatrix} -2 & +5 \\ +5 & -2 \end{bmatrix}, \tag{4.67}$$

and we can apply Equations, 4.16, 4.17 and 4.12 to obtain :

$$q(A) = \left[\frac{3}{4} \quad \frac{1}{4} \right] \left(\left[\begin{bmatrix} -2 & +5 \\ +5 & -2 \end{bmatrix} \circ \left[\begin{bmatrix} \frac{5}{6} & \frac{1}{6} \\ \frac{1}{2} & \frac{1}{2} \end{bmatrix} \right] \right) \begin{bmatrix} 1 \\ 1 \end{bmatrix} = -1 \tag{4.68}$$

4.5 The matrix technique for the first moment

and

$$q(B) = \begin{bmatrix} \frac{1}{4} & \frac{3}{4} \end{bmatrix} \left(\left(\begin{bmatrix} -2 & +5 \\ +5 & -2 \end{bmatrix} \circ \begin{bmatrix} \frac{1}{2} & \frac{1}{2} \\ \frac{1}{6} & \frac{5}{6} \end{bmatrix} \right) \begin{bmatrix} 1 \\ 1 \end{bmatrix} \right) = -1. \quad (4.69)$$

If we mix Games A and B in strictly equal proportions then we obtain the following value for the return from the games:

$$q(C) = \begin{bmatrix} \frac{1}{2} & \frac{1}{2} \end{bmatrix} \left(\left(\begin{bmatrix} -2 & +5 \\ +5 & -2 \end{bmatrix} \circ \begin{bmatrix} \frac{2}{3} & \frac{1}{3} \\ \frac{1}{3} & \frac{2}{3} \end{bmatrix} \right) \begin{bmatrix} 1 \\ 1 \end{bmatrix} \right) = +1. \quad (4.70)$$

Games A and B are losing and the mixed time-average game, $C = \frac{1}{2}(A + B)$, is winning, and so we have Parrondo's paradox for the two-state games, A and B, as defined in Equations 4.65 and 4.66. We can simulate the dynamics of this two-state version of Parrondo's games. Some typical sample paths are shown in Figure 4.16.

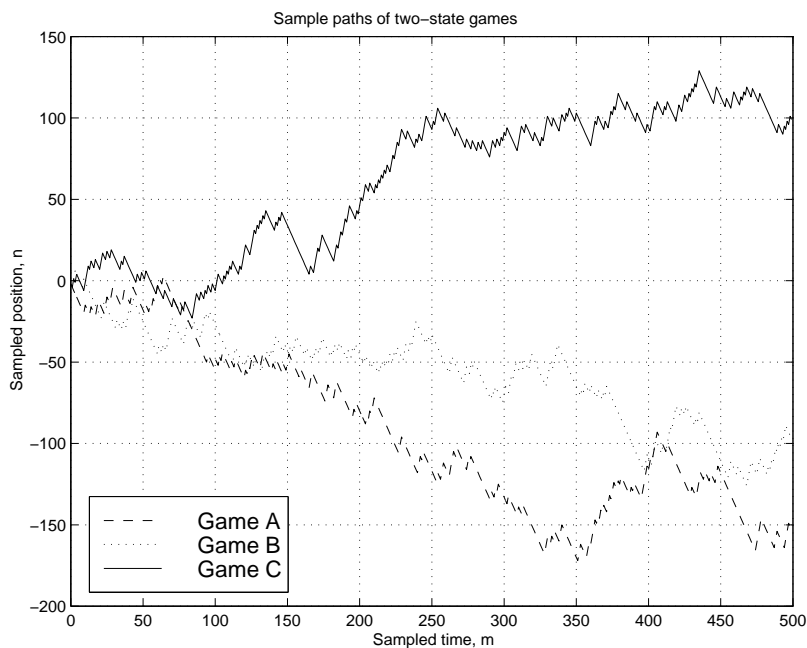


Figure 4.16. Simulation of a two-state version of Parrondo's games. The sample paths for Game A and for Game B, are both generally sloping downwards or are *losing*. Game C is a combination of Games A and B in equal proportions. The sample path for Game C is generally sloping upwards and is *winning*.

The results from the simulations are consistent with the algebraic results. If we refer back to Figure 4.15 then an intuitive explanation for this phenomenon is possible. The negative or punishing rewards are associated with transitions that do not change

state. The good positive rewards are associated with the changes of state. If we play a homogeneous sequence of Games A or B then there are relatively few changes of state and the resulting weighted sum of all the rewards is negative. If we play the mixed game then the rewarding changes of state are much more frequent and the resulting weighted sum of rewards is positive. These results show that it is possible to

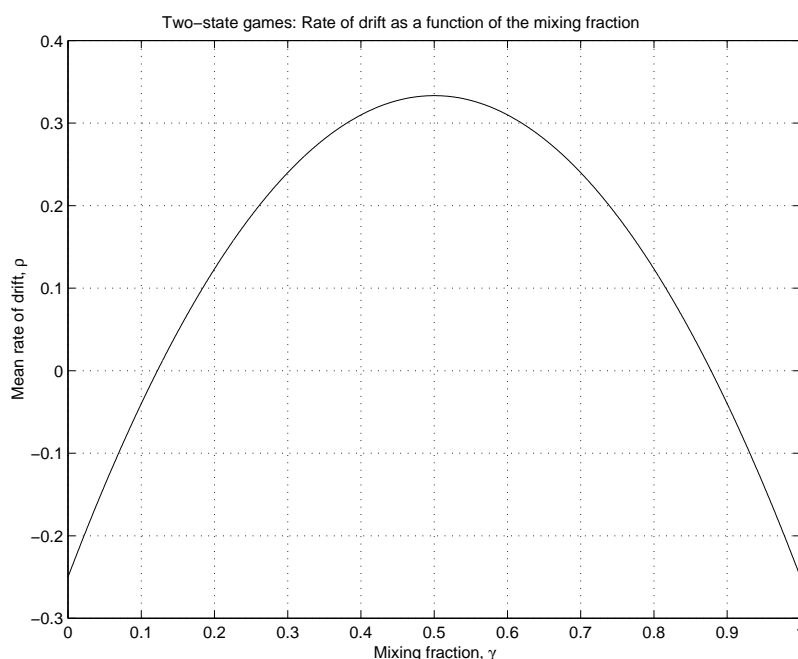


Figure 4.17. The expected rates of return ρ for various choices of the mixing fraction γ .

The parameters for Games A and B are fixed, using the values given in the text. The parameters for the mixed game, C, are derived as a linear convex combination of the parameters for Games A and B. The rate of return for Game C is calculated and plotted.

demonstrate a Parrondo effect, using games that only have two states, and include self-transitions, if we are prepared to accept a complicated reward structure that is not skip-free.

4.5.5 Astumian's games

Dean Astumian²² described a set of games, played on a checker board, and using dice (Astumian 2001). The probabilities of various outcomes were defined in terms of sets of outcomes, in a manner similar to the game of "craps." The moves, forward,

²²The family name 'Astumian' is pronounced as 'osterman.'

4.5 The matrix technique for the first moment

Action	From White	From Black
Forward	$q = 4/36, R = +1$	$q = 2/36, R = +1$
Backward	$q = 4/36, R = -1$	$q = 5/36, R = -1$
No change	$q = 24/36, R = 0$	$q = 29/36, R = 0$

Table 4.1. Rule-set number one, for Astumian's games. This table defines the probabilities of transition, q , and the rewards, R , associated with rule-set number one, from Astumian's games, as described in Astumian (2001). Moves are described as forward (with a certain probability, q), backward (with a certain probability, q) or stationary (by default). The probabilities of the stationary moves are calculated using the law of total probability.

Action	From White	From Black
Forward	$q = 2/36, R = +1$	$q = 8/36, R = +1$
Backward	$q = 5/36, R = -1$	$q = 4/36, R = -1$
No change	$q = 29/36, R = 0$	$q = 24/36, R = 0$

Table 4.2. Rule-set number two, for Astumian's games. This table defines the probabilities of transition, q , and the rewards, R , associated with rule-set number one, from Astumian's games, as described in Astumian (2001). Moves are described as forward (with a certain probability, q), backward (with a certain probability, q) or stationary (by default). The probabilities of the stationary moves are calculated using the law of total probability.

backward or stationary, on the checker-board were defined in terms of rule-sets. These are recorded in concise form in Tables 4.1 and 4.2.

It has been claimed (Astumian 2001, Astumian 2005) that these games have only two states, *white* and *black*, but this over-simplifies the analysis. If we define a *state* in the sense used by Karlin and Taylor (1975) then more states will be required.

In the original version, of Astumian's games, there were absorbing states. If our only interest is to demonstrate a transport effect and to estimate rates of flow, as functions of the probabilities of transition, then the absorbing boundary conditions are a non-essential detail. We leave them out, for the time being. These versions of the games are sometimes called *generalized Astumian's games* (Astumian 2005).

In order to correctly represent the transport effect it is necessary to distinguish between moving forward from a white square (to a black square) or moving backward from a white square (to a black square). Alternatively, it is necessary to store some information about past history. Given that the present position of the checker is on a black square, it is necessary to record whether the transition was forward (from a white square) or backward (from a white square). If we do not do this then it is not possible to allocate rewards of $R = +1$ or $R = -1$ to the transition, since we do not know which transition actually occurred. If we insist on regarding the process as a Markov process then the information about history has to be stored in the states of the system. This means that Astumian's games, without absorbing boundary conditions, require four states: $\{W1, B1, W2, B2\}$, two white states and two black states.

The state transition diagrams for Astumian's Game A and Game B, corresponding to rule-set 1 and rule-set 2, are shown in Figures 4.18 and 4.19.

The state transition matrix for Game A is:

$$A = \frac{1}{36} \begin{bmatrix} 24 & 8 & 0 & 4 \\ 5 & 29 & 2 & 0 \\ 0 & 4 & 24 & 8 \\ 2 & 0 & 5 & 29 \end{bmatrix}. \quad (4.71)$$

The state transition matrix for Game B is:

$$B = \frac{1}{36} \begin{bmatrix} 29 & 2 & 0 & 5 \\ 4 & 24 & 8 & 0 \\ 0 & 5 & 29 & 2 \\ 8 & 0 & 4 & 24 \end{bmatrix}. \quad (4.72)$$

The reward matrix is the same for both games:

$$R = \begin{bmatrix} 0 & +1 & +2 & -1 \\ -1 & 0 & +1 & +2 \\ -2 & -1 & 0 & +1 \\ +1 & -2 & -1 & 0 \end{bmatrix}. \quad (4.73)$$

We can use Equation 4.13, with $C = \gamma \cdot A + (1 - \gamma) \cdot B$, to calculate the return from Astumian's games. The only difficulty, in calculating Π_C , is the increased amount

4.5 The matrix technique for the first moment

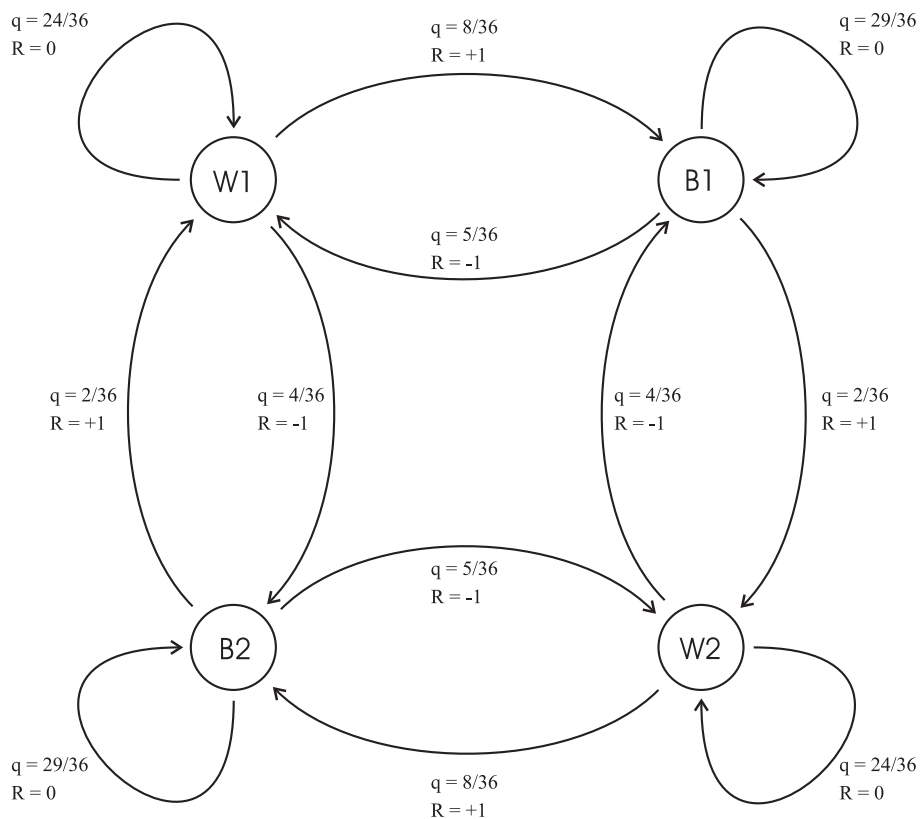


Figure 4.18. State transitions for Astumian's rule-set number 1. There are two white states, W1 and W2, and two black states, B1 and B2. Without this duplication of states, the state transition diagram would reduce to a two-state diagram. There would be no way to detect the difference between clockwise transition about the state-diagram (winning) and anti-clockwise progression around the state-diagram (losing). There would be no way to allocate the correct reward, from the limited set of possible rewards $\{-1, 0, +1\}$, for each different transition. In the true two-state game the set of possible rewards is much more complicated, $\{-2, +5\}$, and the process is not skip free.

of computation required. The Markov chain has four states and the polynomials are fourth order. A numerical approach would seem to be more appropriate here. This is achieved in Matlab. The vector Π_C is calculated from the eigenvector associated with the dominant eigenvector, $\lambda = 1$. The results from the calculation are shown in Figure 4.20. The change of sign is clearly evident. Parrondo's games and Astumian's games both exhibit a change of sign with change in the mixing fraction, γ . They both combine losing games to win.

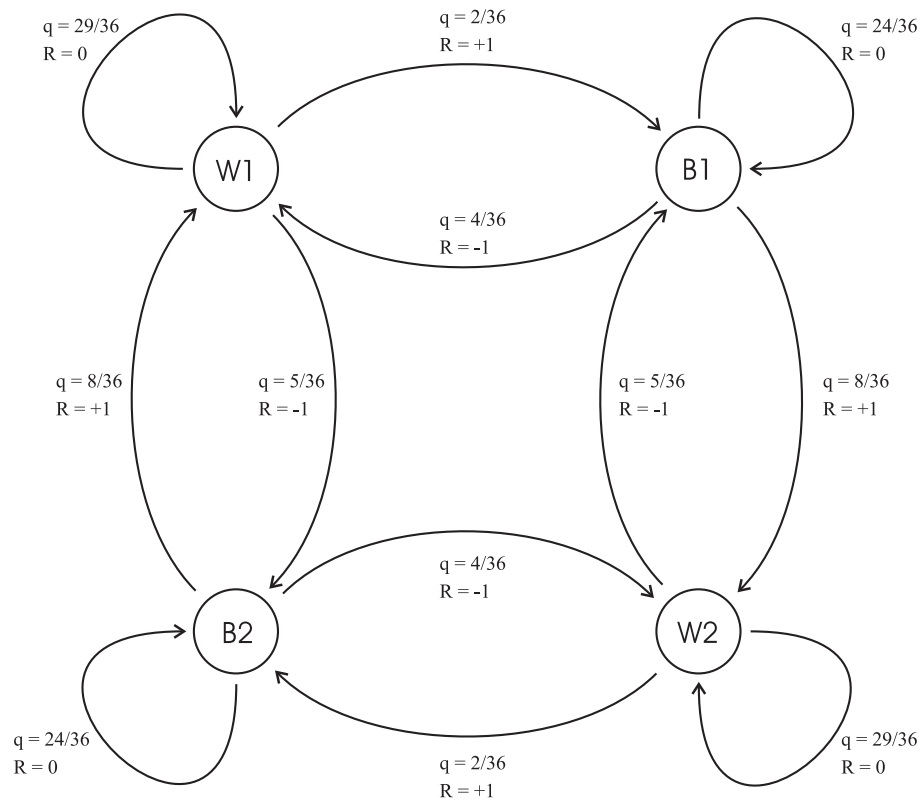


Figure 4.19. State transitions for Astumian's rule-set number 2. This is really the dual of Figure 4.18. The topology of the state-diagram is not changed. The probabilities have not changed, but some of the numbers have been transposed to other branches in the state-diagram. It is the alternation between these two state-diagrams that generates an equivalent state-diagram, with different weights, and demonstrates the required change of sign in the mean direction of probability flow.

4.5.6 Astumian's games, with absorbing boundary conditions

In the original version of Astumian's games (Astumian 2001) there were a total of five states. The system did not extend indefinitely, but had absorbing states at the upper and lower boundaries. In this sense, Astumian's games resemble a two-sided gambler's ruin problem. This is shown schematically in Figure 4.21. We shall refer to these games as *Astumian's Original Games*. These games are Markovian because the probabilities of transition, at any given moment in time, do not depend on past history. It is sufficient to know which state the system is in and which set of rules is being followed at that moment in time, m . The system jumps stochastically between five different states, in the range $1 \leq n \leq 5$, as indicated in Figure 4.21.

4.5 The matrix technique for the first moment

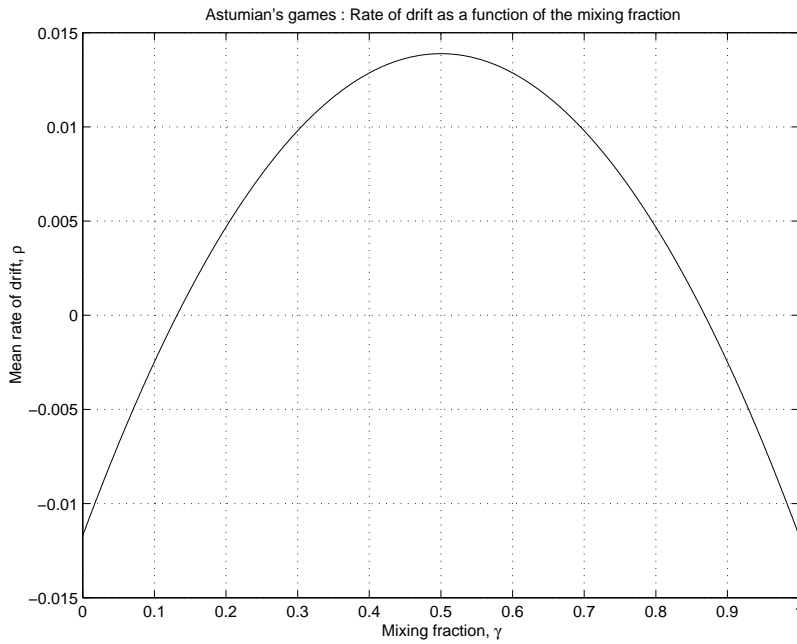


Figure 4.20. The expected rates of return q for various choices of the mixing fraction γ . The parameters for Games A and B are fixed, using Astumian's original values, for rule-set 1 and rule-set 2, respectively. The parameters for the mixed game, C, are derived as a linear convex combination of the parameters for Games A and B. The rate of return for Game C is calculated and plotted. The change of sign, with mixing fraction, is clear.

The transition matrices for both rule-sets take the form:

$$\mathbf{A} = \begin{bmatrix} 1 & 0 & 0 & 0 & 0 \\ \psi_2 & 1 - \psi_2 - \phi_2 & \phi_2 & 0 & 0 \\ 0 & \psi_3 & 1 - \psi_3 - \phi_3 & \phi_3 & 0 \\ 0 & 0 & \psi_4 & 1 - \psi_4 - \phi_4 & \phi_4 \\ 0 & 0 & 0 & 0 & 1 \end{bmatrix}. \quad (4.74)$$

Astumian's original parameter values for the two rule-sets are given in Table 4.3. The initial state was specified as $n = 3$, this is known with certainty at the start of the game, when discrete-time is, $m = 0$, so the initial time-varying probability vector is

$$\underline{P}_0 = [0, 0, 1, 0, 0]. \quad (4.75)$$

The laws of conditional probability apply and after m time steps, the time-varying probability vector is given by:

$$\underline{P}_m = \underline{P}_0 \cdot \mathbf{A}^m. \quad (4.76)$$

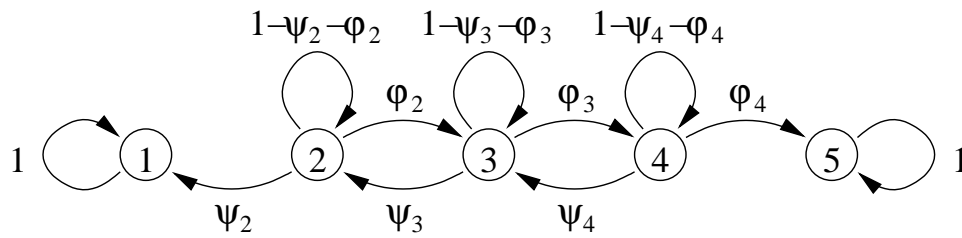


Figure 4.21. A rule-set for Astumian's games. Both rule-sets, 1 and 2, can be represented in this form. The symbols written above and below the arrows are the probabilities of transitions between neighbouring states. Winning moves are represented by right facing arrows with labels ϕ_n . Losing moves are represented by left facing arrows, with labels ψ_n . Null moves are self-transitions, and are represented by arrows that originate and terminate at the same state. Null transitions have probabilities of the form $1 - \psi_n - \phi_n$. This choice of notation avoids the use of redundant symbols and automatically takes account of the fact that the total conditional probability must be 1. In a typical Monte Carlo simulation of a kinetic network, with appropriate choices of spatial and temporal scales, the transition probabilities out of a state should be much less than 1. That is $\psi_n + \phi_n \ll 1$. In any given time tick, or iteration, at most one, and more often zero, transitions will occur. The initial state is state $n = 3$. The game is declared to be *won* if state 5 is reached. It is declared to be *lost* if state 1 is reached. The action of reaching state 1 is analogous to gambler's ruin, and the action of reaching state 5 is analogous to breaking the bank, at a casino.

Because there are absorbing states, it is not very useful to calculate expected values for the asymptotic rates of return, since they will always be zero. Astumian's games, with absorbing states, will either end up in absorbing state 1 or absorbing state 5, with probability of one. We only have to wait long enough for this to happen. After a short period of transition, with reward of ± 2 , there would be no further change, and no reward. The weighting from an indefinitely long sequence, with zero reward, will always overwhelm any contribution from the initial transitions, where the reward is finite. In either case, win or lose, the mean asymptotic rate of return would be zero.

It is more sensible to calculate the asymptotic values of the probabilities of occupancy of the various states. For some stochastic matrices, this can be carried out by considering the eigenvector associated with the dominant eigenvalue, which will always be 1. Unfortunately, this cannot be carried out for the stochastic matrix in Equation 4.74, because the dominant eigenvalue is repeated. There are two dominant eigenvectors, each

4.5 The matrix technique for the first moment

Rule-set	ψ_2	ϕ_2	ψ_3	ϕ_3	ψ_4	ϕ_4
1	4/36	8/36	5/36	2/36	4/36	8/36
2	5/36	2/36	4/36	8/36	5/36	2/36
mixed	9/72	10/72	9/72	10/72	9/72	10/72

Table 4.3. Parameters for the rule-sets, for Astumian's games. This table defines the probabilities of transition, for both rule-sets, for Astumian's games, as described in Astumian (2001). The mixed rule-set is the result of choosing rule-set 1 or rule-set 2, at random, each with a probability of 1/2. The probabilities of transition were calculated by aggregating individual events over the event space of two die, which is a Cartesian product of two integer sub-ranges, $[1,2,3,4,5,6] \times [1,2,3,4,5,6]$. There are 36 individual events. They are all independent, so the probabilities can be calculated by adding the probabilities of the events, as specified by Astumian. The probabilities in rule-sets 1 and 2 are multiples of 1/36. The parameters of rule-sets 1 and 2 are averaged to give parameters for the mixed rule-set. The probabilities in the mixed rule-set are multiples of 1/72.

with eigenvalues of 1. There is one eigenvector for each absorbing state:

$$\underline{\Lambda}_1 = [1, 0, 0, 0, 0] \quad (4.77)$$

$$\underline{\Lambda}_2 = [0, 0, 0, 0, 1]. \quad (4.78)$$

This means that there is a linear sub-space of possible stable states. This space is spanned by the two dominant eigenvectors. In fact, the sub-space is composed of all linear convex combinations of the two dominant eigenvectors. All vectors of the form

$$\underline{\Pi} = [\zeta, 0, 0, 0, 1 - \zeta] \quad (4.79)$$

$$= \zeta \cdot \underline{\Lambda}_1 + (1 - \zeta) \cdot \underline{\Lambda}_2 \quad (4.80)$$

are stable states. They can be reached, given suitable initial conditions, provided, $0 \leq \zeta \leq 1$.

The final asymptotic value of the time-varying probability vector could lie anywhere within the subspace of stable states, depending on the initial conditions. The final stable value depends strongly on the initial conditions, and involves contributions from all of the modes in the response, not just the dominant ones.

In order to calculate the final value of the time varying probability vector, $\underline{\Pi}$, it is necessary to solve Equation 4.76, for the limiting case as $m \rightarrow \infty$. We can define a limit as:

$$\underline{\Pi} = \lim_{m \rightarrow +\infty} (\underline{P}_0 \cdot \mathbf{A}^m), \quad (4.81)$$

given the initial probability vector, in Equation 4.75, associated with state $n = 3$. It is possible to solve this problem using the z-transform and the final-value theorem. This leads to an expression for the limit

$$\underline{\Pi} = \lim_{z \rightarrow 1} \left((1 - z^{-1}) \cdot \underline{P}_0 \cdot (I - z^{-1} \mathbf{A})^{-1} \right). \quad (4.82)$$

The matrix inverse can be calculated using Gauss reduction, or using Cramer's rule. If we apply this technique to Equation 4.74 then we obtain an exact closed-form expression for $\underline{\Pi}$. All the components of $\underline{\Pi}$ are zero, excepting for the first and last components, $\underline{\Pi}[1]$ and $\underline{\Pi}[5]$. We have

$$\underline{\Pi}[1] = \frac{\frac{\psi_2}{\psi_2 + \phi_2} \cdot \frac{\psi_3}{\psi_3 + \phi_3}}{1 - \frac{\phi_2}{\psi_2 + \phi_2} \cdot \frac{\psi_3}{\psi_3 + \phi_3} - \frac{\phi_3}{\psi_3 + \phi_3} \cdot \frac{\psi_4}{\psi_4 + \phi_4}} \quad (4.83)$$

and

$$\underline{\Pi}[5] = \frac{\frac{\phi_3}{\psi_3 + \phi_3} \cdot \frac{\phi_4}{\psi_4 + \phi_4}}{1 - \frac{\phi_2}{\psi_2 + \phi_2} \cdot \frac{\psi_3}{\psi_3 + \phi_3} - \frac{\phi_3}{\psi_3 + \phi_3} \cdot \frac{\psi_4}{\psi_4 + \phi_4}}. \quad (4.84)$$

These results are equivalent to formulae published by Behrends (2004). He refers to matrices containing the coefficients, of the form $\psi_k / (\psi_k + \phi_k)$ or $\phi_k / (\psi_k + \phi_k)$, as *reduced matrices*. The individual coefficients could be called *reduced* or *normalised* probabilities. It is possible to calculate a likelihood ratio, using these reduced probabilities:

$$\frac{p_w}{p_l} = \frac{p(\text{win})}{p(\text{lose})} = \frac{(\psi_2 + \phi_2) \cdot \phi_3 \cdot \phi_4}{\psi_2 \cdot \psi_3 \cdot (\psi_3 + \phi_3)}. \quad (4.85)$$

This has simpler form and is possibly more informative than the raw probabilities in Equations 4.83 and 4.84. The games are winning if $p(\text{win}) / p(\text{lose}) > 1$, or equivalently, the games are winning if

$$(\psi_2 + \phi_2) \cdot \phi_3 \cdot \phi_4 > \psi_2 \cdot \psi_3 \cdot (\psi_3 + \phi_3). \quad (4.86)$$

The system has detailed balance if $(\psi_2 + \phi_2) \cdot \phi_3 \cdot \phi_4 = \psi_2 \cdot \psi_3 \cdot (\psi_3 + \phi_3)$. Astumian's rule-sets 1 and 2 and the mixed rule-set all follow the same pattern and the steady state probabilities are given by Equations 4.83 and 4.84, using different ψ and ϕ values. If we use Astumian's original values, from Table 4.3, then we obtain the corresponding values for the steady-state probabilities. These are listed in Table 4.4.

4.5 The matrix technique for the first moment

Rule-set	$\Pi[1]$	$\Pi[5]$	Most Frequent Outcome
1	5/9	4/9	losing
2	5/9	4/9	losing
mixed	81/181	100/181	winning

Table 4.4. Steady state probabilities, for Astumian's games. The steady state probabilities for the various rule-sets prove that Astumian's games exhibit the same change of sign that was shown in Parrondo's games. Rule-sets 1 and 2, individually, are *losing*. The mixed rule-set, composed of a mixture of rule-sets 1 and 2, is *winning*. The numbers in this table are confirmed by numerical evaluations of Equation 4.76.

There are a few points that follow from this work, on Astumian's games with absorbing states:

- Our analysis is independent of Astumian, but we do confirm his calculations regarding the probabilities of transition (Astumian 2005, Astumian 2004). These are further supported by Behrends (2004). These values were challenged by Piotrowski and Sladkowski (2004), but these claims have not been widely accepted. Our values for the probabilities of transition are summarised in Table 4.3.
- Our analysis is independent of Behrends (2004), but we do confirm his result regarding the probability of a win, for $\Pi[5] = 100/181$, which we present in Equation 4.84. We present a summary of our results in Table 4.4.
- We confirm that the probabilities of occupancy are shifted in the way that was suggested in the original articles (Astumian 2001, Astumian 2004, Astumian 2005, Behrends 2004). This point has been challenged in the past by Piotrowski and Sladkowski (2004), but our analysis confirms that of Astumian and Behrends. We assert that the probability of winning is increased when the rule-sets are mixed.

4.5.7 Summary of common features of the discrete games

The following games have been analysed:

- Parrondo's original games,
- Parrondo's games with natural diffusion,

- Discrete games with only two states,
- Astumian's generalised games,
- Astumian's original games.

These games all have certain features in common.

- They all discrete Markov processes.
- They were all developed in order to simulate aspects of Brownian motors (or Brownian ratchets).
- They can all be reduced to some finite number of states, modulo L , in the spatial dimension.
- The probabilities of transition can be represented using stochastic matrices, such as A and B .
- The rewards associated with the transitions can be written using some reward matrix, R .
- Mixed games can be represented using an equivalent transition matrix, C , which is a linear convex combination of A and B .
- The expected rates of return, from the games is given by Equation 4.13.
- The rate of return is a non-linear function of the component games, A and B .
- It is possible to choose the coefficients in the matrices in such a way that $\varrho[\mathbf{A}] < 0$ and $\varrho[\mathbf{B}] < 0$ and $\varrho[\mathbf{C}] > 0$.

All of these games show that the essential transport properties of Brownian motors can be demonstrated using greatly simplified discrete models.

In order to function correctly, Astumian's games require four, or five, states. Parrondo's games require only three states. Allison *et al.* (2005) published a set of games with two states, but strictly speaking, this is only two states, modulo 2, and the full spatial structure is not skip-free, which does not seem to be very realistic from a physical point of view. The minimum number of states in any *useful* model would seem to be three. This

4.6 Visualisation of the process

confirms the earlier work of Lee *et al.* (2003).

In conclusion, we believe that Parrondo's games with natural diffusion and three, or more, states leads to the best simulation.

Parrondo's games and Astumian's games can both be analysed using the same mathematical machinery.

Parrondo's games are also simple enough to serve as pedagogic models for Brownian ratchets, since they can be solved analytically.

4.6 Visualisation of the process

4.6.1 Time-homogeneous Markov chains and notation

Finite discrete-time Markov chains can be represented in terms of matrices of conditional transition probabilities. These matrices are called Markov transition operators. We denote these by capital letters in brackets, eg: $[A]$ where $A_{i,j} = \Pr \{K_{t+1} = j | K_t = i\}$ and $K \in \mathcal{Z}$ is some measure of the state of the system. The Markov property requires that $A_{i,j}$ cannot be a function of K but it can be a function of time, m . In Parrondo's original games, K , represents the amount of capital that a player has. There is a one-to-one mapping between Markov games and the Markov transition operators for these games. We will refer to the games and the transition operators interchangeably.

The probability that the system will be in any one state at a given instant of time can be represented by a distribution called the time-varying probability vector. We shall also refer to this as the probability-vector. We represent this probability mass function, at time m , using a row vector, \underline{p}_m . We can represent the evolution of the Markov chain in time using a simple matrix equation,

$$\underline{p}_{m+1} = \underline{p}_m \cdot [\mathbf{A}]. \quad (4.87)$$

This can also be viewed as a multi-dimensional finite difference equation.

As a simple example, we can consider the regular Markov transition operator

$$[\mathbf{A}] = \begin{bmatrix} \frac{13}{16} & \frac{3}{16} \\ \frac{1}{16} & \frac{15}{16} \end{bmatrix} \quad (4.88)$$

using the initial condition

$$\underline{p}_m = [p_0, p_1] = \left[\frac{3}{4}, \frac{1}{4} \right] \text{ when } m = 0. \quad (4.89)$$

A fundamental question in the study of dynamical systems is to classify how they behave in the long-time limit, as $m \rightarrow \infty$ and all transient effects have decayed. The evolution of the probability-vector of a discrete-time Markov chain generally traces out a sequence of points or trajectory in the phase-space. The natural technique would be to draw a graph of this trajectory. As an example of this, we can consider the trajectory of the time homogeneous Markov chain, described by Equations 4.88 and 4.89, which is shown in Figure 4.22.

The probability-vector, \underline{p}_m , always satisfies the constraint, $p_0 + p_1 = 1$. This follows from the law of total probability. The probability-vector is always constrained to lie within an $L - 1$ dimensional subspace of the L dimensional phase-space. The dynamics of the system all occur within this sub-space. This is clearly visible in Figure 4.22. We can think of the set

$$M = \{[p_0, p_1] \mid (0 \leq p_0 \leq 1) \wedge (0 \leq p_1 \leq 1) \wedge (p_0 + p_1 = 1)\}, \quad (4.90)$$

as a phase-space for the dynamical system defined by Equations 4.88 and 4.89. The phase-space has a dimension, which is smaller than the embedding-space. This is a result of the fact that there is a conservation law²³, which constrains the dynamics of the system. For this example, the sequence converges to a stable fixed-point at $\mathbf{\Pi} = \left[\frac{1}{4}, \frac{3}{4} \right]$. It can be shown that sequences of this type always converge to single stable fixed-points as long as the Markov transition operators are regular and time-homogeneous. The convergent points are the representations, in phase-space, of the limiting stationary probabilities for the Markov chain.

²³the law of total probability.

4.6 Visualisation of the process

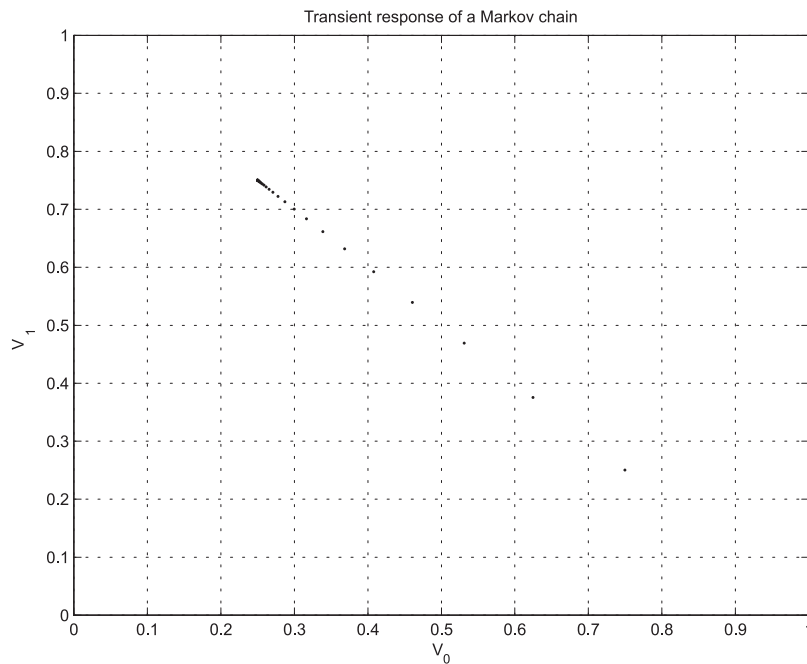


Figure 4.22. The phase-space of a simple Markov chain. The points on the graph represent the trajectory of the probability-vector within the phase space. These points do not represent the physical state of a system. They represent our state of knowledge about the system, given an initial state of knowledge, followed by several iterations of a discrete Markov game. The time-varying probability vector has the components $\underline{p} = [p_0, p_1]$. After many iterations of the game and no further direct observations of the actual state, n , our entire knowledge about the state is summarised by the numbers in the steady-state probability vector, $\underline{\Pi} = [\frac{1}{4}, \frac{3}{4}]$. There will be a probability of $1/4$ that the player is in the first state and a probability of $3/4$ that the player is in the second state.

4.6.2 Time-inhomogeneous Markov chains

The existence, uniqueness and dynamical stability of the fixed-point are important parts of the theory of Markov chains, but we must be careful not to apply these theorems to systems where the basic premises are not satisfied. If the Markov transition operators are not homogeneous in time then there may no longer be a single fixed-point in phase-space. The probability-vector can perpetually move through two or more points without ever converging to any single stable value. To demonstrate this important point, we present a simple example, using two regular Markov transition operators :

$$[S] = \begin{bmatrix} \frac{3}{4} & \frac{1}{4} \\ \frac{3}{4} & \frac{1}{4} \end{bmatrix} \quad (4.91)$$

and

$$[T] = \begin{bmatrix} \frac{1}{4} & \frac{3}{4} \\ \frac{1}{4} & \frac{3}{4} \end{bmatrix}. \quad (4.92)$$

The rows of these matrices are all identical. This indicates that the outcome of each game is completely independent of the initial state. The limiting stable probabilities for these regular Markov transition operators are $\mathbf{\Pi}_S = \left[\frac{3}{4}, \frac{1}{4} \right]$ and $\mathbf{\Pi}_T = \left[\frac{1}{4}, \frac{3}{4} \right]$ respectively. The time-varying probability vector immediately moves to the stable limiting value after even a single play of each game.

$$[Q] \cdot [S] = [S] \quad (4.93)$$

and

$$[Q] \cdot [T] = [T] \quad (4.94)$$

for any conformable stochastic matrix $[Q]$. This leads to some interesting corollaries:

$$[T] \cdot [S] = [S] \quad (4.95)$$

and

$$[S] \cdot [T] = [T]. \quad (4.96)$$

If we play an indefinite alternating sequence of these games, $\{STST \dots\}$, then there are two simple ways in which we can associatively group the terms:

$$\underline{p_{2m}} = \underline{p_0} ([S] [T]) ([S] [T]) \dots ([S] [T]) \quad (4.97)$$

$$= \underline{p_0} [T] \quad (4.98)$$

$$\Rightarrow \mathbf{\Pi} = \mathbf{\Pi}_T \quad (4.99)$$

and

$$\underline{p_{2m+1}} = \left(\underline{p_0} [S] \right) ([T] [S]) ([T] [S]) \dots ([T] [S]) \quad (4.100)$$

$$= \underline{p_0} [S] \quad (4.101)$$

$$\Rightarrow \mathbf{\Pi} = \mathbf{\Pi}_S. \quad (4.102)$$

If we *assume* that there is a unique probability limit then we must conclude that $\mathbf{\Pi}_S = \mathbf{\Pi}_T$ and hence $\frac{1}{4} = \frac{3}{4}$, which is a contradiction. We can invoke the principle of excluded middle, *reductio ad absurdum*, to conclude that the assumption of a single limiting stable value for $\lim_{m \rightarrow \infty} \left(\underline{p_m} \right)$ is false. In the asymptotic limit as $m \rightarrow \infty$, the probability-vector alternately assumes one of the *two* values $\mathbf{\Pi}_S$ or $\mathbf{\Pi}_T$. We refer to the set of all

4.7 Long sequences of operators

recurring probability-vectors of this type, $\{\Pi_S, \Pi_T\}$, as the *attractor* of the system. In more general terms an attractor is a set of points in the phase-space, which is invariant under the system dynamics in the asymptotic limit as $m \rightarrow \infty$.

4.6.3 Reduction of the periodic case

In the last section, we considered a short sequence of length 2. This can be generalised to an arbitrary length, $L \in \mathcal{Z}$. It is possible to associatively group the operators into sub-sequences of length L . As with the sequences of length two, the choice of time origin is not unique. We are free to make an arbitrary choice of time origin with the initial condition at $m = 0$. We can think of the operators as having an offset of $k \in \mathcal{Z}$, where $0 \leq k \leq L - 1$ within the sub-sequence. We can also calculate a new equivalent operator to represent the entire sequence, $A_{\text{eq}} = \prod_{k=0}^{L-1} A_k$. We can then calculate the stationary probabilities associated with this operator, $\Pi_{\text{eq}} = \Pi_{\text{eq}} \cdot A_{\text{eq}}$. We can refer the asymptotic trajectory of the probability-vector to this fixed-point, $p_{(m \pmod L)} = \Pi_{\text{eq}} \cdot \prod_{k=0}^{(m \pmod L)-1} A_k$. In the periodic case, there is generally not a single fixed-point in the original phase-space but the probability-vector settles into a stable limit cycle of length L . If we aggregate time, modulo L then we can re-define what we mean by *state* and we can define a new phase-space in which the probability-vector does converge to a single point.

If we allow the length of the period, N , to become indefinitely long $N \rightarrow \infty$ then our new definition of *state* becomes extremely complicated. We would have to contemplate indefinitely large offsets, n , within the very long cycle. It is not clear whether limits will exist. If we wish to avoid the many paradoxes that infinity can introduce then we should only consider the case with finite period, N .

4.7 Long sequences of operators

If we allow the sequence to become indefinitely long then the amount of memory required grows without bound. It is still possible, in principle, to define these indefinitely long periodic sequences as a homogeneous Markov process although the definition,

and encoding, of the states would require some care. We can consider any one indefinite sequence of operators as being one of many possible indefinite sequences of operators. If we do this then most of the possible sequences will appear to be random. We can learn something about the general case by studying indefinitely long random sequences.

If the sequence of operators is chosen at random then the probability-vector, as defined in the original phase-space, does not generally converge to a single unique value. Simulations show that the time-varying probability vector assumes a distribution in the original phase-space, which is self-similar, or fractal, in appearance. The existence of fractal geometry is established, with rigour, for some particular Markov games. We establish a transcendental equation, which allows the calculation of the Hausdorff dimensions of these fractal objects.

If state-transitions of the time-inhomogeneous Markov chains are associated with rewards then it is possible to show that even simple two-state Markov chains can generate a Parrondo effect, as long as we are free to choose the reward matrix. Homogeneous sequences of the individual games generate a net loss over time. Inhomogeneous mixtures of two games can generate a net gain.

We show that the expected rates of return, or moments of the reward process, for the time-inhomogeneous games are identical to the expected rates of return from a homogeneous sequence of a time-averaged game. This is a logical consequence of the law of total probability and the definition of expected value.

Two different views of the time-inhomogeneous process emerge, depending of the viewpoint that one takes:

- If you have access to the history of the time-varying probability vector and you have a memory to store this information and you choose to represent this data in phase-space then you will see distributions with fractal geometry. This is more or less the view that a casino, with many players, might have if they were to visualise the states of all of their players. (This would be the case if we had a real ensemble of many players playing this game.)

4.8 Phase-space visualisation and fractal properties

- If you do not compute the time-varying probability vector, or you have no memory in which to store the history of this information, then all that you can see is a sequence of rewards from a stochastic process. The internal details of this process are hidden from you. You have no way of knowing precisely how this process was constructed (ie. from an inhomogeneous sequence of Markov operators). There is no experiment that you can perform to distinguish between the time-inhomogeneous process and the time-averaged process. The time-averaged process is a homogeneous sequence of a single operator. We can calculate a single unique limiting value for the time-varying probability-distribution vector, which we could also refer to as the stationary probability-vector. This is more or less the view that a single, mathematically inclined, casino patron might have if they were playing against some elaborate poker machine, over a long period of time. The internal workings of the machine would be hidden from the player, but it would be possible to perform some analysis of the outcomes and form an estimate of the parameters for the time-averaged model.

We show that the time inhomogeneous process is consistent in the sense that the casino and the player will always agree on the expected winnings or losses of the player. In more technical terms, the time-average, which the player sees, is the same as the ensemble-average over phase-space, which the casino can calculate.

4.8 Phase-space visualisation and fractal properties

4.8.1 Two Markov games that generate simple fractals

We construct a simple system in which operators are selected at random and we will use the standard theories regarding probability and expected values to derive some useful results. If we modify the system specified by Equations 4.91 and 4.92, as follows:

$$[S] = \begin{bmatrix} \frac{5}{6} & \frac{1}{6} \\ \frac{1}{2} & \frac{1}{2} \end{bmatrix} \quad (4.103)$$

and

$$[T] = \begin{bmatrix} \frac{1}{2} & \frac{1}{2} \\ \frac{1}{6} & \frac{5}{6} \end{bmatrix} \quad (4.104)$$

and select the sequence of transition operators at random, then the attractor becomes an indefinitely large set. If we were to play a homogeneous sequence of either of these

games then they would have the same stable limiting probabilities as before, Π_S and Π_T , and the dynamics would be similar to those shown in Figure 4.22. In contrast, if we play an indefinite *random* sequence of the new games S and T, $[S, T, T, S, T, S, T, S \dots]$, then there are no longer any stable limiting probabilities and the attractor has a fractal or self-similar appearance, as shown in Figure 4.23.

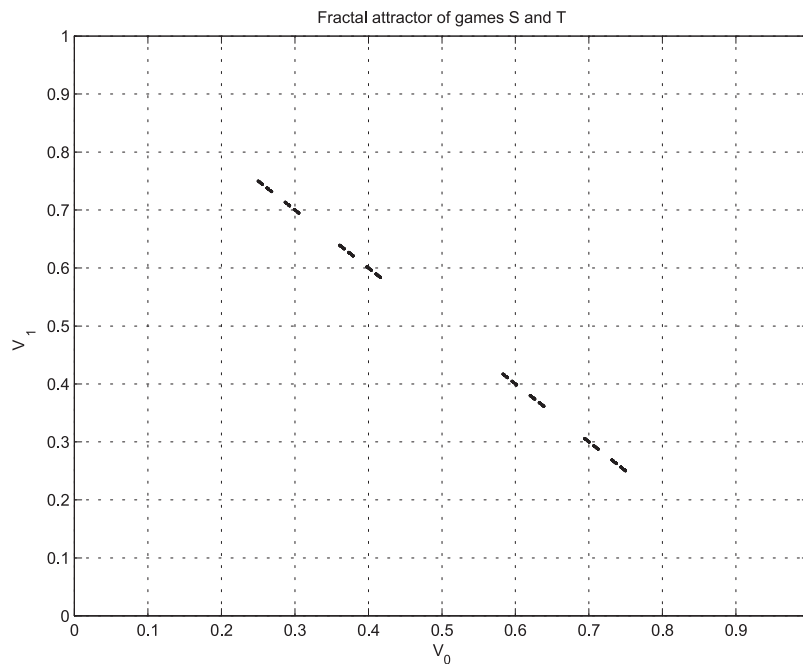


Figure 4.23. A fractal attractor generated by games S and T. These points were generated by the trajectory of a probability vector, operated on by a long, but finite, set of Markov operators, S , and T . They clearly approximate the Cantor set, on a line segment between, $[1/4, 3/4]$ and $[3/4, 1/4]$, which are the fixed points for the two individual operators, S and T . The coverage is only approximate due to the finite resolution of the graphing process. These two operators form an Iterated Function System (IFS) in the sense used by Barnsley (1988).

4.8.2 The Cantor middle-third fractal

Games S and T have been constructed in such a way that they approach the Cantor middle-third set. This was described by Cantor (1883) and has been described by a number of text books (Simmons 1963, Kolmogorov and Fomin 1970). The set is also discussed in the context of its self-similar fractal properties, by Mandelbrot (1977), who calls it *Cantor dust*. The construction of the Cantor set, using an Iterated Function System (IFS) is described by Barnsley (1988).

4.8 Phase-space visualisation and fractal properties

We note that the Cantor set is uncountable. Kolmogorov and Fomin (1970) points out that the Cantor set has the same power ²⁴ as the interval, $[0, 1]$, which has the same power as the entire real line, c . Any countably infinite, sequence of operators only has power of \aleph_0 , and will ever generate enough points to cover the entire Cantor set. The points generated by a random sequence of games cling to the boundaries of the Cantor set, but do not generate the entire set.

If we choose $\underline{p}_0 = [1/2, 1/2]$ then the initial condition lies outside the Cantor set. The operators never map the point \underline{p}_m into the Cantor set. There is always a slight gap. The distance between the point \underline{p}_m and the nearest point in the Cantor set will be $3^{-m}/6$ and this will tend inexorably towards zero with increasing time, as $m \rightarrow \infty$, but the point \underline{p}_m will always lie outside of the Cantor set.

Ergodic properties

Perhaps the best solution to the problem of coverage is to show that the quasi-ergodic hypothesis of Ehrenfest applies to our system: *“During the course of time, the path of [the system in phase space] goes as near as desired to any point in the surface.”* (Perrot 1998). In this case the ‘surface’ is understood to mean the set of points that is invariant under transformation by the transition operators that is the fractal attracting set. If the system were quasi-ergodic then the countable set of points, generated by the sequence of operators, will contain points that are within any given finite distance, $\epsilon > 0$, of any given point in the attractor. As long as we are prepared to wait long enough, and consider the effects of very many operators. This should apply, even if ϵ is very small, as $\epsilon \rightarrow 0^+$.

Hartfiel (2002) states a sufficient condition for a series of matrix operators, P_v to be ergodic, where $P_1 = A_1$, $P_2 = A_1 \cdot A_2$, $P_m = \prod_{v=1}^m A_v$. The sequence, $P_1, P_2 \cdots P_v \cdots$ is ergodic if, and only if, $\lim_{v \rightarrow \infty} \tau_B(P_v) = 0$, where τ_B is the Birkhoff contraction coefficient.

²⁴The word *power* can mean several different things in physics and mathematics. We use the word here in the sense used by Cantor, and later by Kolmogorov and Fomin (1970). Power is an extension of the idea of cardinality, the number of elements in a set. Finite sets have cardinality. For example, the set $\{1, 2, 3, 4, 5, 6\}$ has a cardinality of 6. The set of all integers $\mathcal{Z} = \{1, 2, 3 \cdots\}$ does not have any finite cardinality. It has a power, defined as \aleph_0 . The set of all real numbers, \mathcal{R} , has a greater power than the integers. This was indicated by Cantor, using his diagonal argument. The power of the real numbers is defined as c , or sometimes as \aleph_1 . There is a theorem, due to Cantor, that $c = 2^{\aleph_0}$.

For matrices S and T in Equations 4.103 and 4.103, we have $\tau_B(S) = \tau_B(T) = 1/5$, and also $\tau_B(A \cdot B) \leq \tau_B(A) \tau_B(B)$, for all operators, A and B , including all choices from the set $\{S, T\}$. It then follows that $0 < \tau_B(P_v) < 1/5^v$ and hence $\lim_{v \rightarrow \infty} \tau_B(P_v) = 0$, so a random sequence of matrices S and T will be ergodic in the sense defined by Birkhoff (Hartfiel 2002).

Alternatively, the complete Cantor set is generated if we consider the set of all possible initial conditions (that is the line segment, $[0, 1]$) and all *possible* sequences of operators and take the union of the resulting sets. We operate on complete sets, rather than single points. This is essentially what Barnsley achieves with his iterated function systems. The set of all possible sequences of operators maps neatly onto the binary representations of all real number in the interval, $[0, 1]$.

We can construct probability measures on the Cantor set. and then we can calculate probabilities and expected values. It is also reasonable to talk about the probability density function, of the probability-vector, within the phase-space. Our way forward can be guided by Figures 4.23 and 4.24. These were constructed using discrete approximations, and standard histogram, or bin-counting, techniques in Matlab. In order to stimulate intuition, we can simulate the process and generate a histogram, showing the distribution of the probability-vector. The result is shown in Figure 4.24.

If the process, in Figure 4.24 could be taken to an infinite limit then then we might expect the histogram to converge to the Probability Density Function (PDF) for the probability vector in phase space. If the limit exists *and* it is self-similar under the mappings S and T , then it would also be a fractal.

The property of self-similarity can be established by construction. The function can be explicitly constructed as a limit of a sequence of rectangular functions. This self-similar sub-division of the histogram, into rectangles, is included in the recursion rule, in Equation 4.119. The resulting PDF would not be a *function*, in the usual sense. It would be a *generalised function*, in the sense described by Schwartz (Zemanian 1965).

The issue of existence, of the PDF, requires us to show that the sub-division into self similar rectangular functions has a limit. Rectangular functions have zero derivatives everywhere, excepting at the edges of the rectangles. It is clear that there is no problem with convergence within the constant parts of the rectangular functions. This is no

4.8 Phase-space visualisation and fractal properties

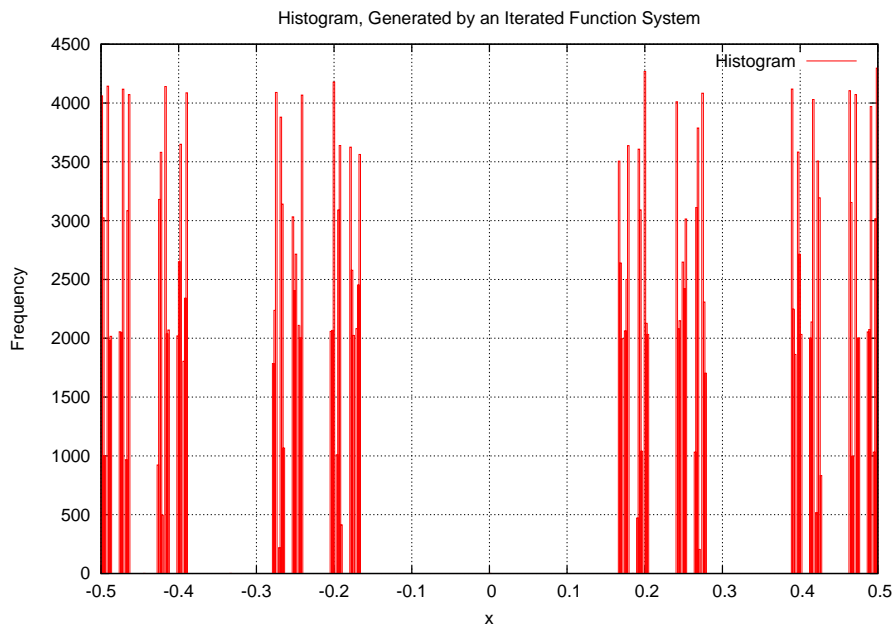


Figure 4.24. A histogram of a distribution in phase-space. This figure shows a histogram of the distribution of p_m , in phase-space. The position along the diagonal of Figure 4.23 can be represented by $x = p_0 - p_1$, which can be regarded as a random variable, and can be subjected to a standard bin-counting technique. This can be used to generate a histogram. It is intuitively clear that this process is building up a picture of a probability density function and that this function is self-similar.

more complicated than the process of allowing a single rectangle to converge to a Dirac delta function.

On the other hand, in the limit there are a potentially infinite number of rectangles, each with singularities at the boundaries. It is reasonable to ask whether these singularities prevent the process from converging to a stable limit. Fortunately, there is a proof, due to Lighthill (1958) that generalised functions can be re-constructed as limits of sequences of good²⁵ functions (Lighthill 1958), and the problem of supposedly infinite derivatives at boundaries can be avoided. One way to approach this would be to construct *nearly* rectangular functions which are still good. We could construct these functions in such a way that the difference, in measure, between these good functions and the rectangles diminishes to zero in the limit.

²⁵A *good* function is one which is everywhere differentiable any number of times and such that all of its derivatives are $\mathcal{O}(|x|^{-N})$ as $|x| \rightarrow \infty$ for all positive values of N .

For the x -axis, of Figure 4.24, we *could* have chosen the first element of the probability-vector, p_0 but this would not have been the easiest way to analyse the dynamics. It is better if we choose another parametrisation. If we examine the eigenvectors of the matrices in Equations 4.103 and 4.104 then we find that a better re-parametrisation is:

$$x = p_0 - p_1 \quad (4.105)$$

and

$$y = p_0 + p_1. \quad (4.106)$$

Of course, we always have $y = 1$ and x is a new variable in the range $-1 \leq x \leq +1$. The Cantor fractal lies in the unit interval $-\frac{1}{2} \leq x \leq \frac{1}{2}$, which is the x interval shown in Figure 4.24. The transformation for matrix $[S]$, in Equation 4.103 reduces to:

$$\left(+\frac{1}{2} - x_{m+1} \right) = \frac{1}{3} \cdot \left(+\frac{1}{2} - x_m \right) \quad (4.107)$$

and the transformation for matrix $[T]$, in Equation 4.104 reduces to:

$$\left(-\frac{1}{2} - x_{m+1} \right) = \frac{1}{3} \cdot \left(-\frac{1}{2} - x_m \right). \quad (4.108)$$

The transformation S has a fixed-point at $x = +\frac{1}{2}$ and the transformation T has a fixed-point at $x = -\frac{1}{2}$. If we choose these transformations as random then the recurrent values of x lie in the interval between the fixed-points, $-\frac{1}{2} \leq x \leq \frac{1}{2}$. This is precisely the iterated function system for the Cantor set (Barnsley 1988).

Fractal dimension, with uniform scale factors

The most elementary analysis that we can perform is to calculate the dimension of this set. If we assume the Iterated Function System (IFS), which generates the fractal is non-overlapping, then there will be conservation of measure.

Every time we perform a transformation, we reduce the diameter by a factor of $\lambda = \frac{1}{3}$ but the transformed object is geometrically half of the original object, $\mu = \frac{1}{2}$. In general, we can write

$$\mu = \lambda^D, \quad (4.109)$$

where λ is the linear scaling factor and μ is the factor by which the measure is scaled and D is the fractal dimension. This is the law of conservation of measure for this particular system. The special cases for line-segments $\mu = \lambda$, squares $\mu = \lambda^2$ and cubes

4.8 Phase-space visualisation and fractal properties

$\mu = \lambda^3$ are well known and not very controversial. The case where D is not an integer had been widely discussed by many authors, including Mandelbrot (1977) and Barnsley (1988), and is now widely accepted. For the case of the Cantor set, Equation 4.109 evaluates to

$$\frac{1}{2} = \left(\frac{1}{3}\right)^D, \quad (4.110)$$

so we can solve this equation, to give $D = \frac{\log(2)}{\log(3)} \approx 0.630929 \dots$.

The fact that the Cantor set has $0 < D < 1$, gives insight into an apparent paradox, in Kolmogorov and Fomin (1970). The total *length* of the Cantor set must be zero. After m steps of substitution, (removing the middle third of the set) the resulting set has length of $(2/3)^n$, so the total length of the Cantor set must lie in the interval, $0 \leq l \leq (2/3)^n$. If we take the limit as $n \rightarrow \infty$ then it follows that the Cantor set has zero length. On the other hand Kolmogorov and Fomin (1970) has established a 1 to 1 mapping between points in the Cantor set and points along the real line. How can a set of zero length can have the same number of points as a set of unit length? The answer is that length is a measure with dimension of 1. It is only appropriate to apply it to sets with a capacity dimension of 1, such as line segments. If we measure a set with dimension of less than one, such as a point, or the Cantor set, then we will obtain a total length of zero. On the other hand, if we attempt to measure the total length contained in a set with a dimension of greater than one, such as a unit square then there will be no upper limit to the process. A square effectively contains infinite length.

Following Mandelbrot (1977), the correct units for measuring line segment, with dimension of $D = 1$, will have dimensions of $[L]^1$. The correct units for measuring an element of area, with dimension of $D = 2$, will have dimensions of $[L]^2$. The correct units for measuring a Cantor set, with dimension of $D = \log(2)/\log(3)$, will have dimensions of $[L]^{\log(2)/\log(3)}$. Sets with different dimensions must be measured using units with different dimensions. If we attempt to use units with a different dimension then we will get a result of zero or infinity, which is not very informative. Measures with dimensions of $[L]^D$ are the natural extensions of length, area, and volume. The powers of sets, such as c , are natural extensions of the concept of cardinality, to infinite sets. These are different concepts.

In the sense that word was used by Cantor, the line segment, the area and the Cantor set all have the power, of c . The fact that the Cantor set has no length is not more remarkable than the fact that the line segment has no area. What is interesting is that all

of these sets have the same power as the entire real line, c .

Fractal dimension, with matrix operators

If the transformations are carried out using linear operators, represented by an L by L , square matrix, A , then it is necessary to calculate the linear scaling factor, λ associated with the transformation, A . This is discussed in Barnsley (1988), and in Meyer (2000), but is stated more explicitly in Doran and Lasenby (2003), where the results for matrices are stated in terms of more general Clifford geometric algebras²⁶. If we consider an L by L , square matrix, A then the ratio of the measures of small elementary of L -dimensional hypervolumes, before and after transformation, are given by the determinant of the transformation matrix,

$$\mu_{\text{hypervolume}} = \det A. \quad (4.111)$$

If we do not consider orientation, then the linear scaling factor is simply

$$\lambda = |\det A|^{\frac{1}{L}}. \quad (4.112)$$

Fractal dimension, with two matrix operators

If we construct an Iterated Function System (IFS) using two L by L , square matrices, A and B , then the form of 4.109 has to be changed,

$$\lambda_A = |\det A|^{1/L} \quad (4.113)$$

$$\lambda_B = |\det B|^{1/L}. \quad (4.114)$$

These two mappings transform the entire fractal set into a subset of itself, with linear scaling factors of λ_A and λ_B . The two subsets both have the same fractal dimension as the whole set and the union of these two subsets reconstruct the whole fractal set.

If the IFS is non-overlapping then we can use conservation of measure to write

$$1 = \lambda_A^D + \lambda_B^D \quad (4.115)$$

$$= |\det A|^{D/L} + |\det B|^{D/L}. \quad (4.116)$$

²⁶Clifford algebras are useful because they maintain all of their properties in higher dimensional spaces.

4.8 Phase-space visualisation and fractal properties

Formulae of this type appear in Barnsley (1988). Equation 4.116 is applicable to Parrondo's original games since there are only two operators, A and B . This could easily be generalised to the case with more operators by including more terms in the sum. The case where the IFS is self-overlapping can be treated in this way, but additional terms need to be subtracted to account for the measure of the overlap. The transformations in Parrondo's original games were non-overlapping.

Moments in phase-space

We can invert the rules described in Equations 4.107 and 4.108 giving:

$$x_t = 3x_{t+1} - 1 \quad (4.117)$$

and

$$x_t = 3x_{t+1} + 1. \quad (4.118)$$

If we consider these equations, together with the law of total probability, then we get a self-similarity rule for the PDF (Probability Density Function), $p(x)$, of the probability-vector, \underline{p}_m :

$$\frac{3}{2}p(3x - 1) + \frac{3}{2}p(3x + 1) = p(x). \quad (4.119)$$

The function $p(x)$ is the density function towards which the histogram in Figure 4.24 converges if we collect enough samples. If the time varying probability vector has a distribution in phase-space then it is reasonable to calculate moments of this distribution. A direct approach leads to infinite sums or infinite products. The self-similarity rule in Equation 4.119 allows a useful simplification. We propose an approach based on generating functions, of the type defined in (Papoulis 1991):

$$\Phi(\Omega) = E[e^{j\Omega x}] = \int_{-\infty}^{+\infty} e^{+j\Omega x} \cdot p(x) dx. \quad (4.120)$$

Generating functions are integral transforms of probability density functions. We can make use of the shifting properties of the transform to prove that

$$\int_{-\infty}^{+\infty} e^{j\Omega x} \cdot p(3x - 1) dx = \frac{1}{3}e^{-j\frac{\Omega}{3}} \cdot \Phi(\Omega/3), \quad (4.121)$$

and

$$\int_{-\infty}^{+\infty} e^{j\Omega x} \cdot p(3x + 1) dx = \frac{1}{3}e^{+j\frac{\Omega}{3}} \cdot \Phi(\Omega/3). \quad (4.122)$$

If we combine Equations 4.121, 4.121 and 4.120, then we can a simple recursion rule for the Moment Generating Function (MGF):

$$\Phi\left(\frac{\Omega}{3}\right) \cdot \cos\left(\frac{\Omega}{3}\right) = \Phi(\Omega). \quad (4.123)$$

We can evaluate the derivatives at $\Omega = 0$ and calculate as many of the moments as we wish. The probability density function must be normalised to one, so it follows that $\Phi(0) = 1$. The other derivatives can be obtained by successively differentiating Equation 4.123,

$$\frac{1}{3} \sin\left(\frac{\Omega}{3}\right) \Phi\left(\frac{\Omega}{3}\right) + \Phi'(\Omega) + -\frac{1}{3} \cos\left(\frac{\Omega}{3}\right) \Phi'\left(\frac{\Omega}{3}\right) = 0, \quad (4.124)$$

which leads to the special case of $\Phi'(0) = 0$, as $\Omega \rightarrow 0$. A second differentiation leads to

$$\frac{1}{9} \cos\left(\frac{\Omega}{3}\right) \Phi\left(\frac{\Omega}{3}\right) + \frac{2}{9} \sin\left(\frac{\Omega}{3}\right) \Phi'\left(\frac{\Omega}{3}\right) + \Phi''(\Omega) - \frac{1}{9} \cos\left(\frac{\Omega}{3}\right) \Phi''\left(\frac{\Omega}{3}\right) = 0, \quad (4.125)$$

which leads to the special case of $\Phi''(0) = -1/8$, as $\Omega \rightarrow 0$. We can then use Equations 4.125 and 4.125 to derive expressions for the first two moments; the mean, μ , and the variance σ^2 :

$$\mu = j\Phi'(0) = 0 \quad (4.126)$$

$$\sigma^2 = -\Phi''(0) + \Phi'(0) = \frac{1}{8}. \quad (4.127)$$

These algebraic results are consistent with results from the numerical simulations that were used to generate the histogram in Equation 4.24. It is interesting to compare the second moment with the result for a uniform distribution, which would have a variance of $\sigma^2 = 1/12$. The variance of the cantor set is larger than the variance of a uniform distribution, over the same domain.

In summary, it is possible to calculate moments of the distributions in phase space using symmetry considerations. These results were published in Allison *et al.* (2005), although some aspects of this result appear to have been anticipated by Elton and Yan (1989). This last paper was communicated by Barnsley and deals with moments and cumulants of sets generated by Iterated Function Systems. There is an unpublished pre-print by Jorgensen *et al.* (2007), which deals with the case of an overlapping IFS. They also include formulae for the moments in terms of infinite products of trigonometric functions. These formulae do not make explicit use of the self-similarity imposed by the IFS and are more complicated than the result in Equation 4.123.

4.8.3 Iterated Function Systems (IFS)

The cause of the fractal geometry is best understood if we realise that Markov transition operators perform affine transformations on the phase-space. An indefinite sequence of different Markov transition operators is equivalent to an indefinite sequence of different affine transformations, which is called an *iterated function system*, or IFS. We refer the reader to Barnsley (1988) showing that fractal geometry is general property of a system of randomly selected affine transformations. Barnsley's work is given further support by Hartfiel (2002), who describes how non-homogeneous products of matrices give rise to fractal geometry. He presents an approach to the construction of the Cantor set that is very similar to the one presented in Figure 4.23.

4.8.4 Parrondo's fractal

The construction in the last section was deliberately kept simple:

- The operators only have two dimensions, so visualisation on paper is easy.
- Uniform sequences of regular Markov operators have known unique stationary probability vectors.
- A mixed sequence of operators is isomorphic to a known iterated function system (IFS).
- The IFS generates a known attracting set in phase space, the Cantor set.
- This attractor is known to be a fractal.
- The points generated by the mixed sequence of operators adhere closely to the boundaries of the attractor, in phase space, as $m \rightarrow \infty$.

We can relax some of these conditions and the result will still be similar:

- The operators can have many dimensions.
- A mixed sequence of operators can still constitute an iterated function system (IFS).

- The IFS still can still generate an attracting set in phase space.
- The attractor can still be a fractal.
- The points generated by the mixed sequence of operators will adhere closely to the boundaries of the attractor, as $m \rightarrow \infty$.

This is the case with Parrondo's original Games A and B. The resulting attractor, in phase space, is shown in Figure 4.25. The similarity to Figure 4.23 is clear.

The matrices for Games A and B, for Parrondo's original games, are three dimensional, $L = 3$. We can apply the methods described in Barnsley (1988), and summarised in Equation 4.116, to obtain an expression for the dimension, D , of Parrondo's original games, in phase-space

$$|\det(A)|^{\frac{D}{3}} + |\det(B)|^{\frac{D}{3}} = 1, \quad (4.128)$$

where A and B are the reduced matrices for Parrondo's games, as described in Equation 4.6. If we use Parrondo's original parameters then the equation for the dimension, D , reduces to:

$$\left(\frac{10003}{40000}\right)^{\left(\frac{D}{3}\right)} + \left(\frac{4463}{40000}\right)^{\left(\frac{D}{3}\right)} = 1, \quad (4.129)$$

and the numerical solution is $D \approx 1.18314737032$. The theory, from Barnsley, can be tested against numerical simulations of Parrondo's games. It is possible to estimate the dimension of a fractal, using the standard box-counting technique. This can be compared with the result from the theory. The correspondence is shown in Figure 4.26. The results agree to about 3 decimal places, which is quite reasonable given the number of points in the simulation.

4.9 Equivalent representation

It is not immediately obvious that expected values calculated over time will always agree with expected values calculated by summing over phase space. We prove that this true, by direct evaluation. If this were not so then we would suspect that the process is not ergodic, which would lead us to doubt some of our earlier results.

4.9 Equivalent representation

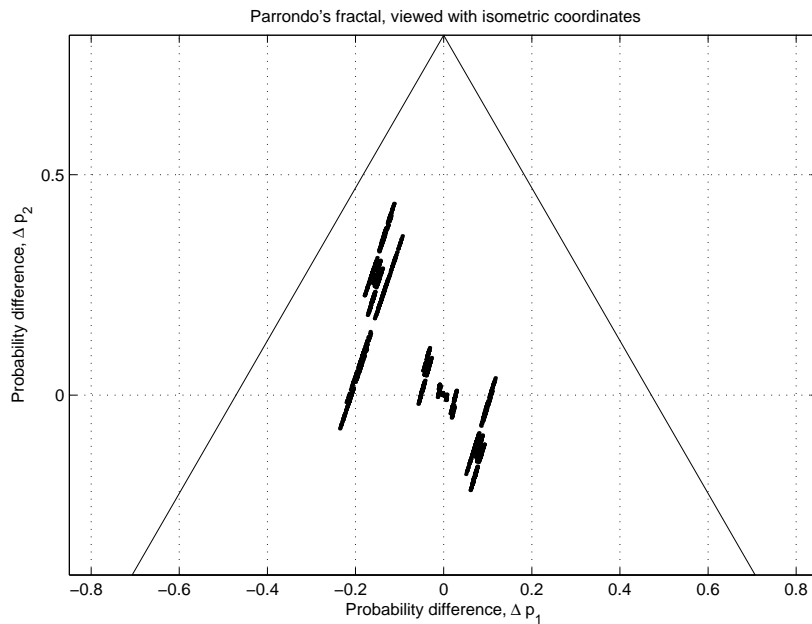


Figure 4.25. The fractal object generated by Parrondo's original games. Parrondo's original games had three states and the probability vector had three dimensions, $\underline{p} = [p_1, p_2, p_3]$. The embedding space is \mathcal{R}^3 . The law of total probability requires $p_1 + p_2 + p_3 = 1$. This constraint implies that the phase-space is actually the plane specified by the equation, $p_1 + p_2 + p_3 = 1$. The phase space is actually two dimensional and can be accurately represented on a printed page. We use a translation, by $[-1/3, -1/3, -1/3]$, followed by rotations in space that preserve length and angle measure. The y -axis of this figure is the projection of the p_3 -axis of the embedding space, denoted by Δp_2 . The other coordinate, the x -axis in this figure is a linear combination of p_1 and p_2 , and is denoted by Δp_1 . The figure represents a true and un-distorted view of the phase-space. There are further constraints on probabilities p_1 , p_2 , and p_3 since $0 \leq p_1 \leq 1$, $0 \leq p_2 \leq 1$ and $0 \leq p_3 \leq 1$. This means that the feasible or reachable region of the phase-space is actually a convex polytope within the phase space. In this case, the boundary is an equilateral triangle, which is shown in the figure. If Parrondo's games are played at random then the probability vector traces out parts of an attracting set. This is the set of all recurrent points in the phase-space. For Parrondo's games, where the games are chosen at random, the attracting set is a fractal, which we call *Parrondo's fractal*. This is self-similar and is a fractal, in the sense defined by Barnsley. It is also a fractal, in the same sense that the Cantor set is a fractal. This was first proposed by Allison *et al.* (2005). This fractal was later independently confirmed by Behrends (2006) and in Behrends (2008).

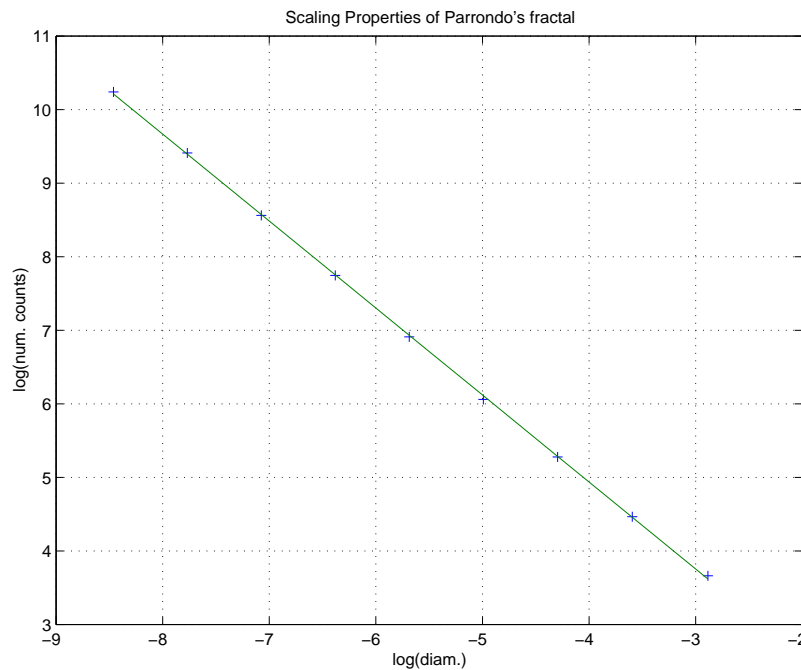


Figure 4.26. The scaling properties of the attractor generated by Parrondo's games. The habitual use of fixed-point theorems has led some mathematicians to query whether or not the attracting set, generated by Parrondo's games is truly a fractal, or whether it is just a transient phenomenon. If the true attractor is just a single fixed-point then it has a fractal dimension of zero, the dimension of a single point. Then any attempt to measure the dimension of the attractor does not converge to a stable value above zero. We use the standard box-counting technique to estimate the capacity dimension of the attracting set for Parrondo's games. This figure shows the results of simulations of more than a billion trials of Parrondo's games. The analysis covers over six orders of magnitude in scale. The horizontal axis represents the size of the boxes, in phase space. The vertical axis represents the number of boxes that enclose one or more points from the simulation. The line of best fit is very clear with very little variation. If the apparent-fractal were only a transient effect, then the slope of the line should change as the number of simulations increased. What we actually observe is a very clear straight line. The slope implies a capacity dimension of 1.18315, which agrees very well with the result from Barnsley's theory, 1.18224. Of course, the *true* proof depends on the logic of Barnsley's approach, but the simulation does support the argument and suggests that there are no grave errors, or fallacies, in the logic.

4.9.1 The average probability vector, over time

At each individual time step, the process is Markov. We do not need to consider past history. We only need to consider the present state, n , or our knowledge of the present

4.9 Equivalent representation

state, p_m . If we average the transitions over time then they will be averaged in proportion to their rate of occurrence. This leads to a time averaged game, with transition probabilities,

$$C_{i,j} = A_{i,j} \cdot \gamma + B_{i,j} \cdot (1 - \gamma). \quad (4.130)$$

The process described in Equation 4.130 has no memory beyond the present state, or our knowledge of the present state. There is a useful thought experiment²⁷ that we can consider, in order to clarify the meaning of this result. We can imagine a casino that owns two game machines. Inside one machine, the algorithm generates a random event, with probability of γ and then plays Game A or Game B depending on the outcome. Inside the other machine, the other algorithm always plays Game C. As players, we do not have access to the detailed mechanisms or algorithms inside the machines. We only have access to the results that come out of the machines, where we receive positive or negative rewards. The key question is: *Is there any analysis that we can perform on the sequences of rewards from these two machines that would allow us to determine which machine was an inhomogeneous random sequence of Games A and B, and which machine was playing an homogeneous sequence of Games C?* The previous result shows that there is no experiment that we can perform to distinguish between the two machines. We refer to Game C as the time-average model. This is analogous to the state-space averaged model found in the theory of control (Middlebrook and Čuk 1976, Levine 1996).

The stationary probability vector, $\underline{\pi}$, has to satisfy the relationship

$$\underline{\pi} = \underline{\pi} \cdot \mathbf{C}, \quad (4.131)$$

together with a normalisation condition,

$$\sum_{n=1}^3 \pi_n = 1. \quad (4.132)$$

These are necessary and sufficient conditions for the complete specification of $\underline{\pi}$, provided \mathbf{C} is regular. These were the conditions used to derive Equation 4.22. Once the stationary probability vector has been specified then the rates of reward from the games can be calculated using Equation 4.13.

²⁷*Gedankenexperiment.*

4.9.2 The average probability vector, over phase-space

We would like to know whether the stationary probability vector, calculated by averaging over time, in Equation 4.131, is the same as the stationary probability vector, calculated by averaging over the attracting set in phase space, as shown in Figure 4.25. This requires changes of variable of the type described in Equations 4.117 and 4.118, and leads to a self-similarity rule, similar to Equation 4.119. This can be manipulated, using an integral transform to yield a recursion rule for the multi-dimensional Moment Generating Function (MGF), similar to the one in Equation 4.123. Finally, it is possible to take the vector gradient of the MGF, to obtain an expression for the mean value of the time varying probability vector, in phase space, similar to the expression in Equation 4.127. Under conditions, which apply to Parrondo's original games, it is possible to show that the two averages must satisfy the same equations and therefore must have the same values. It then follows that the rates of reward are the same, whether we average over time or over phase-space.

Linear transformations of phase-space

If we play Game A, for example, then we perform a linear transformation on the phase-space and we map the entire attracting set onto a subset of itself. We denote the vector in phase space by \underline{p}_m , at time m . We denote the density function over the phase space as $\mathcal{P}(\underline{p})$. The fonts are intended to be significant here. Also, the density function has a vector argument, $\mathcal{P}(\dots)$, and the probability vector has an \underline{p}_m , and does represent a row vector. After transformation by Game A, the new density function will be related to the old one through the relationship

$$\mathcal{P}(\underline{p}') = \frac{1}{\det(\mathbf{A})} \mathcal{P}(\mathbf{A}^{-1}\underline{p}). \quad (4.133)$$

The factor of $1/\det(\mathbf{A})$, is to account for the change in ratio of volumes, before and after transformation. This expression would work in higher (or lower) dimensions, but in these cases we would be dealing with elements of hyper-volume (or area) rather than elements of volume, when the density functions are integrated. The corresponding rule for Game B is

$$\mathcal{P}(\underline{p}') = \frac{1}{\det(\mathbf{B})} \mathcal{P}(\mathbf{B}^{-1}\underline{p}). \quad (4.134)$$

4.9 Equivalent representation

The self-similarity rule for Parrondo's games

If we play Games A and B, at random, with probability of γ , then the self-similarity rule for the density function becomes

$$\frac{\gamma}{\det(\mathbf{A})} \mathcal{P}(\mathbf{A}^{-1}\underline{p}) + \frac{1-\gamma}{\det(\mathbf{B})} \mathcal{P}(\mathbf{B}^{-1}\underline{p}) = \mathcal{P}(\underline{p}). \quad (4.135)$$

This is a generalisation of the rule in Equation 4.119, and would apply for Parrondo's Games, or any system that could be written using an inhomogeneous sequence of Markov operators. There are only two terms on the left hand side of Equation 4.135. This is because the IFS for Parrondo's games is non-overlapping. If overlap did occur then additional terms would have to be included, to account for the overlap. The use of the determinants in the denominators, and the use of inverse matrices assumes that the operators are non-singular. If we use the notation in Equation 4.6, then the determinant of a transition matrix, for the original form of Parrondo's Games has the form

$$\det(\mathbf{A}) = (1 - q_1)(1 - q_2)(1 - q_3) - q_1q_2q_3, \quad (4.136)$$

which is nonzero for Parrondo's original values, for Games A, B and C.

The moment generating function for the distribution of the probability vector

The multi-dimensional Moment Generating Function (MGF) has to be integrated over the entire phase-space. It should be understood that the bounds of integration are the entire phase-space. An infinitesimal element of volume is represented by

$$d\mathbf{V} = dp_1 \cdot dp_2 \cdot dp_3 = \prod_{n=1}^3 dp_n. \quad (4.137)$$

For Parrondo's original games we had, $L = 3$, for three dimensions. This result can be readily generalised to higher numbers of dimensions, $L > 3$, by altering the upper limit of the sum in Equation 4.137. We can define the multi-dimensional MGF for a multi-dimensional density function as

$$\Phi(\underline{\Omega}) = \int \int \int e^{j\underline{\Omega} \cdot \underline{p}^T} \cdot \mathcal{P}(\underline{p}) d\mathbf{V}. \quad (4.138)$$

This is a volume integral of a scalar function, which is defined over the multi-dimensional phase-space. The vector form, $\underline{\Omega} \cdot \underline{p}^T$, is an inner vector product. The moment generating function is an integral transform, similar to the Fourier Transform, and has a

general scaling property of

$$\int \int \int e^{j\underline{\Omega} \cdot \underline{p}^T} \cdot \mathcal{P}(\underline{p} \mathbf{E}) d\mathbf{V} = \det(\mathbf{E}^{-1T}) \cdot \Phi(\underline{\Omega} \mathbf{E}^{-1T}), \quad (4.139)$$

where \mathbf{E} is an general non-singular linear transformation of the phase-space. This essentially is a multi-dimensional version of the scaling property of the Fourier Transform. If we take the MGF of Equation 4.135 and apply the rule for re-scaling then we obtain

$$\gamma \cdot \Phi(\underline{\Omega} \mathbf{A}^T) + (1 - \gamma) \cdot \Phi(\underline{\Omega} \mathbf{B}^T) = \Phi(\underline{\Omega}). \quad (4.140)$$

This is the generalisation of Equation 4.123.

The average probability vector, in phase-space

To calculate the moments of the vector \underline{p} in phase space, we need to take gradients of the MGF, in the $\underline{\Omega}$, or frequency, space.

Using standard manipulations of vector calculus, it can be shown that

$$\nabla_{\underline{\Omega}}(\Phi(\underline{0})) = \lim_{\underline{\Omega} \rightarrow \underline{0}} (\nabla_{\underline{\Omega}}(\Phi(\underline{\Omega}))) = j \int \int \int \underline{p} \cdot \mathcal{P}(\underline{p}) d\mathbf{V}. \quad (4.141)$$

If we apply this result to the recursion rule in Equation 4.140, and apply the distributive law, we can show that

$$\nabla_{\underline{\Omega}}(\Phi(\underline{0})) (\gamma \mathbf{A} + (1 - \gamma) \mathbf{B}) = \nabla_{\underline{\Omega}}(\Phi(\underline{0})). \quad (4.142)$$

It is also necessary to make use of the lemma, $\nabla_{\underline{\Omega}}(\underline{\Omega} \mathbf{A}) = \mathbf{A}^T$, for a general linear transformation, \mathbf{A} .

4.9.3 Consistency of the two averages

Expected values and gradients of multi-dimensional moment generating functions are related by

$$E[\underline{p}] = -j \nabla_{\underline{\Omega}}(\Phi(\underline{0})), \quad (4.143)$$

which follows from Equation 4.141. We evaluate the gradient of $\Phi(\underline{\Omega})$ with respect to $\underline{\Omega}$ and take the limit as $\underline{\Omega} \rightarrow \underline{0}$, and multiply the result by the inverse of the square root of minus-one, $-j$. We also recall that we defined a time-average game as $\mathbf{C} = \gamma \mathbf{A} + (1 - \gamma) \mathbf{B}$. Equation 4.142 now reduces to

$$E[\underline{p}] \mathbf{C} = E[\underline{p}], \quad (4.144)$$

4.10 An optimised form of Parrondo's games

which is identical to Equation 4.131. This means that $\underline{\pi} = E[\underline{p}]$. The stationary probability vector is identical with the expected value of the time-varying probability vector, evaluated over the phase-space.

4.10 An optimised form of Parrondo's games

Simulations reveal that *periodic* inhomogeneous sequences of Parrondo's games have the strongest Parrondo effect. It can be shown that a powerful (locally optimal) form of the games is a set of three games that are played in a strict periodic sequence $\{G_0, G_1, G_2, G_0, G_1, G_2, \dots\}$. The transition probabilities are as follows :

$$\text{Game } G_0 : [a_0, a_1, a_2] = [\zeta, (1 - \zeta), (1 - \zeta)]$$

$$\text{Game } G_1 : [a_0, a_1, a_2] = [(1 - \zeta), \zeta, (1 - \zeta)]$$

$$\text{Game } G_2 : [a_0, a_1, a_2] = [(1 - \zeta), (1 - \zeta), \zeta]$$

where ζ is a small probability, $0 < \zeta < 1$. We can think of ζ as being a very small, ideally microscopic, positive number, $\zeta \rightarrow 0$. These matrices can be written out in the form of Equation 4.6 as follows:

$$[\mathbf{G}_0] = \begin{bmatrix} 0 & \zeta & 1 - \zeta \\ \zeta & 0 & 1 - \zeta \\ 1 - \zeta & \zeta & 0 \end{bmatrix}, \quad (4.145)$$

and

$$[\mathbf{G}_1] = \begin{bmatrix} 0 & 1 - \zeta & \zeta \\ 1 - \zeta & 0 & \zeta \\ 1 - \zeta & \zeta & 0 \end{bmatrix}, \quad (4.146)$$

and

$$[\mathbf{G}_2] = \begin{bmatrix} 0 & 1 - \zeta & \zeta \\ \zeta & 0 & 1 - \zeta \\ \zeta & 1 - \zeta & 0 \end{bmatrix}. \quad (4.147)$$

The rate of return from any **pure sequence** of any one game is approximately

$$\varrho \approx \frac{1}{2} \cdot \zeta, \quad (4.148)$$

which is close to zero and yet the return from the **cyclic combination** of these games is approximately

$$\varrho \approx 1 - 3 \cdot \zeta, \quad (4.149)$$

which is close to a certain win. We can engineer a situation where we can deliver an almost certain win every time using games that, on their own, would deliver almost no benefit at all! These games clearly work better as a team than on their own. Just as team players may pass the ball in a game of soccer, the games $\{G_0, G_1, G_2\}$ carefully pass the probability-vector from one trial to the next as this sequence of Parrondo's games unfolds.

4.10.1 An interesting fractal object

It is possible to de-rate these games by increasing ζ . In the limit as $\zeta \rightarrow \frac{1}{2}$ the Parrondo effect vanishes and the attractor collapses to a single point in phase-space. Just before this limit, the attractor takes the form of the very small and exquisite fractal shown in Figure 4.27.

This fractal is embedded in a two dimensional sub-space of the three dimensional phase-space of the games $\{G_0, G_1, G_2\}$. The two dimensional sub-space has been projected onto the page in order to make it easier to view. The projection preserves dot product, length, and angle measure. The coordinates x and y are linear combinations of the components of the original probability-vector, $\underline{p}_m = [p_0, p_1, p_2]$. The orientation of the image is such that the original p_2 -axis is projected onto the new y -axis. (The orientation of the upward direction is preserved.) The negative numbers on the axes represent negative offsets rather than negative probabilities. This is the same concept that is used when we write down a probability $(1 - p)$. If p is a valid probability then so is $(1 - p)$. The number $-p$ is an offset that just happens to be negative.

The dimension of this fractal is $D \approx \frac{\log(9)}{\log(4)} \approx 1.585$. We define the amount of Parrondo effect, Δp , as the difference in rate of return, ϱ , between the mixed sequence of games $\{G_0, G_1, G_2\}$ and the best performance from any pure sequence of a single game. For

4.11 Chapter summary

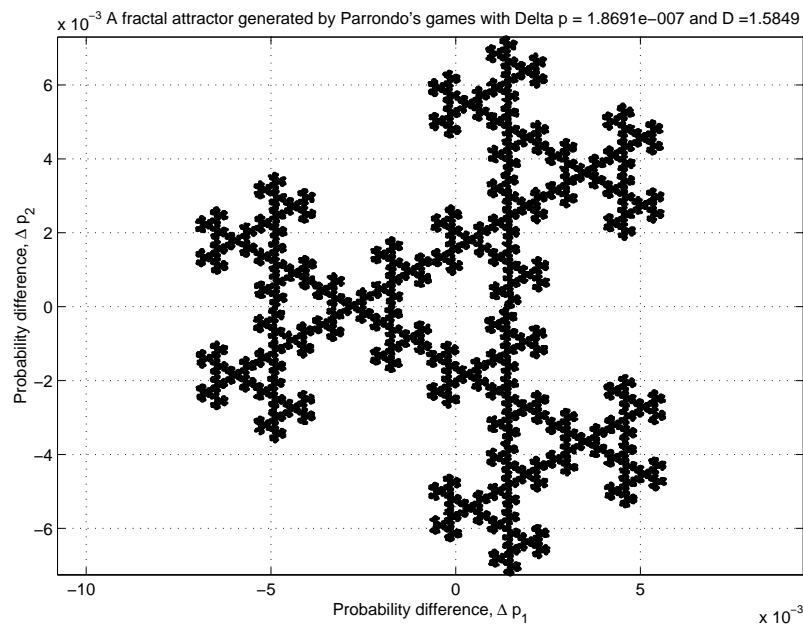


Figure 4.27. Fractal attractor generated by a limiting case of Parrondo's games. In the limiting case as $\lim_{\xi \rightarrow \frac{1}{2}}$, the fractal attractor becomes very small in size and adopts a very symmetrical, even beautiful, mathematical object. This figure shows a two-dimensional, greatly enlarged, projection of the attracting set. It is possible to see that this is a fractal, even without any formal proof that the fractal dimension $D \approx 1.5849$ is not an integer. The quantity, $dp \equiv \Delta p \approx 1.8691 \times 10^{-7}$ is the difference in rate of return, ϱ , between the mixed sequence of games $\{G_0, G_1, G_2\}$ and the best performance from any pure sequence of a single game. This fractal can be poetically described as the “last-gasp” of the Parrondo effect as $\lim_{\xi \rightarrow \frac{1}{2}}$.

this limiting case, $\Delta p \approx 0$. There are some interesting qualitative relationships between the Hausdorff dimension and the amount of Parrondo effect, which deserve further investigation to see if it is possible to formulate general quantitative law.

4.11 Chapter summary

In this chapter we have analysed Parrondo's games in terms of the theory of Markov chains with rewards. We have illustrated the concepts constructively, using a simple two-state version of Parrondo's games and we have shown how this gives rise to fractal geometry in phase-space. We have arrived at a simple method for calculating the expected value of the asymptotic rate of reward from these games and we have shown

that this can be calculated in terms of an equivalent time-averaged game. We have used graphic representations of trajectories and attractors in phase-space to motivate some of the arguments.

The use of phase-space concepts opens up new lines of enquiry. Simulation and visualisation encourage intuition and help us to grasp the essential features of a new system. This would be much more difficult if we were to use a purely formal algebraic approach at the start. We do not propose visualisation as a *replacement* for rigorous analysis. We see it as a guide to help us to decide, which problems are worthy of more detailed attention, and which problems might later yield to a more formal approach. We believe that phase-space visualisation will be as useful for the study of the dynamics of Markov chains as it has already been for the study of other dynamical systems.

Finally, we conclude that the apparent paradox of Parrondo's games arises because the reward process is a nonlinear function of the Markov transition operators, whereas our naïve common sense tells us the reward process ought to be linear. When we combine the games by selecting them at random, we perform a linear convex combination of the operators, but the expected asymptotic value of the rewards from this combined process is not a linear combination of the rewards from the original games.

Much of the earlier work used models with discrete states and continuous time. This is apparent in Westerhoff *et al.* (1986) and in Simon *et al.* (1992), for example. It would be natural to ask whether there are other systems, with discrete states and continuous time, which also exhibit paradoxical behaviour. Allison and Abbott (2001) showed that this is the case for switched circuits, as shown in the next chapter.

Chapter 5

switched-mode circuits and switched Markov systems

IN this chapter we use an analogy with Parrondo's games to design a second order switched mode circuit, which is unstable in either mode but is stable when switched. We do not require a sophisticated control law. The circuit is stable, even if it is switched at random. We use a stochastic form of Lyapunov's second method to prove that the randomly switched system is stable with probability of one.

We perform state-space simulations of our system, with a randomised discrete-time switching policy. The limiting case where switching is very rapid, but random, is examined. This leads to a consideration of Stochastic Differential Equations (SDEs).

5.1 Switched-mode circuits and switched Markov systems

In this section we suggest that deep similarities exist, between systems governed by randomly selected Markov operators, such as Parrondo's games (Harmer and Abbott 1999b, Harmer and Abbott 1999a, Pearce 2000b, Pearce 2000a, Harmer *et al.* 2000a), systems governed by time-varying transition matrices, such as switched-mode circuits (Middlebrook and Čuk 1976, Billings 1989, Gottlieb 1992) and physical systems with randomised control laws (Lai 1977, Hui *et al.* 1997, Wu and Tse 1996, Skafidas *et al.* 1999). The defining property of Parrondo's games is that it is possible to combine two losing games to achieve a winning result.

5.1.1 Switched-mode circuits

Firstly, we work through a simple and specific example of a switched-mode circuit, in order to demonstrate the method of the state-space²⁸ time-average model developed by Middlebrook and Čuk (1976).

A very simple switched-mode circuit is shown in Figure 5.1. The source of energy is modelled as a general Thévenin linear source, with source impedance of R_s and open-circuit voltage of V_s . The load is modelled as a linear load, with an impedance of R_l . This energy conversion-circuit only contains one energy-storage element, the capacitor, C . We can denote the voltage across the capacitor by V_c . The capacitor is switched back and forth between the input side of the circuit and the output side of the circuit, using switching devices. In this case, the switching devices are Metal Oxide Field Effect Transistors (MOSFETs). These switching elements are turned on and off by control voltages, Q and \bar{Q} . It is usual for only one of Q or \bar{Q} to be high at any one time. This means that only one switching device is turned on at any one time. The other device should be turned off. If this condition is not maintained then it is possible for the load to be directly connected to the source. This can lead to waste of energy, loss of control

²⁸We note that electrical engineers regularly use the term *state-space* to refer to what physicists and mathematicians might prefer to call *phase-space*. We prefer to use the term *phase-space* in order to avoid ambiguity with the other use, in the theory of Markov chains. We are occasionally constrained to use the words *state-space* in the sense that engineers use the term, when we quote existing works by engineers.

or even damage to the switching elements. The mutually-exclusive aspect of Q and \bar{Q} can be maintained by controlling MOSFETs using outputs from a *toggle flip-flop*, which will toggle every time a pulse is fed into it. The output of this circuit is generally considered to be the voltage across the load R_l . This depends on the average current in R_l and can be controlled, within certain limits, by varying the duty cycle, that is the fraction of the time, for which Q is high and \bar{Q} is low. The switching devices are usually designed to switch from fully *OFF* to fully *ON* in a very short time, because the circuit wastes energy when the switching devices are in a half-on and half-off condition. If we know the value of V_c as well, as the input, V_s and the modes of the switching devices, Q and \bar{Q} then it is possible to specify all the voltages and currents in the entire circuit. In the parlance of the theory of state variables, this is enough to establish that V_c is a *state-variable* and is the only state-variable for this circuit. More formally Dorf and Bishop (1998) state that “*The state of a system is a set of variables such that the knowledge of these variables and the input functions will, with the equations describing the dynamics, provide the future state and output of the system.*” The choice of state variables is not unique. The total stored energy in this circuit can be deduced from the state-variable. In particular, we have $\mathcal{U} = \frac{1}{2}CV_c^2$.

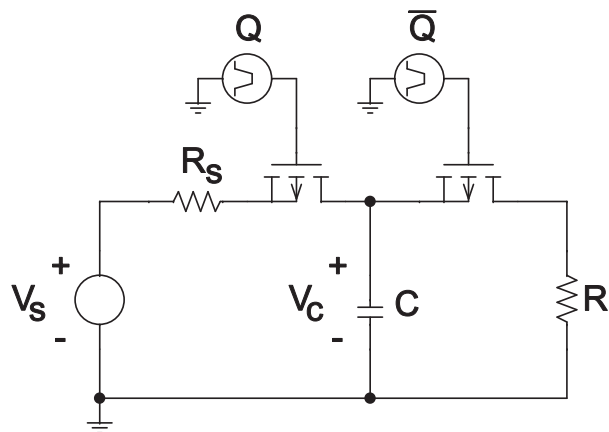


Figure 5.1. A simple switched capacitor energy converting circuit. The capacitor is switched back and forth between the input side of the circuit and the output side of the circuit, using switching devices. The average voltage at the output depends on the average current in R_l and can be controlled, within certain limits, by varying the duty cycle, that is the fraction of the time, for which Q is high and \bar{Q} is low.

5.1 Switched-mode circuits and switched Markov systems

Equivalent circuits in the two modes

When the circuit is in the *ON* mode is equivalent to the circuit shown in Figure 5.2. When the circuit is in this mode then the *state variable*, V_c , is controlled by an Ordinary Differential Equation (ODE):

$$\frac{\partial V_c}{\partial t} + \frac{1}{R_s C} V_c = \frac{1}{R_s C} V_s. \quad (5.1)$$

The time constant for this circuit is $R_s C$. The inverse of the time constant has the value, $\omega_1 = 1 / (R_s C)$, and is called the angular corner frequency, in radians per second. The source voltage, V_s , is understood to be constant, or very nearly so. The solution, to Equation 5.1, is given by

$$V_c(t) = V_s - (V_s - V_c(t_0)) \cdot \exp(-\omega_1 \cdot (t - t_0)). \quad (5.2)$$

This equation can be used to explicitly calculate the value of the state variable, V_c , at the end of a switching period, where the circuit was in the *ON* state, with Q being high.

When the circuit is in the *OFF* mode, it is equivalent to the circuit shown in Figure 5.3. When the circuit is in this mode then the state variable, V_c , is controlled by a different ODE:

$$\frac{\partial V_c}{\partial t} + \frac{1}{R_l C} V_c = 0. \quad (5.3)$$

The constant $R_l C$ is the new time constant for the circuit when it is in this mode and the inverse of this, $\omega_2 = 1 / (R_l C)$, is called the angular corner frequency, in radians per second for the circuit, when it is in this mode. More general circuits will have many time constants. The source voltage, V_s , does not affect V_c when the circuit is in this mode. The solution, to Equation 5.3, is given by

$$V_c(t) = V_c(t_0) \cdot \exp(-\omega_2 \cdot (t - t_0)). \quad (5.4)$$

This equation can be used to explicitly calculate the value of the state variable, V_c , at the end of a switching period, where the circuit was in the *OFF* state, with \bar{Q} being high.

Equilibrium, steady-state value for V_c

We denote the period of time, for which the circuit is in the *ON* state by T_1 and the period of time, for which the circuit is in the *OFF* state by T_2 . We consider the case

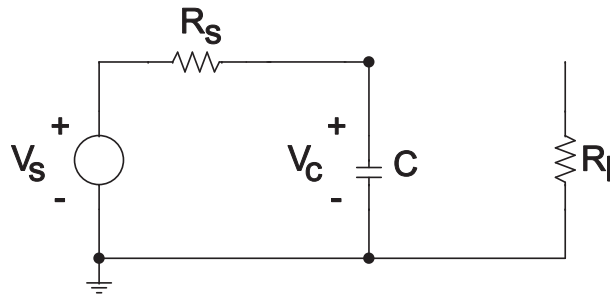


Figure 5.2. Switched-capacitor, equivalent circuit, during the ON mode. We designate the time periods when the capacitor is connected to the source as being in the *ON* mode. This will be the case when Q is high and \bar{Q} is low. In this mode, the capacitor is charged up, from the source. Please note that R_s is the source impedance associated with the linear source, V_s . The “ON” resistance of the left hand transistor, in Figure 5.1, is represented by a short circuit. If this resistance is nonzero then it will be necessary to modify the value of R_s . The open circuit on the right, approximates the off resistance of the right hand transistor, of Figure 5.1. If this resistance is not actually infinite then it will be necessary to include a modified value of R_l , in parallel with the capacitor, C . It is possible to apply Thévenin’s theorem to eliminate the parallel value of R_l and incorporate it with the linear source, leading to modified values of V_s and R_s . These details have been left out of the figure because they add complicating detail and do not introduce any essential new features to the circuit.

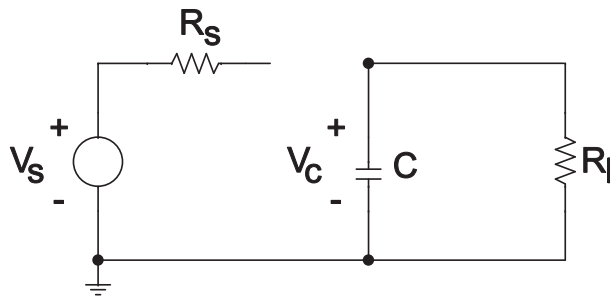


Figure 5.3. Switched-capacitor, equivalent circuit, during the OFF mode. We designate the time periods when the capacitor is connected to the load as being in the *OFF* mode. This will be the case when Q is low and \bar{Q} is high. In this mode, the capacitor is discharged into the load. The left hand transistor is approximated by an open circuit and the right hand transistor is approximated by a closed circuit.

of strictly periodic switching, *ON* for T_1 , *OFF* for T_2 , *ON* for T_1 , *OFF* for T_2 , etc.. The total switching period is $T = T_1 + T_2$. If we consider one entire switching cycle then Equations 5.2 and 5.4 will determine the value of V_c and this is shown schematically in Figure 5.4. In this case, the *ON* mode applies for a period of time $T_1 = DT$, where D is

5.1 Switched-mode circuits and switched Markov systems

the duty cycle. The *OFF* mode applies for a period of time $T_2 = (1 - \mathcal{D}) T$.

We can apply Equations 5.2 and 5.4 to obtain

$$V_2 = V_s - (V_s - V_1) \cdot \exp(-\omega_1 \cdot T_1) \quad (5.5)$$

and

$$V_3 = V_2 \cdot \exp(-\omega_2 \cdot T_2), \quad (5.6)$$

which leads to

$$V_3 = (V_s - (V_s - V_1) \cdot \exp(-\omega_1 \cdot T_1)) \cdot \exp(-\omega_2 \cdot T_2). \quad (5.7)$$

Now the condition for equilibrium is $\delta V = V_3 - V_1 = 0$, so the equilibrium, or steady-state voltage, for V_1 is

$$V_1 = \frac{1 - \exp(-\omega_1 T_1)}{\exp(-\omega_2 T_2) \cdot \exp(-\omega_1 T_1)} \cdot V_s. \quad (5.8)$$

For very small switching times, that is $T_1 \ll R_s C$ and $T_1 \ll R_l C$ and $T_2 \ll R_s C$ and $T_2 \ll R_l C$, Equation 5.8 reduces to

$$V_1 = \frac{\omega_1 T_1}{\omega_1 T_1 + \omega_2 T_2} \cdot V_s, \quad (5.9)$$

which can be further reduced to

$$\frac{V_1}{V_s} = \frac{\omega_1 \mathcal{D}}{\omega_1 \mathcal{D} + \omega_2 (1 - \mathcal{D})}, \quad (5.10)$$

where \mathcal{D} is the duty cycle. It should be noted that V_1 is a lower bound for V_c . Equation 5.10 shows how the steady state voltage, across the capacitor, is controlled by the corner frequencies and by the duty cycle.

The switched capacitor is equivalent to an admittance

For general switching times, T_1 and T_2 , the switched capacitor transfers charge in a manner that is equivalent to an admittance of

$$Y = \frac{C}{T_1 + T_2} \cdot \frac{1 - \exp(-\omega_2 T_2)}{1 - \exp(-\omega_1 T_1) \cdot \exp(-\omega_2 T_2)}. \quad (5.11)$$

This result follows from calculating the total charge transferred during a switching cycle and regarding the charge transferred per unit time as being equivalent to a current.

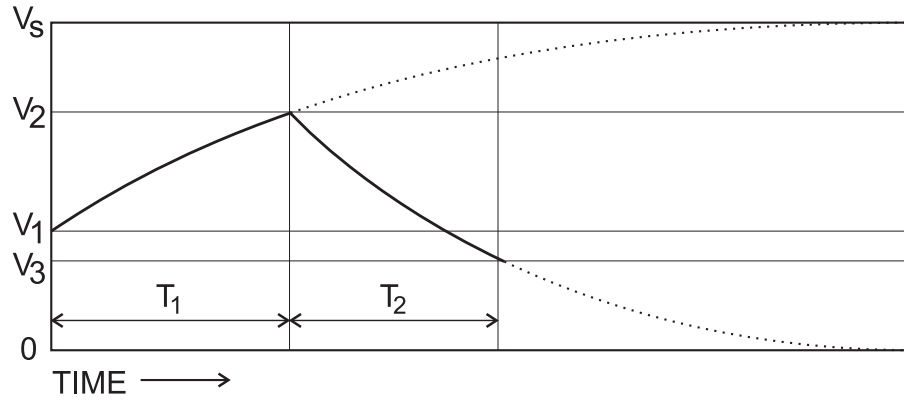


Figure 5.4. A sketch of V_c as a function of time. This figure shows the effect of one full switching cycle on the value of the capacitor voltage V_c . The initial voltage is V_1 at time $t = 0$. This climbs to a voltage V_2 at time $t = T_1$, during the ON mode. The voltage then falls to a value of V_3 at time $t = T_1 + T_2 = T$, during the OFF mode. In general, voltages V_1 and V_3 do not have to be identical. The final voltage, V_3 , may be higher or lower than the initial voltage V_1 . In general, if $V_3 < V_1$ then the medium-term average value of V_c is getting smaller. If $V_3 > V_1$ then the medium-term average value of V_c is getting larger. We define *medium-term* to refer to time intervals that are long compared with the period of the switching cycle, $T_1 + T_2$, but short compared with the time constants in the circuit $R_s C$ and $R_l C$. The circuit has to be switched at a high enough speed to make this possible, $T = T_1 + T_2 \ll \min(R_s C, R_l C)$.

The ratio of mean current to the applied voltage, V_s , is the equivalent admittance. If the switching times, which are large in relation to the time constants, that is $T_1 \gg R_s C$ and $T_1 \gg R_l C$ and $T_2 \gg R_s C$ and $T_2 \gg R_l C$, then Equation 5.11 reduces to

$$Y = \frac{C}{T_1 + T_2}. \quad (5.12)$$

This last result is reported in many textbooks, including (Sedra and Smith 2004), where $R = 1/Y = T/C$. If the switching is very fast, in relation to the time constants, that is $T_1 \ll R_s C$ and $T_1 \ll R_l C$ and $T_2 \ll R_s C$ and $T_2 \ll R_l C$, then Equation 5.11 reduces to

$$Y = \frac{C}{T} \cdot \frac{\omega_2 (1 - \mathcal{D})}{\omega_1 \mathcal{D} + \omega_2 (1 - \mathcal{D})}, \quad (5.13)$$

so the equivalent admittance depends on source impedance, R_s , and the load impedance, R_l , and on duty cycle, \mathcal{D} , as well as capacitance C and the period of switching $T = T_1 + T_2$.

5.1 Switched-mode circuits and switched Markov systems

It may seem paradoxical that a completely lossless component, such as a capacitor, C , behaves like a dissipative component, such as a resistor, $R = 1/Y$. How does the lossless component manage to dissipate energy? The answer to this apparent paradox is that the switching of the capacitor induces losses in the surrounding components, R_s and R_l .

Switching noise, or ripple

Even if the switching is very fast, there will still be a certain amount of switching noise $\Delta V = V_2 - V_1$. We can use Equations 5.5, 5.6 and 5.7, to show that

$$\Delta V = \frac{(1 - \exp(-\omega_1 T_1)) \cdot (1 - \exp(-\omega_2 T_2))}{1 - \exp(-\omega_1 T_1) \cdot \exp(-\omega_2 T_2)} \cdot V_s, \quad (5.14)$$

which further simplifies to

$$\Delta V = \frac{V_s}{\frac{1}{2 \tanh(\frac{1}{2} \omega_1 T_1)} + \frac{1}{2 \tanh(\frac{1}{2} \omega_2 T_2)}}. \quad (5.15)$$

For the case of very small switching times, T_1 and T_2 , this reduces to

$$\Delta V = \frac{V_s}{\frac{1}{\omega_1 T_1} + \frac{1}{\omega_2 T_2}}. \quad (5.16)$$

It is possible to predict how much switching noise will be observed, given various corner frequencies and switching times.

A finite difference model for transient behaviour

We can still write $\delta V = V_3 - V_1$, even when the system is not in equilibrium. Using Equation 5.7, we can write

$$\delta V = V_3 - V_1 = (V_s - (V_s - V_1) \cdot \exp(-\omega_1 \cdot T_1)) \cdot \exp(-\omega_2 \cdot T_2) - V_1, \quad (5.17)$$

so a finite difference estimate for the rate of change of V_1 is:

$$\frac{\delta V}{\delta T} \approx \frac{(V_s - V_1) \cdot \exp(-\omega_2 T_2) \cdot (1 - \exp(-\omega_1 T_1)) - V_1 \cdot (1 - \exp(-\omega_2 T_2))}{T_1 + T_2}. \quad (5.18)$$

For small values of T_1 and T_2 , we can ignore the higher order terms in the Taylor series to obtain

$$\frac{\delta V}{\delta T} \approx (V_s - V_1) \cdot \omega_1 \cdot \frac{T_1}{T_1 + T_2} - V_1 \cdot \omega_2 \cdot \frac{T_2}{T_1 + T_2}, \quad (5.19)$$

which reduces to

$$\frac{\partial V_1}{\partial t} + (\mathcal{D}\omega_1 + (1 - \mathcal{D})\omega_2) \cdot V_1 \approx \mathcal{D}\omega_1 V_s. \quad (5.20)$$

If we define some new time averaged angular corner frequencies, of $\omega_3 = \mathcal{D}\omega_1 + (1 - \mathcal{D})\omega_2$ and $\omega_4 = \mathcal{D}\omega_1 + 0$, then we obtain a much more simple ODE for the transient behaviour of the switched-mode circuit

$$\frac{\partial V_1}{\partial t} + \omega_3 \cdot V_1 \approx \omega_4 V_s. \quad (5.21)$$

This ODE describes the transient behaviour of V_1 , which is a lower bound for V_c . This lower-bound aspect is seen in Figure 5.4. On the other hand, Equation 5.21 is based on a finite difference approximation. This leads to an accumulation of small errors, if the equation is integrated over a long time. This means that V_1 may not remain a lower bound for V_c , unless the initial conditions are reset at some stage. This can be seen if we compare the solution to Equation 5.21 with the results from a detailed simulation, as shown in Figure 5.5. It is clear that the solution to Equation 5.21 is similar to the exact solution to within an error margin of about the size of to ripple, ΔV . If we are prepared to accept errors of about that magnitude then we can use the estimate of V_1 , from Equation 5.21, to estimate V_c .

A numerical simulation of the switched-capacitor circuit

In order to estimate the magnitudes of the errors involved in Equation 5.21, and in order to check the general validity of the model, we will need to perform more detailed and exact simulations of the process using Equations 5.2 and 5.4. The result is shown in Figure 5.5.

The essential features, of the medium-term transient behaviour and the switching noise can be clearly seen. The broken lines, using the symbol \times , are generated using the exact equations of state, 5.2 and 5.4. The solid line shows the solution to Equation 5.21, which is equivalent to the state-space time-average model of Middlebrook and Čuk (1976). It can be seen that the over all medium-term dynamics of the circuit are described quite well by the state-space time-average model. Towards the end of the simulated time interval, near $t = 0.016$ s, the circuit reaches a steady-state equilibrium condition, which resembles the detailed balance condition, of Markov chains. There is switching noise and the actual value of V_c varies up and down in a sawtooth fashion around the equilibrium value. The total amount of variation about the equilibrium voltage, ΔV is called

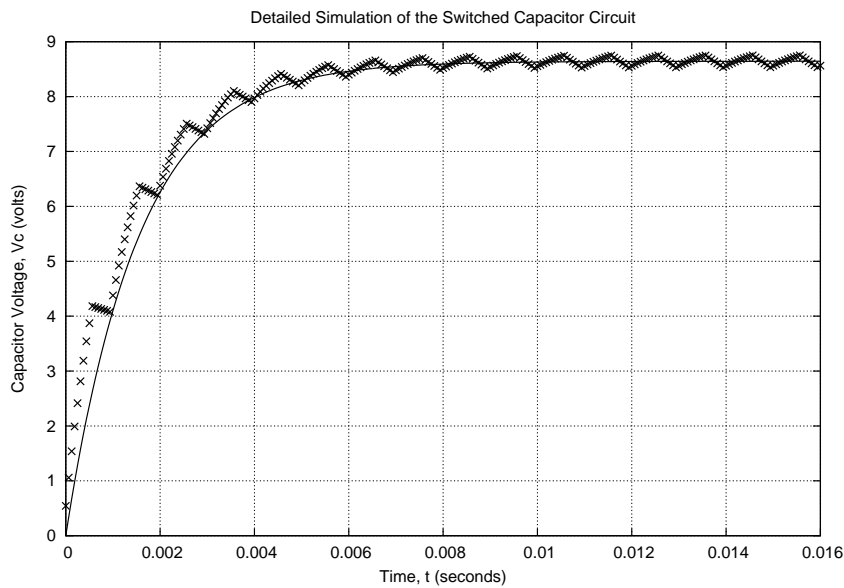


Figure 5.5. A detailed numerical simulation of the switched-capacitor circuit. This figure shows the results from a direct numerical simulation of the switched-capacitor circuit. The broken lines, using the symbol \times , were generated using the exact equations of state, appropriate each of the two modes, *ON* and *OFF*. The solid line shows the solution to the state-space time-average model of Middlebrook and Čuk (1976) is shown by the solid line. The numerical values of the parameters were $\mathcal{D} \approx 0.6180$, $R_s = 1 \Omega$, $R_l = 15 \Omega$, $C = 1000 \mu\text{F}$ and $f = 1/(T_1 + T_2) = 1 \text{ kHz}$. The similarities and differences between the two functions are interesting to consider. The overall effect of a time-average model is to retain the lower frequency components of the signals and to discard the higher frequency components. This means that time-average models ignore the detailed dynamics within a switching cycle.

ripple or *switching noise*. The state-space time-average model allows us to determine: the general form of the transient response of the circuit (in the medium-term), the equilibrium or steady-state values of the state-variable, and the amount of switching noise that we will expect to observe. This can all be carried out with a lot less effort than the complete and detailed simulation, shown in this figure. In addition, the solutions to the state-space time-average model are often simple enough to be solved analytically, which gives insight into the general form of the transient response for a wide range of different parameters. This gives better insight into the behaviour of the circuit than a large number of purely numerical simulations.

The ODE that governs the transient response, Equation 5.21, can be used to identify the modes of response of the switched-mode circuit. These can then be used to carry out stability analysis. This is an important feature of the time-average model.

The time-average switched state-space model

The key insight of the time-average switched state-space approach is that if we switch a circuit rapidly between two modes then we can create an ODE, to describe the transient behaviour of the switched mode circuit, by forming an average of the different ODEs that apply for each mode. We can weight Equation 5.1 by \mathcal{D} to obtain

$$\mathcal{D} \frac{\partial V_c}{\partial t} + \mathcal{D} \omega_1 V_c = \mathcal{D} \omega_1 V_s. \quad (5.22)$$

We can weight Equation 5.3 by $1 - \mathcal{D}$ to obtain

$$(1 - \mathcal{D}) \frac{\partial V_c}{\partial t} + (1 - \mathcal{D}) \omega_2 V_c = 0. \quad (5.23)$$

If we add Equations 5.22 and 5.23 then we obtain

$$\frac{\partial V_c}{\partial t} + (\mathcal{D} \omega_1 + (1 - \mathcal{D}) \omega_2) V_c = \mathcal{D} \omega_1 V_s. \quad (5.24)$$

This is a time weighted average of the ODEs for each of the modes and is identical with Equation 5.21. Time-averaging is less effort, and less susceptible to error, than the more complicated finite-difference argument. Time-averaging is widely used as a general and unified approach for modelling switched-mode circuits (Middlebrook and Čuk 1976).

The time-average switched state-space approach can be used to calculate equilibrium values for state-variables by setting $\partial/\partial t = 0$. For the switched-capacitor circuit, Equation 5.24 leads directly to

$$V_{c0} = \frac{\mathcal{D} \omega_1}{\mathcal{D} \omega_1 + (1 - \mathcal{D}) \omega_2} \cdot V_s, \quad (5.25)$$

which is identical with Equation 5.9. Once again, time-averaging arrives at the same result, but with less effort and less opportunity for error.

5.1 Switched-mode circuits and switched Markov systems

If the equations are weighted in a slightly different way then it is also possible to use a time averaged model to estimate the switching noise, or ripple, in the circuit. The increase in voltage during the *ON* mode is approximately

$$+\Delta V \approx T_1 \cdot \frac{\partial V_c}{\partial t} = -\omega_1 T_1 V_c + \omega_1 T_1 V_s. \quad (5.26)$$

The decrease in voltage during the *OFF* mode is approximately

$$-\Delta V \approx T_2 \cdot \frac{\partial V_c}{\partial t} = -\omega_2 T_2 V_c. \quad (5.27)$$

We can average Equations 5.26 and 5.27 to obtain

$$2\Delta V = (\omega_2 T_2 - \omega_1 T_1) \cdot V_1 + \omega_1 T_1 V_s \quad (5.28)$$

and if we combine this with the equilibrium condition of Equation 5.25 then we obtain

$$\Delta V = \frac{V_s}{\frac{1}{\omega_1 T_1} + \frac{1}{\omega_2 T_2}}, \quad (5.29)$$

which is identical with Equation 5.16.

In summary, The time-average switched state-space approach can be used to predict the transient response of a switched-mode circuit, to carry out stability analysis and to predict the amount of switching noise. The analysis is fairly easy and the results are rigorous. It is a widely used tool in the analysis of switched-mode circuits (Levine 1996).

5.1.2 Switched state-space and switched Markov systems

The results in the previous subsection assumed a periodic switching regime. This is analogous to the periodic choice of Parrondo's Games, $[A, B, A, B, \dots]$. We could press this analogy further, if we could establish a homomorphism between the two types of system.

In Parrondo's games, we have discrete time, m , and discrete space, n and time-varying probability vector in phase-space, \underline{p}_m . The time evolution of Parrondo's games is given by

$$\underline{p}_{m+1} = \underline{p}_m \cdot [\mathbf{A}], \quad (5.30)$$

for Game A, or

$$\underline{p}_{m+1} = \underline{p}_m \cdot [\mathbf{B}], \quad (5.31)$$

for Game B.

Fortunately it is possible to represent the dynamics of switched-mode systems in vector and transition-matrix formalism, by using the method of homogeneous coordinates (Graustein 1930, Harrington 1987). In this system, points at infinity, with fixed directions, are included as points with finite coordinates, within the homogeneous system. For electrical systems it is possible to include independent voltage sources or currents into the homogeneous coordinate system. For the switched capacitor circuit, in Figure 5.1, the fixed source voltage, V_s , appears in the state-vector. This means that the state-vector has two coordinates

$$\underline{V} = [V_c, V_s]. \quad (5.32)$$

We can regard the coordinate with $n = 1$ as the voltage across the capacitor, V_c , and the coordinate with $n = 2$ as the source voltage V_s . The discrete coordinate, n , must lie in the range $1 \leq n \leq 2$. In general finite lumped-component switched-mode circuits have only a finite number of state-variables.

We can use Equations 5.5 and 5.6 to represent the time evolution of the switched mode system over a sampling interval of τ . The equation for the *ON* mode is

$$[V_c(t + \tau), V_s(t + \tau)] = [V_c(t), V_s(t)] \cdot \begin{bmatrix} \exp(-\omega_1\tau) & 0 \\ 1 - \exp(-\omega_1\tau) & 1 \end{bmatrix}, \quad (5.33)$$

which can be written more concisely as

$$\underline{V}_{m+1} = \underline{V}_m \cdot \mathbf{B}, \quad (5.34)$$

where \underline{V}_{m+1} is the state-vector at discrete time $m + 1$, \underline{V}_m is the state-vector at discrete time m and \mathbf{B} is the state transition matrix, for the *ON* mode. In a similar fashion we can write the equation for the *OFF* mode as

$$[V_c(t + \tau), V_s(t + \tau)] = [V_c(t), V_s(t)] \cdot \begin{bmatrix} \exp(-\omega_2\tau) & 0 \\ 0 & 1 \end{bmatrix}, \quad (5.35)$$

which can be written more concisely as

$$\underline{V}_{m+1} = \underline{V}_m \cdot \mathbf{B}, \quad (5.36)$$

5.1 Switched-mode circuits and switched Markov systems

where \underline{V}_{m+1} is the state-vector at discrete time $m + 1$, \underline{V}_m is the state-vector at discrete time m and \mathbf{A} is the state transition matrix, for the *OFF* mode.

Written in this form, the time evolution for the switched mode circuit has the same form as the time evolution of a sequence of Parrondo's games. If we turn the field of a Brownian ratchet on and off in a certain pattern, say [*OFF*, *ON*, *ON*, *OFF*, *ON*], then this will correspond to a sequence of Markov transition matrices, [A, B, B, A, B], and the effect of this sequence of matrices on the time varying probability vector is the same as an equivalent matrix, $C = ABBAB$. In a similar way we can choose Q and \bar{Q} in such a way that the switched capacitor circuit has a certain sequence of modes, say [*OFF*, *ON*, *ON*, *OFF*, *ON*]. The effect of this sequence, on the state vector, will correspond to sequence of transition matrices, [A, B, B, A, B], and the effect of this sequence of transition matrices on the state vector, \underline{V} , is the same as one equivalent transition matrix, $C = ABBAB$.

The time-average switched state-space model takes a particularly simple form, if matrix notation is used. We can represent the average effect of the various modes on the state-vector by using a time-average transition matrix. We have

$$\underline{V}_{m+1} = \underline{V}_m \cdot \mathbf{C}, \quad (5.37)$$

where

$$\mathbf{C} = \mathcal{D}B + (1 - \mathcal{D})A \quad (5.38)$$

and if we define the compliment of the duty cycle as $\gamma = 1 - \mathcal{D}$ then we can write

$$\mathbf{C} = \gamma A + (1 - \gamma)B, \quad (5.39)$$

which has exactly the form required for the time-average form of Parrondo's games.

It is interesting to note that a duty-cycle is the fraction of time, for which a system is in the *ON* mode. For historical reasons, Parrondo's games are parametrised in terms of a factor, γ , which corresponds to the fraction of the time, for which Game A is played and this corresponds to the fraction of time, for which the field of the Brownian ratchet is turned off. The selection parameter, γ , is effectively a complementary duty cycle, $\gamma \equiv 1 - \mathcal{D}$.

In summary, it can be seen that the time evolution of switched state-space and switched Markov systems have the same form, if we choose to use appropriate notation.

5.1.3 Fractals in the phase-space of switched-mode circuits

We defer the question of what we might mean by return, or gain or loss until later. The issue that we address here is that of geometry in phase space. Parrondo's games generate a fractal set in phase-space. We show that it is possible for the switched capacitor circuit to generate a fractal set in phase space. It is fairly easy to show this by construction. We can, for example consider special cases of the transition matrices described in Equations 5.33 and 5.35. A very simple case is the one where $\exp(-\omega_1\tau) = \exp(-\omega_2\tau) = 1/3$. This would require us to choose $R_s = R_l = 1$ and to choose $\tau = \ln(3)RC$, but these are not difficult constraints and we could build a practical circuit to do this. Under these constraints, the transition matrices reduce to

$$B = \begin{bmatrix} 1/3 & 0 \\ 2/3 & 1 \end{bmatrix} \quad (5.40)$$

and

$$A = \begin{bmatrix} 1/3 & 0 \\ 0 & 1 \end{bmatrix}. \quad (5.41)$$

If we perform a change of variable on V_c The the effects of these transitions can be more clearly shown.

If we choose $x = V_c/V_s - 1/2$ and denote the value of x at discrete time m as x_m then we can write

$$\left(+\frac{1}{2} - x_{m+1}\right) = \frac{1}{3} \cdot \left(+\frac{1}{2} - x_m\right) \quad (5.42)$$

for time intervals with the *ON* state and

$$\left(-\frac{1}{2} - x_{m+1}\right) = \frac{1}{3} \cdot \left(-\frac{1}{2} - x_m\right). \quad (5.43)$$

If these transformations are chosen at random then they form an Iterated Function System (IFS) and they are known to generate the Cantor set (Barnsley 1988). This means that it would be possible to generate a fractal, the Cantor set, in the phase space for the capacitor of the switched capacitor circuit by selecting *ON* and *OFF* modes at random. This is simulated in Figure 5.6.

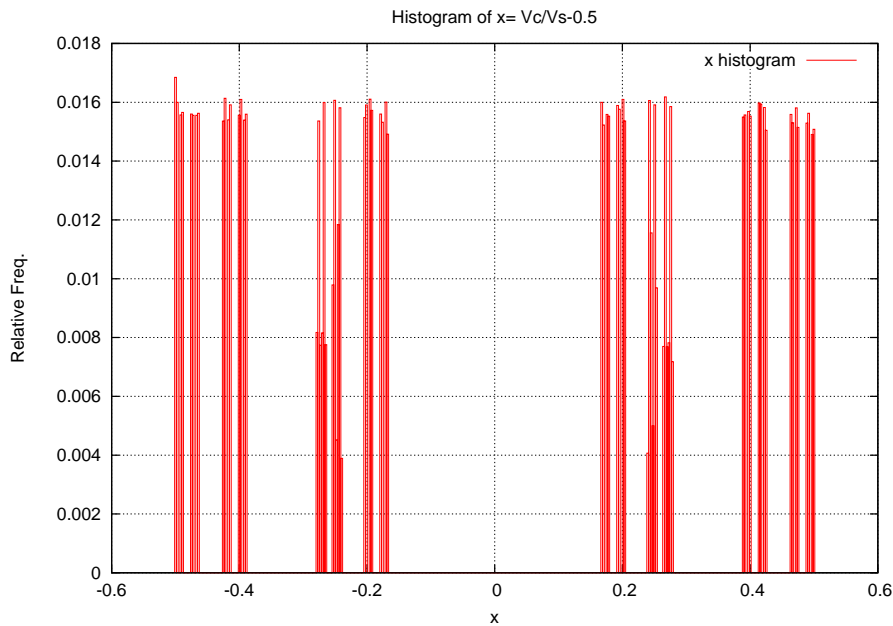


Figure 5.6. A histogram of the scaled voltage, $x = V_c/V_s - 1/2$. The process in Equations 5.42 and 5.43 is simulated in GNU Octave 2.9. The number of points in the sample is $N_s = 2^{17} = 131,072$ and the number of bins in the histogram process is $N_b = 362 \approx \sqrt{N_s}$. The resolution of the x-axis is $1/N_s \approx 0.028$. This is the relative error in the x-axis. Using a Poisson approximation for the number of samples in each bin, the relative error between the number of samples in a bin, x_B , and the expected value $E[x_B]$, is $\sigma_B/\mu_B = 1/\sqrt{N_B} \approx 1/19.026 \approx 0.053$. This is the relative error in the y-axis. The resemblance to the Cantor set in Barnsley (1988) is clear but not exact. Unfortunately, the Cantor set is a fractal and has detail at all levels of scale. This means that no finite representation on the page can ever represent it completely. A simulation, and histogram, does not *prove* the results of Barnsley (1988), but it is an indication that the argument is plausible.

The process in Equations 5.42 and 5.43 could be realised in a physical circuit by driving the switching elements using a Pseudo Random Binary Sequence (PRBS), which could be generated using a shift register and some XOR gates. This is described in the textbooks (Horowitz and Hill 1991) and (Proakis and Manolakis 1992), for example.

We have shown that vectors can be used to represent the present condition or state of an electrical system and that the time evolution of this state can be represented using a transition matrix. This type of model is called a *state-space* model and is quite

general. State-space models can be used to represent a wide variety of different electrical systems. This is covered in quite a wide range of references and texts, including (DeRusso *et al.* 1965, Pierre 1986, Stengel 1986, Levine 1996, Dorf and Bishop 1998, Karnopp *et al.* 2000). It should also be clear that state-space models are appropriate for a variety of different types of system, including translational-mechanical, rotational-mechanical mechatronic and hydraulic, as well as electrical (Karnopp *et al.* 2000).

5.1.4 The limiting case of fast switching as $\tau \rightarrow 0$

We consider the case where the switching is very fast, so τ is much less than the time constants in the circuit, $\tau \ll R_s C$ and $\tau \ll R_l C$. We can use Equation 5.25 to calculate the equilibrium or steady state value of the capacitor voltage, V_{c0} . Suppose that instead of using a periodic switching function, the mode is chosen at random with a probability of $\gamma = 1 - \mathcal{D}$ for the *OFF* mode, and $1 - \gamma = \mathcal{D}$ for the *ON* mode. We can employ Equations 5.5 and 5.6 to show that the changes in V_c , associated with each of the two modes. for finite time-steps, are as follows:

ON: The capacitor voltage increases:

$$\Delta V_c = (1 - \exp(-\omega_1 \tau)) \cdot (-V_c + V_s). \quad (5.44)$$

OFF: The capacitor voltage decreases:

$$\Delta V_c = -\exp(-\omega_2 \tau) \cdot V_c. \quad (5.45)$$

This means that V_c undergoes a random walk, but it is not uniform, like the Bernoulli process, because the changes in V_c are functions of V_c . In the limiting case of fast switching, as τ approaches zero, this will lead to an equation that has a differential aspect and a stochastic aspect. It will be a Stochastic Differential Equation (SDE). A direct simulation of Equations 5.44 and 5.45 is shown in Figure 5.7. This shows a case where $\tau \approx 5 \mu s$, which is small compared with the time constants but is still finite. The output from this circuit gives some qualitative insight into the type of output that we can expect from a randomly switched switched-capacitor circuit.

In the case of Parrondo's games, by choosing operators, A or B , at random, the discrete spatial state, n , undergoes a random walk that is similar to the Bernoulli process. If we switch modes of a switched-mode circuit at random then the value of the

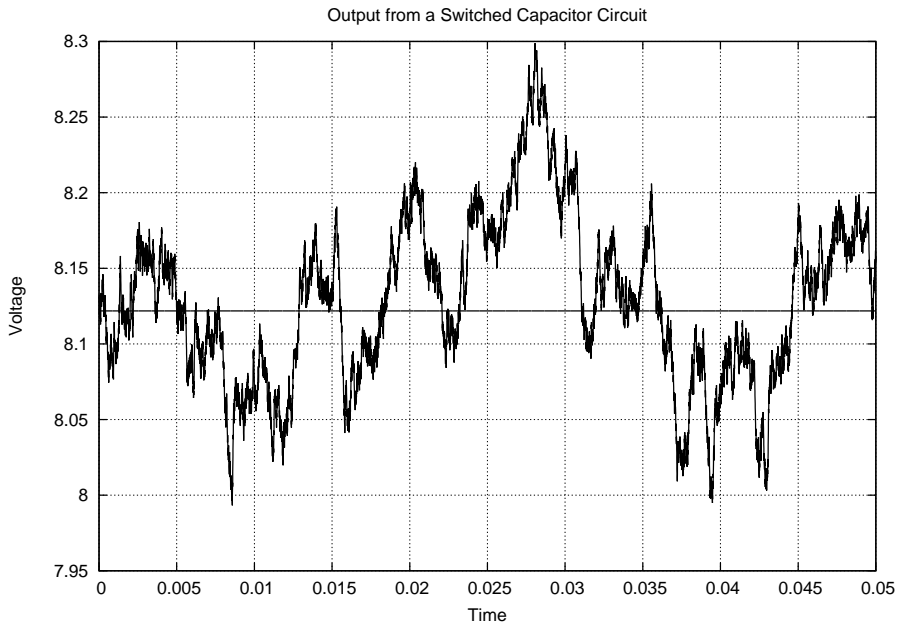


Figure 5.7. The output from a switched-capacitor circuit. If the switched-capacitor is switched very quickly and the modes of *OFF* or *ON* are chosen at random then the voltage across the capacitor is not constant. It follows a stochastic process. The equilibrium voltage across the capacitor is V_{c0} and is shown by the horizontal line. The actual voltage across the capacitor at any given instant of time is V_c and is shown as a set of calculated points. The fluctuations, due to switching, can easily be seen. The capacitor voltage is a unique valued function of time, $V_c(t)$, but it is a very rapidly varying function of time. It may assume many values within a short time interval, ΔT . It is not clear whether certain limits will exist. For example, it is not clear whether $V_c(t)$ is rectifiable. Here, V_c is a generalised function and needs to be handled according to certain special rules, that differ from the rules for ordinary real functions.

state variable, V_c , also undergoes a random walk that is similar to the Bernoulli process. The process differs from a Bernoulli process because the size of the steps depends on the value of the state variable. In the Bernoulli process, the steps are uniform in size.

The time average for Equations 5.44 and 5.45 is

$$\Delta V_c \approx (D \cdot (V_s - V_c) \cdot \omega_1 - (1 - D) \cdot V_c \cdot \omega_2) \cdot \Delta t. \quad (5.46)$$

This is the time-average model for the stochastically-switched case. It is analogous to Equation 5.24, which applies to the periodically switched case. Equation 5.46 does accurately represent the medium-term dynamics of the randomly switched system but

the equation is incomplete because it does not represent fluctuations, due to the random switching.

The process, shown in Figure 5.7 is a non-uniform random walk, where the step lengths are functions of the state variable. Analysis would be easier if we could represent this by a more uniform, infinitely-divisible process, such as Brownian Motion, B_t . In order to complete this model, we need to match up the moments of the non-uniform random walk with the moments of a scaled version of Brownian motion. If we evaluate Brownian motion at time, t , then the result is a Gaussian random variable with mean, $\mu = 0$, and variance, $\sigma^2 = t$. This is the key to deriving equivalent expressions for μ and σ .

If the important parameters of the process do not vary significantly during the switching time, τ , then we can regard the non-uniform random walk as quasi-uniform and we can apply the earlier results for a Bernoulli process with asymmetric rewards, called *Taleb's game*. In particular, the variance for Taleb's game is given by $\sigma^2(m) = q \cdot (1 - q) \cdot (R_1 - R_2)^2 \cdot m$, where q is the probability of a win, and $1 - q$ is the probability of a loss, and R_1 is the reward in the case of a win and R_2 is the reward in the case of a loss. Using this result in the present context, and re-writing the notation, we obtain

$$\sigma^2 = \mathcal{D} \cdot (1 - \mathcal{D}) \cdot ((V_s - V_c) \cdot \omega_1 + V_c \cdot \omega_2)^2 \cdot \tau^2. \quad (5.47)$$

We consider the case as τ approaches zero, but has not yet reached zero, and obtain a Stochastic Differential Equation (SDE) which approximately represents the dynamics of the circuit,

$$dV_c = \mu(V_c, t) dt + \sigma(V_c, t) dB_t, \quad (5.48)$$

where dB_t is an infinitesimal increment of Brownian motion, dt is an infinitesimal increment of time, and dV_c is a corresponding infinitesimal increment of V_c . This model is an idealisation of the full simulation, shown in Figure 5.7, in a similar sense to the time-average model shown in Figure 5.5. The solutions will differ in detail but they have the same measure. The explicit equations for μ and σ are are:

$$\mu(V_c, t) = \mathcal{D} \cdot (V_s - V_c) \cdot \omega_1 - (1 - \mathcal{D}) \cdot V_c \cdot \omega_2 \quad (5.49)$$

and

$$\sigma(V_c, t) = \sqrt{\mathcal{D} \cdot (1 - \mathcal{D})} \cdot |(V_s - V_c) \cdot \omega_1 + V_c \cdot \omega_2| \cdot \tau. \quad (5.50)$$

5.1 Switched-mode circuits and switched Markov systems

We can use the Euler approach to the integration of Equation 5.48 to obtain a finite difference equation that is suitable for computer simulation, SDE for the switched-mode circuit

$$\begin{aligned} \Delta V_c = & (\mathcal{D} \cdot (V_s - V_c) \cdot \omega_1 - (1 - \mathcal{D}) \cdot V_c \cdot \omega_2) \cdot \Delta t \\ & + \sqrt{\mathcal{D} \cdot (1 - \mathcal{D})} \cdot |(V_s - V_c) \cdot \omega_1 + V_c \cdot \omega_2| \cdot \tau \cdot N_t, \end{aligned} \quad (5.51)$$

where N_t is a Gaussian random variable with zero mean and unit variance. An indication of the similarity of the solutions is shown in a direct evaluation of Equation 5.51 in Figure 5.8. This is qualitatively similar to Figure 5.7, but differs in detail, because both processes are stochastic.

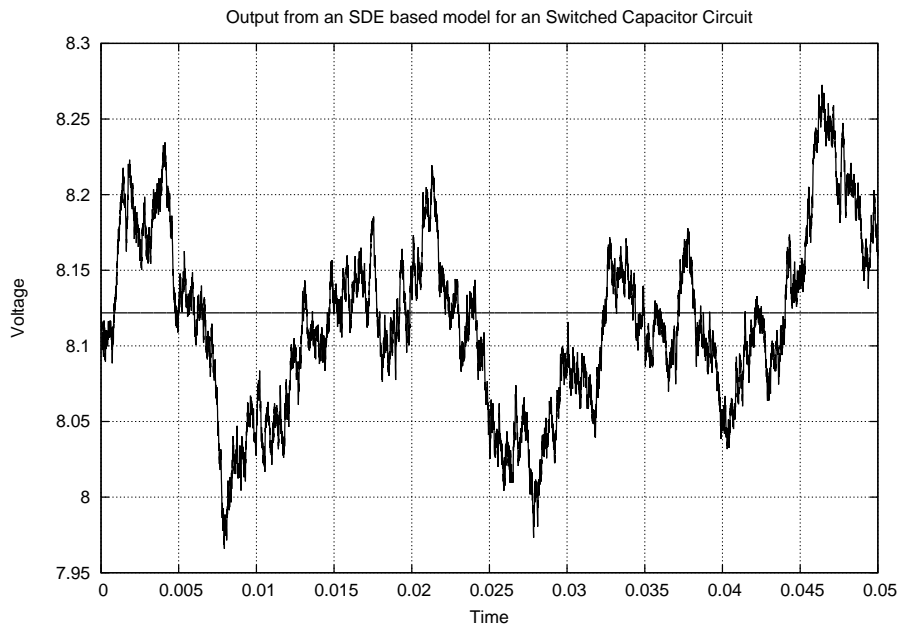


Figure 5.8. The result from an SDE model for a switched capacitor circuit. In this model, the dichotomous noise from the switching between states *ON* and *OFF* is replaced by a continuous Gaussian process, having the same mean and variance. This is reasonable, since the Central Limit Theorem (CLT) implies that the random variation will converge to a Gaussian random variable, in the case where we combine a very large number of bounded and independent increments. This demonstration indicates that it is reasonable to use Stochastic Differential Equations (SDEs) to model the dynamics *and* noise of a switched-mode circuit. This is similar to the way in which the time-average model uses an Ordinary Differential Equation (ODE) to model the medium-term dynamics of a switched-mode circuit, without the fluctuations.

The sample paths in Figures 5.7 and 5.8 suggest that the use of an SDE model might be reasonable, but this is far from a proof. It would be desirable to show that the

solutions from Equations 5.44 and 5.45 are equivalent, in measure, to the solution of Equation 5.48. The mean value is not a difficult issue, since it is already addressed in the time-average model of Middlebrook and Čuk (1976). The noise term is more complicated to evaluate, and needs at least some verification. Equation 5.50 predicts the value of the variance, σ^2 that we should observe for different choices of switching time, τ . This can be tested against a direct simulation, using Equations 5.44 and 5.45. We have to regard the switching time τ as being small in relation to the time constants in the circuit, but still finite.

In Figure 5.9, Equations 5.44 and 5.45 are used to simulate the behaviour of the circuit for a variety of switching times, τ and switching frequencies, $f = 1/(2\tau)$. The value of f can be controlled, within the simulation. Each simulation covers a period of $n_s = 2^{16} = 65536$ time ticks. so the period of time for each simulation is $2^{16} \cdot \tau$. A range of values for f is chosen over three decades, from 10^5 Hz to 10^8 Hz. These switching times are all much faster than the time constants in the circuit. The variance, σ^2 can be estimated using the standard formula from statistics, as realised in GNU Octave v2.9. These are the simulation points, plotted using the symbol \times , in Figure 5.9. Equation 5.50 predicts that the value of σ^2 should follow a scaling law of

$$\sigma^2 = \frac{1}{4} \mathcal{D} \cdot (1 - \mathcal{D}) \cdot ((V_s - V_c) \cdot \omega_1 + V_c \cdot \omega_2)^2 \cdot f^{-2}, \quad (5.52)$$

which is shown as the solid line in the figure. The agreement is very close, showing that the variance, of V_c , as measured from simulations using Equations 5.44 and 5.45, is accurately modelled by Equation 5.50. It is important to note that the straight line is not a least-squares fit to the results from the simulations. The straight line is the prediction of a model. The points are the results from simulations. The correspondence of the two results indicates that the model for the variance is accurate over a wide range of different time scales.

We conclude that the medium term dynamics of the circuit, including transient behaviour *and* noise, can be modelled using an SDE, in Equation 5.48, where the mean rate of change is given by Equation 5.49 and the standard deviation is given by Equation 5.50.

It is possible to control a switched-mode circuit without a sophisticated control law. We can select the modes at random, and the average voltage would be determined by

5.1 Switched-mode circuits and switched Markov systems

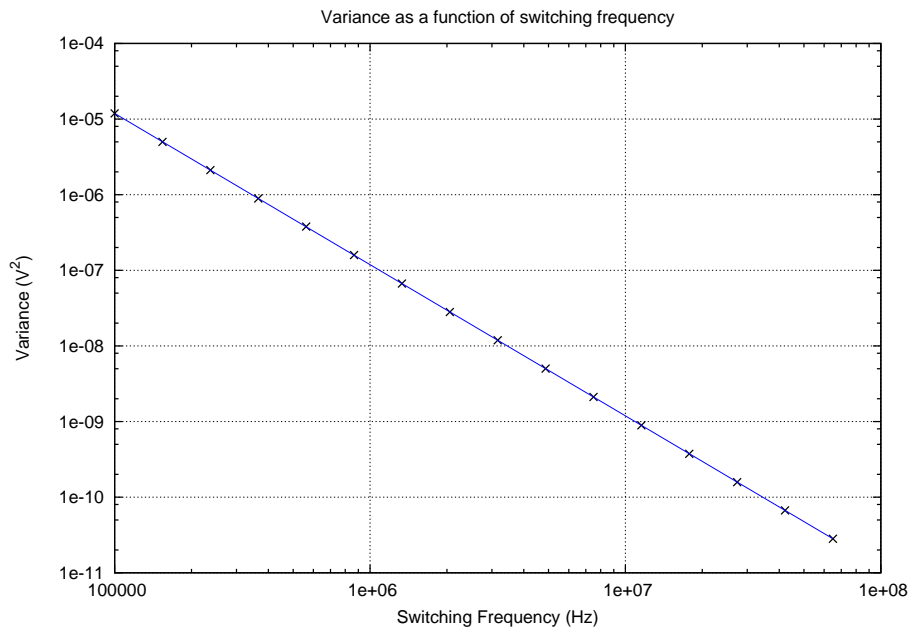


Figure 5.9. The scaling of variance with switching frequency. Equations 5.44 and 5.45 are used to simulate the behaviour of the circuit for a variety of switching times, τ and switching frequencies, $f = 1/(2\tau)$. The variance is estimated empirically and plotted using the symbol, \times . Equation 5.50 predicts that a value of σ^2 , which should follow a scaling law, of $\mathcal{O}(f^{-2})$, which is shown in the solid line in the figure. The agreement is very close, showing that the variance can be estimated using Equation 5.50, with good accuracy. The straight line is not a least-squares fit to the results from the simulations. The straight line is the prediction of the model, represented by Equation 5.50. The medium terms dynamics of the circuit, including transient behaviour *and* noise, can be modelled using an SDE in Equation 5.48.

the probabilities of the various modes, \mathcal{D} and $(1 - \mathcal{D})$. A cost of this approach is that the state-variable is subject to more variation than would be the case for a periodic switching rule, but this can be overcome by switching the circuit more rapidly, making τ very small.

Summary of the switched capacitor circuit

We have shown that a switched-mode circuit can be represented using a switched state-space model. We have shown that one particular switched-mode circuit can be represented using a time-average switched state-space model, although result is quite general. It can be used to represent any switched mode circuit, where the circuit is linear

in each mode (Middlebrook and Čuk 1976, Levine 1996).

If switching always occurs at integral multiples of a switching time, τ , then the time-evolution for a switched-mode circuit and a particular switched-Markov system, Parrondo's games have the same mathematical form. Equilibrium, steady-state voltages, for the switched-mode circuit, can be calculated using a time-average switched state-space model. This is similar to the calculation of the equilibrium, steady-state probabilities, for Parrondo's games, using a time-average game.

We have shown that there are fractals in the phase-space of the switched capacitor circuit²⁹. This is similar to the result for fractals in the phase-space of Parrondo's games.

Finally, just as Parrondo's games can be derived by sampling a Fokker-Planck equation or a Langevin equation, it is possible to work backwards from Parrondo's games to an equivalent Langevin equation, as long as the first two moments are matched up. The same procedure is possible for the switched-mode circuit. The discrete equations for the two modes, Equations 5.44 and 5.45, can be used to derive an equivalent SDE for the dynamics and the fluctuations of the process, Equation 5.48.

Switched-mode circuits and switched-Markov systems can both be modelled using the one formalism, of the switched state-space model. This gives rise to a number of similarities in the two types of system. Given these common features, it is natural to ask whether it is possible to construct a version of Parrondo's paradox for switched-mode dynamical systems. In Parrondo's games, this involves changes in the rates of change of the expected value of discrete-position, $E[n]$. For dynamical systems this may not make very much sense because the state-variable for $n = 1$ may be a voltage and the state-variable for $n = 2$ might be a current or even a fixed source, such as V_s , for the switched capacitor circuit. Looking at changes in the value of n does not have the same meaning for dynamical systems as it does for Parrondo's games. As we shall see, it is possible to construct a situation that is similar to Parrondo's paradox by looking at rates of change in stored internal energy of the system.

²⁹The process is described in Equations 5.42 and 5.43 and illustrated in Figure 5.6, and reproduces results in Barnsley (1988).

5.2 A Parrondo effect for a switched-mode circuit

The starting point for this enquiry is Parrondo's games. The work presented here is the continuation of earlier papers (Allison and Abbott 2000b, Allison and Abbott 1999, Allison and Abbott 2000a, Allison and Abbott 2001). We show that it is possible to combine two losing games to create a new process, which is winning. We extend the apparent paradox of Parrondo's games to the case of a real physical system, obeying the laws of conservation of energy and charge. The flow of reward in Parrondo's games is replaced with a flow of energy in a physical circuit.

In Parrondo's games, a set of games, and associated rules, are said to be *winning* if the expected value of the capital as a function of time, $E[x(t)]$, is increasing, $\frac{\partial}{\partial t}E[x(t)] > 0$. In the winning case of Parrondo's games, there is an accumulation of capital. A dynamical system is said to be *stable*, in the sense of Lyapunov, if the expected value of the stored energy in the system $E[U(t)]$, is decreasing in time, $\frac{\partial}{\partial t}E[U(t)] < 0$, or alternatively $E[\dot{U}] < 0$. The stored energy in the system can serve as a Lyapunov function (Stengel 1986, Levine 1996). In an unstable dynamical system, there is an accumulation of stored energy.

The properties of *winning* and *losing*, can be investigated by studying the geometric and topological properties of certain sets within the parameter space of the system. If we visualise Parrondo's games appropriately then it is apparent that boundary between the winning and losing regions of the parameter space is not planar. The winning and losing regions are not convex, as was suggested by Moraal (2000b). This is considered further by Harmer *et al.* (2001). Costa *et al.* (2005) have used arguments of this type to suggest that Parrondo's paradox is *ubiquitous*.

The analogous result for a switched-mode device is that it is possible to combine two unstable systems together to achieve a stable result. This is feasible because the unstable region is not convex.

The analogy between Parrondo's games and switched-mode systems can be made more rigorous if we consider the mathematical structures that they have in common:

- The macroscopic state of each system at each moment of time can be completely described by a state vector, \underline{X}_m .
- The time evolution of both systems is governed by an indefinite sequence of randomly selected transition operators:

$$\underline{X}_{m+1} = \underline{X}_m \cdot \mathbf{A}_m \quad (5.53)$$

where \mathbf{A}_m is the transition operator that applied at discrete time m .

- We can classify the responses of the systems in terms of asymptotic rates of flow of conserved quantities. In the case of a switched-mode system, we can consider power, $E[\dot{U}] = E\left[\frac{\partial}{\partial t}U\right] = \frac{\partial}{\partial t}E[U]$, as a flow of internal stored energy, U . If the mean rate of flow is always inwards, without bound, then system will accumulate an indefinite amount of energy and must be unstable. In the case of Parrondo's games, we must consider the flow of reward to determine whether the games are winning or losing. If the flow of reward is away from the player, without bound, then the game is losing.
- The effect of selection at random is to generate a new time-averaged system, which will be governed by a linear convex combination of the original transition operators (Middlebrook and Čuk 1976).
- The rate of flow associated with the time-averaged system is generally *not* the same as the time average of the flows associated with the original transition operators. The rate of flow is a non-linear function of the transition operators.

The losing region of the parameter space for Parrondo's games is not convex. We show that it is possible to construct a switched-mode system, which has a non-convex unstable region in its parameter space. For the sake of simplicity, we limit the system to one free real parameter, which is a loop gain, K . The main body of this section contains five key subsections:

1. the construction of a simple switched-mode system with a non-convex unstable region in the parameter space
2. the formulation of this system in terms of a state vector \mathbf{X}_t and two transition operators A_1 and A_2

5.2 A Parrondo effect for a switched-mode circuit

3. the determination of the internal stored energy as a quadratic function of the state vector:

$$U = \mathbf{X}^T P \mathbf{X} \quad (5.54)$$

for some positive definite matrix P . This energy function can be used as a Lyapunov function.

4. the proof of instability of processes governed by the original pure transition operators A_1 and A_2
5. the proof of stability, with probability one, of processes governed by a randomly selected mixed sequence of transition operators A_1 and A_2 .

This shows that the Parrondo effect applies, with rigour, to at least one real switched-mode electronic system.

Simulations indicate that the particular system, which we constructed has further interesting properties. We show the key results from the simulations and speculate about some interesting open questions, which (we believe) are worthy of future investigation.

5.2.1 Construction of a simple switched-mode system

Our immediate aim is to design a system in the Laplace, or s , domain that has a non-convex unstable region in the parameter space. We achieve this by constructing a system with a disjoint unstable region in the parameter space. For simplicity, we choose a parameter space with a single free variable, a loop gain: $K \in \mathcal{R}$.

If a linear system, or plant, is placed inside a feedback control loop then a new system, with new properties, is created. A possible system topology is shown in Figure 5.10. We can write the equations for this system as:

$$F(s)^{-1} = G(s)^{-1} + K \cdot H(s) \quad (5.55)$$

where $G(s)$ is called the open loop transfer function and $F(s)$ is called the closed loop transfer function. The loop gain, K , is a free parameter and $H(s)$ is the transfer function

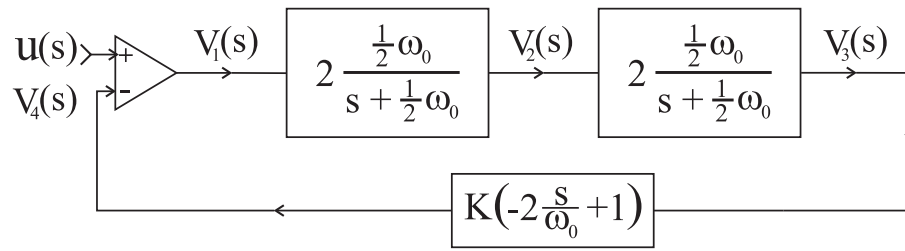


Figure 5.10. General plan of a second-order system with one feedback loop. The inputs to the system at the left are denoted by $U(s)$. The output from the differencing amplifier, V_1 , is called an error signal. This is fed through a plant, which is represented as two single poles. The variables $V_2(s)$ and $V_3(s)$ are the state variables for this system. The feedback path takes a copy of $V_3(s)$, filters it, and then feeds the result, $V_4(s)$ into the differencing amplifier. Superficial consideration of the circuit might lead one to suspect that $V_4(s)$ should be a state variable but closer analysis reveals that this is not so.

of the return path. For this particular system, we have

$$G(s) = \frac{(\omega_0)^2}{\left(s + \frac{1}{2}\omega_0\right)^2} \quad (5.56)$$

and

$$H(s) = K \cdot \left(-2\frac{s}{\omega_0} + 1\right). \quad (5.57)$$

It is customary to analyse the stability of closed loop systems in terms of the poles of the closed-loop transfer function, $F(s)$, which are the zeros of $F(s)^{-1}$. These poles will generally move about in the complex plane in response to changes in the loop gain, K . A graph of the positions of the poles, as a function of gain, is called a *root locus* plot and is shown in Figure 5.11. Some choices of gain may cause one, or more, of the poles to move into the unstable region, on the right hand side of the s -plane, which would mean that the closed loop system would then be unstable. This is the basis of the Routh-Hurwitz criterion (Levine 1996). In general, there will be stable and unstable values for the gain, K .

In this case, we can think of the neutral position of the system as being the case where $K = 0$ and there are repeated poles at $s = -\frac{1}{2}\omega_0$. The system is stable in the neutral position. The general positions of the poles are given by the roots of the characteristic equation:

$$F(s)^{-1} = \left(\frac{s}{\omega_0}\right)^2 + (1 - 2K) \left(\frac{s}{\omega_0}\right) + \left(\frac{1}{4} + K\right) = 0. \quad (5.58)$$

5.2 A Parrondo effect for a switched-mode circuit

K	s_1/ω_0	s_2/ω_0	Routh-Hurwitz stability
$K \rightarrow -\infty$	$2K - 3/2$	$+1/2$	unstable
-1	$-3/2 - \sqrt{3}$	$-3/2 + \sqrt{3}$	unstable
$-1/4$	$-3/2$	0	marginal
0	$-1/2$	$-1/2$	stable
$+1/2$	$-j\sqrt{3}/2$	$+j\sqrt{3}/2$	marginal
$+1$	$+1/2 - j$	$+1/2 + j$	unstable
$+2$	$+3/2$	$+3/2$	unstable
$K \rightarrow +\infty$	$+1/2$	$2K - 3/2$	unstable

Table 5.1. Some values for the poles, s_1 and s_2 , as functions of the loop gain K . The regions of stability and instability of the plant are indicated in the final column of the table. The stable range of values for K is $(-\frac{1}{4} < K < +\frac{1}{2})$. All other values are unstable or marginally stable. The stable region is convex. The unstable region is not convex. The loci of these poles, s_1 and s_2 , as functions of the loop gain K , are shown graphically in Figure 5.11.

Fortunately this is a quadratic function of s and we can readily calculate the loci of the roots:

$$s = \omega_0 \cdot \left(\left(K - \frac{1}{2} \right) \pm \sqrt{K \cdot (K - 2)} \right). \quad (5.59)$$

The loci of these roots of the characteristic equation, in the s -plane, are shown on the root locus plot of Figure 5.11. Some particular values of K have special interest. For $K = -1$ we get closed loop poles at $s = \omega_0(-\frac{3}{2} \pm \sqrt{3})$. The pole at $s = \omega_0(-\frac{3}{2} + \sqrt{3})$ is a positive real number and gives rise to the exponentially increasing response shown in Figure 5.15. For $K = +1$ we get closed loop poles at $s = \omega_0(\frac{1}{2} \pm j)$, which have positive real parts and give rise to the exponentially increasing oscillations shown in Figure 5.16.

There is a range of stable values for K surrounded by two unstable ranges. Analysis of Equation 5.59 reveals that the stable range of values for K is $(-\frac{1}{4} < K < +\frac{1}{2})$. The other intervals, $(-\infty < K < -\frac{1}{4})$ and $(+\frac{1}{2} < K < +\infty)$ are associated with unstable values of K . Some of the critical values for K are shown in Table 5.1 and the locus of the poles, in the complex plane, is shown graphically in Figure 5.11.

The unstable region, within the parameter space for K , is composed of two disjoint open intervals and is not convex. Our choice for $G(s)$ was guided by the need to develop a second order system with an appropriate root locus and a non-convex unstable region in the parameter space for the loop gain K .

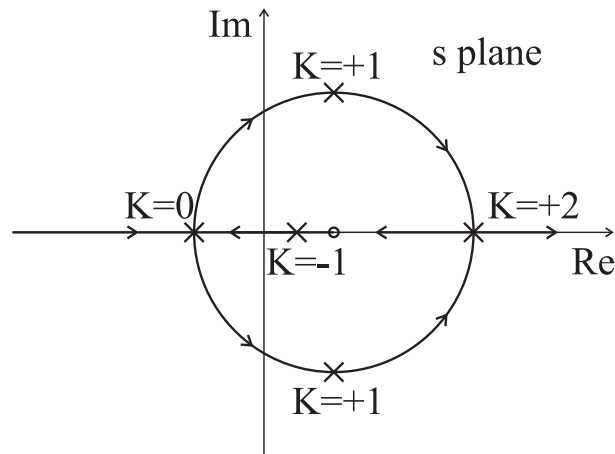


Figure 5.11. Root locus plot for a second order system. The poles, in the s -plane, for particular values of K are represented by crosses. The direction of movement of the poles, with increasing K , within the locus, is indicated by the arrows. The radius of the circle is ω_0 . The neutral position for the plant corresponds to a pair of repeated poles at $s = -\frac{1}{2}\omega_0$. Some of the critical values for the loop gain K and the associated poles, s_1 and s_2 , are listed in Table 5.1.

It is possible to think of this plant³⁰, with variable gain, K , as a switched-mode system. We can think of the system with $K = -1$ as being unstable plant number 1. We can think of the system with $K = +1$ as being unstable plant number 2. The mean value of these two values of gain would be $K = 0$, which corresponds to the neutral system, which is stable. We could switch rapidly between the two *unstable* control systems and we might expect that the result would be a *stable* control system that somehow corresponds to the neutral system.

We proceed to re-formulate this switched-mode system in state space and to derive the necessary mathematical machinery to establish that the switched system actually

³⁰In the terminology of control theory a *plant* is the combination of a *process* and an *actuator*. The word *plant* is used more generally, by control engineers, to refer to a whole system. The etymology of the term derives from the idea of a manufacturing plant, such as a chemical refinery or a rolling mill.

is stable.

5.2.2 A switched state-space formulation

We formulate the system in terms of a state vector \mathbf{X}_t and two transition operators A_1 and A_2 . The choice of state variables is not unique. The strategy used here is to imagine the system $G(s)$ as being constructed of two function blocks in series:

$$G(s) = \left(\frac{+\omega_0}{\left(s + \frac{1}{2}\omega_0\right)} \right) \cdot \left(\frac{+\omega_0}{\left(s + \frac{1}{2}\omega_0\right)} \right). \quad (5.60)$$

The variables, $\{V_1, V_2, V_3, V_4\}$ are the voltages at the outputs of the various function blocks shown in Figure 5.10. Analysis reveals that only voltages V_2 and V_3 are needed to store the internal state of the system. All other variables can be written as linear combinations of these state variables. The state variables $\{V_2, V_3\}$ constitute a set of generalised coordinates for the system.

We can analyse the system using signal flow concepts that lead to a state-space model for the whole closed-loop system:

$$\dot{\mathbf{X}} = \mathbf{A}\mathbf{X} + \mathbf{B}u \quad (5.61)$$

where \mathbf{X} is the state vector, \mathbf{A} is the transition matrix, \mathbf{B} is an input vector and u is an input voltage, shown in Figure 5.10. Equation 5.61 is known in the literature as a state-space model. This is described in quite a wide range of references (DeRusso *et al.* 1965, Pierre 1986, Stengel 1986, Levine 1996, Dorf and Bishop 1998, Karnopp *et al.* 2000).

The state vector is composed of two state variables:

$$\mathbf{X} = \begin{bmatrix} V_2 \\ V_3 \end{bmatrix}. \quad (5.62)$$

The transition matrix defines the way that the system evolves over time,

$$A = \omega_0 \cdot \begin{bmatrix} \left(+2K - \frac{1}{2}\right) & -2K \\ +1 & -\frac{1}{2} \end{bmatrix}. \quad (5.63)$$

We can consider the matrix, A , to be a linear function of a single real scalar variable, K . We can denote this as $A = A(K)$. The function is linear, so $A(K_1 + K_2) = A(K_1) + A(K_2)$.

The input vector is:

$$\mathbf{B} = \begin{bmatrix} +1 \\ 0 \end{bmatrix} \quad (5.64)$$

and the input voltage is $u(t)$. If we are only interested in the asymptotic stability of the system then can consider $u(t)$ to be simply a Dirac delta function, $u(t) = \delta(t)$. Alternatively, we could choose $u(t) = 0$ and select initial conditions, $\mathbf{X} = \mathbf{X}_0$ at time, $t = 0$. This approach leads to a homogeneous equation in time:

$$\dot{\mathbf{X}} = A\mathbf{X}. \quad (5.65)$$

All the simulations presented in this section are for the homogeneous system described in Equation 5.65, with non-zero initial conditions $\mathbf{X} = \mathbf{X}_0$.

We can make use of the two special values for A corresponding to the two special values of K discussed earlier, $K_1 = -1$ and $K_2 = +1$. We can define: $A_1 = A(K_1)$ and $A_2 = A(K_2)$. We can also define the state transition matrix corresponding to the neutral position as $A_0 = A(0)$. We note that A_0 is the average of A_1 and A_2 , and therefore $A_0 = \frac{1}{2}(A_1 + A_2)$. This follows from the fact that $A(K)$ is a linear function of K .

We can now imagine an inhomogeneous process where we switch at random with equal probability between the two systems defined by transition matrices A_1 and A_2 at regular time intervals, ΔT . The time evolution of such a system can be simulated using a discrete time model:

$$\mathbf{X}_{t+\Delta T} = \exp(A_t \cdot \Delta T) \mathbf{X}_t, \quad (5.66)$$

where $\exp(A_t \cdot \Delta T)$ is the matrix exponential function applied to the matrix $A_t \cdot \Delta T$.

Equation 5.66 is an exact solution to the homogeneous ordinary differential equations governing the plant, over the time interval, ΔT (Dorf and Bishop 1998). We can join many of these exact solutions together, to simulate the exact solution of the switched system. It is worth noting the relationships between Equation 5.66 and Equation 5.53.

5.2 A Parrondo effect for a switched-mode circuit

The matrix exponential function can be evaluated numerically, using power series, or algebraically, using Laplace transform techniques.

The symbol A_t really refers to $A(K(t))$, since A only varies, in time, because K varies, in time. In this sense, we now consider A to be a function of t although it only takes one of two values. The symbol A_t represents the transition operator that applies at time t , which will either be A_1 or A_2 .

The stability of this stochastic inhomogeneous system cannot be analysed using linear techniques, like the Routh-Hurwitz criterion. The system is no longer strictly linear because of the multiplicative operation, introduced by the switching. A different, approach must be used. We proceed to use Lyapunov's second, or direct method, to analyse this problem.

5.2.3 Internal stored energy

It is not possible to determine the amount of stored energy in a system, without some reference to the scale of the system. We could be modelling a large national energy grid, delivering many megawatts of power; or a microscopic MEMS system, dissipating micro-watts of power. Both systems could have the same description in the Laplace domain.

Even given an indication of scale, it is possible for several different physical circuits to have the same description, in the Laplace domain. The synthesis of physical circuit, to match a mathematical model, is not unique. What we provide here is a single possible physical implementation for $G(s)$ and $H(s)$ and show that it is possible to represent the stored energy, in this implementation, as a quadratic function of the state variables, V_2 and V_3 .

One possible physical implementation of the system

There are well established techniques for synthesising physical circuits in the Laplace domain. The standard design problem is to design a physical circuit that has a transfer function, which closely approximates a given, or required, transfer function. This is often achieved using operational amplifiers (Peyton and Walsh 1993, Sedra and Smith 2004). The open-loop system, or plant, given in Equation 5.56, can be constructed

by placing two function blocks, each with a single real pole, in cascade. A circuit to achieve this is shown in Figure 5.12. This circuit will synthesise $G(s)$, provided that

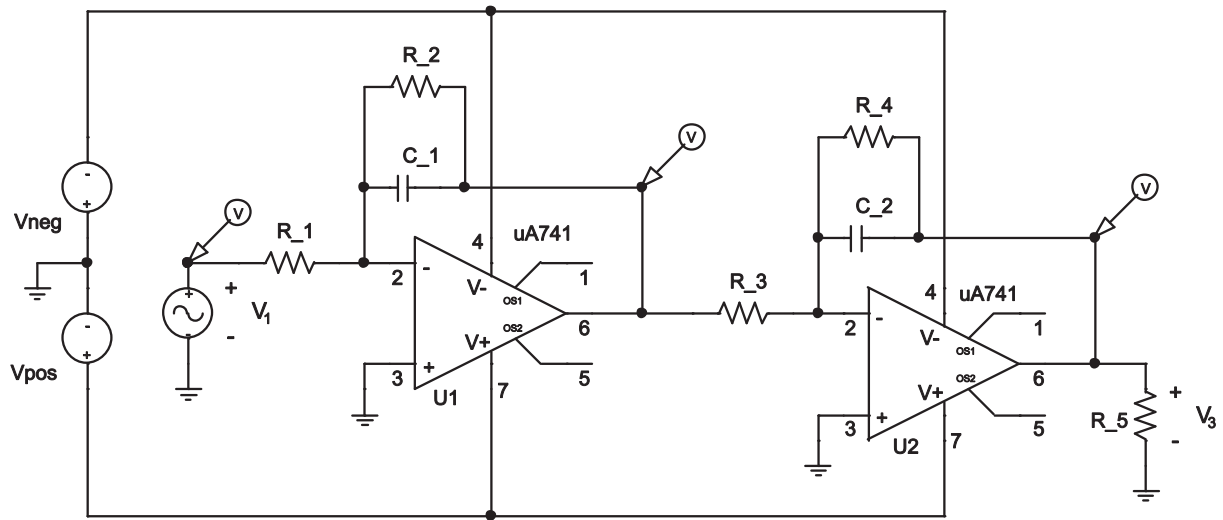


Figure 5.12. A model for the open-loop transfer function, $G(s)$. This operational amplifier circuit implements two single, and identical, real poles by cascading two circuits in series. The required transfer function is produced as long as we satisfy the constraints, $\omega_0/2 = 1/(R_2C_1) = 1/(R_4C_2)$ and $R_2/R_1 = R_4/R_3 = 2$.

certain constraints are met. The poles will be located at the correct angular frequencies if we require that $\omega_0/2 = 1/(R_2C_1) = 1/(R_4C_2)$. The circuit will have the correct low-frequency, or steady-state, gain if we choose our components in such a way that $R_2/R_1 = R_4/R_3 = 2$. Simulations and experience show that this circuit is practical. The stored energy in this part of the circuit has two components: $U_1 = \frac{1}{2}C_1V_2^2$ and $U_2 = \frac{1}{2}C_2V_3^2$.

The feedback transfer function, $H(s)$, described in Equation 5.57 is more difficult to synthesise, because it requires differentiation. Peyton and Walsh (1993) points out that there are practical issues with differentiation:

- Differentiators tend to accentuate the higher frequency components of the noise in a signal.
- Differentiators can have stability issues at DC, as frequency tends towards zero.
- The presence of parasitic resistance at the input, and parasitic capacitance in the feedback path, add additional poles to the circuit. This limits performance at high frequency and may create stability issues if a differentiator is used as a sub-system in a feedback control system.

5.2 A Parrondo effect for a switched-mode circuit

- All operational amplifiers have finite gain. Most practical operational amplifiers are internally compensated, which has the effect of adding another low-frequency pole to the system. These effects limit performance at high frequency.

These issues can be managed, with careful design, but it must be noted that we only approximate the correct transfer function within a range of frequencies. Simulations show that the circuit, in Figure 5.13, can be made to work well over the audio range of frequencies. Detailed formulae for the limits of performance are given in (Peyton and Walsh 1993). If we choose $R_8 = R_9$ and $R_6 C_3 = 2/\omega_0$ then the transfer function of the

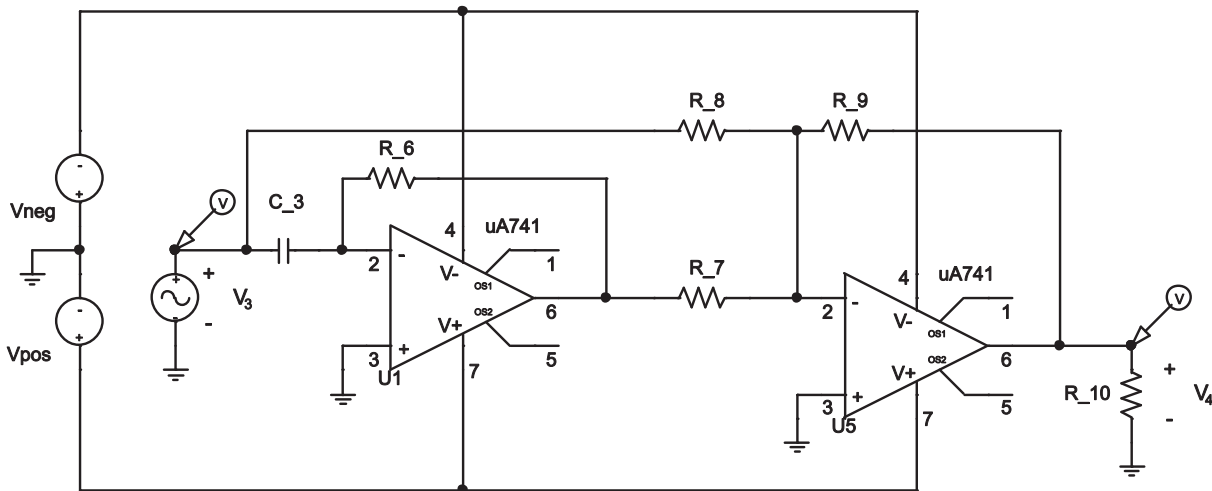


Figure 5.13. A model for the feedback transfer function, $G(s)$. The feedback circuit is essentially a simplified version of a Proportional, Integral and Derivative (PID) circuit. In this case we are simply implementing the proportional and derivative parts of the circuit, using operational amplifiers. At first sight, one might think that the capacitor, C_3 , would be an additional energy storage element, which could affect the stability of the system. More detailed analysis shows that C_3 affects the value, but not the general form of the Lyapunov function.

circuit, in Figure 5.13, is

$$\frac{V_4(s)}{V_3(s)} = - \left(1 - \frac{s}{\frac{1}{2}\omega_0} \right), \quad (5.67)$$

which is of the same general form as Equation 5.57. The change of sign between Equation 5.67 and Equation 5.57 can be accommodated in the design of the summing amplifier that will be used to complete the feedback loop.

The feedback path contains one energy storage element, C_3 , which has stored energy of $U_3 = \frac{1}{2}C_3 V_3^2$. The summing and differencing amplifiers contain no energy storage

elements so they do not contribute to the net stored energy. This means that the total stored energy of this implementation of the system is:

$$U = U_1 + U_2 + U_3 \quad (5.68)$$

$$= \frac{1}{2}C_1V_2^2 + \frac{1}{2}(C_2 + C_3)V_3^2, \quad (5.69)$$

which is a quadratic function of the state variables, V_2 and V_3 . This supports our earlier claim that these state variables are sufficient to describe the system. Other voltages, such as V_1 , are only linear combinations of the state variables. They may appear in our output equations but are not needed in the equations of state transition.

In order to simplify the notation, in the next section, we can define a matrix with capacitance elements:

$$C = \begin{bmatrix} C_{11} & C_{12} \\ C_{21} & C_{22} \end{bmatrix} = \begin{bmatrix} C_1 & 0 \\ 0 & C_2 + C_3 \end{bmatrix}. \quad (5.70)$$

This allows us to represent stored energy U , using a convenient matrix notation.

Energy and power matrices

We can represent the internal stored energy of the system as a quadratic function of the state vector, \mathbf{X} . Using notation from Levine (1996), we can define the internal stored energy as:

$$U = \mathbf{X}^T P \mathbf{X} \quad (5.71)$$

where X is the state vector and P is a positive-definite matrix, called an *energy matrix*. If we differentiate the stored energy along the trajectories of the system, as defined by Equation 5.65, then we get:

$$\dot{U} = \mathbf{X}^T Q \mathbf{X} \quad (5.72)$$

where

$$A^T P + P A = -Q \quad (5.73)$$

and Equation 5.73, is called the *Lyapunov equation*. The choices of P and Q are related through the Lyapunov equation but we are *free* to choose one of them.

In order to construct a workable Lyapunov function, we use stored energy in the entire circuit, in Equation 5.68. We use the definitions in Equation 5.70, to obtain:

$$P = \begin{bmatrix} \frac{1}{2}C_{11} & 0 \\ 0 & \frac{1}{2}C_{22} \end{bmatrix}. \quad (5.74)$$

5.2 A Parrondo effect for a switched-mode circuit

If we use Equation 5.73 to solve for the power matrix, Q , then we obtain:

$$Q = \omega_0 \cdot \begin{bmatrix} \frac{1}{2}C_{11} - 2KC_{11} & KC_{11} - \frac{1}{2}C_{22} \\ KC_{11} - \frac{1}{2}C_{22} & \frac{1}{2}C_{22} \end{bmatrix}. \quad (5.75)$$

We require this matrix to be positive definite for some range of values of K . We can establish when the matrix is positive definite by evaluating all the top left hand minor determinants of Q . We get: $\Delta_1 = C_{11} \left(\frac{1}{2} - 2K \right)$ and $\Delta_2 = \frac{1}{4}C_{22} (C_{11} - C_{22}) - K^2 (C_{11})^2$. We can obtain the largest admissible range of values for K if we choose $C_{11} = 2C$ and $C_{22} = C$ for some standard capacitance C . This gives an admissible range of values of K as

$$-\frac{1}{4} < K < +\frac{1}{4}. \quad (5.76)$$

We can use this Lyapunov function to establish that the system is stable when K is in the admissible range. Since the un-switched system is linear, we can actually calculate a larger range of values, for which the un-switched system is stable, using the Routh-Hurwitz criterion: $-\frac{1}{4} < K < +\frac{1}{4}$. This is larger than the admissible range for the present Lyapunov function, which we can only use when $-\frac{1}{4} < K < +\frac{1}{4}$. We know that the present Lyapunov function is adequate in the smaller range. We also know that the un-switched system would also be stable for values of K in this smaller range.

We can think of ω_0 as a characteristic frequency for the system and $R_0 = 1/(\omega_0 C)$ as a characteristic resistance. This implies that Equation 5.72, describing the rate of change of stored energy, is dimensionally consistent with Joule's law, $\dot{U} = \frac{\partial U}{\partial t} = V^2/R_0$.

We can consider the system near its neutral position, when $K = 0$ and $A = A_0$. Lyapunov's theorem establishes that the system A_0 is stable since both P and Q are positive definite. It seems desirable to test this analytical result. We simulated the system using the values of $K = 0$, $A = A_0$, the value of P from Equation 5.74 and the value of Q from Equation 5.75. The results are shown in Figure 5.14.

The energy is always positive, since P is positive definite. The energy is always decreasing, which is consistent with the fact that the power \dot{U} is always negative. This is also consistent with the fact that Q is positive definite. This was found to be true for a variety of initial conditions, \mathbf{X}_0 .

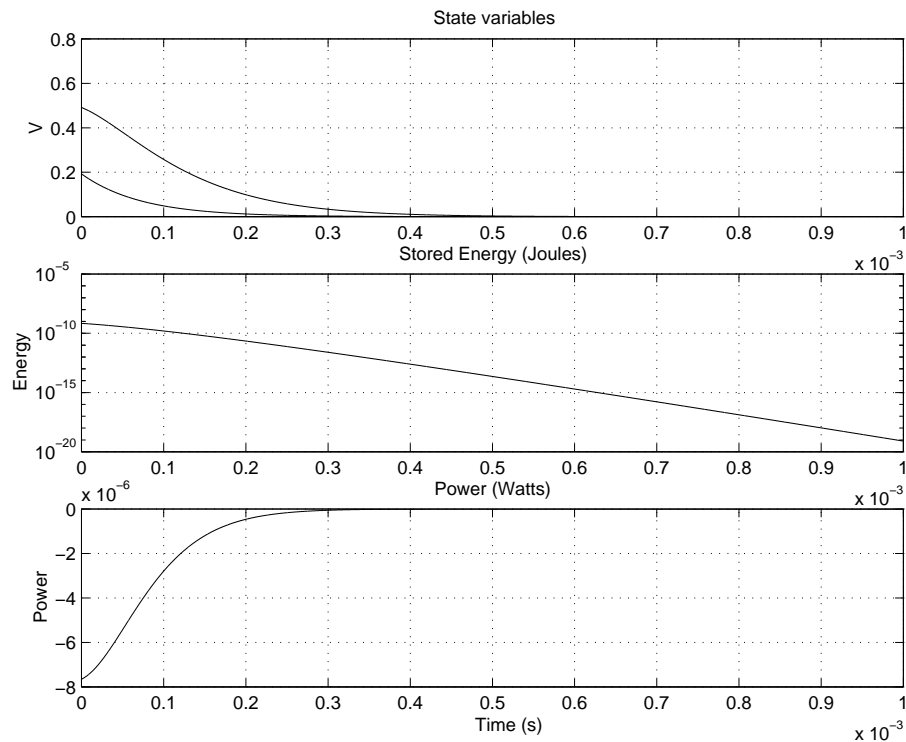


Figure 5.14. Discrete state-space simulation of the neutral system. We describe the system, with $A = A_0$ and $K = 0$ as the *neutral system*. This figure depicts a discrete state-space simulation of the neutral system. The state variables V_2 and V_3 are shown in the top of the figure. The stored energy is shown on a logarithmic scale in the middle and the power dissipation is shown in the bottom graph. All units are SI and correspond to a characteristic frequency of about 2.2 kHz, and a characteristic resistance of 33 k Ω . The power converges to zero. The rate of convergence is limited by the slowest mode in the response.

We note that there is no stochastic element in the simulation in Figure 5.14. This is only a simulation of the time-averaged plant A_0 and is not sufficient to establish the stability of the stochastic inhomogeneous process where A_1 and A_2 are chosen at random.

5.2.4 Proof of instability of plants A_1 and A_2

The plants A_1 and A_2 were *designed* to be unstable. This is supported by simulations. Figure 5.15 shows a simulation of the plant A_1 . All variables clearly diverge exponentially to infinity. Figure 5.16 shows a simulation of the plant A_2 . All variables diverge to infinity in an exponentially growing sinusoidal fashion.

5.2 A Parrondo effect for a switched-mode circuit

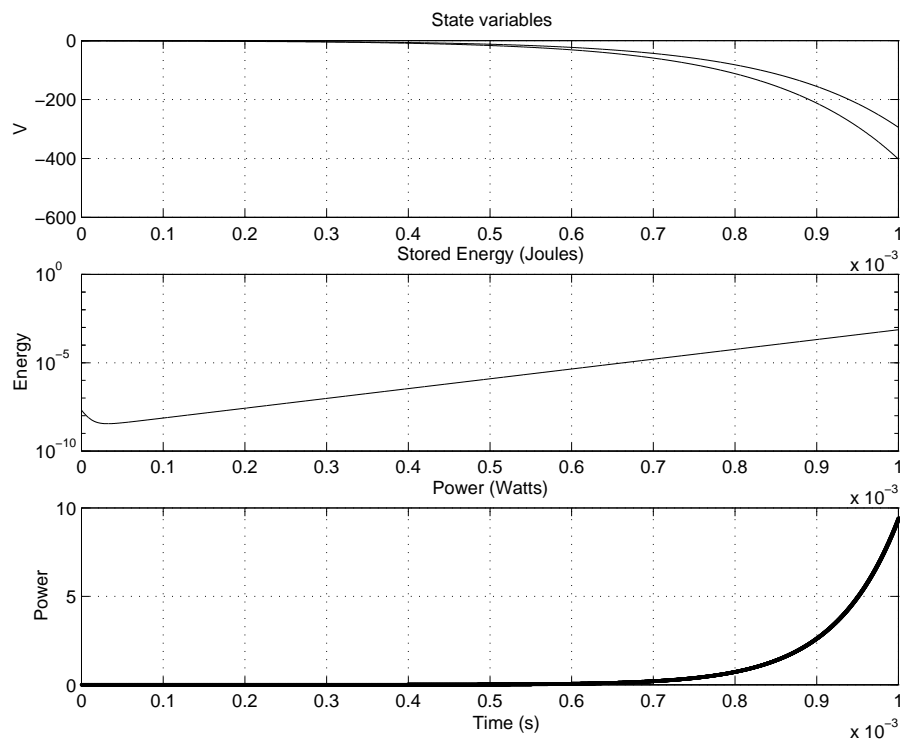


Figure 5.15. Discrete state-space simulation of system A_1 . The system has a real exponential unstable mode. The stored energy increases exponentially, without bound. Exponential functions appear linear on a logarithmic scale. After about one millisecond, the voltages, V_2 and V_3 , have built up to levels of hundreds of volts. This would clearly exceed the capabilities of most operational amplifiers. If the simulation were continued for long enough then the voltages would eventually exceed the ratings of all components in the system, and the system would fail catastrophically. This is clearly non-physical. The actual outcome for a real physical circuit would depend on factors that are not included in the linear model. There are a few possible outcomes that are often observed in unstable systems, (i) The voltages can get locked into a fixed state (saturated near the supply voltages) (ii) the plant can destroy itself (iii) the plant could oscillate between two or more quasi-stable states (near the supply voltages). The purpose of this simulation is not to represent what would actually happen to any specific physical circuit. The purpose is to verify that the design is unstable. This is an adjunct to a proof of instability and helps with motivation but is not an actual *proof* of instability, in the strict sense.

The formal proof for plants A_1 and A_2 is really just a re-statement of the Routh-Hurwitz result, for linear systems, within the context of the matrix notation. This is described in Levine (1996), for example.

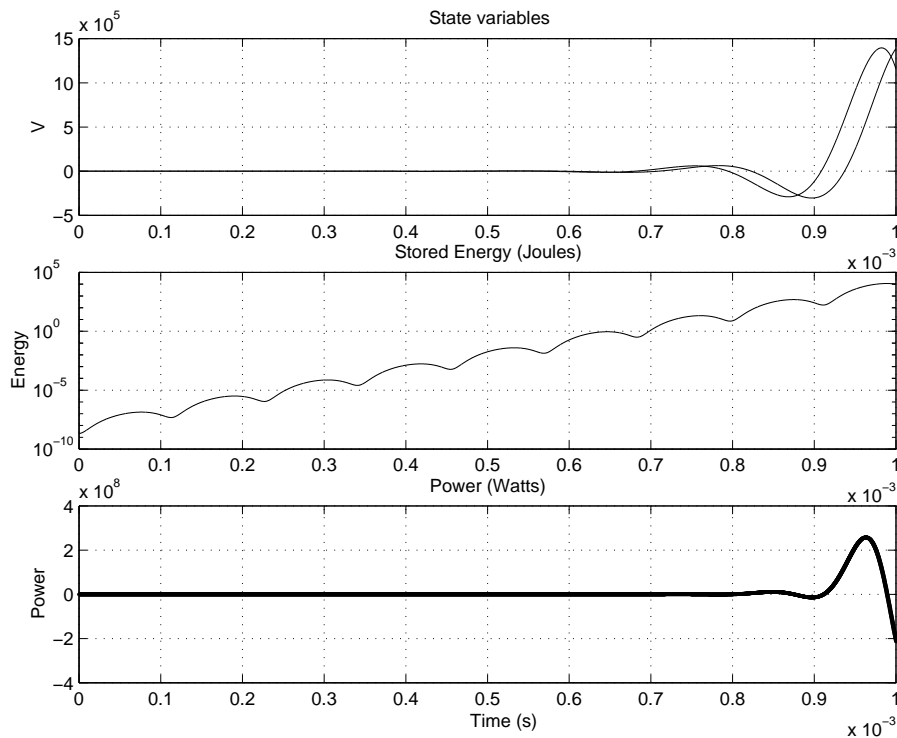


Figure 5.16. Discrete state-space simulation of system A_2 . This system also has a complex exponential unstable mode. A complex conjugate pair of poles on the right hand side of the complex s -plane (with positive real part) are associated with growing exponential functions of the form $\exp(+\sigma t) \cdot \cos(\omega t + \phi)$. Functions of this type can be seen in the top of the figure, in the state variables. The stored energy does have a periodic aspect but can be bracketed between upper and lower exponential bounds. The lower bound for the stored energy increases exponentially, without bound. This means that the system is unstable. After about one millisecond, the voltages, V_2 and V_3 , have built up to levels of millions of volts. This would clearly exceed the capabilities of all components in the system, and the system would fail catastrophically. The actual outcome for a real physical circuit would depend on factors that are not included in the linear model. There are a few possible outcomes that are often observed in unstable systems, (i) the voltages can get locked into a fixed state (saturated near the supply voltages) (ii) the plant can destroy itself (iii) the plant could oscillate between two or more quasi-stable states (near the supply voltages). The purpose of this simulation is not to represent what would actually happen to any specific physical circuit. The purpose is to verify that the design is unstable. This is an adjunct to a proof of instability and helps with motivation but is not an actual *proof* of instability, in the strict sense.

5.2.5 Proof of stability of the stochastically mixed processes

The mathematical issue with the *switched* system is that, in general, switching introduces a multiplication operation and the resulting system may not be linear. That is why the more general approach of Lyapunov has to be used, rather than the more limited approach of Routh and Hurwitz.

Simulations strongly suggest that the mixed process should be stable, but this is not a proof. A sample path is shown in Figure 5.17. The system appears to converge to the point $\mathbf{X}^T = [0, 0]$ in the state-space. We note that the instantaneous power may vary

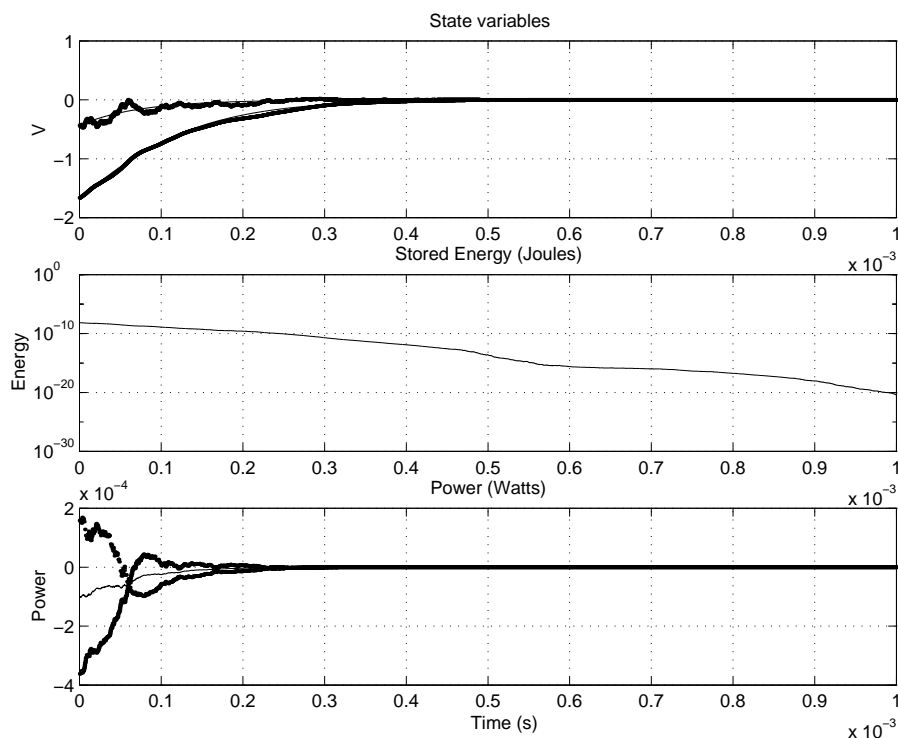


Figure 5.17. Discrete state-space simulation of the randomly switched system. The response of the time-averaged system is included for comparison. For this example, the state variables all tend towards zero, the stored energy is exponentially decreasing and the instantaneous power does eventually decrease to zero. The instantaneous power may diverge wildly from the expected value of the power, but it does tend to zero in the end.

greatly and is often positive. We also note that the *average* power is always decreasing, this is supported by the fact that the curve for stored energy is decreasing in some average sense. We need to make these ideas more precise.

There is a theorem due to Kushner, which is reproduced in Levine (1996), on p. 1108, which states that: The mixed system is stable with probability one if: $\mathcal{L}U \leq 0$ and $U \geq 0$, where \mathcal{L} is the infinitesimal generator for the process:

$$\mathcal{L}U(\mathbf{X}_0) = \lim_{\Delta t \rightarrow 0} \frac{E[U(\mathbf{X}_{\Delta t})] - U(\mathbf{X}_0)}{\Delta t}, \quad (5.77)$$

where $E[\mathbf{X}]$ is the expected value of \mathbf{X} . We can make use of the fact that $E[U(\mathbf{X}_0)] = U(\mathbf{X}_0)$ when $U(\mathbf{X}_0)$ is known so we can write:

$$\mathcal{L}U(\mathbf{X}_0) = \lim_{\Delta t \rightarrow 0} \frac{E[U(\mathbf{X}_{\Delta t})] - E[U(\mathbf{X}_0)]}{\Delta t} \quad (5.78)$$

$$= \lim_{\Delta t \rightarrow 0} E \left[\frac{U(\mathbf{X}_{\Delta t}) - U(\mathbf{X}_0)}{\Delta t} \right]. \quad (5.79)$$

This reduces to

$$\mathcal{L}U(\mathbf{X}_0) = E \left[\frac{\partial U(\mathbf{X})}{\partial t} \right] = E[\dot{U}(\mathbf{X})] \quad (5.80)$$

wherever the limit exists, at the point in state-space, $\mathbf{X} = \mathbf{X}_0$. This raises the question of whether or not $E[\dot{U}(\mathbf{X})]$ converges uniformly. We recall Equation 5.54 so we can write

$$E[U(\mathbf{X})] = E[\mathbf{X}^T P \mathbf{X}] \quad (5.81)$$

but $\dot{\mathbf{X}} = A\mathbf{X}$, where $A = A_1$ or $A = A_2$ so

$$E[\dot{\mathbf{X}}] = E[A\mathbf{X}] \quad (5.82)$$

$$= E[A] \mathbf{X}. \quad (5.83)$$

Equation 5.80 now reduces to

$$\mathcal{L}U(\mathbf{X}) = E \left[\frac{\partial U(\mathbf{X})}{\partial t} \right] \quad (5.84)$$

$$= \mathbf{X}^T \left(E[A]^T P + P E[A] \right) \mathbf{X}. \quad (5.85)$$

We are choosing $A = A_1$ or $A = A_2$ at random with equal probability so $E[A] = \frac{1}{2}(A_1 + A_2) = A_0$ and we arrive at an expression for $\mathcal{L}U(\mathbf{X})$:

$$\mathcal{L}U(\mathbf{X}) = +\mathbf{X}^T \left(A_0^T P + P A_0 \right) \mathbf{X} \quad (5.86)$$

and we know from Equation 5.76 that this is negative since $Q_0 = -A_0^T P - P A_0$ corresponds to the case with $K = 0$ and is positive definite. This can all be summarised by the statement:

$$\mathcal{L}U(\mathbf{X}) = \frac{\partial E[U(\mathbf{X})]}{\partial t} = -\mathbf{X}^T Q_0 \mathbf{X} \leq 0. \quad (5.87)$$

5.3 Sources of noise

We have $\mathcal{L}U \leq 0$ and $U \geq 0$ so, applying the theorem from Kushner, *the mixed system will be stable with probability of one*. A simulation of this process is shown in Figure 5.17. The stored energy in the system does increase, about half of the time for a short intervals, but the overwhelming effect is a consistent reduction of stored energy. The presence of switching noise implies that the instantaneous power can be quite large even though the expected value is very small and negative.

We have constructed a switched-mode system, in which both pure modes are unstable but the random mixture of the two modes is stable. This shows that the Parrondo effect can be applied to energy flow in at least one real physical system.

5.3 Sources of noise

In the switched capacitor circuit there was always certain amount of switching noise in the state variable, V_c . This is the case for ripple, when there is a periodic switching regime, shown in Figure 5.5. There is also switching noise when the switching regime is randomised. This is shown in Figure 5.7, for example. In either case, the act of switching the configuration of the circuit causes noise to appear in the circuit. In the switched control circuit of Figure 5.10, the loop gain is switched between two values and switching noise appears in the state variables. This is shown in Figure 5.17, for example. In addition to switching noise, there are other internal sources of noise in electronic circuits. All dissipative elements, such as resistors have thermal noise. Transistors and other switching elements can suffer from shot noise and avalanche noise.

In all situations noise cannot be rectified, to give rise to a biased change in the state variables, without an external source of energy.

In fact, if we could successfully rectify noise without any other energy input then we would have an example of Maxwell's demon.

It is not possible to construct a demon that can overcome the laws of thermodynamics (Zurek 1989). All such demons contain errors in the physical modelling of the devices or in the mathematical technique for modelling noise. This is well established and will not be pursued here.

The earlier problem, of modelling noise in electronic circuits using Langevin equations, is still open, and of interest. If we could take the continuum limit of a switched mode circuit, such as the one shown in Figure 5.7, then future work can develop mathematical models for handling noisy functions of this type, such as the SDE in Equation 5.48. These problems are considered further in the next chapter.

5.4 Chapter summary

In this chapter, the following major topics have been covered:

- The time-average switched state-space model has been introduced, through the use of a worked example.
- It has been shown that the time-evolution of a switched mode circuit and a switched Markov system, Parrondo's games, have the same mathematical formalism.
- It has been established that fractals can be generated in the phase-space of switched-mode circuits, when modes are chosen at random.
- The limiting case, of fast switching, has been considered and a time-average Langevin equation, has been introduced to model the dynamics and random fluctuations of a rapidly but randomly selected switched-mode circuit. This Langevin equation generalises the time averaged ordinary differential equations, of Middlebrook and Čuk (1976), since it can represent average dynamics *and* random fluctuations.
- A Parrondo-effect has been established for a switched-mode circuit. We can switch, at random, between two unstable control systems to obtain a stable control system.
- The winning and losing regions of Parrondo's games have been considered and it has been noted that these are non-convex. Parrondo's paradox is ultimately a statement about convexity, or lack of convexity. We confirm the earlier claims by Moraal (2000b). The unstable regions of the parameter space for the switched-mode circuit have the same lack of convexity as the winning, or losing, regions of Parrondo's games.

5.4 Chapter summary

In the next chapter we develop some general tools, for analysing noise in electronic circuits, based on the stochastic calculus of Itô (Øksendal 1998, Levine 1996). These include, but are not limited to the SDE in Equation 5.48.

Chapter 6

Langevin equations as models for noise in circuits

WE show that stochastic differential calculus of Itô (Itô 1942, Itô 1951) is a rigorous, and yet convenient, tool for the analysis of noise in electronic circuits. This chapter extends earlier work (Allison and Abbott 2005). We begin by showing how the nodal and mesh equations of ordinary circuit analysis can be extended to model the effects of thermal fluctuations. We describe models for the basic lumped components of electronics. These developments are non-trivial, because white noise is not a function, in the usual sense of the word. It is a *generalised function* in the sense used by Schwartz. Special techniques have to be used. The calculus of Itô provides the necessary tools. Our analysis leads to a systematic method for formulating Langevin equations for electronic circuits. These can then be transformed into ordinary differential equations, allowing the calculation of average voltages, or noise power, without the need to explicitly solve the stochastic differential equations.

We argue that the SDE approach to noise estimation is systematic and should find wide application amongst the other basic tools of circuit theory.

6.1 Introduction, to noise techniques in electronics

The traditional approach to thermal noise in circuits can be traced back to Johnson (1928) and Nyquist (1928). Over the years, a number of empirical techniques have been developed to estimate noise in circuits that filter the thermal noise, and these appear in standard textbooks (Lathi 1965, Carlson *et al.* 2002). Our aim is to extend these results in a systematic manner, using the stochastic calculus of Itô (Itô 1942, Itô 1951). In more recent years, Itô's techniques have been formulated in ways that make them easier to apply (Durrett 1996, Øksendal 1998, Kloeden and Platen 1999). There has been some work in the literature on the application of stochastic calculus to electronic systems (Demir *et al.* 2000, Mehrotra and Sangiovanni-Vincentelli 2004, Gitterman 2005), but these works suppose that the relevant Stochastic Differential Equations (SDEs) have already been formulated. We address the problem of the systematic formulation of the equations, based on physical principles. Once the equations have been formulated then it is possible to use standard techniques to solve the equations (Durrett 1996, Øksendal 1998), or failing that, to solve the equations numerically (Kloeden and Platen 1999).

Clearly, the central issue in any analysis of noise is the way in which white noise is represented. One surprising aspect of white noise is that it cannot be constructed as an ordinary function of time, say $Z(t)$. It should be regarded a generalised function, or *distribution* of the type described by Schwartz (Mandelbrot 1977, Kloeden and Platen 1999). Generalised functions, such as noise, $Z(t)$, should always appear inside an integration over a finite time interval (Lighthill 1958, Papoulis 1962, Zemanian 1965, Bracewell 2000). For example, compare

$$I_1 = \int_{T_1}^{T_2} f(t) \cdot Z(t) dt \quad \text{and} \quad I_2 = \int_{T_1}^{T_2} f(t) \cdot \delta(t) dt \quad (6.1)$$

(6.2)

where $f(t)$ is an ordinary, well behaved or *good*³¹ function of time, $Z(t)$ is white noise and $\delta(t)$ is the Dirac delta function. The functional forms and applications are identical. It is not possible to specify the instantaneous values of either of the distributions, $Z(t)$ or $\delta(t)$, at each instant of time but it is always possible to express the effect of these distributions over a finite interval of time, using a functional. In short, noise can be correctly described in terms of distributions but not in terms of ordinary functions.

It is customary to represent noise in terms of infinitesimal increments of another process called Brownian motion, $B(t)$, where

$$dB \equiv Z(t)dt, \quad (6.3)$$

which is really a concise notation for

$$\int_{T_1}^{T_2} f(t)dB \equiv \int_{T_1}^{T_2} f(t)Z(t)dt. \quad (6.4)$$

This form of Brownian motion, $B(t)$, is a mathematical abstraction, based on the real physical phenomenon of the same name (Durrett 1996, Øksendal 1998, Kloeden and Platen 1999).

There is a proof, due to Kolmogorov, that it is possible to construct a function which is continuous almost everywhere and yields all the properties that we expect of Gaussian white noise, $Z(t)$ (Karlin and Taylor 1975, Norris 1997, Durrett 1996). This is known as the Wiener process³², and also as *Brownian motion*. Wiener showed that it was possible to define integrals of the form in Equation 6.4 for well behaved or *good* functions, $f(t)$.

The theory of stochastic differential equations (Lamberton and Lapeyre 1991, Baxter and Rennie 1996, Durrett 1996, Øksendal 1998, Kloeden and Platen 1999) establishes

³¹We use the term *good* function, in the sense used by Lighthill (1958). Lighthill defines a good function, $\gamma(t)$, as one which is everywhere differentiable, any number of times, and one that decays asymptotically towards zero rapidly enough, that the integral $\int_{-\infty}^{+\infty} \gamma(t) \cdot t^N dt$ converges for $N \geq 0$. The Gaussian function is the classic example of a good function. We use Lighthill's notion that distributions, or "generalised functions," are obtained using regular sequences of good functions. More generally, distributions, or "generalised functions," are obtained by completing the space of continuous functions, and making use of a suitable (possibly weak) definitions of convergence. Different definitions lead to different function spaces.

³²In some of the literature, noise is represented by $dW = Z(t)dt$ that is an infinitesimal increment of the Wiener process. For our purposes, we regard dW and dB as mathematically equivalent.

6.1 Introduction, to noise techniques in electronics

the existence of integration with respect to white noise, over a finite time interval:

$$I_3 = \int_{T_1}^{T_2} F_t dB_t, \quad (6.5)$$

even in the case where the function, F_t is a distribution, or *generalised function*, which contains noise. We follow the convention used in the literature, where generalised functions of time are represented with subscripts, F_t , rather than as functions with bracketed arguments, $F(t)$.

The forms and terminology used today derive largely from the work of Kiyosi Itô (Itô 1942, Itô 1951). His formulation has the advantage that the integrals can be defined for a large class of functions and that the solutions are martingales. An alternative formulation, proposed independently by Stratonovich and Fisk, has the disadvantage that it is only defined for a very narrow class of functions and the solutions are not martingales.

The one disadvantage of Itô's approach to integration is that the formula for change of variable is different to the one used for the commonly used, Riemann-Stieltjes, type of integration. Itô's formula is:

$$df(X_t) = f'(X_t)dX_t + \frac{1}{2}f''(X_t)d[X, X]_t \quad (6.6)$$

where $d[X, X]_t$ is understood to be an inner product, roughly $dX \cdot dX$. The Stratonovich formulation preserves the more usual rule for change of variable at the expense of less general application. A very interesting history of the development of the theory and techniques of SDEs may be found in Protter (1990).

We argue that the calculus of stochastic differential equations, as defined by Itô is the best tool to use to analyse noise in electronic circuits. We show that in many cases we do not actually have to solve the SDEs explicitly in order to evaluate parameters of interest, such as noise power. It is possible to derive an ODE from the SDE to describe the evolution of the parameters in time.

6.2 Stochastic analysis of circuits

Since noise is a generalised function, it must appear inside an integration. Itô's differential equation

$$dX_t = \sigma(X_t)dB_t + \mu(X_t)dt \quad (6.7)$$

is really short hand for an integral equation

$$X_t - X_{t_0} = \int_{t_0}^t \sigma(X_\tau)dB_\tau + \int_{t_0}^t \mu(X_\tau)d\tau. \quad (6.8)$$

Durrett (1996) points out that detached stochastic differentials, such as dX_t are fictitious. We can only use these symbols on the understanding that expressions like Equation 6.7 can be integrated to create expressions of the form Equation 6.8. We can make a finite difference approximation for a very short time interval $\Delta t = t - t_0$:

$$\Delta X_t \approx \sigma(X_t)\Delta B_t + \mu(X_t)\Delta t. \quad (6.9)$$

From a philosophical point of view, we can consider the behaviour of a circuit over a short but finite time interval, Δt . This interval needs to be large enough to avoid problems with physical representation, such as infinite bandwidth, and yet short enough to represent the changing behaviour of the system under investigation.

In short, we shall work with infinitesimal increments, of the form of Equation 6.7, knowing that these are really short hand for integrals over finite time intervals of the form of Equation 6.8 and we can approximate the process in computer simulations using Equation 6.9, known as an *Euler approximation* (Kloeden and Platen 1999, Davis 2000).

6.2.1 Outline of stochastic calculus of Itô

We provide a very brief outline of Itô's stochastic calculus (Itô 1942, Itô 1951). Since the time of Itô a tremendous amount of material has been published, establishing general theorems. There are theorems regarding construction of probability spaces, convergence of measures, existence and uniqueness of solutions, changes of measure and many other foundational issues. Summaries and bibliographies can be found in (Gikhman and Skorokhod 1969) and (Durrett 1996). Much of this material is very detailed and is very necessary to establish the rigour of the technique, but the degree

6.2 Stochastic analysis of circuits

of detail makes it difficult to immediately apply the techniques to practical problems, such as the analysis of noise in an electronic circuit.

The situation, with stochastic calculus, is similar to the case where an engineer may want to measure the mass of an object, in kilograms, and model that quantity as a real number. Of course, *pure* mathematicians will tell us that the construction of the real numbers is a very complicated process, first devised by Dedekind (Harrison 1998). Pure mathematicians might prefer that we read an entire thesis before using a single real number to represent the mass of a single object. This situation would be intolerable to a practical person, who just wants to get a job done. The applied approach is to accept that we do not quite know what a real number *is*, but we do know the rules that a real number will follow. We do know that real numbers must obey the standard field axioms (Apostol 1974), and we can use those axioms to carry out our computations. We rely on the specialists to provide the foundation, and we are assured by their efforts, even if we do not read them in detail. In more recent years, Itô's techniques have been formulated in ways that make them easier to apply for non-specialists, who mainly want to carry out computations (Øksendal 1998, Kloeden and Platen 1999). Some of the recent interest is motivated by a desire to solve problems in the area of finance (Lamberton and Lapeyre 1991, Baxter and Rennie 1996).

We present an outline of the theory of stochastic differential equations, but only what we need to solve the problems arising in the analysis of noise within electronic circuits.

Properties of Brownian motion

Brownian motion has a long history where Brown (1828) studied the irregular motion of fragments of pollen in water. There is an excellent summary of a century of the history, in Hänggi and Marchesoni (2005). In the early 1900s both Einstein and Smoluchowsky independently worked on a mathematical framework for Brownian motion (Abbott *et al.* 1996). This work formed the stepping stone for a Noble prize, awarded to Perrin, in 1926. During the following decades the subject becomes far more mathematical and abstract, see Uhlenbeck and Ornstein (1930) and Wang and Uhlenbeck (1945), for example Itô (1951) cites the earlier work of Kolmogorov (1931) and Feller (1937). These works are also very mathematical and abstract. Modern models for Brownian

motion have now been reduced to idealised mathematical abstractions. The theory no longer includes all the messy details, of any specific problem, such as particles in water. On the other hand, the power of this abstraction is that the models can be applied, with some accuracy, to a very wide range of different problems.

The version of Brownian motion that we describe here is the mathematical abstraction, formulated by Kolmogorov (1931). Brownian motion, B_t , can be constructed in such a way that it has the following properties:

Translational invariance $B_t - B_0$ is independent of B_0 and has the same distribution as Brownian motion with $B_0 = 0$. This means that we can make an arbitrary standard choice for the initial condition.

Initial Condition Brownian motion has a zero initial condition, $B_0 = 0$,

Continuity Brownian motion can be constructed in such a way that it is continuous almost everywhere (a.e.). This construction is due to Kolmogorov (Durrett 1996),

Random Variable B_t is a random variable with a Normal (or Gaussian) distribution $B_t \sim N(\mu, \sigma^2)$, with $\mu = 0$ and $\sigma^2 = t$,

Markov Brownian motion is a Markov process. $B_{s+t} - B_s$, with $t > 0$ is independent of anything that happened before time, s ,

Martingale The expected value, $E[B_{s+t}]$, with $t > 0$, is not affected by any information about events before time s , X_{s-u} , for $u > 0$. If we only have information about events up to time, s , then our best estimate for the future expected value is $E[B_{s+t}] = E[B_s]$,

Independent Increments The increments of Brownian motion are independent. If $\{t_1, t_2, t_3, t_4\}$ are different instants in time, such that $t_1 < t_2 < t_3 < t_4$, then $E[(B_{t_4} - B_{t_3}) \cdot (B_{t_2} - B_{t_1})] = 0$,

Fractional Dimensions Brownian motion is a fractal, and has dimensions of time to the half, $[B_t] = [T]^{1/2}$.

Karatzas and Shreve (1988) provide detailed descriptions of four different methods for constructing Brownian motion, with the required properties. For operational purposes, we can use the properties, secure in the knowledge that mathematical objects with these properties can be constructed.

The Itô integral

Itô defined an integral, I_1 , of a function f_t with respect to Brownian motion, B_t ;

$$I_1 = \int_{T_1}^{T_2} f_t \cdot dB_t. \quad (6.10)$$

This is defined in a way that is a natural extension of the Riemann-Stieltjes integral. The important properties of the Itô integral are listed in (Øksendal 1998).

- The Itô integral I_1 is a random variable.
- If T_1 is fixed and $T_2 = t$ is an independent variable then the resulting Itô integral, $I_1(t)$, is a martingale.
- The Itô integral is summative over ranges:

$$\int_{T_1}^{T_2} f_t \cdot dB_t = \int_{T_1}^{T_3} f_t \cdot dB_t + \int_{T_3}^{T_2} f_t \cdot dB_t. \quad (6.11)$$

- The Itô integral is linear

$$\int_{T_1}^{T_2} (\alpha \cdot f_t + \beta \cdot g_t) \cdot dB_t = \alpha \cdot \int_{T_1}^{T_2} f_t \cdot dB_t + \beta \cdot \int_{T_1}^{T_2} g_t \cdot dB_t, \quad (6.12)$$

where $\alpha \in \mathcal{R}$ and $\beta \in \mathcal{R}$ are constants.

- An Itô integral always has an expected value of zero

$$E \left[\int_{T_1}^{T_2} f_t \cdot dB_t \right] = 0. \quad (6.13)$$

- Itô integrals are \mathcal{F}_T measurable.

The existence and properties of the Itô integral are discussed in a number of references (Gikhman and Skorokhod 1969, Durrett 1996, Øksendal 1998). One Itô integral can be evaluated directly, by definition,

$$\int_0^\tau 1 \cdot dB_t = B_\tau. \quad (6.14)$$

Many Stochastic Differential Equations (SDEs) can be solved, using changes of variable to manipulate the stochastic parts of the equation into the same form as Equation 6.14. There are stochastic analogues to integration by parts and integrating factors (Øksendal 1998). The stochastic analogue to the chain rule is called Itô's Formula (Durrett 1996, Øksendal 1998, Kloeden and Platen 1999).

Itô's formula

Itô's rules for change of variable differ from the rule Riemann-Steiltjes integrals. We consider an SDE of the form

$$dX_t = u(t, x) \cdot dt + v(t, x) \cdot dB_t. \quad (6.15)$$

We now consider another variable Y_t , such that

$$Y_t = g(t, x) = g(t, X_t), \quad (6.16)$$

which is a function of X_t and t , in general. Itô's formula states that

$$dY_t = \frac{\partial g}{\partial t}(t, X_t) dt + \frac{\partial g}{\partial x}(t, X_t) dx + \frac{1}{2} \frac{\partial^2 g}{\partial x^2}(t, X_t). \quad (6.17)$$

This formula must be interpreted together with some other rules:

$$dt \cdot dt = 0 \quad (6.18)$$

$$dt \cdot dB_t = 0 \quad (6.19)$$

$$dB_t \cdot dt = 0, \quad (6.20)$$

and

$$dB_t \cdot dB_t = dt. \quad (6.21)$$

This last rule, in Equation 6.21, is of particular interest. It differs from what we are used to, compared with the rules for Riemann-Steiltjes integrals, where the increments are not stochastic. It is also worth noting that dB_t has fractional dimensions, $[dB_t] = [T]^{1/2}$. Brownian motion is a fractal and the sample paths have dimension of $1/2$. This is noted in Mandelbrot (1977). The units of dB_t are root-seconds, $s^{1/2}$.

Itô's formula is widely reported in the literature (Durrett 1996, Øksendal 1998, Kloeden and Platen 1999). It is widely used to integrate SDEs, by using a change of variable.

A worked example

We consider the problem of Geometric Brownian motion (GBM). We use the following equation, to model value of an investment, X_t , over time

$$dX_t = r \cdot X_t \cdot dt + \alpha \cdot X_t \cdot dB_t, \quad (6.22)$$

6.2 Stochastic analysis of circuits

where X_t models the value of an investment at time t , $r \in \mathcal{R}^+$ is a positive real constant called the *interest rate*, and $\alpha \in \mathcal{R}^+$ is a positive real constant called *the volatility*. Equation 6.22 is widely used as a basis for modelling the variation of prices in financial systems (Lamberton and Lapeyre 1991, Baxter and Rennie 1996).

It is possible to simulate Equation 6.22 numerically. Many sample paths are required to give an accurate picture of the situation, because this equation is stochastic. Figure 6.1 shows seven sample paths. The number of paths has been limited in order to show the individual paths more clearly. The aim is to give a qualitative feel for what the solutions might be like, before explicitly solving Equation 6.22 analytically.

The first step in the solution is to write Equation 6.22 as

$$\int_0^t \frac{dX_t}{X_t} = rt + \alpha B_t, \quad (6.23)$$

with the initial condition $B_0 = 0$. Itô's formula is now applied with $g(t, x) = \ln(x)$. We obtain

$$d \ln(X_t) = \frac{dX_t}{X_t} - \frac{1}{2}\alpha^2 dt. \quad (6.24)$$

This last term being due to Equation 6.21. We can now combine Equations 6.23 and 6.24, to obtain a complete solution

$$X_t = X_0 \cdot \exp \left(\left(r - \frac{1}{2}\alpha^2 \right) \cdot t + \alpha \cdot B_t \right). \quad (6.25)$$

The presence of the stochastic process, B_t , in Equation 6.25, is the source of variation, which is why all sample paths are unique. Each sample path will include its own unique instance of B_t , as indicated in Figure 6.1.

The model for GBM is instructive. If we know the full solution for this simple case then more complicated problems can be seen as extensions of a known problem and might not seem to be as difficult as they would first appear. For example, Equation 6.25 forms the basis for the modelling of multiplicative noise in physical systems.

The model for GBM forms the basis of the Black-Scholes model for the pricing of financial derivatives (Lamberton and Lapeyre 1991, Baxter and Rennie 1996). Of course,

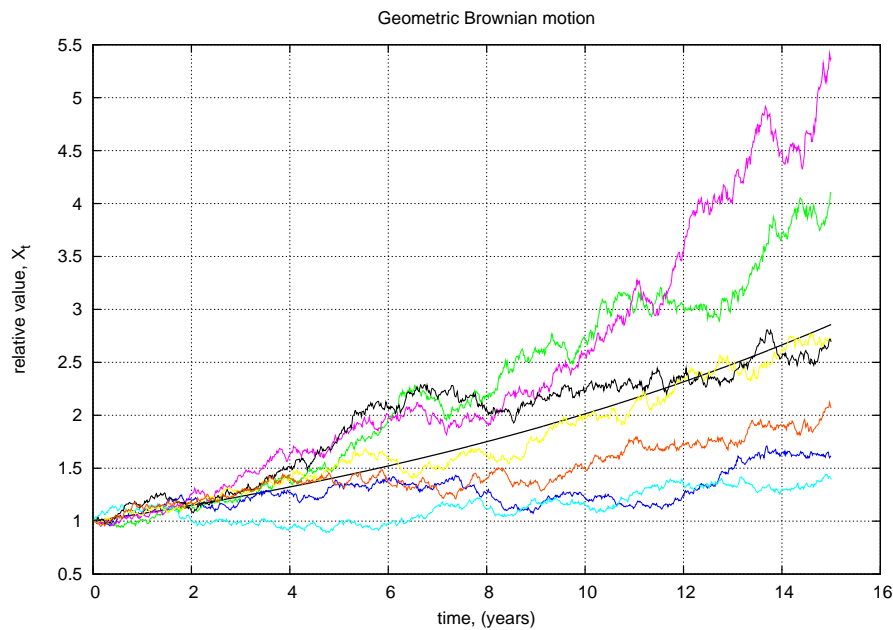


Figure 6.1. Some sample paths from Geometric Brownian Motion (GBM). The equation for Geometric Brownian Motion (GBM) is approximated numerically using the Euler integration formula (Kloeden and Platen 1999, Davis 2000). The simulation is executed in Octave v2.9. The time step is kept small, in order to prevent the (neglected) second-order terms from introducing large errors into the results. There are 1024 samples in each of the seven instances of the sample paths. The parameters are scaled to suggest a financial application; the value of a financial investment, for example. The time unit is chosen as years. The proportional rate of increase is $r = 0.07 \equiv 7\%$ per annum, for all of the sample paths. The paths are made very volatile, with $\alpha = 0.7$. This is done in order to make the effect of volatility easy to see. The black smooth continuous line shows the mean path $E[X_t]$. The coloured jagged lines are the sample paths. The individual paths may diverge quite widely from the expected path. This is a fundamental effect of volatility. Actual returns can be very different from expected returns.

it is always up to the user to decide whether a model is appropriate for any given application. The downturn and bail-out of Long-Term Capital Management (LTCM)³³, in 1998, suggests that even sophisticated models may not adequately represent risk

³³Myron Scholes and Robert C. Merton made important contributions to the Black-Scholes model and they were on the board of LTCM but this was not sufficient to prevent the company from experiencing difficulties. Soros (2008) states that the main problem with the model used by LTCM was that it did not take into account the empirical fact that deviations [from equilibrium] may be self-reinforcing, or *reflexive*. This misunderstanding caused LTCM to radically underestimate their risk. We could say that, in financial markets, price increments do not depend *only* on the present state and that the process of price variation is not Markov.

in a very complex situation. Problems with one inappropriate application of a theory do not affect the fact that Equation 6.22 can be solved exactly, to yield Equation 6.25. Geometric Brownian Motion (GBM) is an internally consistent and valid model, even if it does not always adequately represent the behaviour of actual phenomena in the real world. There is an account of the social history of the Black-Scholes model in (Bernstein 2008).

6.2.2 The Fokker Planck equation and the Langevin SDE

If we accept that the dynamics of a particular system are governed by an SDE, such as the Langevin Equation, then it is reasonable to ask what the corresponding PDE is for the probability density function, as a function of time and position. Analysis shows that the resulting PDE is identical to the Fokker-Planck equation (Gikhman and Skorokhod 1969, Kloeden and Platen 1999). When the equation is derived in this way, from an SDE via the Chapman-Kolmogorov equations, the resulting PDE is called *The Kolmogorov backward equation*, or the *second direct equation of Kolmogorov*.

Gikhman and Skorokhod (1969) attribute the following theorem to Kolmogorov. Suppose that we represent the position of a diffusing particle in one-dimensional space, x , with a stochastic function of time X_t . Suppose, further, that time is represented by t and dt is an infinitesimal increment of time and dB_t is an infinitesimal increment of Brownian motion. Given

$$dX_t = a(t, X_t) \cdot dt + b(t, X_t) \cdot dB_t, \quad (6.26)$$

where $a(t, x)$ and $b(t, x)$ are good functions of t and x , then the probability density of the particle, over x and t , can be represented by $p(t, x)$, where

$$\frac{\partial}{\partial t} p(t, x) = -\frac{\partial}{\partial x} (a(t, X_t) \cdot p(t, x)) + \frac{1}{2} \frac{\partial^2}{\partial x^2} (b(t, X_t) \cdot p(t, x)), \quad (6.27)$$

which is identical in form with the Fokker-Planck equation. This is an important result. Given an SDE, in Equation 6.26, we can write down the corresponding PDE in Equation 6.27.

6.3 Modelling of electronic circuits, using SDEs

If we are given an SDE for an electronic circuit then we have some of the tools required to determine the solution (Durrett 1996, Øksendal 1998, Kloeden and Platen 1999). For example, we can use techniques, similar to the ones for Geometric Brownian Motion, in Equation 6.22. There is some material in the literature regarding the use of SDEs for the analysis of noise in electronic circuits (Demir *et al.* 2000, Mehrotra and Sangiovanni-Vincentelli 2004, Gitterman 2005), but the modelling does not always go right down to the detailed level, of single components, and does not relate to established results, such as those of Nyquist (1928). That is our purpose here, to place the existing work on a firmer foundation. We begin with a re-evaluation of the laws of Kirchhoff.

6.3.1 Infinitesimal forms of Kirchhoff's laws

We can re-write Kirchhoff's laws for infinitesimal intervals of time. The advantage of writing the circuit laws in this way is that the new equations provide a single simple systematic basis for combining signals of different types.

It is possible to write statistical fluctuations in terms of generalised functions, such as $dB \equiv Z_t dt$ or $\delta(t)dt$. We can also write contributions from deterministic functions in infinitesimal form, $f(t)dt$. We can then combine noise contributions freely with other contributions from deterministic functions. We do this in the knowledge that we could always convert the resulting Stochastic Differential Equations (SDEs) into Stochastic Integral Equations (SIEs), through integration. In this way, we avoid many of the philosophical difficulties connected with the manipulation of generalised functions. We must always be able to write the generalised functions in terms of integral functionals, such as Equation 6.5.

6.3.2 Kirchhoff's current law

The infinitesimal version of Kirchhoff's Current Law (KCL) is written in terms of infinitesimal increments of electric flux (electric charge) flowing out of a node:

$$\sum_{\forall k} dQ_k = 0. \quad (6.28)$$

6.3 Modelling of electronic circuits, using SDEs

This is shown in Figure 6.2 If all the contributions, dQ_k are not stochastic, then we can

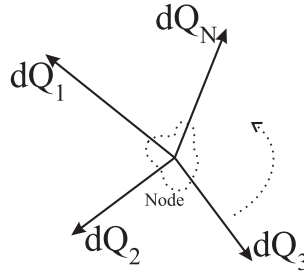


Figure 6.2. The infinitesimal form of Kirchhoff's Current Law (KCL). This figure represents the total effect of currents flowing into, and out of, a node of a circuit, during an infinitesimal period of time, dt .

write the increments of charge in terms of currents, $dQ_k = I_k dt$, and the Equation 6.28 reduces to

$$\sum_{\forall k} (I_k dt) = \left(\sum_{\forall k} I_k \right) dt = 0 \quad (6.29)$$

and if this is true for all dt , we can integrate and get

$$\sum_{\forall k} I_k = 0, \quad (6.30)$$

which is the more usual form of the law. The proof of the infinitesimal form follows from one of Maxwell's equations (Hayt 1988), called Gauss's electric law:

$$\oint_A \underline{D} \cdot d\underline{A} = \int_v \rho \cdot dv = Q \quad (6.31)$$

where the vector, \underline{D} , is the electric flux density, the vector, $d\underline{A}$, is a directed element of the surface, A , and the scalar, the scalar ρ is the volume charge density, the scalar, dv , is an infinitesimal element of the volume, v , enclosed by the surface, A , and Q , is the total charge enclosed within the surface.

Suppose that we divide the complete surface, A , into a finite number, N , of small disjoint sub-surfaces, A_k such that $\bigcup_{k=1}^N A_k = A$ and $A_i \cap A_j = \emptyset$, if $i \neq j$. We can express the electric flux through each sub-surface as:

$$Q_k = \int_{A_k} \underline{D} \cdot d\underline{A} \quad (6.32)$$

and we can write

$$\sum_{k=1}^N Q_k = Q. \quad (6.33)$$

If we consider the variation in total electric flux, charge, over an infinitesimal time interval, dt , then we get:

$$\sum_{k=1}^N dQ_k = dQ. \quad (6.34)$$

The correct modelling of dQ is a non-trivial problem. It depends on the relationship of the surface, A , to the surrounding electrical environment. Specifically, we need to know the capacitance, C , of the surface, A , with respect to earth.

The stored energy of the total charge in the node is: $U = \frac{1}{2C}Q^2$ If we assume that the system is at thermodynamic equilibrium with the surroundings then we can use thermodynamic and statistical arguments. It is possible to show that $E[Q] = 0$, because this is the minimum energy configuration for the system³⁴. Using the principle of equipartition of energy, it is possible to show that $E\left[\frac{1}{2C}Q^2\right] = \frac{1}{2}kT$, which is simply the mean energy for each degree of freedom, in a classical thermodynamic system at temperature T . This implies that $E[Q^2] = kT \cdot C$.

It can be shown that this formula is divisible. That is, a node can be arbitrarily divided into two complete sub-nodes, enclosed by two complete surfaces, A_1, A_2 . These enclose two sets of charge, Q_1 and Q_2 .

The charge within the surfaces must be the same, no matter how we choose to partition the node, $Q = Q_1 + Q_2$. Energy is also partitioned, $E[U] = [U_1] + E[U_2]$. Capacitance of the two surfaces must also add, if the surfaces are conducting and are at the same potential, $C = C_1 + C_2$ and yet each sub-node follows same the formula for fluctuations: $E[Q_1^2] = kT \cdot C_1$ and $E[Q_2^2] = kT \cdot C_2$. This seems to be a paradox, until we realise that the fluctuations of charges enclosed in the two nodes are independent, $E[Q_1 \cdot Q_2] = 0$.

We regard the charge enclosed in a node as being a normally distributed random process, $Q \sim N(0, kT \cdot C)$ so we can model the natural thermal fluctuations of charge enclosed inside the node, over a time interval dt , as $dQ = \pm\sqrt{kTC} \cdot dB$ where dB is an infinitesimal increment of Brownian motion. This means that Equation 6.34 can be

³⁴We have used the symbols, $E[Q]$, to denote an ensemble average of a stochastic process, Q . We use the symbols, $\langle Q \rangle$, to denote the time average of Q . If the process is ergodic then $E[Q] = \langle Q \rangle$

written as

$$\sum_{k=1}^N dQ_k = \sqrt{kTC} \cdot dB. \quad (6.35)$$

This differs from the homogeneous form of Kirchhoff's current law, in Equation 6.28. This is an indication that Kirchhoff's laws are ultimately statistical and there will be small fluctuations. The fluctuations can usually be ignored, as long as the circuit is well constructed and the capacitance of the node to earth, C is small. If this is not the case, then we would need to include the parasitic capacitance, C , in our model of the circuit.

In the remainder of this chapter, we will use the homogeneous, differential form of Kirchhoff's current law, Equation 6.28, where infinitesimal increments of charge are represented in the form, $dQ = Idt$ for deterministic currents, and also in the form, $dQ = i_n dB$ for noise currents³⁵.

6.3.3 Kirchhoff's voltage law

The infinitesimal version of Kirchhoff's Voltage Law (KVL) is written in terms of infinitesimal increments of magnetic flux through a mesh:

$$\sum_{\forall k} d\Phi_k = 0. \quad (6.36)$$

This is shown in Figure 6.3. If all the contributions, $d\Phi_k$, are not stochastic then we can write the increments of flux in terms of voltages, $d\Phi_k = V_k dt$ and Equation 6.36 reduces to

$$\sum_{\forall k} (V_k dt) = \left(\sum_{\forall k} V_k \right) dt = 0 \quad (6.37)$$

and if this is true for all dt , we can integrate and get

$$\sum_{\forall k} V_k = 0, \quad (6.38)$$

³⁵Note that the units are $[dQ] = [I][T]$, $[dt] = [T]$, $[i_n] = [I][T]^{-\frac{1}{2}}$ and $[dB] = [T]^{\frac{1}{2}}$. The units of noise current are $A \cdot Hz^{-1/2}$, or amperes per root Hz. The fractional units are a consequence of the fact that Brownian motion is a fractal (Mandelbrot 1977). Brownian motion is statistically self-similar under a change of scale.

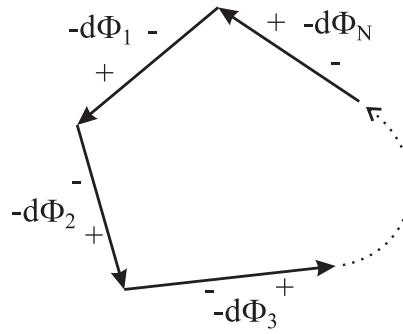


Figure 6.3. The infinitesimal form of Kirchhoff's Voltage Law (KVL). This figure represents the total effect of flux flowing through a mesh, in either direction, during an infinitesimal period of time, dt .

which is the more usual form of the law. If we sum the voltage increments around the mesh then we must get zero. This is equivalent to saying that electric fields are the product of a static potential field, $\underline{E} = -\nabla V$. The proof of the infinitesimal form of Kirchhoff's voltage law follows from one of Maxwell's equations (Hayt 1988), called Faraday's law:

$$\oint_{\lambda} \underline{E} \cdot d\underline{\lambda} = -\frac{\partial}{\partial t} \int_S \underline{B} \cdot d\underline{A} = -\frac{\partial \Phi}{\partial t} \quad (6.39)$$

where the vector, \underline{E} , is the electric field strength, the vector, $d\underline{\lambda}$, is a directed line element of the contour, λ , the vector, \underline{B} , is the magnetic flux density and the vector, $d\underline{A}$ is a directed element of the surface, S , enclosed by the contour, λ .

Suppose that we divide the complete contour, λ , into a finite number, N , of small disjoint sub-curves, λ_k , such that $\bigcup_{k=1}^N \lambda_k = \lambda$, and $\lambda_i \cap \lambda_j = \emptyset$, if $i \neq j$. We can express the voltage increments in each sub-curve as

$$V_k = \int_{\lambda_k} \underline{E} \cdot d\underline{\lambda} \quad (6.40)$$

and we can write

$$\sum_{k=1}^N V_k = -\frac{\partial \Phi}{\partial t}. \quad (6.41)$$

If we consider the variation in total magnetic flux over an infinitesimal time interval, dt , then we get:

$$\sum_{k=1}^N V_k dt = \sum_{k=1}^N d\Phi_k = -d\Phi. \quad (6.42)$$

The correct modelling of $d\Phi$ is a non-trivial problem. It depends on the actual physical geometry of the current path. Specifically, we need to know the inductance, L , of the

current path.

The stored energy of the total charge in the node is: $U = \frac{1}{2L}\Phi^2$. If we assume that the system is at thermodynamic equilibrium with the surroundings, then we can use thermodynamic and statistical arguments. It is possible to show that $E[\Phi] = 0$, because this is the minimum energy configuration for the system. Using the principle of equipartition of energy, it is possible to show that $E\left[\frac{1}{2L}\Phi^2\right] = \frac{1}{2}kT$, which is simply the mean energy for each degree of freedom in a classical thermodynamic system at temperature T . This implies that $E[\Phi^2] = kT \cdot L$.

It can be shown that this formula is divisible. That is, the contour, λ , can be arbitrarily divided into two complete sub-contours, λ_1, λ_2 . These enclose two sets of flux, ϕ_1 and ϕ_2 . The flux linked by the contours must be the same, no matter how we choose to partition the mesh, $\Phi = \Phi_1 + \Phi_2$. Energy is also associated with magnetic flux. It is conserved and partitioned as, $E[U] = [U_1] + E[U_2]$.

Inductance of the two contours must also add, if the surfaces are connected and are carrying the same current, $L = L_1 + L_2$ and yet each sub-node follows the same formula for fluctuations: $E[\Phi_1^2] = kT \cdot L_1$ and $E[\Phi_2^2] = kT \cdot L_2$. This seems to be a paradox, until we realise that the fluctuations of the flux enclosed in each the two nodes are independent, $E[\Phi_1 \cdot \Phi_2] = 0$.

We regard the magnetic flux linked by the contour, λ , as being a normally distributed random process, $\Phi \sim N(0, kT \cdot L)$ so we can model the natural thermal fluctuations of flux linked by the contour over a time interval dt , as $d\Phi = \pm\sqrt{kT \cdot L} \cdot dB$ where dB is an infinitesimal increment of Brownian motion. This means that Equation 6.42 can be written as

$$\sum_{k=1}^N d\Phi_k = \sqrt{kT \cdot L} \cdot dB. \quad (6.43)$$

This differs from the homogeneous form of Kirchhoff's voltage law, in Equation 6.36. This is an indication that Kirchhoff's laws are ultimately statistical and that there will be small fluctuations. The fluctuations can usually be ignored, as long as the circuit is well constructed and the inductance of the current carrying path, L , is small. If this is not the case, then we would need to include the parasitic inductance, L , in our model

of the circuit.

In the remainder of this chapter, we will use the homogeneous, differential form of Kirchhoff's voltage law, Equation 6.36, where infinitesimal increments of magnetic flux are represented in the form $d\Phi = Vdt$ for deterministic currents, and also in the form, $d\Phi = v_n dB$ for noise currents³⁶.

6.3.4 Models for resistors

There are two possible linear models for thermal noise in a resistor, a Thévenin and a Norton model, which are shown in Figure 6.4. The Thévenin model, Figure 6.4(a), places a noise voltage source in series with an ideal noiseless resistor. During an infinitesimal time interval, dt , the source contributes a magnetic flux of $v_n dB$ to all circuit meshes in which it sits. We can use the results of Johnson (1928) and Nyquist (1928), $\Delta \langle V^2 \rangle = 4kTR \cdot \Delta f$, to estimate intensity of the noise voltage, $v_n = \sqrt{2kTR}$. The units of noise voltage are $V/\sqrt{\text{Hz}}$.

The use of the constant “2” rather than “4” is due to the convention that we use for frequency. We consider all frequencies in the real line, positive and negative. This is the definition of frequency used for complex exponentials, rather than sinusoids. It is consistent with widely used definitions of power spectral density and autocorrelation functions (Reif 1965, Bracewell 2000, Yates and Goodman 1999, Peebles 2001, Razavi 2001). It is sometimes called the two-sided power spectrum (Razavi 2001).

The flat spectrum described by Johnson (1928) is really only a special case which applies at low frequencies. The high frequency cutoff of the spectrum is determined by quantum mechanical effects (Nyquist 1928). This was also noted in Feynman *et al.* (1963) and Reif (1965). The power spectrum of the output of a system governed by a Langevin equation, driven by white noise will generally be Lorentzian (Papoulis 1991)

³⁶Note that the units are $[d\Phi] = [V][T] = [M][L]^2[T]^{-2}[I]^{-1}$, $[dt] = [T]$, $[v_n] = [V][T]^{1/2}$ and $[dB] = [T]^{1/2}$. The units of noise voltage are $V \cdot \text{Hz}^{-1/2}$, volts per root Hz. The fractional units are a consequence of the fact that Brownian motion is a fractal (Mandelbrot 1977).

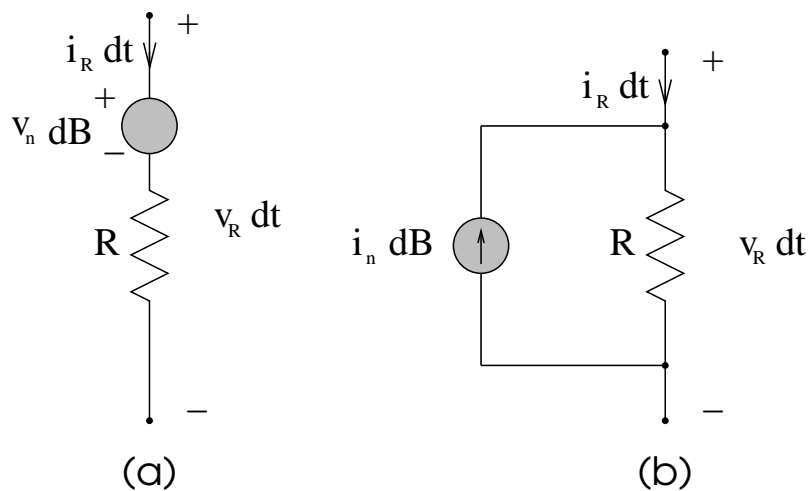


Figure 6.4. Linear noise models for a resistor. This figure shows the total contribution to electric flux (charge) and magnetic flux, caused by a resistor, during an infinitesimal interval of time, dt . The Thévenin equivalent model, is shown in part (a), on the left. The increment of charge is $dQ = i_r dt$. The increment of magnetic flux is $v_R dt$. The resistor is represented as a noiseless ideal resistance (obeying Ohm's law) in series with a noise voltage source. Noise sources are represented shading the corresponding circuit symbols, in order to distinguish them from deterministic sources. We can apply Kirchhoff's voltage law to the Thevenin circuit to obtain an SDE to describe the terminal behaviour of this component, $v_R \cdot dt = i_R \cdot R \cdot dt + v_n dB$. The Norton equivalent model, is shown in part (b), on the right. The increments of electric and magnetic flux are the same as for the Thévenin model. The resistor is represented as a noiseless ideal conductance (obeying Ohm's law) in parallel with a noise current source. We can apply Kirchhoff's current law to the Norton circuit to obtain another SDE to describe the terminal behaviour of this component $i_R \cdot R dt + R \cdot i_n dB = v_R dt$. The Thevenin and Norton noise models have equivalent behaviour, at the terminals, provided, $v_n = R i_n$. These infinitesimal models can be incorporated with the infinitesimal models for other components, using the infinitesimal versions of Kirchhoff's laws, to arrive at Stochastic Differential Equations (SDEs) for complete circuits. The noise sources in a circuit are typically the dissipative components, such as resistors, or the semiconductor components, such as diodes and transistors.

and the high frequency cutoff due to the dynamics of the Langevin equation will usually be several orders of magnitude below the cutoff due to quantum mechanical effects. This is why the abstraction of a flat spectrum is adequate. An interesting summary of the history of Power Spectral Density (PSD) for noise can be found in Abbott *et al.* (1996).

The Norton model, Figure 6.4(b), places a noise current source in parallel with an ideal noiseless resistor. During an infinitesimal time interval, dt , the source contributes an electric flux, or charge³⁷, of $dQ_1 = i_n dB$ to the node into which the terminal flows. A corresponding opposite charge of $dQ_2 = -i_n dB$ is added at the other terminal³⁸. The corresponding intensity of noise current is $i_n = \sqrt{2kT/R}$. The units of noise current are $A/\sqrt{\text{Hz}}$.

The equivalence of the Thévenin and Norton models is consistent with the fact that $v_n = Ri_n$ which is the same as the accepted rule for deterministic signals. Wannier (1966) notes that the Norton model more accurately describes the physical process of fluctuations within a resistor.

We can write the increments of electric flux associated with a resistor as

$$dQ = i_n dB \quad (6.44)$$

where dB is an infinitesimal increment of Brownian motion. These increments of electric flux can be used directly in the differential form of KCL, Equation 6.28.

We can write the increments of magnetic flux associated with a resistor as

$$d\Phi = v_n dB \quad (6.45)$$

where dB is an infinitesimal increment of Brownian motion. These increments of magnetic flux can be used directly in the differential form of KVL, Equation 6.36.

We can also imagine other noise models for other devices. These will generally have different expressions for current and voltage noise intensities, v_n and i_n , but the calculations will generally be of the same form as for the resistor.

³⁷Electric flux has the units of charge (Hayt 1988).

³⁸The signs only determine the directions of the symbols. The direction of the noise current will change indefinitely often within any finite time interval. The instantaneous value of the noise current at any given instant of time cannot be specified, even in principle, since noise current is a *generalised* function.

6.3 Modelling of electronic circuits, using SDEs

A functional mapping between electrical and mechanical systems

There is a widely used functional mapping between quantities in electrical and mechanical systems. These can be expressed in terms of the Hamiltonian function, \mathcal{H} , using Hamilton's canonical equations (Lanczos 1949).

Variable	Electrical Quantity	Mechanical Quantity
Effort	Voltage, $-V = +\frac{\partial\Phi}{\partial t} = -\frac{\partial\mathcal{H}}{\partial Q}$	Force, $+F = +\frac{dp}{dt} = -\frac{\partial\mathcal{H}}{\partial x}$
Flow	Current, $I = +\frac{\partial Q}{\partial t} = +\frac{\partial\mathcal{H}}{\partial\Phi}$	Velocity, $v = +\frac{dx}{dt} = +\frac{\partial\mathcal{H}}{\partial p}$
Momentum	Magnetic flux, Φ	Momentum, p
Displacement	Electric flux, Q	Displacement, x
Power	$\mathbf{P} = V \cdot I$	$\mathbf{P} = F \cdot v$
Energy	$\mathbf{E} = \int^Q V dQ \equiv \int^\Phi I d\Phi$	$\mathbf{E} = \int^x F dx \equiv \int^p v dp$

Further details of the mapping are described by Karnopp *et al.* (2000). There are differences of sign in the definitions of the effort variables. These are due to historical differences of convention in the way that the symbols are defined³⁹. The mapping applies to all equations of motion, including the Langevin equation.

Variable	Electrical Quantity	Mechanical Quantity
Viscous damping force	$-V = -R \cdot I$	$+F = -\alpha \cdot v$
Noise intensity	$E[v_n^2] = 2kT \cdot R$	$E[f_n^2] = 2kT \cdot \alpha$
Langevin Equation	$LdI + RI dt = v_n dB_t$	$mdv + \alpha v dt = f_n dB_t$

This demonstrates that the resulting equations for electrical circuits are Langevin equations in the literal sense. Of course, all established results for mechanical systems can be applied directly to electrical systems, by mapping solutions to the mechanical problems into the electrical domain. These considerations also suggest that we should use the generalised coordinates, Φ and Q to describe the dynamics of electrical systems, as an analogy of the use of p and x for mechanical systems.

$$dQ = i_c dt = C dv_c$$

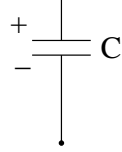
$$d\Phi = v_c dt$$


Figure 6.5. Modelling of capacitors. The modelling of capacitors is complete, for SDE applications, if the infinitesimal increments of flux are completely specified. In this case, the increment of electric flux (charge) is given by $dQ = i_c dt = C dv_c$. The increment of magnetic flux is given by $d\Phi = v_c dt$.

6.3.5 Modelling of capacitors

For a fixed capacitor, C , with terminal voltage, v_C , and terminal current, i_C , we require the following equivalent forms for infinitesimal increments of electric flux

$$dQ = i_C \cdot dt = Cd \cdot v_C. \quad (6.46)$$

The increment of magnetic flux follows the usual rule for any component

$$d\Phi = v_C \cdot dt. \quad (6.47)$$

There are two equivalent forms for dQ , but only one for $d\Phi$. The capacitor model can be combined with Norton and Thévenin models, to create more complex circuits. The equations for the increments of flux, Equations 6.46 and 6.47, can be combined directly with the differential form of KCL, Equation 6.28.

6.3.6 Modelling of inductors

For a fixed inductor, L , with terminal voltage, V , and terminal current, I , we require the following equivalent forms for infinitesimal increments of magnetic flux

$$d\Phi = v_L \cdot dt = L \cdot di_L. \quad (6.48)$$

The increment of electric flux follows the usual rule for any component

$$dQ = i_L \cdot dt. \quad (6.49)$$

³⁹In the electrical case, the minus sign is known as Lenz' law, $V = -\partial\Phi/\partial t$.

6.4 A one-dimensional Langevin equation (SDE)


$$\begin{aligned} dQ &= i_L dt \\ d\Phi &= v_L dt = L di_L \end{aligned}$$


Figure 6.6. Modelling of inductors. The modelling of inductors, for SDE applications, is complete if the infinitesimal increments of flux are completely specified. In this case, the increment of electric flux (charge) is given by $dQ = i_L dt$. The increment of magnetic flux is given by $d\Phi = v_L \cdot dt = L \cdot di_L$.

There are two equivalent forms for $d\Phi$, but only one for dQ . The inductor model can be combined with Norton and Thévenin models, to create more complex circuits. The equations for the increments of flux, Equations 6.48 and 6.49, can be combined directly with the differential form of KVL, Equation 6.36.

6.4 A one-dimensional Langevin equation (SDE)

We consider the case of a resistor in parallel with a capacitor. This problem has been considered by many authors, including (Feynman *et al.* 1963, Lathi 1965, Carlson *et al.* 2002). The circuit is represented in Figure 6.7 We expect to find a mean-square voltage across the capacitor of,

$$\langle V^2 \rangle = \frac{kT}{C}. \quad (6.50)$$

This is clear if we regard the voltage across the capacitor as a single degree of freedom and apply the principle of equipartition of energy, $\langle \frac{1}{2}CV^2 \rangle = \frac{1}{2}kT$. Equilibrium and quasi-equilibrium arguments, of this type, are presented in Feynman *et al.* (1963), Reif (1965) and Wannier (1966). The history of this approach, for mechanical systems, can be traced at least as far back as Gibbs (1902).

6.4.1 An approach, based on power spectral density

If we consider a resistor and a capacitor in parallel, then the equivalent circuit could be represented as a parallel (Norton equivalent) circuit, as shown in Figure 6.7. A

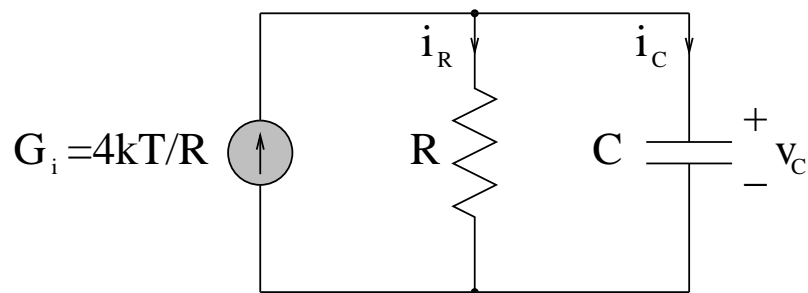


Figure 6.7. Parallel, or Norton, representation of an RC circuit. Johnson (1928) and Nyquist (1928) suggested an approach to the estimation of mean-square noise voltage, based on Power Spectral Density (PSD). This approach is used here. This figure shows a Norton equivalent representation of the resistor. The noise source is represented as a noise current source, with Power Spectral Density, $G_i(f)$. The source is represented by the standard symbol for a current source, but it is shaded, to indicate that it is a noise source, which represents a generalised function. Nyquist showed that, for thermal noise in a resistor, we would expect that $G_i(f) = 4kT/R$. This circuit can be analysed as a parallel circuit but it is usually represented as a series (Thevinin equivalent) circuit.

resistor and capacitor in parallel can also be represented as a Thevinin-equivalent circuit. It is common in the literature to regard the voltages as the signals of interest, and to use a Thévenin-equivalent circuit, as shown in Figure 6.8. In the traditional approach, due to Nyquist (1928), increments of time, dt , or Brownian motion, dB_t , are not considered explicitly. The source voltage for the circuit is the Thévenin-equivalent voltage, represented here as $v_n(t)$. No attempt is made to represent $v_n(t)$ directly, but the Fourier transform, $V_N(f)$, has a spectral representation in the frequency domain, $G_1(f) = E[|V_N(f)|^2] = 4kTR$, where $k \approx 1.3806503 \times 10^{-23} \text{ J} \cdot \text{K}^{-1}$, is Boltzmann's constant and T is the temperature in degrees Kelvin. The Fourier transform of a noise function, $V_N(f) = \mathcal{F}[v_n(t)]$, is a random variable, which is distributed over the complex plane. The corresponding PSD involves a magnitude-squared, and an expected value so it reduces to a real function of frequency $G_1(f)$. In the case of thermal noise, the PSD, $G_1(f)$, reduces to a constant real number, which does not depend on frequency, $G_1(f) = 4kTR$. This result was derived by Nyquist (1928). The result is nearly correct for low frequencies, $|f| \ll kT/h$, where $h \approx 6.62606876 \times 10^{-34} \text{ J} \cdot \text{s}$, is Planck's constant. This PSD, $G_1(f) = 4kTR$, is a *one sided* power spectral density that only considers non-negative frequencies $f \geq 0$. The output from the circuit is considered to be $v_C(t)$, but no attempt is made to represent $v_C(t)$ directly, but the Fourier transform, $V_C(f)$, also has a spectral representation in the frequency domain, which is related

6.4 A one-dimensional Langevin equation (SDE)

to the input $V_N(f)$, through the transfer function of the RC circuit. We can define, $G_2(f) = E \left[|V_C(f)(f)|^2 \right]$, and write

$$G_2(f) = |H(j2\pi f)|^2 \cdot G_1(f), \quad (6.51)$$

where $H(s)$ is the transfer function of the circuit in the Laplace domain. We note that $G_1(f) = 4kTR$ does not vary with frequency. It is constant, so is can be taken outside of any integration. The total noise energy can be calculated by integrating Equation 6.51 over all frequencies, to give

$$E \left[|v_c(t)|^2 \right] = G_1(f) \cdot \int_{-\infty}^{+\infty} |H(j2\pi f)|^2 \cdot df. \quad (6.52)$$

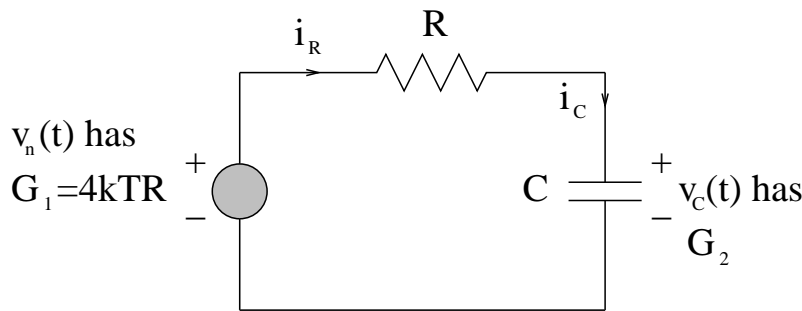


Figure 6.8. A Thévenin Equivalent Circuit for the RC circuit. The resistor and capacitor in parallel can be represented as a Thevenin-equivalent circuit. It is common in the literature to regard the signal of interest as the noise voltage source, associated with the resistor, and to use a Thévenin-equivalent circuit, shown here. Viewed from this point of view, the circuit is a Linear Time-Invariant (LTI) system driven by a noise source. The input to the circuit is nominally represented by $v_n(t)$ and the output from the circuit is nominally represented by $v_c(t)$. These are generalised functions, in the time domain, but their power spectral densities are good functions, in the sense used by Lighthill (1958). The PSD of $v_n(t)$ is denoted by $G_1(f) = |\mathcal{F}[v_n(t)]|^2$, and the PSD of $v_c(t)$ is denoted by $G_2(f) = |\mathcal{F}[v_c(t)]|^2$. Nyquist's analysis considers the PSD of the input function, $G_1(f)$, the PSD of the output function, $G_2(f)$, and the way in which they are related through the transfer function of the circuit, $G_2(f) = |H(j2\pi f)|^2 \cdot G_1(f)$. The total noise energy, observed at the output, can be calculated by integrating this last expression over all frequencies.

The transfer function for the RC circuit has only one real pole. In the Laplace domain, we can write

$$H(s) = \frac{\omega_0}{s + \omega_0}, \quad (6.53)$$

where $\omega_0 = 1/(RC)$. This can be written in terms of angular frequency

$$H(j\omega) = \frac{1}{1 + j\left(\frac{\omega}{\omega_0}\right)} \quad (6.54)$$

We can then normalise the frequency variable:

$$H(j\Omega) = \frac{1}{1 + j\Omega}, \quad (6.55)$$

where $\Omega = \omega/\omega_0$.

The Power Spectral Density (PSD) of the circuit can be calculated as the magnitude-squared response of the circuit. This can be written as

$$|H(j\Omega)|^2 = H(j\Omega) \cdot H(j\Omega)^* \quad (6.56)$$

$$= H(+j\Omega) \cdot H(-j\Omega). \quad (6.57)$$

Equation 6.56 is quite general. The special case, for a single pole reverts to

$$|H(j\Omega)|^2 = \frac{1}{1 + j\Omega} \cdot \frac{1}{1 - j\Omega} = \frac{1}{\Omega - j} \cdot \frac{1}{\Omega + j}. \quad (6.58)$$

This can be explicitly written as a polynomial in Ω ,

$$|H(j\Omega)|^2 = \frac{1}{\Omega^2 + 1}. \quad (6.59)$$

The power spectral density function, represented by Equation 6.59 is called a *Lorentzian* function.

We would like to be able to reduce the entire effect of a filter, on noise, back to a single number. This is the role of the Noise Equivalent Bandwidth (NEB) (Carlson *et al.* 2002), which is defined as:

$$B_N = \frac{1}{2} \int_{-\infty}^{+\infty} \left| H\left(j\frac{f}{f_0}\right) \right|^2 df \quad (6.60)$$

This can be evaluated in terms of the normalised PSD:

$$B_N = \frac{f_0}{2} \cdot \int_{-\infty}^{+\infty} |H(j\Omega)|^2 d\Omega. \quad (6.61)$$

This leads to an expression for the particular case, of a single-pole RC circuit,

$$B_N = \frac{f_0}{2} \cdot \int_{-\infty}^{+\infty} \frac{1}{\Omega^2 + 1} d\Omega, \quad (6.62)$$

6.4 A one-dimensional Langevin equation (SDE)

where $f_0 = 1/(2\pi RC)$. Integrals of this type can be evaluated using Cauchy's integral formula. An integral along the real line can be shown to be equivalent to the integral around a contour in the complex plane, which can be reduced to a finite sum of residues, at the poles. This reduces an improper integral of the type of Equation 6.62 to a simple result.

Cauchy's integral formula states that

$$\oint \frac{g(z)}{z - z_0} = j2\pi \cdot g(z_0), \quad (6.63)$$

where the path of integration includes z_0 . The quantity, $j2\pi g(z_0)$ is called the residue of g at z_0 . Cauchy's integral formula is central to mathematical analysis with complex variables and can be found in many text books, including (Goursat 1916, Courant and McShane 1966, Apostol 1974, LePage 1980, Doran and Lasenby 2003, Kreyszig 2006). The formula equation is linear, so sums of functions lead to sums of residues. This means that many rational functions can be integrated by resolving them into partial fractions. The conditions under which the formula can be used to evaluate real integrals are discussed in (Goursat 1916, Courant and McShane 1966, Apostol 1974, LePage 1980). The essential requirement is that the PSD, $|H(j\Omega)|^2$ must tend towards zero as the radius, $|\Omega| \rightarrow \infty$ with a power index of less than -2 . Specifically, there must be a positive real constant constant, $M \in \mathcal{R}^+$, such that

$$|H(j\Omega)|^2 < \frac{M}{|\Omega|^2}. \quad (6.64)$$

These conditions are met for PSD functions with one or more poles, because one pole in the transfer function gives rise to two poles in the PSD.

The improper integral in Equation 6.62 can be evaluated using Cauchy's integral formula. The first step is to break the PSD function into a partial fraction expansion. We can re-write $|H(j\Omega)|^2$ as

$$\frac{1}{\Omega^2 + 1} = +\frac{j}{2} \cdot \frac{1}{\Omega - j} + \frac{-j}{2} \cdot \frac{1}{\Omega + j} \quad (6.65)$$

The PSD function has poles at $\Omega = \pm j$. These are shown in Figure 6.9.

Cauchy's formula then leads to a concise expression for the integral,

$$\int_{-\infty}^{+\infty} \frac{1}{\Omega^2 + 1} d\Omega = \theta = (2\pi j) \cdot \left(\frac{-j}{2}\right) = \pi. \quad (6.66)$$

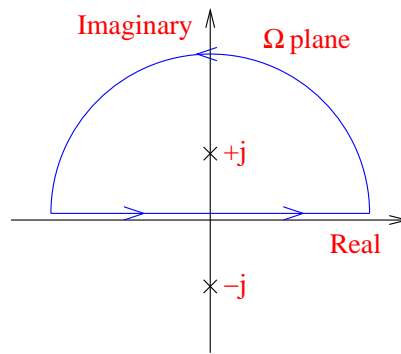


Figure 6.9. The Poles of the PSD function for an RC circuit. This figure represents the complex plane. The x-axis represents the real part and the y-axis represents the imaginary part of complex numbers. The PSD function, $|H(j\Omega)|^2$, has poles at $\Omega = \pm j$. The integral around the D-shaped contour is the same as the integral along the real axis. For clarity, the horizontal part of the contour is represented slightly above the real axis. In practice this part of the contour runs along the real axis. For clarity, the semi-circular part of the contour (the return path) is shown as having finite radius, r . In practice this radius approaches infinity, $r \rightarrow \infty$. Under these conditions, the contribution, to the integral, from the return path approaches zero.

If we combine Equation 6.62 and Equation 6.66 then we can deduce that

$$B_N = \frac{\pi f_0}{2}, \quad (6.67)$$

but $\omega_0 = 2\pi f_0 = 1/(RC)$, which leads to the final result,

$$B_N = \frac{1}{4RC}. \quad (6.68)$$

This is a *one-sided* bandwidth, which applies for $f \geq 0$ so it has to be used together with a one-sided estimate for the PSD at the input, $G_1(f) = 4kTR$. We can predict the noise power observed at the resistor, in the RC circuit, in Figure 6.8.

$$E[x^2] = 4kTB_N \quad (6.69)$$

$$= 4kT \frac{1}{4RC} \quad (6.70)$$

$$= \frac{kT}{C}. \quad (6.71)$$

This result is recorded in many of the standard textbooks, including Carlson *et al.* (2002). It is also derived in a very direct way by Feynman *et al.* (1963), who uses a quasi-equilibrium thermodynamic argument. A capacitor is treated as though it were an over-sized particle with one degree of freedom. Equipartition of energy is a classical

6.4 A one-dimensional Langevin equation (SDE)

approximation due to Boltzmann and Maxwell. On average each degree of freedom has mean energy of $kT/2$. One can understand that extreme deviations from this equality should be rare. If we imagine a single high energy particle, amongst a large number of more slowly moving particles. This would be equivalent to a fast moving white ball breaking up a frame of balls, in eight-ball. After a few collisions, the energy in the white-ball is more evenly distributed amongst the other coloured balls. After many collisions, between all of the balls, we would expect the mean energy of each ball to be about the same. A formal proof of the classical equipartition theorem is given by Reif (1965). Classically, we expect the mean energy in the capacitor to satisfy

$$E[\mathcal{U}_c] = \frac{1}{2}CE[v_c^2] = \frac{1}{2}kT. \quad (6.72)$$

Given that the voltage across the capacitor is $v_c = x$, then Equation 6.72 leads directly to Equation 6.69. Feynman *et al.* (1963) uses this argument to show that $E[v_c^2] = kT/C$ for a capacitor and $E[i_l^2] = kT/L$ for an inductor. Equilibrium and quasi-equilibrium arguments, of this type, are presented in (Feynman *et al.* 1963, Reif 1965) and (Wannier 1966). The fact that Nyquist's procedure is consistent with the result from equipartition of energy might tempt us to calculate *all* noise levels using equipartition arguments. A problem with this special technique is that it only works if we measure the voltage *directly* across a capacitor or *directly* through an inductor. In addition, some noise sources are not thermal. A further issue is that the presence of a circuit to filter noise will introduce autocorrelation, which will affect the higher cumulants. We might be able to estimate mean expected values but it is not clear whether we could estimate variances without accounting for the autocorrelation. The use of equipartition serves as a sanity check for some circuits but it is not clear how to generalise the technique to more complex situations. This is an important motivation for developing a more general theory based on Stochastic Differential Equations (SDEs).

6.4.2 The Langevin SDE

We represent the resistor using a Norton model of an noiseless resistor, R , in parallel with a noise source, denoted by $i_0 dB$ where $i_0 = \sqrt{2kT/R}$. This is shown in Figure 6.10. The circuit is drawn and labelled in a manner that is consistent with analysis, using an Stochastic Differential Equations (SDEs). We consider the nodal equation for the circuit. We require $\sum dQ = 0$. For the capacitor, we have $dQ = Cdv_c$, where C is

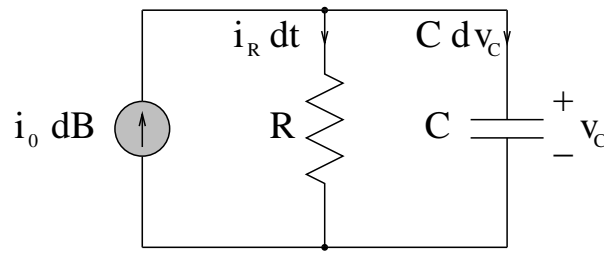


Figure 6.10. SDE models for an RC parallel circuit. This figure shows an RC parallel circuit, with resistor, R , noise current source, $i_0 dB$, and capacitor, C . The noise source in this circuit is embodied in the resistor, and contributes an increment of electric flux of $i_0 dB$. The increment of electric flux in the resistor is $i_R dt$. The increment of electric flux in the capacitor is $i_C dt = C dv_C$. The infinitesimal models for the resistor and the capacitor can be combined using Kirchhoff's current law to arrive at an SDE for the complete circuit.

the capacitance and dv_C is an infinitesimal increment of the capacitor voltage. For the resistor, we have $dQ = \frac{v_C}{R} dt$ and for the equivalent noise source in the resistor, we have $dQ = i_0 dB$, as discussed above. The nodal equation then becomes

$$C dv_C + \frac{1}{R} v_C dt = i_0 \cdot dB = \sqrt{2kT/R} \cdot dB, \quad (6.73)$$

which is the SDE for this system. It has the same form and plays exactly the same role as the Langevin equation in statistical physics (Reif 1965, Hecht 1990, Wannier 1966, Risken 1996).

It is possible to evaluate the infinitesimal moments implied by a Langevin equation and to formulate a Partial Differential Equation (PDE), describing the probability density of an ensemble of solutions to the SDE in Equation 6.73. This PDE is known as the Fokker-Planck equation (Reif 1965, Tuckwell 1988, Risken 1996). If we could solve the Fokker-Planck equation then we could apply operators to the solutions to calculate quantities of interest, such as the noise power as a function of time, $w(t)$. Unfortunately, this approach is cumbersome. Instead, we suggest the application of a method described by Gubner (1996), where the SDE is transformed into a much simpler ODE in the noise power.

Equation 6.73 can be re-written as an SDE in the narrow sense:

$$dv_C = \frac{-1}{RC} v_C dt + \frac{i_0}{C} dB. \quad (6.74)$$

6.5 A two-dimensional Langevin equation (SDE)

This is of the form

$$dv_C = \alpha(t)v_C dt + \beta(t)dB \quad (6.75)$$

where $\alpha(t) = \alpha = -1/(RC)$ and $\beta(t) = \beta = +i_0/C = \sqrt{2kT/(RC^2)}$. If we define the expected value of v_C as $\mu = E[v_C]$ and the variance as $w = E[(v_C - \mu)^2]$ then it can be shown (Gubner 1996) that

$$\frac{dw(t)}{dt} = 2\alpha(t)w(t) + \beta(t)^2. \quad (6.76)$$

We have now derived an Ordinary Differential Equation (ODE) in the variable of interest, noise power. If we consider the steady-state situation after all transients have decayed then we have $\frac{dw(t)}{dt} = 0$, which implies that

$$w = E[(V - \mu)^2] = -\frac{\beta(t)^2}{2\alpha(t)} = \frac{kT}{C}, \quad (6.77)$$

which is the classical result in Equation 6.50, which appears in the literature (Feynman *et al.* 1963, Lathi 1965, Carlson *et al.* 2002).

We did not solve the SDE directly. We only used it to derive an ODE. We did not solve the ODE but only used it to derive an algebraic equation, which we then used to solve for the steady state value of the noise power. We believe that this simple and systematic method is general and should find wide application in the analysis of noise in circuits.

In summary: We proceed from the circuit to nodal, or mesh, equations to an SDE to an ODE to an algebraic equation and then obtain estimates of noise power.

6.5 A two-dimensional Langevin equation (SDE)

6.5.1 Nyquist's approach, based on power spectral density

We consider the parallel RCL circuit shown in Figure 6.11. Standard analysis of this circuit, in the Laplace domain gives the transfer function:

$$\frac{v_C}{i_n} = \frac{1}{\frac{1}{R} + sC + \frac{1}{sL}} \quad (6.78)$$

where i_n is the current noise source with PSD, of $G_i = 4kT/R$. This is a one-sided PSD. Equation 6.78 can be written as

$$\frac{v_C}{v_n} = \frac{\frac{1}{RC}s}{s^2 + \frac{1}{RC}s + \frac{1}{LC}} \quad (6.79)$$

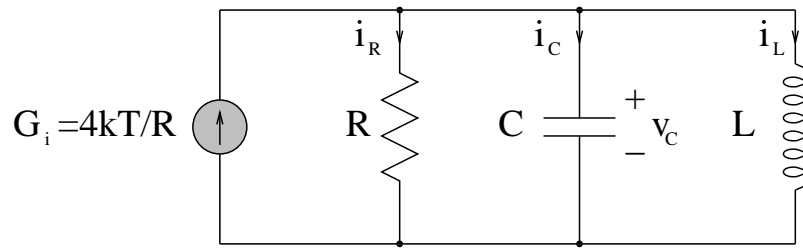


Figure 6.11. A parallel RCL circuit. Using the approach of Nyquist and Johnson, the parallel RCL circuit is a Linear Time Invariant (LTI) system being driven by a noise source, with Power Spectral Density (PSD) of $G_i = 4kT/R$. The output voltage, of interest, is the voltage across the capacitor, v_C .

where v_n is a voltage noise source with a PSD, of $G_v = 4kTR$. This is also an one sided PSD. The transfer function in Equation 6.79 can be written in the canonical form, of Equation 6.80, provided that we allow, $\omega_0^2 = 1/(LC)$ and $\zeta = \sqrt{L/C}/R$. This approach, to the scaling of the problem, means that we can solve the noise problem for all second order circuits, regardless of the actual values of the angular frequency, ω_0 , or the impedance, R . With this in mind, it is worth taking some time to consider the standard definitions and terms for second-order systems.

Some definitions and terms, for the second-order transfer function

We are given a standard second-order resonant band-pass transfer function:

$$H(s) = \frac{2\zeta\omega_0 s}{s^2 + 2\zeta\omega_0 s + \omega_0^2} \quad (6.80)$$

where $2\pi f_0 = \omega_0$ is the *angular resonant frequency* and ζ is the *damping ratio*. For sinusoidal signals, we have $\omega = 2\pi f$. The *damping coefficient* is often defined as $\sigma = \omega_0\zeta$. The *damped natural angular frequency of oscillation* is defined as $\omega_d = \omega_0\sqrt{1-\zeta^2}$. This definition means that $\omega_0^2 = \omega_d^2 + \sigma^2$. These relationships are shown in Figure 6.12.

The Transfer function can be normalised to give:

$$H(S) = \frac{2\zeta S}{S^2 + 2\zeta S + 1} \quad (6.81)$$

where $S = s/\omega_0 = j\omega/\omega_0 = jf/f_0$. The scaled poles are now located at $\Lambda_1 = -\zeta + j\Omega_d$ and $\Lambda_2 = -\zeta - j\Omega_d$, where $\zeta = \sigma/\omega_0$ and $\Omega_d = \omega_d/\omega_0$. The scaled poles, in the scaled *big S* plane are shown in Figure 6.13.

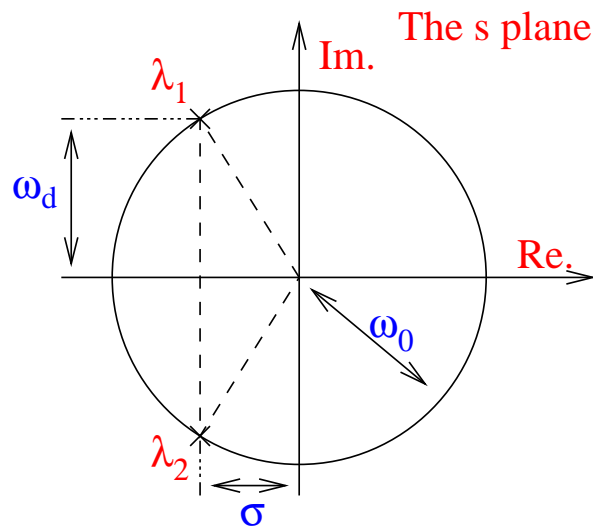


Figure 6.12. Positions of poles of a second-order under-damped circuit. The poles are located in the s plane at $\lambda_1 = -\sigma + j\omega_d$ and $\lambda_2 = -\sigma - j\omega_d$. These form a complex conjugate pair, so $\lambda_2 = \lambda_1^*$. The radius of the circle is given by ω_0 , where $\omega_0^2 = \omega_d^2 + \sigma^2$.

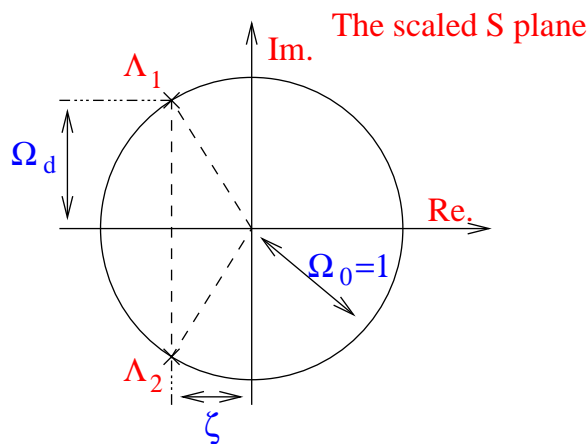


Figure 6.13. The normalised poles of a second-order under-damped circuit. the angles are preserved but the angular frequencies are all normalised to $\omega_0 = 1$ radian per second.

The second order transfer function $H(s)$ can be written in the form:

$$H(s) = \frac{2\zeta\omega_0s}{(s - \lambda_1)(s - \lambda_2)} \tag{6.82}$$

This relationship can be used to locate all of the poles, and zeros of the Power Spectral Density (PSD) function, $|H(s)|^2$. If Equation 6.82 is multiplied by its complex conjugate then it is possible to show that the normalised PSD has the general form:

$$|H(j\Omega)|^2 = \frac{4\zeta^2\Omega^2}{\Omega^4 + (4\zeta^2 - 2)\Omega^2 + 1} \tag{6.83}$$

where $\Omega = \omega/\omega_0$ and $\zeta = \sigma/\omega_0$. This can also be written as:

$$|H(j\Omega)|^2 = \frac{4(1 - \Omega_d^2)\Omega^2}{\Omega^4 + (2 - 4\Omega_d^2)\Omega^2 + 1}, \quad (6.84)$$

since $\zeta^2 + \Omega_d^2 = 1$.

The poles of the normalised PSD are located at the corners of a rectangle in the complex S plane:

- $\Lambda_1 = -\zeta + j\Omega_d$
- $\Lambda_2 = -\zeta - j\Omega_d = \Lambda_1^*$
- $\Lambda_3 = +\zeta + j\Omega_d = -\Lambda_1^*$
- $\Lambda_4 = +\zeta - j\Omega_d = -\Lambda_1$

where $\zeta = \sigma/\omega_0$, $\Omega_d = \omega_d/\omega_0$, and $S = s/\omega_0$.

If we wish to view the situation from the point of view of normalised angular frequency Ω then these poles get rotated through $\pi/2$ when we view the situation from the point of view of the Ω plane, where real normalised angular frequencies lie along the real line. This follows from the fact that $S = j\Omega$. The poles in the Ω plane are shown in Figure 6.14.

The PSD can be written as a product of linear factors in Ω :

$$|H(j\Omega)|^2 = \frac{4\zeta^2\Omega^2}{(\Omega - j\Lambda_1)(\Omega - j\Lambda_1^*)(\Omega + j\Lambda_1)(\Omega + j\Lambda_1^*)}. \quad (6.85)$$

The usual approach to this problem is to resolve the function into a sum of first order partial fractions. The amount of labour involved is reduced if we realise that the four poles can be arranged into two pairs of complex conjugate poles: $\{-j\Lambda_1^*, +j\Lambda_1\}$ and $\{-j\Lambda_1, +j\Lambda_1^*\}$. It is sensible to multiply these factors first:

$$\begin{aligned} (\Omega + j\Lambda_1^*) \cdot (\Omega - j\Lambda_1) &= \Omega^2 + 2\Omega_d\Omega + 1 \\ (\Omega + j\Lambda_1) \cdot (\Omega - j\Lambda_1^*) &= \Omega^2 - 2\Omega_d\Omega + 1. \end{aligned}$$

6.5 A two-dimensional Langevin equation (SDE)

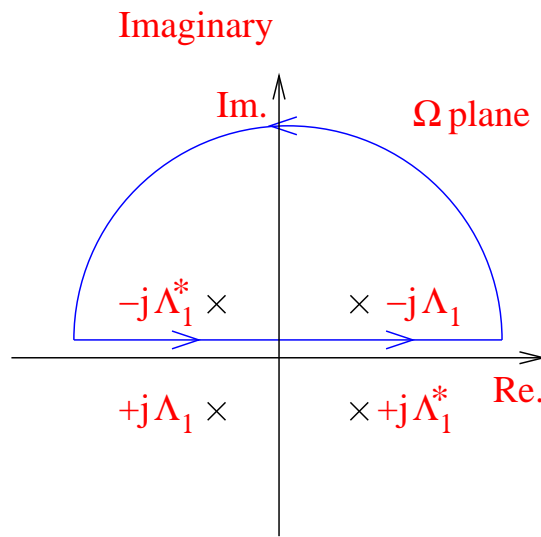


Figure 6.14. Poles of the power spectral density function. This figure shows the poles of the Power Spectral Density (PSD) function in the Ω plane. We can integrate with respect to Ω , using Cauchy's theorem by integrating along the real axis. We can imagine the return path being effectively at infinity. It can be shown that the integral around the return path converges to zero as the radius goes to infinity. This is because the power spectral density drops off faster than radius of the path.

After that, one can use the formula for the difference of two squares, $(A + B)(A - B) = A^2 - B^2$, to obtain:

$$\begin{aligned}
 & (\Omega + j\Lambda_1^*) \cdot (\Omega - j\Lambda_1) \cdot (\Omega + j\Lambda_1) \cdot (\Omega - j\Lambda_1^*) \\
 &= (\Omega^2 + 2\Omega_d\Omega + 1) \cdot (\Omega^2 - 2\Omega_d\Omega + 1) \\
 &= \Omega^4 + (4\zeta^2 - 2)\Omega^2 + 1,
 \end{aligned}$$

which proves that Equations 6.85 and 6.83 are equal. Equation 6.84 follows from the fact that $\zeta^2 + \Omega_d^2 = 1$. We could use Equations 6.85 or Equation 6.84, depending on the application and depending on which ever form was more convenient.

The normalised PSD, expressed in terms of Ω , can be written, as a sum of linear partial fractions,

$$\begin{aligned}
 |H(j\Omega)|^2 &= |H(s)|^2 \\
 &= \frac{+\zeta}{2\Omega_d} \cdot \frac{\Lambda_1}{\Omega - j\Lambda_1} + \\
 &\quad \frac{+\zeta}{2\Omega_d} \cdot \frac{\Lambda_1^*}{\Omega + j\Lambda_1^*} + \\
 &\quad \frac{-\zeta}{2\Omega_d} \cdot \frac{\Lambda_1}{\Omega + j\Lambda_1} + \\
 &\quad \frac{-\zeta}{2\Omega_d} \cdot \frac{\Lambda_1^*}{\Omega - j\Lambda_1^*}, \tag{6.86}
 \end{aligned}$$

where $\Lambda_1 = -\zeta + j\Omega_d$.

Noise equivalent bandwidth for a second-order system

It is then possible to use Cauchy's Integral Formula to derive an expression for the Noise Equivalent Bandwidth, B_N , of a standard second-order resonant band-pass circuit:

$$B_N = \frac{f_0}{2} \cdot \int_{-\infty}^{+\infty} |H(j\Omega)|^2 d\Omega, \tag{6.87}$$

where $2\pi f_0 = \omega_0$.

If a function can be written as:

$$F(\Omega) = \sum_{k=1}^N c_k \cdot \frac{1}{\Omega - z_k}, \tag{6.88}$$

then the poles are z_k , for $1 \leq k \leq N$ and the residues are $2\pi j c_k$, for $1 \leq k \leq N$. The Cauchy Integral Formula implies that the integral of $F(z)$ is given by the sum of the residues:

$$\oint F(\Omega) d\Omega = j2\pi \sum_{k=1}^N c_k \cdot b_k, \tag{6.89}$$

where the b_k coefficients are either 0 or 1. The coefficient, $b_k = 1$, if the pole, z_k , lies inside the contour and the coefficient, $b_k = 0$, if the pole, z_k , lies outside of the contour.

The poles and residues are all described in Equation 6.86, so to apply Cauchy's formula, all that we need to do is to identify which poles lie inside the contour and then sum those residues, and multiply by $j2\pi$. The poles and the contour are shown in

6.5 A two-dimensional Langevin equation (SDE)

Figure 6.14. The required integral can be written as

$$\int_{-\infty}^{+\infty} |H(j\Omega)|^2 d\Omega = j2\pi \sum_{k=1}^N c_k \cdot b_k. \quad (6.90)$$

The only difficult part is deciding which poles lie inside the contour. The poles and the contour are shown in Figure 6.14. Equation 6.87 can then be applied to obtain the Noise Equivalent Bandwidth, B_N .

We can sum and scale the appropriate residues in Equation 6.86 to evaluate the integral of $|H(j\Omega)|^2$, along the real axis of the Ω plane. The residues at $\Omega = -j\Lambda_1^*$ and $\Omega = -j\Lambda_1$ are relevant because they lie inside the contour of integration. When we apply Cauchy's Integral Formula, we obtain:

$$\int_{-\infty}^{+\infty} |H(j\Omega)|^2 d\Omega = j2\pi \left(\frac{\zeta}{2\Omega_d} (\Lambda_1^* - \Lambda_1) \right) = 2\pi\zeta, \quad (6.91)$$

which gives the final result of

$$B_n = \pi \cdot f_0 \cdot \zeta = \frac{\pi}{2} \cdot \frac{f_0}{Q}. \quad (6.92)$$

This is closely related to the *half-power* bandwidth, which is given by

$$B_{1/2} = 2 \cdot f_0 \cdot \zeta = \frac{f_0}{Q}. \quad (6.93)$$

The derivation of this last result can be found in Hayt *et al.* (2002). The noise-bandwidth and half-power-bandwidth are not equal but are closely related, for the second-order band-pass circuit.

For the parallel LRC circuit we have $\zeta\omega_0 = 1/(2RC)$, and hence

$$B_n = \frac{1}{4RC}, \quad (6.94)$$

which is the same result as for the RC circuit. This gives an expression for the mean-square voltage across the resistor as,

$$E[|v_n|^2] = \frac{kT}{C}, \quad (6.95)$$

which is also the same as for the RC circuit. The value, or presence, or even complete absence of the inductor, makes no difference to the mean square voltage across the capacitor. This is also consistent with an argument, based on equipartition of energy, where $\frac{1}{2}CE[|v_n|^2] = \frac{1}{2}kT$, because the mean energy per degree of freedom is $\frac{1}{2}kT$. If we view the capacitor as a single lumped element then it has one degree of freedom.

6.5.2 An approach, using the the Langevin stochastic differential equation

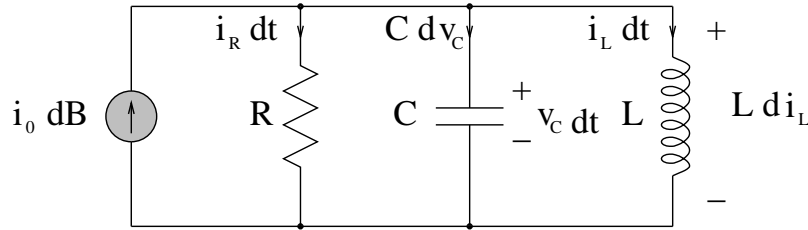


Figure 6.15. An RCL parallel circuit. This parallel circuit has two energy storage elements, so the state-space model has two dimensions. The choice of state variables is not unique but a sensible choice is to use the energy variables, the capacitor voltage, v_c , and the inductor current, i_L . If we apply Kirchhoff's Current Law (KCL) then we obtain $dv_C = (-1/(RC))v_C dt - (1/C)i_L dt + (i_0/C)dB$. If we apply Kirchhoff's Voltage Law (KVL) then we obtain $di_L = (1/L)v_C dt$. These are the two equations of state for this circuit.

This parallel RCL circuit In Figure 6.15 is identical with the circuit in Figure 6.11, but the symbols that are used to describe the circuit have been changed, in order to be consistent with an SDE representation. The symbols represent infinitesimal increments of flux that occur in an infinitesimal time interval, dt . Increments of electric flux (charge) are represented using conventional current symbols, along a conductors. Increments of magnetic flux are represented using conventional voltage symbol, across components. The circuit is already in a form where the infinitesimal forms of Kirchhoff's laws can be applied. There are two energy storage elements, so the state-space model has two dimensions. We choose state variables of the capacitor voltage, v_c , and the inductor current, i_L . If we apply Kirchhoff's Current Law (KCL), to the common node at the top of the figure, then we obtain

$$dv_C = -\frac{1}{RC} \cdot v_C \cdot dt - \frac{1}{C} \cdot i_L \cdot dt + \frac{i_0}{C} \cdot dB. \quad (6.96)$$

If we apply Kirchhoff's Voltage Law (KVL), to the mesh that includes L and C only, then we obtain

$$di_L = +\frac{1}{L} \cdot v_C \cdot dt. \quad (6.97)$$

Equations 6.96 and 6.97 are the two equations of state for the circuit in Figure 6.15. These can be written in matrix form as

$$\begin{bmatrix} dv_C \\ di_L \end{bmatrix} = \begin{bmatrix} -\frac{1}{RC} & -\frac{1}{C} \\ +\frac{1}{L} & 0 \end{bmatrix} \cdot \begin{bmatrix} v_C \\ i_L \end{bmatrix} \cdot dt + \begin{bmatrix} \frac{i_0}{C} \\ 0 \end{bmatrix} \cdot B_t. \quad (6.98)$$

6.6 Noise models for the JFET

This has the general form of

$$d\underline{X}_t = \mathbf{A} \cdot \underline{X}_t \cdot dt + \mathbf{K} \cdot d\underline{B}_t, \quad (6.99)$$

where \underline{X} is the state vector (in phase space), \mathbf{A} is the state-transition matrix, \mathbf{K} is a mixing matrix (that can introduce linear mixtures of noise into the state variables) and $d\underline{B}_t$ is a vector of independent infinitesimal increments of Brownian motion. Specifically, these variables can be defined, for the circuit in Figure 6.15, as follows,

$$\underline{X} = \begin{bmatrix} v_C \\ i_L \end{bmatrix}, \quad (6.100)$$

$$\mathbf{A} = \begin{bmatrix} -\frac{1}{RC} & -\frac{1}{C} \\ +\frac{1}{L} & 0 \end{bmatrix} \quad (6.101)$$

$$\mathbf{K} = \begin{bmatrix} \frac{i_0}{C} \\ 0 \end{bmatrix} \quad (6.102)$$

$$d\underline{B}_t = [dB_t], \quad (6.103)$$

which is a rather degenerate one-dimensional vector that is equivalent to the scalar, dB_t . This problem is of a standard form, that has been solved by Øksendal (1998), as follows

$$\underline{X}_t = \exp(\mathbf{A}t) \cdot \left(X_0 + \exp(-\mathbf{A}t) \cdot \mathbf{K} \cdot d\underline{B}_t + \int_0^t \exp(-\mathbf{A}s) \cdot \mathbf{A} \cdot \mathbf{K} \cdot \underline{B}_s \cdot ds \right). \quad (6.104)$$

It is clear that circuits, leading to equations of the form of Equation 6.99 can be solved using solution of the form of Equation 6.104. This technique can be extended to all linear circuits with finite numbers of energy storage elements, and noise generating elements.

6.6 Noise models for the JFET

The noise model that we use here, shown in Figure 6.16 is the one used by Abbott *et al.* (1997) and is essentially a van der Ziel model (Streetman 1995, Razavi 2001) with all noise sources referred to the input. For a JFET, the gate currents are limited by reverse biased PN junctions. We regard the gate leakage current as negligible and have not included it in the model.

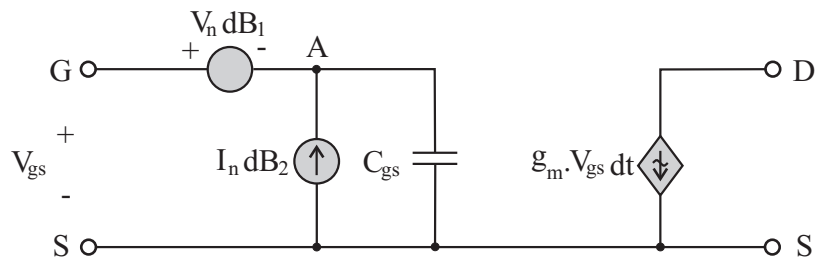


Figure 6.16. Noise model for a JFET. This is a van der Ziel model with all noise sources referred to the input. The gate to source capacitance is represented by C_{gs} . This model includes the standard noise-free small signal model for a JFET. The amplifying effect of the JFET is represented by the dependent current source, $g_m \cdot V_{gs}$. The noise is represented by two sources at the input, $V_n \cdot dB_1$ and $I_n \cdot dB_2$ where dB_1 and dB_2 are infinitesimal increments of Brownian motion.

6.7 A simple JFET circuit

allows reference to this section We use a very simple version of the Colpitts oscillator with a FET as the amplifying element. This is shown in Figure 6.17. In the Colpitts topology, the chain of capacitors, C_1 and C_2 , allows for a feedback path with high impedance and voltage amplification.

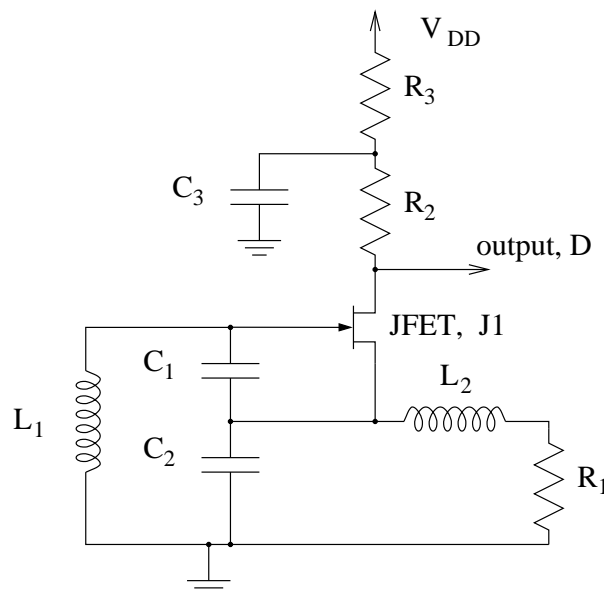


Figure 6.17. Large-signal, schematic circuit diagram for a Colpitts oscillator. This circuit uses a JFET as the amplifying element. There are noise sources in R_1 , R_2 and J_1 .

6.8 Analysis of the JFET circuit

If we analyse the circuit in Figure 6.17, using small-signal technique, and insert the noise model from Figure 6.16, then we obtain the complete small signal noise model for the Colpitts oscillator, shown in Figure 6.18. If the circuit did not have noise sources

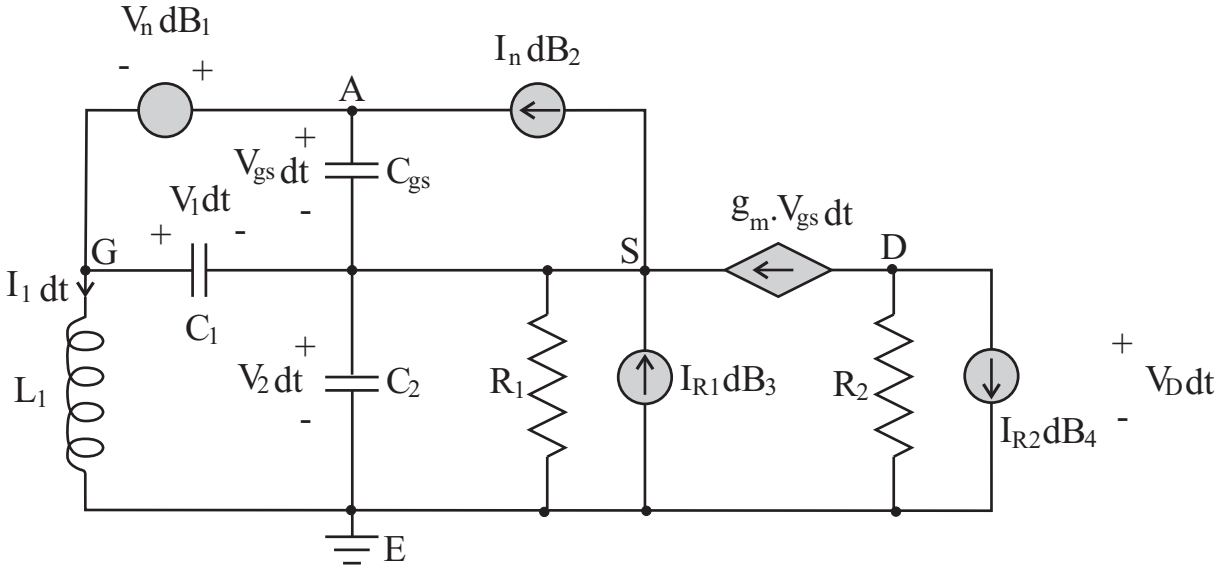


Figure 6.18. Small signal equivalent circuit of a Colpitts oscillator. This circuit model, includes the van der Ziel noise model. The FET is mapped into the equivalent circuit with Source, S, Gate, G, Drain D. The earth is represented by E. The circuit has four energy storage elements, C_{gs} , C_1 , C_2 and L_1 . There are four corresponding state variables, V_{gs} , V_1 , V_2 and I_1 . Further analysis shows that only three of these are independent. There are four noise sources, $V_n \cdot dB_1$, $I_n \cdot dB_2$, $I_{R1} \cdot dB_3$ and $I_{R2} \cdot dB_4$. The nominal output is the drain voltage, V_D .

then ordinary mesh and nodal analysis could be performed and we obtain a standard state-variable model (DeRusso *et al.* 1965). With the presence of noise sources, we can still write down mesh equations. Kirchhoff's voltage law takes the form: $\sum d\Phi = \sum V dt = 0$ where the contribution from a noise voltage source would be $d\Phi = V_n dB$. We obtain a mesh equation for the mesh including the Gate G and the node A,

$$V_1 dt - V_{gs} dt + V_n dB_1 = 0, \quad (6.105)$$

which indicates that the state-variables, V_1 and V_{gs} are not independent. We can obtain a mesh equation including L_1 , C_1 and C_2 ,

$$dI_1 = \frac{1}{L_1} \cdot V_1 dt + \frac{1}{L_1} \cdot V_2 dt. \quad (6.106)$$

The current through the noise source, $V_n dB_1$ is undetermined but we can regard G and A as an enlarged node and write

$$I_1 dt + C_1 dV_1 + C_{gs} dV_{gs} - I_n dB_2 = 0. \quad (6.107)$$

Finally, the source is simply a very large node

$$C_1 dV_1 - C_2 dV_2 + C_{gs} dV_{gs} = \frac{V_2}{R_1} dt - g_m V_{gs} dt + I_n dB_2 - I_{R1} dB_3. \quad (6.108)$$

Equations 6.105, 6.106, 6.107 and 6.108 are the equations of state for this system.

The nominal output of the circuit is the drain voltage, V_D . This can be expressed with an output equation,

$$V_D dt = -R_2 g_m V_{gs} dt - I_{R2} R_2 dB_4. \quad (6.109)$$

This completes the formulation of the circuit. We could solve the resulting SDEs exactly if we could write these equations in matrix form:

$$d\underline{X}_t = \mathbf{A} \cdot \underline{X}_t dt + \mathbf{K} d\underline{B}_t \quad (6.110)$$

where \mathbf{A} is a square state-transition matrix and $\exp(+\mathbf{A}t)$ is defined, \underline{X}_t is a state vector containing the state-variables, $\{V_{gs}, V_1, V_2, I_1\}$ and \mathbf{K} is a matrix that combines the independent noise sources, $\{dB_1, dB_2, dB_3, dB_4\}$. In this case the matrix, \mathbf{K} is square but this does not have to be the case. There will be an explicit solution of the form:

$$\underline{X}_t = \exp(+\mathbf{A}t) \cdot \left[\underline{X}_0 + \exp(-\mathbf{A}t) \cdot \mathbf{K} \cdot \underline{B}_t + \int_0^t \exp(-\mathbf{A}s) \cdot \mathbf{A} \cdot \mathbf{K} \underline{B}_s ds \right]. \quad (6.111)$$

The derivation of this solution relies on the multi-dimensional form of Itô's lemma and may be found in Øksendal (1998). Of course, these equations can also be solved using numerical methods described in the literature, see for example (Kloeden and Platen 1999, Pensi 2000).

6.9 Summary and open questions

So far, we have constructed models for L , R and C . We have devised practical and consistent forms for Kirchhoff's laws. We have shown that the noise equations for electrical circuits are completely equivalent to the Langevin equations of statistical mechanics. We have shown that explicit solution of the SDEs is not always necessary, since we

6.9 Summary and open questions

can often formulate much simpler ODEs in the variables of interest. Finally, we have made some progress on the formulation of a practical and consistent noise models for a JFET.

A cursory examination of the JFET in Figure 6.18 circuit would suggest that the state variables should be: $\{V_1, V_2, V_{gs}, I_1\}$. There ought to be 4 state variables. There seem to be 4 independent equations 6.105, 6.106, 6.107 and 6.108, so we might expect that these equations could be written directly in the form of Equation 6.110. This turns out not to be the case, because Equation 6.105 is degenerate. It does not contain any explicit reference to dV_1 or dV_{gs} and we might expect that the noise components of these variables are not independent. We do not appear to have enough independent equations for the number of (apparently) independent variables.

Our unsolved problem of noise is that we cannot yet implement the noise model for the JFET until we can put Equations 6.105, 6.106, 6.107 and 6.108 into the form of Equation 6.110.

It seems that the solution must ultimately depend on a reduction of the number of state variables required to describe the circuit. We must somehow reduce V_1 and V_{gs} to a single variable. We would then have three truly independent variables in three truly independent equations, in the whole circuit, and the equations could be solved.

At first sight, this problem looks like it might be a simple oversight. If the noise source, $v_n \cdot dB_1$ were a deterministic voltage source, say $V_3 \cdot dt$ then there would be no problem. Equation 6.105 would reduce to an ordinary mesh equation of the usual type, $V_1 - V_{gs} + V_3 = 0$, and the elimination of one of the state-variables, V_1 or V_{gs} would be trivial. Unfortunately, the circuit *does* contain a noise source, $v_n \cdot dB_1$, and the mesh equation does not reduce in the usual way. We cannot simply “cancel by dt ,” as it were.

We suspect that the required reduction will depend on the unique decomposition of semi-martingales as expounded by Doob (Protter 1990). The state-variables V_1 and V_{gs} cannot be independent because they do not have independent decompositions.

This chapter completes the exposition of the work of this thesis. We now summarise this work in the following concluding chapter.

Chapter 7

Conclusions and future challenges

WE review the original contributions made in this thesis and consider future possible developments that have potential for further development.

7.1 Original contribution

This thesis makes a number of important contributions to the application of models of the type used in Parrondo's games.

- We establish the physical basis for Parrondo's games, which places the work of earlier authors on a more rigorous basis.
- We establish conditions for realistic simulations of Brownian ratchets, using Parrondo's games.
- We also show how to evaluate all of the moments of Parrondo's games using a discrete transform method. This can be done without explicitly solving the difference equations, represented by Parrondo's games.
- We establish a unified small-matrix technique for evaluating expected return from all sets of games in the same class at Parrondo's games.
- We establish, by construction, that Parrondo's games still manifest their apparently paradoxical behaviour, even if null transitions are included.
- We also examine the conditions for the minimum number of states and develop a set of games with only two states, which demonstrates the same paradoxical behaviour as Parrondo's games.
- We reveal that fractals are generated in the phase-space for Parrondo's games.
- We devise methods for evaluating all the moments of fractals, including second and higher moments.
- The concepts embodied in Parrondo's games are applied to electrical circuits.
- We extended the methods of Middlebrook and Čuk (1976) and use stochastic differential equations (SDEs) to model switching noise in switched-mode circuits, in the case where there is a random aspect in the switching rule.
- We show fractals exist in the phase spaces of switched mode circuits, where there is a random, or stochastic, aspect in the switching rule.
- We develop methods to model electrical circuits using stochastic differential equations (SDEs).

7.2 Future prospects

Towards the end of his life Isaac Newton is reported to have said, “*I do not know what I may appear to the world, but to myself I seem to have been only like a boy playing on the sea-shore, and diverting myself in now and then finding a smoother pebble or a prettier shell than ordinary, whilst the great ocean of truth lay all undiscovered before me.*” What we know is always such a small fraction of what *can* be known.

Each new discovery that we make, whether it is large or small, leads us on to ask new questions. The scientist is always in a situation like triage in a hospital. Unfortunately, some problems are lost causes and must be abandoned. Some problems do not need our attention. Somebody else can solve them. Some questions can be answered, using the available resources, and are worth solving. So it is with this thesis. There are many questions that *could* be asked. The questions that are presented here are the ones that seem to be new to the world, capable of solution and would produce useful results if they were answered. We present some unsolved problems of noise, in this spirit.

7.2.1 The physical basis of Parrondo’s games

Choice of basis functions

If we are to solve partial differential equations, using a sum of basis functions then, the basis-functions and operators must be chosen together, as parts of a working ensemble. Ideally, we want the set of functions to be closed under the operators. If this does not apply then, each time we apply the differential operators, $\partial/\partial x$, $\partial^2/\partial x^2$ then we will increase the number of function that need to be tracked in the algorithm. This increase occurs at each time step. There may be many steps in a simulation. The algorithm will soon run up against storage or computational limits.

Polynomials may not always be ideal basis functions but they are closed under differentiation. This is an important property. Sinusoidal functions also have closure under differentiation. Sinusoidal expansions are used in Fourier’s solution to the diffusion equation, for heat (Farlow 1982). They naturally occur in an approach, based in separation of variables. There are some difficulties with polynomial and sinusoidal basis

7.2 Future prospects

functions though. They do not have good locality and they do not automatically guarantee continuity in parabolic partial differential equations, where total probability is conserved. Conservation only arises out of an infinite sum and it is not clear what will happen if the sum is truncated. This is the same issue that arises in the truncation of the Kramers-Moyal expansion, where truncation can lead to negative probability densities.

With these ideas in mind, it is plausible that Gaussian functions of the form

$$p(x) = \frac{1}{\sigma\sqrt{2\pi}} \cdot \exp\left(\frac{-(x-\mu)^2}{2\sigma^2}\right) \quad (7.1)$$

might be good basis functions. The function $p(x)$ automatically has locality near $x = \mu(t)$, with a defined variation each side of the order of $\pm\sigma(t)$. These basis function also have a well defined total probability,

$$\int_{-\infty}^{+\infty} p(x)dx = 1, \quad (7.2)$$

regardless of the values of $\mu(t)$ or $\sigma(t)$. This is important for parabolic differential equations, where total probability is conserved. A good example is Equation 3.69, which is first devised by Fourier (Maxwell 1888) and is used by Einstein (1905). The solution has the form of a Gaussian function that scales with time.

Unfortunately, Gaussian functions are not orthogonal but they are *almost* orthogonal if they are located in different positions. If we define

$$\mathcal{N}(x, \mu, \sigma^2) = \frac{1}{\sigma\sqrt{2\pi}} \cdot \exp\left(\frac{-(x-\mu)^2}{2\sigma^2}\right) \quad (7.3)$$

then it can be shown that

$$\mathcal{N}(x, \mu_1, \sigma_1^2) \cdot \mathcal{N}(x, \mu_2, \sigma_2^2) = \mathcal{N}(\mu_1, \mu_2, \sigma_4^2) \cdot \mathcal{N}(x, \mu_3, \sigma_3^2) \quad (7.4)$$

where

$$\mu_3 = \frac{\sigma_1^2}{\sigma_1^2 + \sigma_2^2} \cdot \mu_2 + \frac{\sigma_2^2}{\sigma_1^2 + \sigma_2^2} \cdot \mu_1, \quad (7.5)$$

and

$$\frac{1}{\sigma_3^2} = \frac{1}{\sigma_1^2} + \frac{1}{\sigma_2^2} \quad (7.6)$$

and

$$\sigma_4^2 = \sigma_1^2 + \sigma_2^2. \quad (7.7)$$

This can be proved by completing the squares in the exponents, and rearranging terms, algebraically. Equation 7.4 allows us to establish a quasi-orthogonal condition for Gaussian functions:

$$\mathcal{I} = \int_{-\infty}^{+\infty} \mathcal{N}(x, \mu_1, \sigma_1^2) \cdot \mathcal{N}(x, \mu_2, \sigma_2^2) dx = \mathcal{N}(\mu_1, \mu_2, \sigma_1^2 + \sigma_2^2). \quad (7.8)$$

This reduces to $\mathcal{I} \approx 1$, when $(\mu_2 - \mu_1)^2 \ll \sigma_1^2 + \sigma_2^2$, and $\mathcal{I} \approx 0$ when $(\mu_2 - \mu_1)^2 \gg \sigma_1^2 + \sigma_2^2$. Gaussian functions are quasi-orthogonal. If we apply linear algebra to the problem of representation then the resulting matrices are not purely diagonal, but they are diagonally dominant, and are well conditioned. It is certainly true, numerically, that Gaussian functions are very good for representation of other functions. This can be seen in Figure 7.1 where a sinc function is approximated, using finite weighted sum of Gaussian functions. The Gaussian function is a very versatile basis function. It is possible to approximate many different functional forms, over finite intervals, using Gaussian functions.

An important, but unfortunate, issue with Gaussian functions, as basis functions, is that they are not closed under differentiation. This limits their utility, for solving differential equations. Consider $p(x)$ in Equation 7.1. Rodrigues' formula allows us to express the derivatives of $p(x)$ in terms of Hermite polynomials (Abramowitz and Stegun 1970),

$$\frac{\partial^k}{\partial x^k} p(x) = (-1)^k \cdot H_k \left(\frac{\sqrt{2}}{2} x \right) \cdot p(x), \quad (7.9)$$

where $H_k(x)$ are Hermite polynomials, satisfying the recurrence relationship

$$H_{k+1}(x) = 2xH_k(x) - 2kH_{k-1}(x). \quad (7.10)$$

The first two Hermite polynomials are $H_0(x) = +1$, $H_1(x) = 2x$. Higher order polynomials and derivatives can be evaluated using Equations 7.10 and 7.9.

This suggests that Gaussian functions, multiplied by polynomials might be good basis functions. The set of polynomial functions, windowed by Gaussian functions, is closed under differentiation. A good example, of this type of function, is the class of Hermite functions, of the form

$$h_k(x, \sigma) = \frac{H_k \left(\frac{x-\mu}{\sigma} \right) e^{-\frac{(x-\mu)^2}{2\sigma^2}}}{\sqrt{2^k k! \sigma \sqrt{\pi}}}, \quad (7.11)$$

7.2 Future prospects

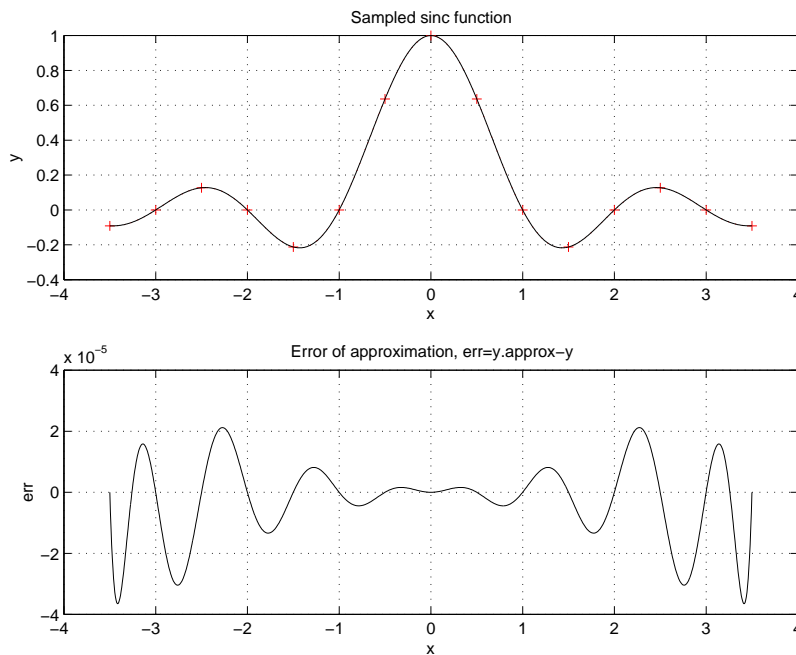


Figure 7.1. The Gaussian function, as a *basis* function. The top half of this figure shows an approximation to the sinc function, $y = \sin(\pi x)/(\pi x)$, using a weighted sum of Gaussian functions, $y_g(x) = \sum_{k=1}^M b_k \cdot \mathcal{N}(x, x_k, \sigma^2)$. The Gaussian approximation collocates at the sampling points, $y_g(x_k) = y_k = y(x_k)$. The collocating points are shown with the symbol, +. The two functions, $y(x)$ and $y_g(x)$ are shown as continuous curves. The two curves are so close that they cannot be distinguished on this scale. The RMS distance between the two curves is approximately 1.3×10^{-5} . This is achieved with 15 equally spaced collocating points. The width of the basis functions is controlled by the parameter, σ . This is chosen to be somewhat larger than the sampling distance, λ . The choice for this figure is $\sigma = 1.68 \cdot \lambda$. This is chosen in order to limit the edge effects that are quite common with collocating functions. The bottom half of the figure shows the error of this approximation, $y_g(x) - y(x)$. It is possible to construct almost anything out of Gaussian functions, if one uses enough of them. Gaussian functions can be useful for windowing other functions, as a part of signal processing. They are used in Gabor wavelets. The Gaussian is an excellent windowing function because it has locality in the time and frequency domains. It has minimum time-bandwidth product and it makes a good testing function because its properties have been extensively studied. Most of the indefinite integrals that one needs to evaluate can be evaluated explicitly, in closed form (without the use of power series).

where $k \geq 0$ is the degree of the Hermite polynomial H_k and σ is a scale parameter, and μ is a position parameter. These functions have a very interesting property that h_k is isomorphic with its own Fourier transform. Hermite functions, of the

form of Equation 7.11, are well behaved in the time and frequency domains. They also appear as the eigenfunctions for Schrödinger's equation for the harmonic oscillator, which has quadratic potential as a function of position. Schrödinger's equation and the Fokker-Planck equation are related through a transformation of relativistic Minkowski space, called a Wick rotation, where the time coordinate is multiplied by $j = \sqrt{-1}$ (Risken 1996). Hermite functions are used for the unification of time-domain and frequency-domain measurements in electronic engineering Rao and Sarkar (1999). Risken (1996) discusses the expansion of distribution functions into Hermite functions, for the solutions of the Kramers equation. The conjecture is that Hermite functions might be very well-behaved and suitable basis functions for solving the partial differential equations, which arise in the study of Brownian ratchets.

The technical issue to be overcome is the choice of position, μ , and scale, σ , for each basis function. There is also the problem of how to accommodate mutual approximation of both the probability density, $p(x)$, and the potential function $v(x)$, within the scheme imposed by the Fokker Planck equation. It is not clear that equally spaced samples are best, but on the other hand, if equal spacing is *not* used then the number of testing functions that are created, during each time step, will grow very quickly, maybe even exponentially. The algorithm may collapse under the weight of demand, for storage or computation. This is the closure issue again. We need the set of basis functions to be closed under the set of operations that we have to perform.

Brownian ratchets with distributed charge

In biological ion channels, and pumps, performance depends strongly on how we model the effect of ion to ion interactions. At high local ion concentrations the effect of the crowding of charge is significant. It is necessary to include this effect in the models. If we are interested in average ion currents then we can replace the complicated many-body problem with a time-average mean-field for the distribution of charge. We can use Poisson's equation.

To date, most analyses of Brownian ratchets neglect the effect of distributed charge. This means that the analysis is only strictly valid for dilute solutions. One exception is Allison and Abbott (2003a), who use Poisson's equation to formulate methods for

7.2 Future prospects

generating difference equations that can be used to model Brownian ratchets with distributed charge. They show that distributed charge reduces the transport effect that is generated by a Brownian ratchet.

Unfortunately, there are technical issues with the resulting equations because there are important transitions at a wide range of different scales. Such equations are regarded as being *stiff*. The standard method for sampling, for finite differences, is not very stable when the partial differential equations are stiff.

Fortunately, there is a good possibility that a different choice of basis functions would help. Hermite functions (Hermite polynomials, weighted by Gaussian functions) appear to be an appropriate basis functions for sampling the resulting equations. The conjecture is that the use of Hermite functions, to examine Brownian ratchets with distributed charge, would lead to a different set of difference equations, which would generalise Parrondo's games in a different way.

Bayesian approach to the analysis of the games

Most of the discussion of probability in this thesis is consistent with the orthodox view, formulated in axiomatic form by Kolmogorov (1950). If we examine the structure of the games then we realise that they are being played sequentially and the outcome from each step is determined by the conditional probabilities that apply at each step. This sequential aspect of the games suggests that an approach based on Bayesian probability might be more natural. It would avoid a lot of arcane discussion about ergodic theory (Jaynes 1957). Some of the apparently paradoxical behaviour might be easier to understand if it were explained in a more natural step-by-step fashion. Jaynes (2003) includes a discussion of the derivation of the Fokker-Planck equation. This could be a useful starting point for the Bayesian analysis of Parrondo's games.

Parrondo's games as a von Neumann game

Juan Parrondo originally left the rule for choosing game A or game B unspecified. Some researchers have studied deterministic, periodic sequences and some have studied randomised sequences. There would be interesting possibilities, from the game

theoretic point of view, if the games were played between agents with objectives. For example in a casino situation, the gambler might have the options of betting long (on a win) or short (on a loss). This would be like a futures market where short selling is possible. The casino could choose to play game A or game B. If the gambler and the casino both had to choose their strategies for the next time-tick *before* playing the games and they made their choices in *secret* without telling the other party, then Parrondo's games would become a true matrix-game, in the sense used by von Neumann and by Nash. It should be possible to use the theorems of Nash to show that equilibrium strategies exist. There should be strategies from which neither player would be willing to diverge. This part of the theory should be fairly routine. These strategies may not be unique, though.

The interesting generalisation of this question would be , what if we played a game against nature? Our *payoff* is determined by our ability, or otherwise to transform energy from one form to another in a Brownian motor. We do this by choosing from a number of available strategies, after the fashion of Maxwell's demon, who opens or does not open the door. Nature seeks to hide her secrets. Nature's *payoff* is that she seeks to maximise the entropy that we produce, as a result of our activities. This imposes an energy cost on us, which has to be factored into our plans. Can games of this type be made physically realistic?

We can consider some electrical examples. In a purely dissipative electrical system, such as networks of resistors, the resulting distribution of currents and voltages always arranges itself in such a way as to minimise the dissipation of power,

$$\mathcal{P} = v_1^2/R_1 + v_2^2/R_2. \quad (7.12)$$

This result has been known since the time of Kirchhoff. In a purely conservative electrical system, such as the LC resonant circuit, the currents and voltages arrange themselves in a way that minimises the action, given by integrating the Lagrangian

$$\mathcal{L} = \mathcal{U}_C - \mathcal{U}_L = \frac{1}{2}Cv^2 - \frac{1}{2}Li^2. \quad (7.13)$$

So in a circuit which is dissipative and also has energy storage, which objective is optimised? Can the currents and voltages serve two masters? The conjecture is that game theory might give the right approach to a problem where we seek to optimise two different objective functions. We can imagine a game being played between agents,

7.2 Future prospects

possibly many agents, each with different objectives. The most probable outcome is a Nash equilibrium where none of the agents are not prepared to change their strategies because that would leave them vulnerable to exploitation.

7.2.2 Rates of return from discrete games of chance

Higher moments of Parrondo's games

In Chapter 3, formulae are developed for evaluating the higher moments to Parrondo's games. The open question is whether these equations can be reduced to more simple expressions, in the way that is carried out for the first moment. The second moment is of particular interest because it measures the amount of spread generated by the action of Parrondo's games. At first sight this would seem to be just a matter of algebra. It might be necessary to carry out a *lot* of algebra but this would seem to be well within the capability of a computer algebra package, such as Mathematica, Maple or Axiom. Evaluation of higher moments would make it possible to predict the Peclet numbers arising from different ratchet designs. Our desire would be to optimise the design to get a strong transport effect without generating too much spreading of the particles.

Moments of fractal objects

In this thesis, we show that it is possible to calculate the moments of fractal objects, generated by an Iterated Function System (IFS), using a Moment Generating Function (MGF). The MGF can be determined by considering the symmetries resulting from the IFS. The moments can be determined by differentiating the MGF. This could have some interesting application for determining the moments of fractal objects, wherever they may be found.

Given a fractal object, the collage theorem of Barnsley allows us to construct an IFS which will generate an approximation to the original fractal object (Barnsley 1988). This is the basis of Fractal image compression. This suggests a procedure for calculating moments. Given a fractal object, we can generate an IFS which can be used to determine an MGF, which can be differentiated to calculate moments. The conjecture is that this will be less labour than evaluating the moments directly from the original

data. The reason for being optimistic about this, is that the IFS requires much less storage than the original data.

Behrends' conjecture regarding fractal dimension

There is the important question of how to optimise the return from Parrondo's games, if the only choice at our disposal is to choose a sequence of games, $[A, B, B, A, B, \dots]$. This can be shown to be equivalent to choosing a binary number in the unit interval $[1, 0, 0, 1, 0, 1, 0, \dots] \equiv .1001010\dots$. Behrends (2006) investigates the question of the optimal sequence of games. He argues that the cost of the search depends on the fractal dimension of the attracting set. He writes, as follows "We denote by $R_{x_0}^{\max}(m)$ the maximum possible reward. The aim of this note is to investigate the behaviour of the sequence $(R_{x_0}^{\max}(m))$ for large m . It will be shown that the growth is nearly linear: there is a constant γ (which does not depend on x_0) such that $(R_{x_0}^{\max}(m)) / m$ tends to γ . However, an explicit calculation of γ might be hard. The complexity depends on the fractal dimension of the smallest nonempty compact subset of M which is invariant with respect to all Γ_ρ ."

The issue here is that the fractal dimension of the attracting set possibly does play a role in the relative ease, or difficulty, of finding good sequences of games, with high reward. This is interesting because the fractal is constructed within a rather abstract phase-space that has no material existence. The results in this thesis show that the averages over phase-space will always be the same as the time average. One might conclude that all we have to do is to analyse the time-average game and we will know everything that *can* be known about the games. If Behrend's conjecture is true then the distribution of probability vectors in phase-space does play a role in determining how much computational effort is required, in order to acquire information about an optimal sequence, for a given set of games. The open question is whether Behrends conjecture *is* true.

7.2.3 Switched-mode circuits and switched Markov systems

Moments of fractal objects, for switched-mode devices

The fractal objects in the phase-spaces of electronic circuits are as physical and real as the voltages and currents in the circuits. They can be measured and displayed, and

7.2 Future prospects

compared against theories. The results in this thesis show that when there is a random element in the switching rule, there will be fractals in the phase space. This should apply to small variations in timing, such as jitter, as it does to binary choices, such as *ON* or *OFF*. The obvious extension of this theory is to build some physical hardware and examine whether uncertainty in the switching law does generate fractals in the phase space. The theory should predict the moments of all the state-variables. This includes the mean values and variances of all the voltages and currents. These results all follow from an analysis of the fractal sets in the phase-space.

SDEs to model large switched-mode circuits

The national power grid is actually an extremely large switched-mode device. Every time we switch on, or off, a new load, the network switches into a new mode. Of course, the number of devices and switching incidents on such a large network is enormous. We cannot track them individually, any more than we can track the individual molecules in a large volume of gas. Statistical methods must be used. The techniques defined in this thesis show how to aggregate the effects of random switching to arrive at Langevin equations that can be used to model the behaviour of the dynamical system.

Classical control theory mostly reduces to the use of time-average ordinary differential equations to model the average behaviour of a system. Langevin equations can be used to model average behaviour, including transients, *and* the fluctuations due to the stochastic switching within the system. One of the more modern trends in the design of power distribution networks is the use of signal processing techniques (Novak 2008). As National networks become larger, the noise due to switching will become more pronounced. This is especially the case if there is a large number of small generators, switching into and out of the national grid. This is likely to become more pronounced if there is a move to renewable energy, generated near the locations of use. We believe that Langevin equations will find a role in the analysis and design of power distribution networks because they have the capability of describing both average transient behaviour and the fluctuations due to switching noise.

7.2.4 Langevin equations to model noise in electronic circuits

As the feature size of microelectronic circuits is reduced, it is necessary to reduce the supply voltages and currents in order to keep power dissipation within manageable limits. This is placing stress on noise margins. It is likely that microelectronic design will run up against noise constraints before quantum limits are reached. We believe that there will be an increasing demand for accurate prediction of noise levels within microelectronic circuits, based on physical modelling. The methods presented in this thesis are an important first step towards algorithmic analysis of noise. If the analysis can be made *completely* algorithmic then it can be programmed into a machine. It can be built into the software of the simulators. We believe that Langevin equations will play an important role here.

Unique decomposition of martingales

The noise model for the JFET, in a Colpitts oscillator, in Figure 6.18, required three capacitors, C_1 , C_{gs} and C_2 to join at a single node. In the analysis that follows, there appear to be too many independent variables and not enough equations.

It seems impossible to specify a unique solution. One might suspect that the answer to this difficulty lies in the fact that supposedly independent variables might not actually be independent. This would depend on the decomposition of martingales into stochastic and deterministic parts. If this decomposition is unique then supposedly independent quantities are actually dependent. This reduces the number of independent quantities in the equations, which would allow the equations to be solved, in a straightforward manner. The conjecture here is that the state variables in systems of SDEs are martingales and that the decomposition into stochastic and deterministic parts is unique.

The two capacitor problem

The three capacitors, C_1 , C_{gs} and C_2 , in Figure 6.18, join at a single node. This problem has a great similarity with a long standing difficulty in circuit theory, called the two-capacitor problem (Powell 1979, Mayer *et al.* 1993). Consider the following thought

7.2 Future prospects

experiment. We place two equal capacitors, $C_1 = C_2 = C$, side by side. They are not connected electrically. We charge up one capacitor, C_1 to an initial voltage, V_1 . The initial stored energy in the system is $\mathcal{U} = \frac{1}{2}CV_1^2$. We then connect the capacitors and current flows through the supposedly lossless wires. Charge is conserved so we can calculate the final voltage as $V_2 = \frac{1}{2}V_1$, and hence the final stored energy of the system is $\mathcal{U} = \frac{1}{4}CV_1^2$. Where did the missing energy go? Is there something wrong with circuit theory?

It appears that constructing a *pure* capacitor is impossible and that inductance may be important and the transient currents and voltages may be oscillatory. It also appears that it is not possible to construct a capacitor of zero size, and therefore radiation will always occur. The proof of this depends on Maxwell's equations, which lie outside of ordinary circuit theory. The solution is to include a small amount of resistance in the circuit, to represent the radiation resistance (Boykin *et al.* 2002).

Possibly the most perceptive insight is given by Zemanian (2005), who also wrote (Zemanian 1965), about distribution theory and generalised functions. He points out that *all* that is required to resolve the apparent paradox is that the circuit contains at least an infinitesimal amount of resistance. This could be Ohmic, in the wires, or it could be resistance of radiation. This is not the most important issue. The oscillations are not the important issue. The important issue is that the circuit must contain some small resistive part. For *very* small amounts of resistance, most of the power is dissipated extremely quickly in the first brief moments after the circuit is completed. This should be obvious to anybody who has ever tried to discharge a large capacitor, say 100,000 μF at 50 volts, using a screwdriver⁴⁰. Zemanian (2005) shows that the estimation of the final energy in the capacitors, calculated using distribution theory gives the same result as expected from a naive consideration of circuit theory. It appears that charge is conserved under these conditions, but energy is dissipated, no matter how small the resistive part of the circuit may be. The final values of the state variables do not depend on the exact path by which this state is reached. We do not need to know the details of the rapid, impulsive transition. The complete solution to the two-capacitor depends on nonstandard analysis, using generalised functions.

⁴⁰The author has tried this experiment, once.

It is possible that the three capacitor problem, in Figure 6.18, has some similarity to the two-capacitor problem. It is possible that both problems cannot be solved without including parasitic components, such as parasitic resistance. We could possibly add parasitic resistance, to the three capacitor problem, solve the resulting model and then take the limit as the resistances become infinitesimally small. This would require nonstandard analysis of the type used by Zemanian (2005). The conjecture is that we can solve the three capacitor problem by adding the right parasitic components. The unsolved problem is, which components must be added, and why?

Closing comments

Niels Bohr is reported to have said “*Prediction is very difficult, especially about the future.*” It is hard to predict which parts of this work will prove to be the most useful, but of one *must* judge then the following summary (of the summary) would seem to be the best short list.

- Parrondo’s games exhibit a real effect that is closely related to real physical transport processes, in nature.
- The moments of these processes can be calculated analytically.
- Various similar games, devised by other authors, can all be analysed within the same mathematical framework.
- Phase-space, state-space and visualisation techniques are helpful.
- The framework is quite general and applies to other physical systems, including electronic circuits.
- In the continuum limit, it seems possible to use stochastic differential equations to model these systems.

Résumé

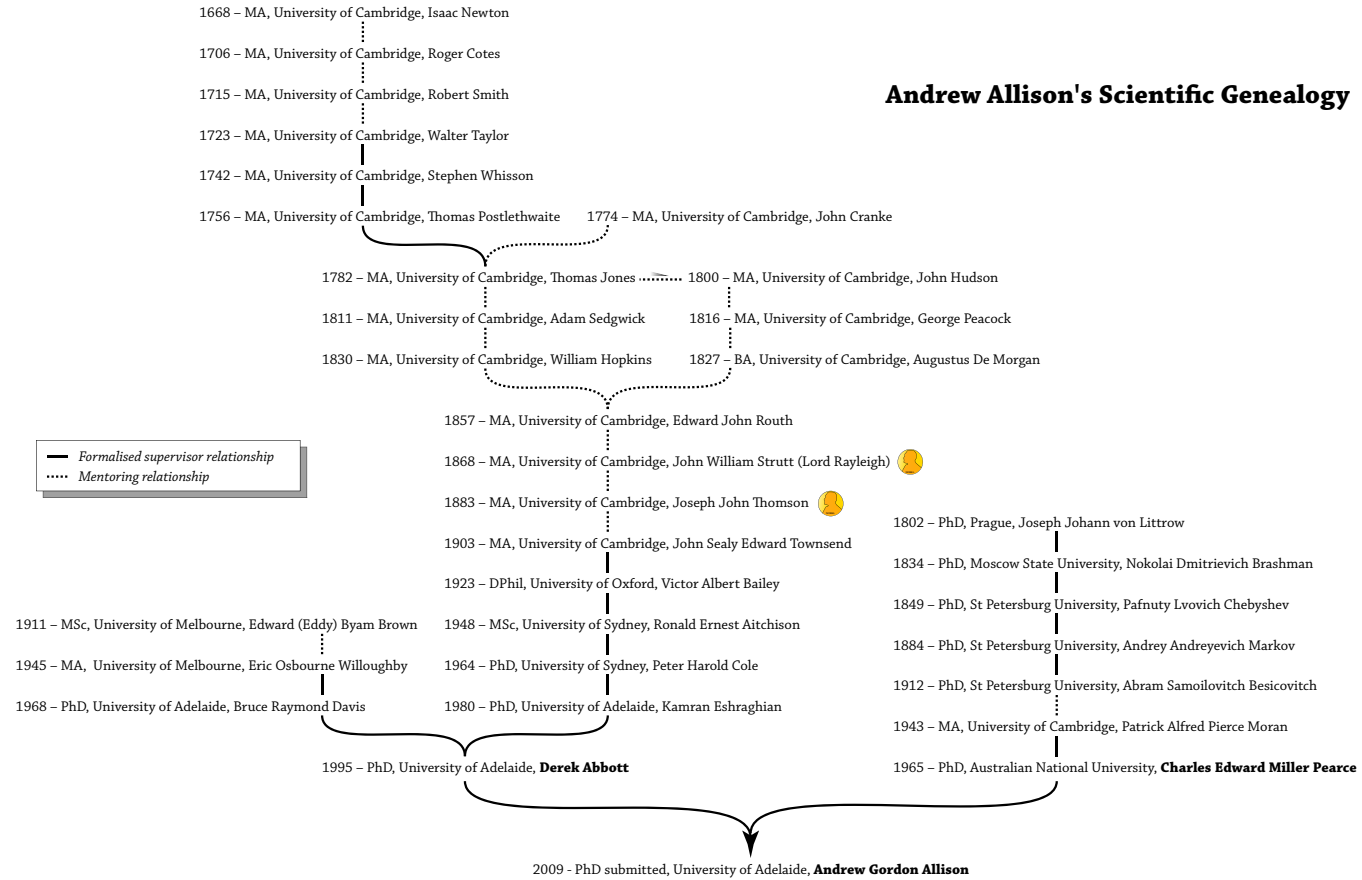


Andrew Allison has bachelor's degrees in Mathematics and Computer Systems Engineering, from the University of Adelaide. He worked at the CSIRO, using High Pressure Liquid Chromatography (HPLC). He then worked for thirteen years at Telstra, where he gained experience with telephony, electronic data processing, local area networks and cable television. He is a member of the IEEE. For the last thirteen years he has been lecturing in the School of Electrical and Electronic Engineering, at the University of Adelaide. His main areas of teaching are practical analogue electronics and the theory of communications. He is secretary of the Centre for Biomedical Engineering (CBME).

His PhD supervisors are Professors Derek Abbott and Charles Pearce. During the course of this thesis, he has authored (and co-authored) one book chapter, 12 papers in refereed journals, and 23 conference papers.

Scientific genealogy

Andrew Allison's Scientific Genealogy



Methods of work

NOTE:

This image is included on page 269 of the print copy of the thesis held in the University of Adelaide Library.

The author is grateful to Mei Sheong Wong for capturing one aspect of his working methods in an etching, on a copper plate. This plate was prepared at Second Valley, in South Australia, in 2007. It shows the author at work on the problem of the moments of Parrondo's games, using a z-transform technique. Mei's WWW site can be found at

<http://www.wastreels.com.au/>

The production of this thesis involved many hours of work, with computers. Many hundreds of lines of source code were written, in a variety of languages, especially

\LaTeX and Matlab. This might lead people to conclude that the computer comes first, but this is not correct. Computers are used to verify and to display ideas that are first developed using other techniques. Most of the geometry, calculus and algebra is first carried out by hand, on paper. Sometimes, quite a lot of paper is used. The results for Astumian's games, with absorbing boundaries, require about thirty pages of hand-written A4 paper, which leads to about five pages of finished images and text, in Section 4.5.6. This is a fairly typical yield factor, throughout the thesis. To include *every* step of *every* mathematical argument would make the thesis very tiresome to read.

Many hundreds of pieces of paper were written, manipulated and stored. The author uses a hierarchical form of document identification. Each project is allocated a working title and acronym. A project called "the Moments of Parrondo's Games via a Transform method" is identified as "MPGT." The project called "Astumian's Games with Absorbing States" is identified as "AGAS" and so on. Collisions between acronyms can always be avoided by making them longer. The use of acronyms is easier for human beings to use than a pure numbering system, with numerical tokens.

All the documents resulting from the first working session on a project are identified with a label that follows the format of a UNIX file system, eg: "MPGT/1". The individual pages can be numbered as "MPGT/1/1" and "MPGT/1/2" and so on. Individual equations and figures can be identified as "MPGT/1/1/3" and so on. Equations can be numbered by counting the relational operators, such as = or \leq , starting from the top of the page. If the second working session follows on directly from the first, in a linear narrative, then the second session will be identified as "MPGT/2", and so on. This can proceed for a very long time. At the present time, the MPGT project extends as far as "MPGT/37". New sessions can be added at any time.

The useful aspect of a tree-oriented notation is that it allows for branching. If an error is found in a page, say "MPGT/3/4/" then a new line of development can be created, starting with "MPGT/3/4.1/" and so on. The labels "MPGT/3/4/" and "MPGT/3/4.0/" are deemed to be equal. The dot numbering convention for the branching follows the convention to IP addresses. It might take many branches and false leads to solve a problem. The label "MPGT/17/9.2/3.1.1/6.1" has occurred, in practice. The

notation does not place any limit on the extent of branching. This approach, to numbering with dots, is very similar to but more systematic than the notation used in the *Tractatus* by Wittgenstein (1918). The metaphor for the labelling system is a UNIX file system with many sub-directories. Each sub-directory stores a document which has an internal numbering system similar to Wittgenstein (1918).

Branching is required in any narrative where old ideas are being corrected or new creative developments are being introduced. A hierarchical tree-oriented numbering system allows for commentary, after commentary, without end, in the fashion of the Talmud. Using this method of labelling, documents can be stored, retrieved and edited. New comments can be added. New lines of thought can be introduced. Commentaries, checks, additions, and new ideas can be added, to any arbitrary level of recursion. In short, the storage method does not place any limit on the creative process.

The documents can be taken out, laid out on a table in arbitrary positions or arbitrary sequences, to assist with creativity. The documents can then be stored away in correct order, to prevent loss of information. This makes it possible to work in a disrupted or temporary workspace and to make use of small fragments of time because it is possible to physically store your mental state and then reconstruct it physically on a table, later on. The author refers to this approach to document labelling as the *Wittgenstein system*, as a reference to the *Tractatus* and to Wittgenstein's Jewish heritage of commentary and debate.

The author has also developed a horizontal form of the Noguchi (Communication-Nation 2005, Patterson 2007) filing system for storing all the paper associated with projects. The system used for this thesis differs from Noguchi's original system in that it is horizontal and makes use of suspension files. This makes it quick and easy to archive old material, back into standard filing cabinets, for long term storage. The central feature of the Noguchi system is that it trades off some searching time (when a document is retrieved) in exchange for a great saving of clerical effort (when a document is stored). The Noguchi system automatically sorts the most frequently used documents to the front of the queue. It automatically identifies the infrequently used documents, which should be placed into archives, in filing cabinets, or placed in the recycling bin.

Epilogue

NOTE:

This figure is included on page 273 of the print copy of the thesis held in the University of Adelaide Library.

Figure 7.2. Fundamental limitations of computation. Thus I have heard: *“There are four incalculables, which cannot be calculated, an attempt to calculate which would lead to frustration and madness. What four? They are the objective field of the Buddhas, the objective field of one who has acquired the meditations, the ripening of action, and the calculation of the world.”* Buddha Gotama, Anguttara Nikāya (IV 77). Translated and arranged by Bhikku Ñānamoli (1978).

Bibliography

- ABBOTT-D., DAVIS-B. R., AND ESHRAGHIAN-K. (1997). Output circuit noise analysis of the xy array imager, in C. Claeys., and E. Simoen. (eds.), *Noise in Physical Systems and $1/f$ Fluctuations*, World Scientific, Leuven, Belgium, pp. 482–487.
- ABBOTT-D., DAVIS-B. R., AND PARRONDO-J. M. R. (2000). The problem of detailed balance for the Feynman-Smoluchowski Engine (fse) and the multiple pawl paradox, in D. Abbott., and L. B. Kish. (eds.), *Proc. AIP, Second Int. Conf. Unsolved Problems of Noise and Fluctuations (UPoN'99)*, Vol. 511, American Inst. Phys., pp. 213–218.
- ABBOTT-D., DAVIS-B. R., PHILLIPS-N. J., AND ESHRAGHIAN-K. (1996). Simple derivation of the thermal noise formula using window-limited fourier transforms and other conundrums, *IEEE Transaction on Education*, **39**(1), pp. 1–13.
- ABRAMOWITZ-M., AND STEGUN-I. (1970). *Handbook of Mathematical Functions*, 9th edn, Dover Publications, Inc., New York.
- AJDARI-A., AND PROST-J. (1992). Drift induced by a periodic potential of low symmetry: pulsed dielectrophoresis, *C.R. Acad. Sci. Paris, Série II*, **315**, pp. 1635–1639.
- ALLISON-A., ABBOTT-D., AND PEARCE-C. E. M. (2005). State-space visualisation and fractal properties of Parrondo's games, in A. S. Nowak., and K. Szajowski. (eds.), *Proceedings of the Ninth International Symposium on Dynamic Games and Applications 2000, Advances in Dynamic Games: Applications to Economics, Finance, Optimization, and Stochastic Control.*, Vol. 7, The International Society of Dynamic Games (ISDG), pp. 613–633.
- ALLISON-A., AND ABBOTT-D. (1999). Simulation and properties of randomly switched control systems, in B. Courtois., and S. N. Demidenko. (eds.), *Proc. SPIE Conference, Design, Characterization, and Packaging for MEMS and Microelectronics*, Vol. 3893, pp. 204–213.
- ALLISON-A., AND ABBOTT-D. (2000a). Some benefits of random variables in switched control systems, *Microelectronics Journal*, **31**, pp. 515–522.
- ALLISON-A., AND ABBOTT-D. (2000b). Stochastically switched control systems, in D. Abbott. (ed.), *Proc. AIP, Second Int. Conf. Unsolved Problems of Noise and Fluctuations (UPoN'99)*, Vol. 511, American Inst. Phys., pp. 249–254.
- ALLISON-A., AND ABBOTT-D. (2001). Control systems with stochastic feedback, *Chaos Journal*, **11**(3), pp. 715–724.
- ALLISON-A., AND ABBOTT-D. (2002). The physical basis for Parrondo's games, *Fluctuation and Noise Letters*, **2**(4), pp. L327–L341.
- ALLISON-A., AND ABBOTT-D. (2003a). Brownian ratchets with distributed charge, in S. M. Bezrukov., H. Frauenfelder., and F. Moss. (eds.), *Fluctuations and Noise in Biological, Biophysical, and Biomedical Systems*, Vol. 5110, SPIE, pp. 302–311.

- ALLISON-A., AND ABBOTT-D. (2003b). Discrete games of chance as models for continuous stochastic transport processes, in L. Schimansky-Geier, D. Abbott, A. Neiman, and C. Van den Broeck. (eds.), *Proc. SPIE: Noise in Complex Systems and Stochastic Dynamics*, Vol. 5114, pp. 363–371.
- ALLISON-A., AND ABBOTT-D. (2005). Applications of stochastic differential equations in electronics, in L. Reggiani and C. Penneta and V. Akimov and E. Alfinito and M. Rosini. (ed.), *Unsolved Problems of Noise and Fluctuations in Physics, Biology and High Technology*, Vol. 800 of *American Institute of Physics Conference Series*, pp. 15–23.
- AMENGUAL-P., ALLISON-A., TORAL-R., AND ABBOTT-D. (2004). Discrete-time ratchets, the Fokker-Planck equation and Parrondo's paradox, *Proceedings of the Royal Society of London*, **460**(2048), pp. 2269–2284.
- APOSTOL-T. M. (1974). *Mathematical Analysis*, Addison-Wesley Publishing Company.
- APOSTOL-T. M., AND MNATSAKANIAN-M. A. (2003). Sums of squares of distances in m-space, *The American Mathematical Monthly*, **110**(6), pp. 516–526.
- ASTUMIAN-D. (2001). Making molecules into motors, *Scientific American*, **285**(7), pp. 56–64.
- ASTUMIAN-R. D. (2004). Gambler's paradox and noise driven flux reversal in kinetic cycles: Response to the preceding paper by Piotrowski and Sladkowski, *Fluctuation Noise Letters*, **4**(4), pp. C13–C20.
- ASTUMIAN-R. D. (2005). Paradoxical games and a minimal model for a Brownian motor, *Am. J. Phys.*, **73**(2), pp. 178–183.
- ASTUMIAN-R. D., AND DERÉNYI-I. (1998). Fluctuation driven transport and models of molecular motors and pumps, *Journal European Biophysics*, **27**(5), pp. 474–489.
- ASTUMIAN-R. D., CHOCK-P. B., TSONG-T. Y., CHEN-Y. D., AND WESTERHOFF-H. V. (1987). Can free energy be transduced from electric noise?, *Proc. Nat. Acad. Sci. USA*, **84**, pp. 434–438.
- ATKINSON-K. (1985). *Elementary Numerical Analysis*, John Wiley & Sons, New York.
- ATKINS-P. W. (1994). *Physical Chemistry*, fifth ed. edn, Oxford University Press, Oxford.
- BADER-J. S., HAMMOND-R. W., HENK-S. A., DEEM-M. W., MCDERMOTT-G. A., BUSTILLO-J. M., SIMPSON-J. W., MULHERN-G. T., AND ROTHBERG-J. M. (1999). DNA transport by a micro-machined Brownian ratchet device, *Proceedings of the National Academy of Sciences*, **96**(23), pp. 13165–13169.
- BARNESLEY-M. (1988). *Fractals Everywhere*, Academic Press.
- BAXTER-M., AND RENNIE-A. (1996). *Financial Calculus*, Cambridge University Press, Cambridge.
- BEHRENDSE-E. (2004). A note on the preceding paper by Piotrowski and Sladkowski and the response of astumian, *Fluctuation and Noise Letters*, **4**(4), pp. C21–C23.
- BEHRENDSE-E. (2006). Walks with optimal reward on metric spaces, *Nonlinearity*, **19**(3), pp. 685–700.
- BEHRENDSE-E. (2008). Stochastic dynamics and Parrondo's paradox, *Physica D*, **237**, pp. 198–206.

- BENNETT-C. H. (1982). The thermodynamics of computation—a review, *Journal International Journal of Theoretical Physics*, **21**(12), pp. 905–940.
- BERNSTEIN-J. (2008). *Physicists on Wall Street and Other Essays on Science and Society*, Springer, New York.
- Bezdek, J. C., and Pal, S. K. (eds.) (1992). *Fuzzy Models for Pattern Recognition*, IEEE Press, New York.
- BHIKKU ÑĀNAMOLI. (1978). *The Life of the Buddha*, Buddhist Publication Society, Kandy, Ceylon.
- Bier, M. (ed.) (1997). *Stochastic Dynamics*, Vol. 484 of *Lecture Notes in Physics*, Springer, Berlin, chapter A Motor Protein Model and How it Relates to Stochastic Resonance, Feynman’s Ratchet, and Maxwell’s Demon, pp. 81–87.
- BILLINGS-K. (1989). *Switchmode Power Supply Handbook*, McGraw-Hill.
- BIRD-R. B., STEWART-W. E., AND LIGHTFOOT-E. N. (1960). *Transport Phenomena*, John Wiley & Sons, New York.
- BLACKMAN-P. F. (1975). *Introduction to Sampling and z-Transforms*, John Wiley & Sons., London, chapter 2, pp. 11–31.
- BOYKIN-T. B., HITE-D., AND SINGH-N. (2002). The two-capacitor problem with radiation, *American Journal of Physics*, **70**(4), pp. 415–420.
- BOYLE-R. (1661). *The Sceptical Chymist*, Printed J. Cadwell for J. Crooke, London.
- BRACEWELL-R. N. (2000). *The Fourier Transform and its Applications*, third ed. edn, McGraw-Hill, Boston.
- BRILLOUIN-L. (1956). *Science and Information Theory*, Academic Press Inc., New York.
- BROWN-R. (1828). A brief account of microscopical observations, made in the months of june, july, and august, 1827, on the particles contained in the pollen of plants; and on the general existence of active molecules in organic and inorganic bodies., *Philos. Mag.*, **4**, pp. 161–173.
- BRYAN-G. H. (1906). Prof. ludwig boltzmann, *Nature*, **74**(1927), pp. 569–570.
- BUCHANAN-G. R. (1995). *Finite Element Analysis*, Schaum’s Outline, McGraw-Hill, New York.
- CANTOR-G. (1883). Über unendliche, lineare punktmannigfaltigkeiten, *Mathematische Annalen*, **21**, pp. 545–591. On infinite, linear point-manifolds.
- CARLSON-A. B., CRILLY-P. B., AND RUTLEDGE-J. C. (2002). *Communication systems: an introduction to signals and noise in electrical communication*, 4th edn, McGraw-Hill, Dubuque, Iowa.
- CARTA-G. (1988). Analytical solution for rate-based chromatography with linear isotherm, *Chem. Eng. Sci.*, **43**, pp. 2877–2883.
- CHAPRA-S. C. (2006). *Numerical Methods for Engineers*, fifth edn, McGraw-Hill, Boston.
- COMMUNICATION-NATION. (2005). The Noguchi filing system.

Bibliography

- COSTA-A., FACKRELL-M., AND TAYLOR-P. G. (2005). Two issues surrounding Parrondo's paradox, in A. S. Nowak., and K. Szajowski. (eds.), *Proceedings of the Ninth International Symposium on Dynamic Games and Applications 2000, Advances in Dynamic Games: Applications to Economics, Finance, Optimization, and Stochastic Control.*, Vol. 7, The International Society of Dynamic Games (ISDG), pp. 599–609.
- COURANT-R., AND MCSHANE-E. J. (1966). *Differential and Integral Calculus*, Vol. II, second edn, Blackie and Son Limited.
- CUSSLER-E. L. (1997). *Diffusion: Mass Transfer in Fluid Systems*, second edn, Cambridge University Press, Cambridge.
- DALTON-J. (1808). *A New System of Chemical Philosophy*, Bickerstaff, London.
- DAVIES-P. C. W. (2001). Physics and life: The Abdus Salam memorial lecture, in J. Chela-Flores., T. Tobias., and F. Raulin. (eds.), *Sixth Trieste Conference on Chemical Evolution*, Kluwer Academic Publishers, Trieste, Italy, pp. 13–20.
- DAVIS-B. R. (2000). Numerical methods for systems excited by white noise, in D. Abbott., and L. B. Kish. (eds.), *Proc. AIP, Second Int. Conf. Unsolved Problems of Noise and Fluctuations (UPoN'99)*, Vol. 511, American Inst. Phys., pp. 533–538.
- DEMIR-A., MEHROTRA-A., AND ROYCHOWDHURY-J. (2000). Phase noise in oscillators: a unifying theory and numerical methods for characterization, *IEEE Transactions on Circuits and Systems I: Fundamental Theory and Applications*, **47**(5), pp. 655–674.
- DE MOIVRE-A. (1730). *Miscellanea Analytica*, J. Tonson & J. Watts, London.
- DERUSSO-P. M., ROY-R. J., AND CLOSE-C. M. (1965). *State Variables for Engineers*, John Wiley&Sons Inc., New York.
- DIACU-F., AND HOLMES-P. (1996). *Celestial Encounters, The Origins of Chaos and Stability*, Princeton University Press.
- DOERING-C. R. (1995). Randomly rattled ratchets, *Il Nuovo Cimento*, **17D**(7–8), pp. 685–697.
- DOETSCH-G. (1974). *Introduction to the Theory and Application of the Laplace Transformation*, Springer-Verlag, Berlin.
- DORAN-C., AND LASENBY-A. (2003). *Geometric Algebra for Physicists*, Cambridge University Press, Cambridge.
- DORF-R. C., AND BISHOP-R. H. (1998). *Modern Control Systems*, eighth edn, Addison-Wesley, Menlo Park, California.
- DOUC-R., MOULINES-E., AND ROSENTHAL-J. S. (2004). Quantitative bounds on convergence of time-inhomogeneous Markov chains, *The Annals of Applied Probability*, **14**(4), pp. 1643–1665.
- DUKE-T. A., AND AUSTIN-R. H. (1998). Microfabricated sieve for the continuous sorting of macromolecules, *Phys. Rev. Lett.*, **80**(7), pp. 1552–1555.
- DURRETT-R. (1996). *Stochastic Calculus*, CRC Press, Boca Raton.

-
- EINSTEIN-A. (1905). Investigations on the theory of the Brownian movement, *Ann. Physik*, **17**, pp. 549–560.
- EINSTEIN-A. (1956). *Investigations on the Theory of the Brownian Movement*, Dover Publications, Inc., New York.
- ELTON-J. H., AND YAN-Z. (1989). Approximation of measures by markov processes and homogeneous affine iterated function systems, *Constructive Approximation*, **5**(1), pp. 69–87.
- ERDŐS-P., FELLER-W., AND POLLARD-H. (1949). A property of power series with positive coefficients., *Bull. Am. Math. Soc.*, **55**, pp. 201–204.
- ERSOY-O. (1997). *Fourier-Related Transforms, Fast Algorithms and Applications*, Prentice Hall PTR, Upper Saddle River, NJ.
- ERTAS-D. (1998). Lateral separation of macromolecules and polyelectrolytes in microlithographic arrays, *Phys. Rev. Lett.*, **80**(7), pp. 1548–1551.
- ETHIER-S. N., AND LEE-J. (2009). Limit theorems for Parrondo’s paradox, <http://arxiv.org/abs/0902.2368>.
- FARLOW-S. J. (1982). *Partial Differential Equations for Scientists and Engineers*, Dover Publications, Inc.
- FAUCHEUX-L. P., BOURDIEU-L. S., KAPLAN-P. D., AND LIBCHABER-A. J. (1995). Optical thermal ratchet, *Phys. Rev. Lett.*, **74**(9), pp. 1504–1507.
- FELLER-W. (1937). Zur theorie der stochastischen prozesse existenz- und eindeutigkeitssätze, *Journal Mathematische Annalen*, **113**, pp. 113–160.
- FELLER-W. (1967). *An Introduction to Probability Theory and its Applications*, Vol. 1, third edn, Wiley, New York.
- FEYNMAN-R. P., LEIGHTON-R. B., AND SANDS-M. (1963). *The Feynman Lectures on Physics*, Vol. 1, Addison-Wesley, Reading, Massachusetts.
- FODOR-G. (1965). *Laplace Transforms in Engineering*, Akadémiai Kiadó, Budapest.
- GALBRAITH-J. K. (1954). *The Great Crash, 1929*, Penguin books, Harmondsworth, Middlesex.
- GARDINER-C. W. (1983). *Handbook of Stochastic Methods*, Springer-Verlag, Berlin.
- GASSENDI-P. (1649). *Syntagma philosophiæ Epicuri cum refutationibus dogmatum quæ contra fidem christianam ab eo asserta sunt*, Guillaume Barbier.
- GIBBS-J. W. (1902). *Elementary Principles in Statistical Mechanics*, Dover, 1960 edn, Dover Publications, Inc., New York.
- GIKHMAN-I. H., AND SKOROKHOD-A. V. (1969). *Introduction to the Theory of Random Processes*, Dover 1996 edn, Dover Publications, Inc., New York.
- GITTERMAN-M. (2005). *The Noisy Oscillator, The First Hundred Years From Einstein Until Now*, World Scientific, New Jersey.

Bibliography

- GOLDBERG-S. (1986). *Introduction to Difference Equations*, Dover edn, Dover Publications, Inc., New York.
- GOTTLIEB-I. M. (1992). *Regulated Power Supplies*, TAB Books.
- GOURSAT-E. (1916). *Functions of a Complex Variable*, Dover edn, Dover Publications, Inc., New York.
- GRAUSTEIN-W. C. (1930). *Introduction to Higher Geometry*, The Macmillan company, New York.
- GREENWOOD-D. T. (1977). *Classical Dynamics*, Dover Publications, Inc.
- GUBA-F., AND GYÖRGYI-A. S. (1946). Fluochrome in muscle, *Nature*, **158**(4010), pp. 343–343.
- GUBNER-J. A. (1996). *The Control Handbook*, CRC Press and IEEE Press, chapter 60, Stochastic Differential Equations, pp. 1067–1078.
- HÄNGGI-P., AND MARCHESONI-F. (2005). Introduction: 100 years of Brownian motion, *Chaos*, **15**(2), p. 026101.
- HARMER-G., ABBOTT-D., TAYLOR-P. G., AND PARRONDO-J. M. R. (2000a). Parrondo's paradoxical games and the discrete Brownian ratchet, in D. Abbott., and L. B. Kiss. (eds.), *Proc. AIP, Second Int. Conf. Unsolved Problems of Noise and Fluctuations (UPoN'99)*, Vol. 511, pp. 189–200.
- HARMER-G. P. (2001). *Stochastic Processing for Enhancement of Artificial Insect Vision*, PhD thesis, Electrical and Electronic Engineering, University of Adelaide.
- HARMER-G. P., ABBOTT-D., AND TAYLOR-P. G. (2000a). The Paradox of Parrondo's games, *Proc. Royal Soc., Series A, (Math. Phys. and Eng. Science)*, **456**(99), pp. 247–251.
- HARMER-G. P., ABBOTT-D., AND TAYLOR-P. G. (2000b). The paradox of Parrondo's games, *Proc. Royal Soc., Series A, (Math. Phys. and Eng. Science)*, **456**(99), pp. 247–251.
- HARMER-G. P., ABBOTT-D., TAYLOR-P. G., AND PARRONDO-J. M. R. (2000b). Parrondo's paradoxical games and the discrete Brownian ratchet, *Proc. AIP, Second Int. Conf. Unsolved Problems of Noise and Fluctuations (UPoN'99)*, 2000, eds. D. Abbott and L. B. Kish, *American Inst. Phys.*, **511**, pp. 149–160.
- HARMER-G. P., ABBOTT-D., TAYLOR-P. G., AND PARRONDO-J. M. R. (2001). Brownian ratchets and parrondo's games, *Chaos*, **11**(3), pp. 705–714.
- HARMER-G. P., AND ABBOTT-D. (1999a). Losing strategies can win by Parrondo's paradox, *Nature*, **402**, p. 864.
- HARMER-G. P., AND ABBOTT-D. (1999a). Parrondo's paradox, *Statistical Science*, **14**(2), pp. 206–213.
- HARMER-G. P., AND ABBOTT-D. (1999b). Losing strategies can win by Parrondo's paradox, *Nature*, **402**(23/30), p. 864.
- HARMER-G. P., AND ABBOTT-D. (1999b). Parrondo's paradox, *Statistical Science*, **14**, pp. 206–213. Parrondo's Games.
- HARMER-G. P., AND ABBOTT-D. (2001). Brownian ratchets and Parrondo's games, *Chaos*, **11**(3), pp. 705–714.
- HARMER-G. P., AND ABBOTT-D. (2002). A review of Parrondo's paradox, *Fluctuation and Noise Letters*, **2**(2), pp. R71–R107.

-
- HARRINGTON-S. (1987). *Computer Graphics: A Programming Approach*, 2nd edn, McGraw-Hill, New York.
- HARRISON-J. (1998). *Theorem Proving with the Real Numbers*, Springer-Verlag.
- HARTFIEL-D. J. (2002). *Nonhomogeneous Matrix Products*, World Scientific, New Jersey.
- Hawking, S.. (ed.) (2005). *God Created the Integers*, Running Press, Philadelphia.
- HAYT-W. H. (1988). *Engineering Electromagnetics*, McGraw-Hill Book Co., New York.
- HAYT-W. H., KEMMERLEY-J. E., AND DURBIN-S. M. (2002). *Engineering Circuit Analysis*, sixth edn, McGraw-Hill, Boston.
- HEATH-D., KINDERLEHRER-D., AND KOWALCZYK. (2002). Discrete and continuous ratchets: From coin toss to molecular motor, *Discrete and Continuous Dynamical Systems Series B*, 2(2), pp. 153–167.
- HECHT-C. E. (1990). *Statistical Thermodynamics and Kinetic '1 Theory*, Dover Publications, Inc., New York.
- HILL-T. L. (1977). *Free Energy Transduction and Biochemical Cycle Kinetics*, Academic Press, New York.
- HOPCROFT-J. E., AND ULLMAN-J. D. (1979). *Introduction to Automata Theory, Languages and Computation*, Addison-Wesley Publishing Company, Reading Massachusetts.
- HOROWITZ-P., AND HILL-W. (1991). *The Art of Eelectronics*, Cambridge University Press, Cambridge, UK.
- HOWARD-R. A. (1960). *Dynamic Programming and Markov Processes*, John Wiley & Sons Inc.
- HUBBARD-B. B. (1998). *The World According to Wavelets*, second edn, A. K. Peters, Natick, Massachusetts.
- HUI-S. Y. R., SATHIAKUMAR-S., AND SUNG-K.-K. (1997). Novel random PWM schemes with weighted switching decision, *IEEE Transactions on Power Electronics*, 12(6), pp. 945–952.
- ISERLES-A. (1996). *A First Course in the Numerical Analysis of Differential Equations*, Cambridge University Press, Cambridge, UK.
- ITÔ-K. (1942). Differential equations determining a Markoff process (in Japanese), *Journ. Pan-Japan Math.* (in English) Kiyosi Itô Selected Papers, Springer-Verlag, 1986.
- ITÔ-K. (1951). On stochastic differential equations, *Mem. Amer. Math. Soc.*, 4, pp. 1–51.
- JAYNES-E. T. (2003). *Probability Theory the Logic of Science*, Cambridge University Press, Cambridge.
- JAYNES-E. T. E. T. (1957). Information theory and statistical mechanics, *Phys. Rev.*, 106(4), pp. 620–630.
- JERRI-A. J. (1996). *Linear Difference Equations with Discrete Transform Methods*, Kluwer Academic Publishers, Dordrecht.
- JOHNSON-J. B. (1928). Thermal agitation of electricity in conductors, *Phys. Rev.*, 32, pp. 97–109.
- JORGENSEN-P. E. T., KORNELSON-K. A., AND SHUMAN-K. L. (2007). Harmonic analysis of iterated function systems with overlap.
-

Bibliography

- JURY-E. I. (1964). *Theory and Application of the z-Transform Method*, John Wiley & Sons, Inc., New York.
- KAC-M. (1947). Random walk and the theory of Brownian motion, *The American Mathematical Monthly*, **54**(7), pp. 369–391.
- KARATZAS-I., AND SHREVE-S. E. (1988). *Brownian Motion and Stochastic Calculus*, Springer-Verlag, New York.
- KARLIN-S. M., AND TAYLOR-H. M. (1975). *A First Course in Stochastic Processes*, Academic Press, San Diego.
- KARNOPP-D. C., MARGOLIS-D. C., AND ROSENBERG-R. C. (2000). *System Dynamics, Modelling and Simulation of Mechatronic Systems*, John Wiley and Sons Inc., New York.
- KING-E. L., AND ALTMAN-C. (1956). A schematic method of deriving the rate laws for enzyme-catalyzed reactions, *J. Phys. Chem.*, **60**, p. 1375.
- KIVIAT-B. (2007). Real estate's fault line, *Time Magazine*, pp. 38–42.
- KLOEDEN-P. E., AND PLATEN-E. (1999). *Numerical Solution of Stochastic Differential Equations*, Springer, Berlin.
- KNUTH-D. (1978). *Fundamental Algorithms*, Vol. 1, second ed. edn, Addison Wesley.
- KOLMOGOROV-A. (1950). *Foundations of the Theory of Probability*, Chelsea Pub. Co., New York.
- KOLMOGOROV-A. N. (1931). Über die analytischen methoden in der wahrscheinlichkeitsrechnung, *Math. Ann. B*, **104**, p. 415.
- KOLMOGOROV-A. N., AND FOMIN-S. V. (1970). *Introductory Real Analysis*, Dover Publications, Inc., New York.
- KORN-G. A., AND KORN-T. M. (2000). *Mathematical Handbook for Scientists and Engineers*, Dover edn, Dover Publications, Inc.
- KREYSZIG-E. (2006). *Advanced Engineering Mathematics*, 9th edn, John Wiley, Hoboken, NJ.
- KRINSMAN-A. N. (2007). Subprime mortgage meltdown: How did it happen and how will it end?, *The Journal of Structured Finance*, **XIII**(2), pp. 1–9.
- KUO-B. J. (1992). *Digital Control Systems*, Saunders College Publishing.
- LAI-Y.-S. (1977). Random switching techniques for inverter control, *Electronics Letters*, **33**(9), pp. 747–749.
- LAMBERTON-D., AND LAPEYRE-B. (1991). *Stochastic Calculus Applied to Finance*, Chapman & Hall, London.
- LAMPORT-L. (1994). *L^AT_EX, A Document Preparation System*, Addison-Wesley, Reading, Massachusetts.
- LANCZOS-C. (1949). *The Variational Principles of Mechanics*, Dover Publications, Inc.
- LANCZOS-C. (1954). *Applied Analysis*, Prentice Hall Inc., Englewood Cliffs, N.J.

-
- LANDAUER-R. (1961). Irreversibility and heat generation in the computing process, *IBM Journal of Research and Development*, 5(3), pp. 183–191.
- LAPIDUS-L. (1962). *Digital Computation for Chemical Engineers*, McGraw-Hill Book Co. Inc., New York.
- LAPLACE-P. S. (1814). *A Philosophical Essay on Probabilities*, Dover.
- LATHI-B. P. (1965). *Signals Systems and Communications*, John Wiley and Sons, Inc., New York.
- LEE-Y., ALLISON-A., ABBOTT-D., AND STANLEY-H. E. (2003). A minimal Brownian ratchet: an exactly solvable model, *Phys. Rev. Lett.* 91 (22), 220601.
- LEON-GARCIA-A. (1994). *Probability and Random Processes for Electrical Engineering*, second edn, Addison-Wesley, Reading, Massachusetts.
- LEPAGE-W. R. (1980). *Complex Variables and the Laplace Transform for Engineers*, Dover edn, Dover Publications, Inc., New York.
- Levine, W. S.. (ed.) (1996). *The Control Handbook*, CRC Press & The IEEE Press.
- LIGHTHILL-M. J. (1958). *Introduction to Fourier analysis and Generalised Functions*, Cambridge, Cambridge.
- LÜKE-H. D. (1999). The origins of the sampling theorem, *IEEE Communications Magazine*, pp. 106–108. April 1999.
- MAGNASCO-M. O. (1993). Forced thermal ratchets, *Phys. Rev. Lett.*, 71(10), pp. 1477–1481.
- MANDELBROT-B. B. (1977). *The Fractal Geometry of Nature*, W. H. Freeman, New York.
- MARON-M. J., AND LOPEZ-R. J. (1990). *Numerical Analysis: A Practical Approach*, Wadsworth, Belmont, CA, USA.
- MAXWELL-J. C. (1888). *Theory of Heat*, Dover Publications, Inc.
- MAYER-R. P., JEFFRIES-J. R., AND PAULIK-G. F. (1993). The two-capacitor problem reconsidered, *IEEE Transactions on Education*, 36(3), pp. 307–309.
- MCCLINTOCK-P. V. E. (1999). Random fluctuations: Unsolved problems of noise, *Nature*, 401, pp. 23–25.
- MCELIECE-R. J., ASH-R. B., AND ASH-C. (1989). *Introduction to Discrete Mathematics*, Random House, New York.
- MEHROTRA-A., AND SANGIOVANNI-VINCENTELLI-A. (2004). *Noise Analysis of Radio Frequency Circuits*, Kluwer Academic Publishers, Boston.
- MEYER-C. D. (2000). *Matrix Analysis and Applied Linear Algebra*, SIAM, Philadelphia.
- MIDDLEBROOK-R. D., AND ČUK-S. A. (1976). A general unified approach to modelling switching converter power stages, *IEEE Power Electronics Specialist's Conf Rec*, pp. 18–34.
- MONK-R. (1991). *Ludwig Wittgenstein, The duty of genius*, Vintage, London.
-

Bibliography

- MORAAL-H. (2000a). Counterintuitive behaviour in games based on spin models, *J. Phys. A, Math. Gen.*, **33**(23), pp. L203–L206.
- MORAAL-H. (2000b). Counterintuitive behaviour in games based on spin models, *J. Phys. A.*, **33**(23), pp. L203–L206.
- MUTH-E. J. (1977). *Transform Methods with Applications to Engineering and Operations Research*, Prentice Hall, Englewood Cliffs, NJ.
- NEWTON-I. (1704). *Opticks*, dover, 1979 edn, Dover Publications Inc.
- NORRIS-J. R. (1997). *Markov Chains*, Cambridge University Press.
- Novak, I. (ed.) (2008). *Power Distribution Network Design Methodologies*, Intl. Engineering Consortium.
- NYQUIST-H. (1928). Thermal agitation of electricity in conductors, *Phys. Rev.*, **32**, pp. 97–109.
- O'BRIEN-G. G., HYMAN-M. A., AND KAPLAN-S. (1951). A study of the numerical solution of partial differential equations, *J. Math. Phys.*, **29**, pp. 223–251.
- OGATA-K. (1987). *Discrete-Time Control Systems*, Prentice-Hall International Inc., Englewood Cliffs, NJ.
- ØKSENDAL-B. (1998). *Stochastic Differential Equations*, sixth edn, Springer, Berlin.
- ONSAGER-L. (1931). Reciprocal; relations in irreversible processes i, *Physical Review*, **37**, pp. 405–426.
- PAPOULIS-A. (1962). *The Fourier Integral and its Applications*, McGraw-Hill Book Co., New York.
- PAPOULIS-A. (1991). *Probability, Random Variables, and Stochastic Processes*, McGraw Hill, New York.
- PARRONDO-J. M. R. (1996a). Criticism of Feynman's analysis of the ratchet as an engine, *American Journal of Physics*, **64**(9), pp. 1125–1130.
- PARRONDO-J. M. R. (1996b). How to cheat a bad mathematician, EEC HC&M Network on Complexity and Chaos, #ERBCHRX-CT 940 546, Torino, Italy.
- PARRONDO-J. M. R., HARMER-G. P., AND ABBOTT-D. (2000). New paradoxical games based on Brownian ratchets, *Physical Review Letters*, **85**, pp. 5226–5229.
- PATTERSON-M. (2007). Time sort (Noguchi) filing system.
- PAULI-W. (1973). *Statistical Mechanics*, Vol. 4 of *Pauli Lectures on Physics*, Dover Publications, Inc., New York.
- PEARCE-C. E. M. (2000a). Entropy, Markov information sources and Parrondo's games, *Proc. AIP, Second Int. Conf. Unsolved Problems of Noise and Fluctuations (UPoN'99)*, 2000, ed. D. Abbott, *American Inst. Phys.*, **511**, pp. 426–431.
- PEARCE-C. E. M. (2000a). On Parrondo's paradoxical games, in D. Abbott., and L. B. Kiss. (eds.), *Proc. AIP, Second Int. Conf. Unsolved Problems of Noise and Fluctuations (UPoN'99)* *American Inst. Phys.*, 2000, Vol. 511, pp. 201–206.

- PEARCE-C. E. M. (2000b). Entropy, Markov information sources and Parrondo's games, in D. Abbott, and L. B. Kiss. (eds.), *Proc. AIP, Second Int. Conf. Unsolved Problems of Noise and Fluctuations (UPoN'99) American Inst. Phys., 2000*, Vol. 511, pp. 207–212.
- PEARCE-C. E. M. (2000b). Parrondo's paradoxical games, *Proc. AIP, Second Int. Conf. Unsolved Problems of Noise and Fluctuations (UPoN'99), 2000*, ed. D. Abbott, *American Inst. Phys.*, **511**, pp. 420–425.
- PEARSON-K. (1905). The problem of the random walk, *Nature*, **72**, pp. 294, 318, 342.
- PEEBLES-P. Z. (2001). *Probability, Random Variables, and Random Signal Principles*, McGraw Hill, Singapore.
- PENROSE-R. (2004). *The Road to Reality*, Vintage Books, London.
- PENSKI-C. (2000). A new numerical method for SDEs and its application in circuit simulation, *Journal of Computational and Applied Mathematics*, **115**(1–2), pp. 461–470.
- PERRIN-J. (1909). Le mouvement Brownien et la Réalité moléculaire, *Ann. Chim. Phys.*, **18**(8^{me} Serie), pp. 5–114.
- PERRIN-J. (1910). *Brownian Movement and Molecular Reality*, Taylor and Francis, London. translated by F. Soddy.
- PERROT-P. (1998). *A to Z of Thermodynamics*, Oxford University Press.
- PEYTON-A. J., AND WALSH-V. (1993). *Analog Electronics with Op Amps*, Cambridge University Press, Cambridge.
- PHILIPS-T. K., AND FELDMAN-A. B. (2004). Parrondo's paradox is not paradoxical.
- PIERRE-D. A. (1986). *Optimization Theory with Applications*, Dover Publications, Inc., New York.
- PIOTROWSKI-E. W., AND SLADKOWSKI-J. (2004). On the applicability of Astumian's model in describing Parrondo effects, *Fluctuation and Noise Letters*, **4**(4), pp. C7–C12.
- POWELL-R. A. (1979). Two-capacitor problem: A more realistic view, *American Journal of Physics*, **47**(5), pp. 460–462.
- PRESS-W. H., TEUKOLSKY-S. A., VETTERLING-W. T., AND FLANNERY-B. P. (1995). *Numerical Recipes in C*, second edn, Cambridge University Press, New York.
- PROAKIS-J. G., AND MANOLAKIS-D. G. (1992). *Digital Signal Processing*, MacMillan Publishing Company, New York.
- PROTTER-P. (1990). *Stochastic Integration and Differential Equations*, Springer Verlag, Berlin.
- RAO-M. M., AND SARKAR-T. K. (1999). Simultaneous extrapolation in time and frequency domains using hermite expansions, *IEEE Transactions on Antenas and Propagation*, **47**(6), pp. 1108–1115.
- RAZAVI-B. (2001). *Design of Analog CMOS Integrated Circuits*, McGraw Hill, Boston.
- REED-R. A. (2007). Two-locus epistasis with sexually antagonistic selection: A genetic Parrondo's paradox, *Genetics*, **176**, pp. 1923–1929.

Bibliography

- REIF-F. (1965). *Fundamentals of Statistical and Thermal Physics*, International Ed. 1985 edn, McGraw Hill, Singapore.
- REIMANN-P., BARTUSSEK-R., AND HÄUßER-P. H. R. (1996). Brownian motors driven by temperature oscillations, *Physics Letters A*, **215**, pp. 26–31. First use of the phrase “Brownian motor”.
- RISKEN-H. (1996). *The Fokker-Planck Equation*, Springer, Berlin.
- ROSS-S. M. (1970). *Applied Probability Models with Optimization Applications*, Dover Publications, Inc., New York.
- SCHEISSER-W. E., AND SILEBI-C. A. (1997). *Computational Transport Phenomena*, Cambridge University Press, Cambridge, UK.
- SEADER-J. D., AND HENLEY-E. J. (2006). *Separation Process Principles*, John Wiley & Sons, Inc.
- SEDRA-A. S., AND SMITH-K. C. (2004). *Microelectronic Circuits*, 5th edn, Oxford University Press, New York.
- SIMMONS-G. F. (1963). *Introduction to Topology and Modern Analysis*, McGraw-Hill Kogakusha, Ltd, Tokyo.
- SIMON-S. M., PESKIN-C. S., AND OSTER-G. F. (1992). What drives the translocation of proteins?, *Proc. Natl. Acad. Sci. USA*, **89**, pp. 3770–3774. First use of the phrase “Brownian ratchet”.
- SKAFIDAS-E., EVANS-R. J., SAVKIN-A. V., AND PETERSEN-I. R. (1999). Stability results for switched controller systems, *Automatica*, **35**(4), pp. 553–564.
- SLATER-G. W., GUO-H. L., AND NIXON-G. I. (1997). Bidirectional transport of polyelectrolytes using self-modulating entropic ratchets, *Phys. Rev. Lett.*, **78**(6), pp. 1170–1173.
- SMOLUCHOWSKI-M. (1912). Experimentell nachweisbare, de ublichen Thermodynamik wider-sprechende Molekularphanomene, *Physikalische Zeitschrift*, **13**, p. 1069.
- SMOLUCHOWSKI-M. (1916). Drei vorträge über diffusion, Brownsche Molekularbewegung und Koagu-lation von Kolloidteilchen, *Phys. Z.*, **17**, pp. 557–571.
- SOROS-G. (2008). *The New Paradigm for Financial Markets*, Scribe, Melbourne.
- STENGEL-R. F. (1986). *Optimal Control and Estimation*, Dover Publications, Inc., New York.
- STREETMAN-B. G. (1995). *Solid State Electronic Devices*, fourth edn, Prentice Hall, Englewood Cliffs, New Jersey.
- SZILARD-L. (1929). Über die entropieverminderung in einem thermodynamischen system bei eingriffen intelligenter wesen, *Journal Zeitschrift für Physik*, **53**(11-12), pp. 840–856.
- TALEB-N. N. (2004). *Foiled by Randomness*, Penguin Books, London.
- TAYLOR-H. M., AND KARLIN-S. (1998). *An Introduction to Stochastic Modelling*, third edn, Academic Press, San Diego.
- TODHUNTER-I. (1865). *History of the Mathematical Theory of Probability from the time of Pascal to that of Laplace*, Macmillan and co., Cambridge.

- TORAL-R. (2001). Cooperative Parrondo's games, *Fluctuation and Noise Letters*, **1**(1), pp. L7–L12.
- TORAL-R., AMENGUAL-P., AND MANGIONI-S. (2003a). A Fokker-Planck description for Parrondo's games, in L. Schimansky-Geier, D. Abbott, A. Neiman, and C. V. den Broeck. (eds.), *Proc. SPIE, Noise in Complex Systems and Stochastic Dynamics*, Vol. 5114, pp. 309–317.
- TORAL-R., AMENGUAL-P., AND MANGIONI-S. (2003b). Parrondo's games as a discrete ratchet, *Physica A*, **327**(1–2), pp. 105–110.
- TREFETHEN-L. N. (2000). *Spectral Methods*, SIAM, Philadelphia.
- TRUSTRUM-K. (1971). *Linear programming*, Routledge & Kegan Paul Ltd., London.
- TUCKWELL-H. C. (1988). *Elementary Applications of Probability Theory*, Chapman&Hall, London.
- UHLENBECK-G. E., AND ORNSTEIN-L. S. (1930). On the theory of the Brownian motion, *Phys. Rev.*, **36**(5), pp. 823–841.
- VAN DEN BROECK-C., REIMANN-P., KAWAI-R., AND HÄNGGI-P. (1999). *Lecture Notes in Physics: Statistical Mechanics of Biocomplexity*, Vol. 527, Springer-Verlag, Berlin, chapter Coupled Brownian motors, pp. 93–111.
- WACKERLEY-D. D., MENDENHALL III-W., AND SCHEAFFER-R. L. (1996). *Mathematical Statistics with Applications*, Duxbury Press, Belmont, USA.
- WANG-M. C., AND UHLENBECK-G. E. (1945). On the theory of Brownian motion II, *Reviews of Modern Physics*, **17**(2 and 3), pp. 323–342.
- WANNIER-G. H. (1966). *Statistical Physics*, Dover 1987 edn, Dover Publications Inc., New York.
- WARRICK-H. M., AND SPUDICH-J. A. (1987). Myosin structure and function in cell motility, *Annual Review of Cell Biology*, **3**(1), pp. 379–421.
- WEISSTEIN-E. W. (1999). *The CRC Concise Encyclopedia of Mathematics*, CRC, Boca Raton.
- WESTERHOFF-H. V., TSONG-T. Y., CHOCK-P. B., CHEN-Y. D., AND ASTUMIAN-R. D. (1986). How enzymes can capture and transmit free energy from an oscillating electric field, *Proc. Nat. Acad. Sci.*, **83**, pp. 4734–4737.
- WITTGENSTEIN-L. (1918). *Tractatus Logico Philosophicus*, Routledge, New York.
- WU-M. K. W., AND TSE-C. K. (1996). A review of EMI problems in switch mode power supply design, *Journal of Electrical and Electronics Engineering Australia*, **16**, pp. 193–204.
- YATES-R. D., AND GOODMAN-D. J. (1999). *Probability and Stochastic Processes*, John Wiley&Sons, Inc., New York.
- ZEMANIAN-A. H. (1965). *Distribution Theory and Transform Analysis*, Dover 1987 edn, Dover Publications, Inc., New York.
- ZEMANIAN-A. H. (2005). A circuit-theoretic anomaly resolved by nonstandard analysis, preprint arXiv:math/0509261v1.
- ZUREK-W. H. (1989). Thermodynamic cost of computation, algorithmic complexity and the information metric, *Nature*, **341**(6238), pp. 119–124.

Glossary

No new technical terms, or acronyms, are defined in this thesis. New concepts are constructed from short phrases of existing concepts. Some existing acronyms are used and are listed here, together with a few technical terms.

AC	Alternating Current, high frequency
AE	Almost Everywhere
AIP	American Institute of Physics
BIOMEMS	Biological- Micro-Electro-Mechanical Systems
BJT	Bipolar Junction Transistor
CBME	Centre for Bio-Medical Engineering
CLT	Central Limit Theorem
CSIRO	Commonwealth Scientific and Industrial Organisation
dB_t	an infinitesimal increment of Brownian motion
DC	Direct Current, zero frequency
det	the determinant of a matrix
DNA	Deoxy-ribo-Nucleic Acid
EMACS	Editing with MACroS, The one true text editor
EPS	Encapsulated Post-Script
FET	Field Effect Transistor
JFET	Junction Field Effect Transistor
GNU	GNU is Not UNIX, devised by Richard M Stallman
HTML	Hyper-Text Markup language
IE	Integral Equation
inkscape	A versatile vector graphics program

KCL	Kirchhoff's Current Law
KVL	Kirchhoff's Voltage law
L ^A T _E X	the T _E X mathematical markup language with macros
LINUX	Linus Torvald's open-source reverse-engineered version of UNIX.
LRC	Adjective for a circuit containing an inductor, L , resistor, R , and a capacitor, C
Matlab	A powerful matrix-oriented scientific and engineering computing language
MEMS	Micro Electro-Mechanical System
MGF	Moment Generating Function
MOSFET	Metal-Oxide Field-Effect Transistor
MULTICS	Multiplexed Information and Computing Service
Octave	The GNU open-source matrix-oriented computing language
ODE	Ordinary Differential Equation
PDE	Partial Differential Equation
Perl	A language for getting your job done, especially with text
PFE	Partial Fraction Expansion, of rational polynomials over a field
PSD	Power Spectral Density
RC	Adjective for a circuit containing a resistor, R , and a capacitor, C
RMS	Root Mean Square
SDE	Stochastic Differential Equation
SIE	Stochastic Integral Equation, the more rigorous form of an SDE
sinc	the function of x , $\sin(\pi x)/(\pi x)$
UNIX	A widely used computer operating system, pun on MULTICS.
UPoN	Unsolved Problems of Noise
WWW	World Wide Web
xfig	A venerable, reliable and compact vector graphics program

Index

- Ćuk
 - and Middlebrook, 162
- absorbing
 - boundary conditions, 122
 - Astumian's games, 125
 - states, 122
- actin, 18
- adenosine, 18
- admittance, 166
- Astumian
 - Astumian's games, 121
 - rule-set 1, 122
 - rule-set 2, 122
- asymmetrical, 21
- asymptotic
 - rates of return, 91, 94
 - not helpful with absorbing states, 126
 - small-matrix technique, 96
 - value
 - of the time-varying probability vector, 128
- average
 - current, 163
 - rate of return
 - from Parrondo's original games, 97
 - small-matrix formula, 95
 - reward, 93
 - state-space time-average model, 170
 - time averaged angular corner frequencies, 169
 - time-average model
 - of Middlebrook and Ćuk, 162
 - time-average SDE
 - for switched-mode circuits, 180
 - time-average switched state-space model, 171
 - time-averaged game, 95
 - small-matrix representation, 96
 - voltage, 163
- average probability vector
 - in phase-space
 - of Parrondo's games, 154
 - over phase-space, 152
- averages
 - consistency of
 - in time and phase-space, 155
- Avogadro's number, 13
- band-pass circuit
 - SDE model for, 236
- Barnsley, 141, 147, 149
 - and Iterated Function Systems (IFS), 139
 - and the Cantor set, 175, 176, 183
 - dimension of Parrondo's fractal, 151
 - testing theory of, 150
- basis functions
 - choice of, 253
- basis functions
 - choice of, 31
- Behrends
 - analysis agrees with Astumian, 130
 - and formulae for Astumian's games, 129
 - conjecture
 - regarding fractal dimension, 261
- Bernoulli, 59, 60, 62, 67
 - distribution, 52
 - process, 52, 65
 - and Parrondo's games, 70
 - solution using z-transforms, 64
 - trials, 61
- Binomial, 61
 - coefficients, 52
 - distribution, 52
 - probability mass function, 59
- Boltzmann, 12
- Boyle, 12
- Brownian motion, 12, 14, 16
 - properties of, 210
- Brownian motor, 17

- Brownian ratchet, 18
 - flashing ratchet
 - physical design, 20
 - inter-digital, 20–23
 - successful physical examples, 22
 - Brownian ratchets
 - with distributed charge, 257
 - Cantor set
 - is a fractal, 138
 - capacitance, 219, 220
 - capacitor, 228, 236
 - in switched-mode circuit, 162
 - randomly switched, 177, 179
 - SDE model, 177
 - SDE model for, 180
 - stochastic model, 227
 - switched, 163, 165, 167
 - equivalent to an admittance, 166
 - fractals in phase-space, 175
 - simulation, 169
 - with fast switching, 177
 - capacitors
 - SDE modelling of, 227
 - catalysis, 24
 - Cauchy
 - integral formula, 232
 - challenges
 - for the future, 251
 - charge
 - electric, 217
 - equivalent to charge, 217
 - electric flux, 217
 - chromatography, 39
 - circuit
 - equivalent
 - switched-mode, 164
 - switched mode, 162
 - circuits
 - electronic
 - modelling using SDEs, 217
 - stochastic analysis of, 209
 - Clifford
 - Clifford algebra, 144
 - geometric algebra
 - meaning of determinant, 144
 - Colpitts oscillator, 245
 - computation
 - fundamental limitations of, 16, 275
 - conclusions
 - summary of, 251
 - configuration space, 83
 - consistency of averages
 - in time and phase-space, 155
 - continuity, 42, 254
 - law of, 53
 - continuity, law of, 41
 - contribution
 - original, 252
 - contributions
 - original
 - in this thesis, 7
 - control
 - control law
 - randomised, 162
 - loop, 186
 - systems
 - stable and unstable, 189
 - theory
 - law can be randomised, 181
 - convex
 - convex set
 - Kolmogorov's definition, 102
 - convexity and concavity, 101
 - linear convex combination, 94
 - current
 - average, 163
 - in the switched capacitor circuit, 167
 - KCL
 - Kirchhoff's current law, 217
 - Kirchhoff's current law
 - infinitesimal form, 217
 - KCL, 217
 - terminal, 227
- current source

-
- noise, 224
 - symbol, 229
 - Norton equivalent, 224
 - currents
 - and voltages
 - as state variables, 163
 - De Moivre, 52
 - debt, 70
 - decomposition
 - unique
 - martingales, 248
 - definitions of terms
 - for Markov transition operators, 82
 - Democritus, 12
 - demon
 - Maxwell's, 14
 - figure, 15
 - role in creative process, xiv
 - density function
 - conditional, 29
 - difference equations
 - partial, 40
 - with periodic coefficients, 72
 - differences
 - finite, 30
 - partial, 30
 - diffusion, 29
 - coefficient
 - effective, 68
 - equation, 41
 - Einstein's use of Fourier's solution, 52
 - Fourier's solution to, 52
 - Fick's law, 30, 41
 - Graham's law, 41
 - minority carriers
 - bipolar transistor, 58
 - operator
 - Parrondo and Ehrenfest, 51
 - Parrondo's games with natural, 57
 - partial difference equation for, 51
 - dimension
 - capacity, 151
 - constraint
 - reduces number by one, 84
 - different from cardinality, 144
 - fractal, 137, 143
 - attracting set, 157
 - generated by matrix operators, 144
 - of attracting set in an IFS, 143
 - with two matrix operators, 145
 - Hausdorff, 137
 - Moment Generating Function
 - multi-dimensional, 152
 - multi dimensional
 - discrete Markov chain, 84
 - multi-dimensional
 - Moment Generating Function, 154
 - scaling property, 154
 - number of
 - very large in Parrondo's games, 88
 - Parrondo's original games, 148
 - three states, 148
 - phase-space
 - multi-dimensional, 154
 - special two dimensional case
 - Parrondo's games, 104
 - dimensions
 - many
 - leads to large matrices, 90
 - discrete games of chance
 - history, 23
 - rates of return from, 81
 - solution using discrete transforms, 59
 - discrete transforms, 35
 - discrete transforms in space
 - the w-transform, 68
 - dynamics
 - and state-variables, 163
 - detailed
 - ignored in time-average models, 170
 - medium-term, 169
 - medium-term and stochastic
 - modelled by SDE, 181
 - state-space models for, 173
-

- Einstein, 24, 41, 43
 - Einstein-Smoluchowski equation, 52
 - solution to the diffusion equation, 52
- energy
 - a apparent paradox resolved, 167
 - a Parrondian paradox with, 184
 - source, 162
 - stored, 162, 163
 - waste, 163
- entropy, 14, 15, 19
- Epicurus, 12
- equilibrium
 - quasi, 228, 233
 - thermodynamic, 219, 222
- equilibrium, steady-state voltages, 164
- equipartition
 - of energy, 219, 222, 228, 233, 242
 - limitations of use, 234
 - mean square voltage, 234
 - proof, 234
- equivalent representation
 - in time and phase-space
 - of Parrondo's games, 150
- ergodic
 - an inhomogeneous Markov chain, 140
 - hypothesis
 - for Cantor's fractal, 140
- feedback
 - control
 - loop, 186
 - path, 187
 - transfer function, 193
- FET
 - Field Effect Transistor, 244
- Feynman, 12, 17, 223
- finite difference equations
 - and Parrondo's games, 38
- finite difference model, for switched-mode circuits, 168
- flashing ratchet, 19, 20
- fluctuations, 13, 16, 19
- flux
 - density
 - electric, 218
- electric
 - charge, 217
 - magnetic, 220, 221
- Fokker-Planck Equation, 29, 30, 41
 - and Brownian ratchets, 39
 - and Parrondo's Game B, 50
 - and Parrondo's game B, 50
 - diffusion equation as a special case, 52
 - equivalent finite partial difference equation, 46
 - methods of obtaining, 41
 - relation to the Kramers-Moyal expansion, 30
 - sampling, 44
 - summary of results, 58
 - sampling the, 38
 - with piecewise-constant coefficients, 42
- Fokker-Planck equation
 - relationship to Langevin equation, 216
- fractal
 - an interesting example, 157
 - Parrondo's, 148
 - snowflake fractal, 157
- fractals
 - moments of, 260
- functional mapping
 - between electrical and mechanical systems, 226
- functions
 - continuous
 - discrete transformations of, 29
 - sampling
 - of, 29
- gain
 - zero gain surface, 98
 - zero-gain surface
 - figure, 116
- gambler
 - gambler's ruin
 - and Astumian's games, 125

-
- gambling as a paradigm
 - for Parrondo's games, 86
 - for probability theory, 86
 - Game A
 - Parrondo's, 47
 - Game B
 - Parrondo's, 47
 - games
 - independent games without memory, 112
 - games of chance
 - discrete
 - history, 23
 - Gauss
 - Gaussian basis function, 34
 - Gaussian conditional density function, 30
 - Gaussian distribution
 - completely determined by first two moments, 59
 - robust when sampled, 69
 - Gaussian function
 - solution to the diffusion equation, 52
 - Gaussian functions
 - as basis functions, 69
 - Gaussian limit of the binomial, 52
 - generalised function, 142, 178, 206
 - Lighthill and, 142
 - generating function, 30, 36, 39
 - generating functions
 - and the z-transform, 59
 - table of, 69
 - Geometric Brownian Motion (GBM)
 - basis for Black-Scholes model, 214
 - Geometric Brownian motion (GBM)
 - exact solution, 213
 - Gibbs, 13, 14, 83, 84, 228
 - Hamiltonian, 226
 - Hurwitz, 187
 - IFS
 - Iterated Function System, 139
 - Iterated Function Systems, 147
 - inductor, 236
 - stochastic modelling, 227, 228
 - inductors
 - modelling of, 227
 - instability, 187
 - and modes of response, 171
 - proof, 197
 - integral
 - Itô, 212
 - ions
 - in solution, 42
 - Iterated Function System
 - IFS, 139
 - Iterated Function Systems
 - IFS, 147
 - Itô
 - stochastic calculus of, 209
 - Itô integral, 212
 - Itô's formula, 213
 - Jaynes, 258
 - JFET
 - Field Effect Transistor
 - simple circuit, 245
 - Junction Field Effect Transistor, 244
 - analysis of circuit, 246
 - Kirchhoff, 259
 - Kirchhoff's laws
 - infinitesimal forms, 217
 - Kirchhoff's voltage law
 - stochastic form, 220
 - Kolmogorov
 - and linear spaces, 84
 - construction of Brownian motion, 207
 - definition of a convex set, 102
 - on continuity of Brownian motion, 207
 - Kushner, 200, 202
 - Lagrangian, 259
 - Langevin, 183, 203
 - Langevin equation, 228
 - applied to electronic circuits, 243
 - for electronic circuits, 234
-

- relationship to the Fokker-Planck equation, 216
- two dimensional, 236
- Langevin equations
 - models for noise in electronic circuits, 263
- Langevin equations, as models for noise in circuits, 205
- Laplace, 31
 - Gaussian limit of the binomial, 52
 - on probability, 41
 - transform, 35
 - one-sided, in time, 35
 - two-sided, in space, 35
- linear transformations
 - of phase-space, 153
- low-pass filter
 - SDE model for, 228
- Lucretius, 12
- Lyapunov
 - equation, 195
 - function, 194
 - stability, 184
 - theorem, 196
- Lyapunov's method
 - second, 192
- Mandelbrot
 - Cantor dust, 139
 - self-similar sets, 139
- Markov chains
 - can generate fractals
 - in phase-space, 138
 - time-homogeneous
 - notation, 132
 - time-inhomogeneous, 134
- martingale, 208
 - decomposition
 - unique, 263
 - definition of, 211
 - property of Itô integrals, 211
 - unique decomposition of, 248
- Maxwell, 13, 14
- Maxwell's demon, xiv, 14, 16
- mean-square
 - noise voltage, 229
 - voltage, 242
- Middlebrook, 162
 - and Ćuk, 162
- modelling of capacitors, 227
- modelling of electronic circuits, using SDE, 217
- modelling of inductors, 227
- moment
 - calculation
 - from z-transforms, 62
 - mean
 - as first moment, 33
 - mean and variance
 - most important moments, 38
 - variance
 - as second moment, 33
- moment generating function
 - in phase-space
 - of Parrondo's games, 154
- moments
 - and derivatives of z-transforms, 65
 - in phase-space, 146
 - of Parrondo's games
 - method for obtaining, 39
- motor
 - Brownian, 17
- motor, Brownian, 4
- multi-dimensional
 - Moment Generating Function
 - to calculate moments, 155
- multiplex
 - Multiplexed spatial function, 72
- multiplexed spatial functions, 72
 - moments of, 73
- myosin, 18
- natural diffusion
 - Parrondo's games
 - with, 115
- NEB
 - Noise Equivalent Bandwidth, 241
- Newton, 12

- and atoms, 12
- and finite differences, 27
- on scientific discovery, 253
- Optiks, 12
- noise
 - current source, 224
 - symbol, 229
 - voltage source, 223, 224, 230, 246, 248
- Noise Equivalent Bandwidth
 - NEB, 241
- noise techniques
 - in electronics
 - introduction to, 206
- non-convex
 - winning and losing regions
 - Parrondo's games, 101
- Norton and Thévenin representations, 225
- Norton equivalent current source, 224
- Nyquist, 14, 236
- ODE
 - Ordinary Differential Equation, 33, 164, 180, 191, 203
- Onsager
 - condition for detailed balance, 98
 - cyclic chemical reaction, 100
- operator
 - description of, 30
- operators
 - choice of, 31
- Ordinary Differential Equation
 - ODE, 164, 180, 191, 203
- Parabolic
 - Partial Differential Equation
 - convergence of numerical method, 51
 - Partial Differential Equation (PDE)
 - methods of solution, 30
- paradoxical circuit
 - Parrondian
 - construction of, 186
 - physical implementation, 192
- Parrondo's fractal, 148
- Parrondo's game
 - average probability vector
 - in phase-space, 154
- Parrondo's game A, 48
 - solution using discrete transforms, 69
- Parrondo's game B, 50
- Parrondo's games, 7, 8, 25, 38, 39, 47, 86, 162, 172, 175, 177, 183, 184, 252
 - a definition, 87
 - an optimised form, 155
 - analogy with switched-mode circuit, 184
 - and finite difference equations, 38
 - and other similar games, 130
 - apparently paradoxical, 100
 - as a realistic simulation of a Brownian ratchet, 55
 - as a von Neumann game, 258
 - as Markov chains with reward, 94
 - as partial difference equations, 47
 - background, 11
 - Bayesian approach, 258
 - condition for detailed balance, 100
 - condition for zero-return, 100
 - equivalent representation
 - in time and phase-space, 150
 - first moment
 - asymptotic value, 94
 - higher moments, 260
 - history, 23
 - large-matrix formulation, 88
 - long sequences of games, 136
 - mean position, 53
 - mean velocity of drift, 53
 - moment generating function of
 - in phase-space, 154
 - moments, 39
 - calculation using z-transforms, 62
 - method for obtaining, 39
 - moments of, 58
 - non-convex winning and losing regions, 101
 - odd and even games
 - with only two states, 118

- original games
 - small-matrix analysis, 96
 - original parameters, 87
 - parameter space for, 104
 - parameter space of, 185
 - periodic sequences of games, 135
 - physical basis, 27
 - reward function
 - properties of, 113
 - self-similarity rule
 - in phase-space, 153
 - simulation
 - including null-transition, 54
 - small-matrix notation for the first moment, 95
 - small-matrix representation of, 77
 - spatially-periodic case
 - reduced modulo L , 92
 - specification of parameter values, 86
 - visualisation
 - in phase-space, 138
 - visualisation of, 132
 - with natural diffusion, 54, 115
 - with null-transitions, 115
 - with only two states, 118
 - with self-transitions, 115
 - zero-gain surface, 98
 - figure, 116
 - zero-return surface, 98
- Parrondo's game B, 74
- Parrondo's paradox, 98, 183
- partial difference equation
 - appropriate choice of scale, 51
- partial difference equations, 40
 - and Parrondo's games, 47
 - numerical methods
 - conditions for convergence, 50
- pawl
 - ratchet and, 16
- PDE
 - Partial Differential Equation, 33
- phase space, 83
- phase-space, 84
 - limit theorems in, 85
 - linear transformations of, 153
 - moments in, 146
 - Parrondo's games
 - moment generating function of, 154
 - relation to configuration space, 84
 - relation to state-space, 84
 - visualisation in, 138
- power, 185, 195
 - change in stored energy, 192
 - matrices, 195
 - in state-space, 195
 - series, 192
- Power Spectral Density
 - PSD, 224, 228, 236
- probabilities
 - of transition, 48
- probability
 - flow, 41
 - flow of, 54
 - of transition, 46
 - in Parrondo's games, 48, 50
 - total, 64
- probability density function, 41
 - Brownian particle, 41
 - Gaussian, 52
- probability density functions
 - transformed, 37
- probability mass functions
 - transformed, 37
- properties of Brownian motion, 210
- prospects
 - future
 - for thesis topics, 253
- PSD
 - Power Spectral Density, 224, 228, 236
- random, 40
 - random part of Brownian motion, 58
 - random-ness and disorder, 58
 - randomised sequence, 48
 - variables, 62

-
- ratchet
 - Brownian, 16, 18, 19
 - on-off, 18
 - ratchet and pawl, 16
 - ratchet, flashing, 4
 - ratchet, on-off, 4
 - resistance
 - characteristic, 196, 197
 - resistor, 168, 193, 228, 236
 - dissipative, 202
 - SDE models for, 223
 - return
 - zero-gain surface
 - figure, 116
 - reward functions
 - linear and non-linear
 - definitions, 106
 - examples, 109
 - summary of results, 111
 - ripple, 168
 - Routh, 187
 - sampling
 - finite difference approach, 258
 - of functions, 29
 - points, 256
 - spacing of points, 257
 - sampling method
 - choice of, 31
 - Schwartz
 - generalised functions, 32
 - SDE
 - multi-dimensional
 - exact solution, 244
 - Stochastic Differential Equation, 161, 177, 179, 181, 203, 206, 208, 213
 - algebraic solution of, 212
 - simulation, 180
 - SDE models
 - large switched-mode circuits, 262
 - Smoluchowski, 14, 17
 - snowflake
 - snowflake fractal
 - and a limiting case of Parrondo's games, 157
 - Soboleff
 - generalised functions, 32
 - stability, 187
 - analysis, 172
 - differentiators
 - marginally stable, 193
 - Lyapunov, 184
 - proof, 200
 - regions in parameter space, 188
 - whole of system property, 184
 - stable region
 - parameter space
 - can be non-convex, 185
 - state space, 83
 - statistical laws, 13, 15
 - statistical methods, 13
 - statistical physics, ix
 - stochastic calculus of Itô, 209
 - Stochastic Differential Equation
 - multi-dimensional
 - exact solution, 244
 - SDE, 161, 177, 179, 181, 203, 206, 208, 213
 - algebraic solution of, 212
 - simulation, 180
 - stochastic processes
 - with stationary probabilities of transition, 66
 - stochastically switched, 178, 200
 - sub-prime crisis, 70
 - correlated downturn, 72
 - switched capacitor circuit, summary, 182
 - switched state-space model, 190
 - switched-Markov chain
 - ODE model, 172
 - switched-mode, 162–164, 166
 - circuit
 - fast random switching, 177
 - fractals in state-space, 175
 - ODE model, 171–174
 - SDE model, 177
-

- stability, 172
- simulation, 169
- switched-mode circuits, 161, 162
- switched-mode devices
 - fractals in phase-space
 - moments of, 261
- switched Markov systems, 161
- switching noise, 168
 - as one of many noise sources, 202
 - SDE for modelling, 202
- Taleb, 70
- Taleb's game
 - definition, 70
 - solution using discrete transforms, 70
- terminal
 - current, 227
 - voltage, 227
- Thévenin and Norton representations, 225
- the w-transform
 - discrete transforms in space, 68
- time and phase-space
 - equivalent representation
 - for Parrondo's games, 150
- time-average
 - switched-mode circuits and switched-Markov chains, 183
- time-average SDE
 - for switched-mode circuits, 180
- transfer function
 - second-order
 - definitions and terms, 237
- Two capacitor problem, 263
- two-state
 - Parrondo's games
 - with only two states, 118
- variables
 - description of, 30
- variance
 - and the Einstein Smoluchowski equation, 52
- visualisation, 85
- in phase-space, 138
- of Parrondo's games, 132
- value of, 158
- volatility
 - definition, 214
- voltage
 - across capacitor
 - state-variable, 166
 - as functions of state variables, 195
 - average, 163
 - capacitor, 177
 - histogram, 176
 - simulation, 167
 - input, 191
 - Kirchhoff's voltage law, 220
 - mean-square, 228
 - noise intensities, 225
 - open circuit, 162
 - source, 164
 - noise, 223, 224, 230, 246, 248
 - stochastic, 224
 - terminal, 227
 - Thévenin-equivalent, 229
- voltages
 - and currents
 - as state variables, 163
- z-transforms
 - and generating functions, 59
 - table of, 69